CRANFIELD UNIVERSITY

Kim Vercruysse

Processes controlling the sources and transport dynamics of suspended sediment in rivers

School of Water, Energy and Environment

PhD
Academic Year: 2016 - 2017

Supervisors: Dr. Robert Grabowski and Dr. Tim Hess
September 2017

CRANFIELD UNIVERSITY

School of Water, Energy and Environment

PhD

Academic Year 2016 - 2017

Kim Vercruysse

Processes controlling the sources and transport dynamics of suspended sediment in rivers

Supervisors: Dr. Robert Grabowski and Dr. Tim Hess
September 2017

This thesis is submitted in partial fulfilment of the requirements for the degree of Doctor of Philosophy

ABSTRACT

Human activity has disturbed the natural suspended sediment (SS) balance and the associated geomorphological and ecological functioning of many rivers. Yet, predicting and managing SS is challenging because the processes controlling SS transport over multiple timescales are not well understood. The aim of this research is to improve the prediction and management of SS by investigating the hydro-meteorological and catchment processes driving temporal variation in SS transport. The objectives are (i) to assess SS transport over multiple timescales to uncover the scale-specific processes and process interactions that determine temporal variation in SS transport; (ii) to apply and test a sediment fingerprinting approach based on infrared spectrometry to identify dominant SS sources; and (iii) to evaluate the role of variations in sediment sources in controlling SS concentrations in response to hydro-meteorological variables. The research was carried out in the River Aire, UK.

The findings show that SS transport in the River Aire is highly event-driven and supply-limited, while also being influenced by long-term changes in land use. Over the studied period, the dominant SS source was grassland, and its contribution was mainly controlled by antecedent moisture conditions. On the contrary, urban street dust, which was also a dominant sediment source, was less hydrologically driven. The research also demonstrated that while infrared-based fingerprinting can be used to estimate SS source contributions with acceptable model errors, sediment apportionment is strongly influenced by the degree of discrimination between source classes. In order to improve methods to quantify SS transport and sources, and to identify sediment management needs, this research underscores the need to (i) recognise different timescales of SS transport to identify the underlying processes; (ii) develop better approaches for source classification and discrimination to accurately represent the sediment in rivers; and (iii) establish further knowledge on sediment sources variations in different contexts and over multiple spatial and temporal scales.

Keywords: Timescale, fluvial geomorphology, connectivity, hydro-meteorology, sediment fingerprinting, processes

This work was funded by an industrial PhD studentship supported by Cranfield University, Leeds City Council and Arup.

ACKNOWLEDGEMENTS

Thank you!

To Bob, for giving me this opportunity to explore the mysteries of the sediment-world, for pushing me to do that little extra work, and especially for your excellent guidance and support during the past three years. To Tim, for your critical eye and your expert advice. To Jane, for asking the right questions and sharing your insights. To Nigel, for chairing the advisory committee. To Irantzu, Milly, Sally, and the rest of the Flood Alleviation Scheme-team at Arup and Leeds City Council for providing funding, logistical, and research support. And to Gary Bilotta and Robert Simmons for critically examining this work and providing constructive feedback.

¡Muchas gracias!

To Mar, for assisting me during my soil sampling in rainy Yorkshire, and for being the perfect partner in crime in getting through PhD-life. And to the Bedfordians, for the pub-nights and the Spanish lunches, which were a great distraction from all the mud.

Dankjewel!

To my family, mama, papa, Alec and Karen, and to my friends back in Belgium, for your solid confidence in me, for your numerous visits to England, and for reminding me that there is life outside the academic universe. And to Maarten, for simply helping me in so many possible ways, for challenging me to think outside the box, and for listening to my dirt talk. But most of all, for being my much-needed home during these past years of moving around.

TABLE OF CONTENTS

LIST OF FIGURES

LIST OF TABLES

LIST OF ABBREVIATIONS

AOD	Above Ordnance Datum
BS	Bed sediment
DEM	Digital Elevation Model
DRIFTS	Diffuse reflectance infrared fourier transform spectrometry
EA	Environment Agency
EM	Embsay
FH	Farnley Hall
HD	Headingly
KS	Knotstrop
LL	Lower Laithe
MD	Mahalanobis distance
MT	Malham Tarn
NRFA	National River Flow Archive
P	Precipitation (mm)
P_{1d}	Precipitation 1 day prior to event (mm)
P_{21d}	Precipitation 21 days prior to event (mm)
P_{7d}	Precipitation 7 days prior to event (mm)
PCA	Principal component analysis
PH	Proctor Heigts
PLSR	Partial least squares regression
Q	River discharge (m^3/s)
Q_{1d}	River discharge 1 day prior to time of sampling ($m^3 s^{-1}$)
Q_{1h}	River discharge one hour prior to time of sampling ($m^3 s^{-1}$)
Q_{21d}	River discharge 21 days prior to time of sampling ($m^3 s^{-1}$)
Q_{7d}	River discharge 7 days prior to time of sampling ($m^3 s^{-1}$)
Q_{max}	Peak river discharge during high flow event ($m^3 s^{-1}$)
Q_{mean}	Mean river discharge during high flow event ($m^3 s^{-1}$)
RMSE	Root mean squared error
RMSEP	Root mean squared error of prediction
SK	Skipton
SL	Sediment load (t per unit of time)
SR	Silsden Reservoir
SRC	Sediment rating curve
SS	Suspended sediment
SSC	Suspended sediment concentration ($mg L^{-1}$)
SSC_C	Suspended sediment concentration from grassland in the Coal measures area
SSC_L	Suspended sediment concentration from grassland in the Limestone and shale area
SSC_M	Suspended sediment concentration from grassland in the Millstone Grit area
SSC_{max}	Maximum suspended sediment concentration during high flow event
SSC_{min}	Minimum suspended sediment concentration during high flow event
SSC_R	Suspended sediment concentration from eroding riverbanks
SSC_U	Suspended sediment concentration from urban area
STW	Sewage Treatment Works
TR	Thornton Reservoir

CHAPTER 1: INTRODUCTION

"A river can cleave a deep canyon and twist like a giant snake across its plains; plunge over great cliffs and stretch fingers of earth into the oceans. Rivers dominate landscapes, eroding and creating them. They are, without doubt, the product of a complex suite of natural processes. But the evolution of many rivers has been driven as much by social systems as by natural ones, surprising though this may at first seem." (Middleton, 2012, p. xv)

Rivers have formed landscapes and directed human history for millennia, while simultaneously, humans have also shaped rivers across the world. River channels are diverted for irrigation and straightened to efficiently convey water. Dams are built to create water reservoirs and generate electricity. Riverbanks are consolidated to stop the river from moving across its floodplain, and to create space for agriculture, industry and housing. Rivers are also used as a water resource, while at the same time they serve as drainage systems to flush down industrial and household waste, introducing a multitude of pollutants into the environment (Castonguay and Evenden, 2012). In addition, land use changes have resulted in increased sediment loads in rivers through soil erosion and the emergence of new sediment sources from urban areas, which are harmful for the ecological, biochemical and physical status of rivers (Taylor and Owens, 2009). Consequently, human activity has not only changed the appearance and quality of rivers, but also altered the natural sediment dynamics, and the ecological and geomorphological functioning of river systems.

Unlike pollutants, sediment is a natural and fundamental part of river systems. For this reason, sediment cannot (and should not) simply be prevented and removed from the river. Instead, sediment in the river needs to be managed sensibly and in line with the specific catchment characteristics. Yet, the challenge to managing sediment is that it is difficult to assess how and when sediment negatively impacts the functioning of a particular river system (Gao, 2008).

1.1 What is suspended sediment?

This research will focus on a particular part of river sediment, namely suspended sediment (SS). Every year, the total delivery of SS from rivers to oceans is estimated to be of the order of 15-20 x 10^9 t yr^{-1} (Owens et al., 2005) or 70% of the total river sediment load towards the coast (Morgan, 2005). This is equivalent to every human being on earth in 2017 delivering 20 wheelbarrows of sediment to the ocean every year.

So, what is SS? In general, sediment in rivers originates from rock and soil erosion on land whereby detached particles are transported by water and wind towards the river. Other particles can also enter the river such as organic and inorganic material from the erosion of roads, combined sewer overflows, and biological and human activity. As a result, the particles constituting the sediment of rivers vary significantly in composition and size, of which the latter is commonly defined by the Wentworth scale: boulders (≥256 mm), cobbles (64-256 mm), gravel (2-64 mm), sand (0.063-2 mm), silt (0.004-0.063 mm) and clay (≤0.004 mm) (Fryirs and Brierley, 2013). The finest sediments (silt and clay) are usually transported within the water column of a river, kept in suspension through turbulence (i.e. SS). Contrarily, coarser, heavier particles are transported in the river along the channel bottom (i.e. bedload) (Fryirs and Brierley, 2013; Sear et al., 2003). Therefore, SS is typically defined as the fine fraction of the river sediment (generally < 63 µm) that is carried in suspension consisting of a mixture of organic and inorganic material. SS is usually measured as suspended sediment concentration (SSC, in mg L^{-1}), from which sediment loads (SL, in t) per unit of time can be calculated.

1.2 Suspended sediment: natural and problematic

SS in rivers is natural. It plays a fundamental role in the geomorphological, hydrological, ecological and even socio-economical functioning of river systems and catchments (Owens et al., 2005). For geomorphologists and geologists, fine sediments form a fundamental part of geomorphological processes and the geological cycle (e.g. formation of coastal deltas) (Bracken et al., 2015; Bridge, 2003). For ecologists and biologists, SS contributes to the functioning of aquatic

habitats (e.g. sediment flocs as habitats) (Droppo, 2001; Owens et al., 2005). For farmers and agronomists, fine sediments deliver valuable nutrients to floodplain soils (Gao, 2008; Horowitz, 2008; Lloyd et al., 2016). Therefore, too little SS in rivers can be problematic, because it can lead to increased erosion of river channels and deltas, scouring of bridges and other infrastructure, and the modification of aquatic habitats (e.g. reduced turbidity can lead to competitive advantages for sight-feeding fish) (Owens et al., 2005).

SSC in a river can also become excessive. Human activity has significantly increased SSCs in rivers due to, for example, increased soil erosion from agriculture, deforestation, construction and mining activities, and urbanisation (Owens et al., 2005). These elevated levels of fine sediment in rivers are damaging for the ecological status of a river system. The combination of light suppression (i.e. high turbidity levels) and a high density of fine particles in the water column, prevents algae and macrophytes from growing, causes abrasion and scouring of aqueous habitats and organisms, and clogs the pores of gravel beds which damages fish spawning sites (Bilotta and Brazier, 2008; Heise and Förstner, 2007; Lloyd et al., 2016; Rossi et al., 2013; Rügner et al., 2013). SS is also the most chemically active component of the river SL, so that many contaminants and nutrients (e.g. dioxins, radionuclides, heavy and trace metals, and phosphorus) are transported (and stored) in association with SS particles, polluting both the sediment and the wider river system (Owens et al., 2005). Furthermore, high SSCs significantly increase water treatment costs (Rickson, 2014; Wohl, 2015), and, when the flow is no longer sufficient to maintain the excessive SS particles in motion, sediment is deposited (Fryirs and Brierley, 2013). Excessive sediment deposition within river channels can block culverts and streams (García-Ruiz et al., 2015), shorten the lifespan of infrastructure such as dams and reservoirs (Hunink et al., 2013) and increase flood risk by reducing the capacity of channels to convey runoff (Gregory, 2006; Slater, 2016; Wallerstein, 2006). Finally, excessive fine sediment deposition outside the river channel can also degrade floodplains by depositing polluted sediment and smothering riparian vegetation (García-Ruiz et al., 2015).

Nevertheless, assessing the potential detrimental impact of SS and developing appropriate management and mitigation strategies is not straightforward. A SS transport system is a continuum of sediment supply, transport and storage at multiple spatial and temporal scales (Sear et al., 2003). As a result, the threshold at which SS becomes harmful strongly depends on the spatial and temporal scales and the context. For example, the effect on aquatic biota is determined by the amount of SS, but also by the duration of exposure, the composition, and the particle-size distribution of the SS (Bilotta and Brazier, 2008). Similarly, when assessing the impact of SS on flood risk, infrastructure, and water treatment, it is important to understand the frequency-magnitude of SS transport to determine potential problems and develop mitigation strategies (Perks et al., 2017).

1.3 Knowledge gap and research needs

Accurate quantification and prediction of SSCs is the first step to assessing the potential impact of SS in rivers and for the development of appropriate management strategies. However, predicting SSCs in rivers is challenging because the temporal dimensions of the processes and process interactions underlying SS transport are not fully understood (Gao, 2008; Poulenard et al., 2009; Rickson, 2014; Sun et al., 2015; Zhang et al., 2013; Zheng et al., 2012). To accurately quantify and predict SSCs in rivers, we need comprehensive insights into how different processes of SS transport interact across temporal scales (Phillips, 2016). To this end, three key research needs were identified.

First, there is a need for studies that identify and synthesise driving factors and underlying processes for SS transport across multiple temporal scales (Blöschl, 2006; Blöschl and Sivapalan, 1995; Evans and Brazier, 2005; McDonnell et al., 2007; Raven et al., 2010; Tetzlaff et al., 2008; Troch et al., 2009; Van Nieuwenhuyse et al., 2011). To date, many sediment studies have been designed to capture SS transport at a particular timescale, and/or the applied predictive models are generally statistical models based on empirical data, which limits our understanding of the potential explanatory factors and processes driving SS transport at different timescales (Cao et al., 2007; Dean et al., 2016; Harvey, 2002; Sun et al., 2015; Zhang et al., 2013).

Second, to support hypotheses about processes underlying SS transport, we also need more detailed information on where SS in rivers comes from and how sediment sources vary over time (Fryirs, 2013). Our understanding of the processes underlying SS transport is often based on hydro-meteorological data, without consideration of the variation in sediment sources and how sediment is transferred across the catchment (Bracken et al., 2015; Francke et al., 2014; Onderka et al., 2012; Perks et al., 2015; Zeiger and Hubbart, 2016). The lack of sediment source information associated with the SS complicates our ability to identify the processes controlling SS transport, and emphasizes the need to combine the analysis of hydro-meteorological data with detailed sediment source information.

Finally, the need for sediment source information requires accurate identification of the sediment sources. Sediment fingerprinting is a possible approach to address this need, and aims to quantify contributions of different sediment sources to the SS in a river based on geochemical and/or physical sediment properties that are characteristic for a particular sediment source (Mukundan et al., 2012). Different techniques have been used to identify sediment properties, such as inductively coupled plasma-optical emission spectrometry (ICP-OAS), atomic absorption spectrometry (AAS), and Diffuse Reflectance Infrared Fourier Transform Spectrometry (DRIFTS) (Cooper et al., 2014a; Laceby and Olley, 2015; Legout et al., 2013; Martínez-Carreras et al., 2010; Poulenard et al., 2009). DRIFTS-based sediment fingerprinting has proved to be especially suitable to gain sediment source information at a high temporal resolution because it is more cost- and time-efficient compared to AAS or ICP techniques, and requires smaller sample volumes (Cooper et al., 2014b; Poulenard et al., 2009). However, to interpret variations in sources in terms of SS transport processes, consideration of all sources of uncertainty related to fingerprinting results is essential. While many studies have quantified statistical model uncertainty, and tested the impact of different sediment properties on the fingerprinting results (Cooper et al., 2014a; Koiter et al., 2013; Laceby et al., 2017), research has not sufficiently investigated how initial sediment source classification influences the interpretation and reliability of the results (Koiter et al., 2013; Pulley et al., 2017a, 2017b).

1.4 Research aim and objectives

Aim: The aim of this study is to improve the quantification and prediction of SS transport in rivers, and to support the development of targeted sediment management strategies, by investigating the hydro-meteorological and catchment processes driving temporal variation in SS transport. This aim will be met through the following objectives.

Objective 1: To assess SS transport over multiple timescales to uncover the scale-specific processes and process interactions that determine temporal variation in SS transport.

Objective 2: To apply a sediment fingerprinting approach based on DRIFTS to identify dominant SS sources, and test the sensitivity of the method to *a priori* sediment source classification.

Objective 3: To investigate the role of variations in SS sources in controlling SSCs in response to hydro-meteorological variables at the intra-annual and event scale.

Case study: The study is applied to the River Aire in northern England, UK.

1.5 Thesis outline

The thesis has been written in a paper format, and thus the novel contributions to science are written as individual academic journal articles (Chapter 2 to 5). Chapter 2 has been published in Earth-Science Reviews (Vercruysse et al., 2017) and Chapter 3 was under review at Water Resources Research at the time of writing. All original work was carried out by the author of this thesis, and the contributions of the co-authors were what would normally be expected from supervisors and advisors (Table 1-1). Chapter 4 and 5 will be submitted for review after completion of this thesis. Please note that due to the format of the thesis, repetition in data description and methodology occur (especially in Chapter 4 and 5).

Chapter 2 provides an up-to-date summary of the main factors controlling spatial and temporal variability in SS transport, evaluates the common methods to

quantify and predict SS concentrations, and identifies the research gaps regarding temporal variability in SS transport. The chapter presents new theoretical knowledge regarding the study and analysis of SS transport through a synthesis of the scale-dependency of processes controlling SS transport and its implications for quantification and management.

Chapter 3 presents a multi-timescale, data-driven statistical investigation of SS transport to uncover the underlying processes and process interactions, and to demonstrate how identification of the scale-dependent processes can aid in more accurate prediction of SSCs (Obj. 1). Based on empirical data, a new framework is developed to serve as a basis towards more holistic process-based approaches to quantify and predict SS transport in rivers.

Chapter 4 describes the DRIFTS-based sediment fingerprinting approach. Different model setups are also presented to investigate how the initial sediment source classification influences the reliability and interpretation of the results (Obj. 2). The chapter provides practical guidance and recommendations for further research on sediment fingerprinting, specifically related to sediment source classification and discrimination.

Chapter 5 presents the results of the DRIFTS-sediment fingerprinting applied to an extensive empirical SSC dataset and investigates how sediment source information can be linked to the total SS transport. The chapter outlines a statistical analysis combining SSCs, sediment source information and detailed hydro-meteorological data to identify the underlying mechanisms for source-specific SS transport at the event and intra-annual scale (Obj. 3).

Chapter 6 discusses how the results presented in the previous chapters contribute to uncovering the temporal variation in SS transport in terms of hydro-meteorological and catchment processes, towards improving quantification and prediction of SS transport, and supporting the development of targeted sediment management strategies. This chapter also outlines recommendations for further research and sediment management based on the findings and limitations of the research.

Finally, ***Chapter 7*** presents the main conclusions of this study in relation to the stated aim.

Additionally, **appendices** are included at the end of the document, which provide more detail on the case study catchment (River Aire), sediment data, and methodologies, including sediment sampling, sediment fingerprinting and statistical approaches.

Table 1-1: Author contributions to the chapter 2 already submitted for publication in peer-reviewed academic journals (Chapters 2 and 3)

	Chapter 2 Earth-Science Reviews Published (2017)	**Chapter 3** Water Resources Research Under review (submitted: 14/07/2017)
Kim Vercruysse	Literature review, synthesis, layout, writing	Data collection and analysis, methodology development, discussion, layout, writing
Robert Grabowski (supervisor)	Guidance on structure, advice, editing	Guidance on method and structure, advice, editing
Tim Hess (co-supervisor)	/	Guidance on method and structure, advice, editing
Jane Rickson (subject advisor)	Advice on sections about soil erosion and editing	/
Irantzu Lexartza-Artza (industrial sponsor)	/	Advice on discussion and editing

1.6 References

Bilotta, G.S., Brazier, R.E., 2008. Understanding the influence of suspended solids on water quality and aquatic biota. Water Res. 42, 2849–2861. doi:10.1016/j.watres.2008.03.018

Blöschl, G., 2006. Hydrologic synthesis: Across processes, places, and scales. Water Resour. Res. 42, 2–4. doi:10.1029/2005WR004319

Blöschl, G., Sivapalan, M., 1995. Scale issues in hydrological modelling: A review. Hydrol. Process. 9, 251–290. doi:10.1002/hyp.3360090305

Bracken, L.J., Turnbull, L., Wainwright, J., Bogaart, P., 2015. Sediment connectivity: a framework for understanding sediment transfer at multiple scales. Earth Surf. Process. Landforms 40, 177–188. doi:10.1002/esp.3635

Bridge, J., 2003. Rivers and Floodplains: Forms, Processes, and Sedimentary Record. Blackwell

Science, Oxford.

Cao, Z., Li, Y., Yue, Z., 2007. Multiple time scales of alluvial rivers carrying suspended sediment and their implications for mathematical modeling. Adv. Water Resour. 30, 715–729. doi:10.1016/j.advwatres.2006.06.007

Castonguay, S., Evenden, M., 2012. Urban Rivers: Remaking Rivers, Cities and Space in Europe and North America. University of Pittsburgh Press, Pittsburgh.

Cooper, R.J., Krueger, T., Hiscock, K.M., Rawlins, B.G., 2014a. High-temporal resolution fluvial sediment source fingerprinting with uncertainty: A Bayesian approach. Earth Surf. Process. Landforms. doi:10.1002/esp.3621

Cooper, R.J., Rawlins, B.G., Lézé, B., Krueger, T., Hiscock, K.M., 2014b. Combining two filter paper-based analytical methods to monitor temporal variations in the geochemical properties of fluvial suspended particulate matter. Hydrol. Process. 28, 4042–4056. doi:10.1002/hyp.9945

Dean, D.J., Topping, D.J., Schmidt, J.C., Griffiths, R.E., Sabol, T.A., 2016. Sediment supply versus local hydraulic controls on sediment transport and storage in a river with large sediment loads. J. Geophys. Res. Earth Surf. 182–110. doi:10.1002/2015JF003436

Droppo, I.G., 2001. Rethinking what constitutes suspended sediment. Hydrol. Process. 15, 1551–1564. doi:10.1002/hyp.228

Evans, R., Brazier, R., 2005. Evaluation of modelled spatially distributed predictions of soil erosion by water versus field-based assessments. Environ. Sci. Policy 8, 493–501. doi:10.1016/j.envsci.2005.04.009

Francke, T., Werb, S., Sommerer, E., López-Tarazón, J.A., 2014. Analysis of runoff, sediment dynamics and sediment yield of subcatchments in the highly erodible Isábena catchment, Central Pyrenees. J. Soils Sediments 14, 1909–1920. doi:10.1007/s11368-014-0990-5

Fryirs, K.A., 2013. (Dis)Connectivity in catchment sediment cascades: A fresh look at the sediment delivery problem. Earth Surf. Process. Landforms 38, 30–46. doi:10.1002/esp.3242

Fryirs, K.A., Brierley, G.J., 2013. Geomorphic analysis of river systems: An approach to reading the landscape. Wiley-Blackwell, West Sussex.

Gao, P., 2008. Understanding watershed suspended sediment transport. Prog. Phys. Geogr. 32, 243–263. doi:10.1177/0309133308094849

García-Ruiz, J.M., Beguería, S., Nadal-Romero, E., González-Hidalgo, J.C., Lana-Renault, N., Sanjuán, Y., 2015. A Meta-Analysis of soil erosion rates across the world. Geomorphology

239, 160–173. doi:10.1016/j.geomorph.2015.03.008

Gregory, K.J., 2006. The human role in changing river channels. Geomorphology 79, 172–191. doi:10.1016/j.geomorph.2006.06.018

Harvey, A.M., 2002. Effective timescales of coupling within fluvial systems. Geomorphology 44, 175–201. doi:10.1016/S0169-555X(01)00174-X

Heise, S., Förstner, U., 2007. Risk assessment of contaminated sediments in river basins--theoretical considerations and pragmatic approach. J. Environ. Monit. 9, 943–52. doi:10.1039/b704071g

Horowitz, A.J., 2008. Determining annual suspended sediment and sediment-associated trace element and nutrient fluxes. Sci. Total Environ. 400, 315–43. doi:10.1016/j.scitotenv.2008.04.022

Hunink, J.E., Niadas, I. a., Antonaropoulos, P., Droogers, P., de Vente, J., 2013. Targeting of intervention areas to reduce reservoir sedimentation in the Tana catchment (Kenya) using SWAT. Hydrol. Sci. J. 58, 600–614. doi:10.1080/02626667.2013.774090

Koiter, A.J., Owens, P.N., Petticrew, E.L., Lobb, D.A., 2013. The behavioural characteristics of sediment properties and their implications for sediment fingerprinting as an approach for identifying sediment sources in river basins. Earth-Science Rev. 125, 24–42. doi:10.1016/j.earscirev.2013.05.009

Laceby, J.P., Evrard, O., Smith, H.G., Blake, W.H., Olley, J.M., Minella, J.P.G., Owens, P.N., 2017. The challenges and opportunities of addressing particle size effects in sediment source fingerprinting: A review. Earth-Science Rev. 169, 85–103. doi:10.1016/j.earscirev.2017.04.009

Laceby, J.P., Olley, J., 2015. An examination of geochemical modelling approaches to tracing sediment sources incorporating distribution mixing and elemental correlations. Hydrol. Process. 29, 1669–1685. doi:10.1002/hyp.10287

Legout, C., Poulenard, J., Nemery, J., Navratil, O., Grangeon, T., Evrard, O., Esteves, M., 2013. Quantifying suspended sediment sources during runoff events in headwater catchments using spectrocolorimetry. J. Soils Sediments 13, 1478–1492. doi:10.1007/s11368-013-0728-9

Lloyd, C.E.M., Freer, J.E., Johnes, P.J., Collins, A.L., 2016. Using hysteresis analysis of high-resolution water quality monitoring data, including uncertainty, to infer controls on nutrient and sediment transfer in catchments. Sci. Total Environ. 543, 388–404. doi:10.1016/j.scitotenv.2015.11.028

Martínez-Carreras, N., Udelhoven, T., Krein, A., Gallart, F., Iffly, J.F., Ziebel, J., Hoffmann, L., Pfister, L., Walling, D.E., 2010. The use of sediment colour measured by diffuse reflectance spectrometry to determine sediment sources: Application to the Attert River catchment (Luxembourg). J. Hydrol. 382, 49–63. doi:10.1016/j.jhydrol.2009.12.017

McDonnell, J.J., Sivapalan, M., Vache, K., Dunn, S., Grant, G., Haggerty, R., Hinz, C., Hooper, R., Kirchner, J., Roderick, M.L., Selker, J., Weiler, M., 2007. Moving beyond heterogeneity and process complexity: A new vision for watershed hydrology. Water Resour. Res. 43, 1–6. doi:10.1029/2006WR005467

Middleton, N., 2012. Rivers: A Very Short Introduction. Oxford University Press, New York.

Morgan, R.P.C., 2005. Soil Erosion & Conservation. Blackwell Publishing Ltd, Oxford.

Mukundan, R., Walling, D.E., Gellis, A.C., Slattery, M.C., Radcliffe, D.E., 2012. Sediment source fingerprinting: transforming from a research tool to a management tool. J. Am. Water Resour. Assoc. 48, 1241–1257. doi:10.1111/j.1752-1688.2012.00685.x

Onderka, M., Krein, A., Wrede, S., Martínez-Carreras, N., Hoffmann, L., 2012. Dynamics of storm-driven suspended sediments in a headwater catchment described by multivariable modeling. J. Soils Sediments 12, 620–635. doi:10.1007/s11368-012-0480-6

Owens, P.N., Batalla, R.J., Collins, A.J., Gomez, B., Hicks, D.M., Horowitz, A.J., Kondolf, G.M., Marden, M., Page, M.J., Peacock, D.H., Petticrew, E.L., Salomons, W., Trustrum, N.A., 2005. Fine-grained sediment in river systems: environmental significance and management issues. River Res. Appl. 21, 693–717. doi:10.1002/rra.878

Perks, M.T., Owen, G.J., Benskin, C.M.H., Jonczyk, J., Deasy, C., Burke, S., Reaney, S.M., Haygarth, P.M., 2015. Dominant mechanisms for the delivery of fine sediment and phosphorus to fluvial networks draining grassland dominated headwater catchments. Sci. Total Environ. 523, 178–190. doi:10.1016/j.scitotenv.2015.03.008

Perks, M.T., Warburton, J., Bracken, L.J., Reaney, S.M., Emery, S.B., Hirst, S., 2017. Use of spatially distributed time-integrated sediment sampling networks and distributed fine sediment modelling to inform catchment management. J. Environ. Manage. 1–10. doi:10.1016/j.jenvman.2017.01.045

Phillips, J.D., 2016. Vanishing point: Scale independence in geomorphological hierarchies. Geomorphology 266, 66–74. doi:10.1016/j.geomorph.2016.05.012

Poulenard, J., Perrette, Y., Fanget, B., Quetin, P., Trevisan, D., Dorioz, J.M., 2009. Infrared spectroscopy tracing of sediment sources in a small rural watershed (French Alps). Sci. Total Environ. 407, 2808–19. doi:10.1016/j.scitotenv.2008.12.049

Pulley, S., Foster, I., Collins, A.L., 2017a. The impact of catchment source group classification on the accuracy of sediment fingerprinting outputs. J. Environ. Manage. 194, 16–26. doi:10.1016/j.jenvman.2016.04.048

Pulley, S., Van Der Waal, B., Collins, A.L., Foster, I.D.L., Rowntree, K., 2017b. Are source groups always appropriate when sediment fingerprinting? The direct comparison of source and sediment samples as a methodological step. River Res. Appl. 1–11. doi:10.1002/rra.3192

Raven, E.K., Lane, S.N., Bracken, L.J., 2010. Understanding sediment transfer and morphological change for managing upland gravel-bed rivers. Prog. Phys. Geogr. 34, 23–45. doi:10.1177/0309133309355631

Rickson, R.J., 2014. Can control of soil erosion mitigate water pollution by sediments? Sci. Total Environ. 468–469, 1187–1197. doi:10.1016/j.scitotenv.2013.05.057

Rossi, L., Chèvre, N., Fankhauser, R., Margot, J., Curdy, R., Babut, M., Barry, D.A., 2013. Sediment contamination assessment in urban areas based on total suspended solids. Water Res. 47, 339–50. doi:10.1016/j.watres.2012.10.011

Rügner, H., Schwientek, M., Beckingham, B., Kuch, B., Grathwohl, P., 2013. Turbidity as a proxy for total suspended solids (TSS) and particle facilitated pollutant transport in catchments. Environ. Earth Sci. 69, 373–380. doi:10.1007/s12665-013-2307-1

Sear, D.A., Malcolm, D.N., Thorne, C.R., 2003. Guidebook for Applied Fluvial Geomorphology, R&D Technical Report FD1914. London.

Slater, L.J., 2016. To what extent have changes in channel capacity contributed to flood hazard trends in England and Wales? Earth Surf. Process. Landforms n/a-n/a. doi:10.1002/esp.3927

Sun, L., Yan, M., Cai, Q., Fang, H., 2015. Suspended sediment dynamics at different time scales in the Loushui River, south-central China. Catena Published. doi:10.1016/j.catena.2015.02.014

Taylor, K.G., Owens, P.N., 2009. Sediments in urban river basins: a review of sediment–contaminant dynamics in an environmental system conditioned by human activities. J. Soils Sediments 9, 281–303. doi:10.1007/s11368-009-0103-z

Tetzlaff, D., McDonnell, J.J., Uhlenbrook, S., McGuire, K.J., Bogaart, P.W., Naef, F., Baird, A.J., Dunn, S.M., Soulsby, C., 2008. Conceptualizing catchment processes: Simply too complex? Hydrol. Process. 22, 1727–1730. doi:10.1002/hyp.7069

Troch, P.A., Carrillo, G.A., Heidbüchel, I., Rajagopal, S., Switanek, M., Volkmann, T.H.M., Yaeger, M., 2009. Dealing with landscape heterogeneity in watershed hydrology: A review

of recent progress toward new hydrological theory. Geogr. Compass 3, 375–392. doi:10.1111/j.1749-8198.2008.00186.x

Van Nieuwenhuyse, B.H.J., Antoine, M., Wyseure, G., Govers, G., 2011. Pattern-process relationships in surface hydrology: Hydrological connectivity expressed in landscape metrics. Hydrol. Process. 25, 3760–3773. doi:10.1002/hyp.8101

Vercruysse, K., Grabowski, R.C., Rickson, R.J., 2017. Suspended sediment transport dynamics in rivers: Multi-scale drivers of temporal variation. Earth-Science Rev. 166, 38–52. doi:10.1016/j.earscirev.2016.12.016

Wallerstein, N., 2006. Accounting for sediment in rivers. FRMRC Research Report UR9.

Wohl, E., 2015. Legacy effects on sediments in river corridors. Earth-Science Rev. 147, 30–53. doi:10.1016/j.earscirev.2015.05.001

Zeiger, S., Hubbart, J.A., 2016. Quantifying suspended sediment flux in a mixed-land-use urbanizing watershed using a nested-scale study design. Sci. Total Environ. 542, 315–323. doi:10.1016/j.scitotenv.2015.10.096

Zhang, Y.Y., Zhong, D.Y., Wu, B.S., 2013. Multiple temporal scale relationships of bankfull discharge with streamflow and sediment transport in the Yellow River in China. Int. J. Sediment Res. 28, 496–510. doi:10.1016/S1001-6279(14)60008-1

Zheng, M., Yang, J., Qi, D., Sun, L., Cai, Q., 2012. Flow-sediment relationship as functions of spatial and temporal scales in hilly areas of the Chinese Loess Plateau. Catena 98, 29–40. doi:10.1016/j.catena.2012.05.013

CHAPTER 2: SUSPENDED SEDIMENT TRANSPORT DYNAMICS IN RIVERS: MULTI-SCALE DRIVERS OF TEMPORAL VARIATION[1]

Abstract

SS is a natural part of river systems and plays an essential role in structuring the landscape, creating ecological habitats and transporting nutrients. It is also a common management problem, where alterations to sediment quantity and quality negatively impact ecological communities, increase flood hazard and shorten the lifespan of infrastructure. To address these challenges and develop sustainable management strategies, we need a thorough understanding of sediment sources, pathways and transport dynamics and the drivers that underlie spatial and temporal variability in SS transport in rivers. However, research to date has not sufficiently addressed the temporal complexity of sediment transport processes, which is limiting our ability to disentangle the hydro-meteorological, catchment, channel and anthropogenic drivers of SS transport in rivers. This review critically evaluates previously published work on SS dynamics to demonstrate how the interpretation of sediment sources and pathways is influenced by the temporal scale and methodology of the study. To do this, the review (i) summarises the main drivers of temporal variation in SS transport in rivers; (ii) critically reviews the common empirical approaches used to analyse and quantify SS sources and SLs, and their capacity to account for temporal variations; (iii) applies these findings to recent case studies to illustrate how method and timescale affect the interpretation of SS transport dynamics; and finally (iv) synthesises the findings of the review into a set of guidelines for a multi-timescale approach to characterise the sediment regime of a river. By recognising a priori that study design and temporal scale have an impact on the interpretation of SS dynamics and employing methods that address these issues, future research will be better able to identify the drivers of SS transport in rivers, improve sediment transport modelling, and propose effective, sustainable solutions to sediment management problems.

[1] Vercruysse, K., R. C. Grabowski, and R. J. Rickson (2017), Suspended sediment transport dynamics in rivers: Multi-scale drivers of temporal variation, *Earth-Science Rev.*, *166*, 38–52, doi:10.1016/j.earscirev.2016.12.016.

The spelling of the original published manuscript has been adjusted to fit the format of this thesis.

2.1 Introduction

SS is a natural part of river systems. It is the organic and inorganic material carried within the water column (Bridge, 2003; Fryirs and Brierley, 2013). SS plays an essential role in structuring the landscape, creating ecological habitats and transporting nutrients (Dean et al., 2016; Koiter et al., 2013b). Despite being an indispensable part of the river system, SS is also linked to a range of problems related to pollution, ecological degradation, flooding and damage to infrastructure in an increasingly built-up world (Bilotta and Brazier, 2008; Horowitz, 2009; Taylor and Owens, 2009). To develop adequate management strategies, we must be able to quantify SS transport, and link these transport dynamics to drivers both within the channel and the wider catchment in order to accurately predict SS transport in rivers over management relevant timescales (Gao, 2008; García-Ruiz et al., 2015; Taylor and Owens, 2009; Vanmaercke et al., 2011). However, despite decades of research, the spatial and temporal dimensions of the factors and process interactions underlying SS transport in rivers have not yet been fully captured and understood.

On a basic level, sediment transport through a catchment is straightforward. Fine organic and inorganic material erode from land surfaces, flow downhill to a river and are then transported downstream as SS. However, research has increasingly highlighted the stochastic and variable nature of each stage of this basic process (Phillips, 2003). In fact, it is this complexity in the field-catchment-river sediment transfer system that makes estimation of the provenance, transport and deposition of sediment in rivers so challenging (Gao, 2008; Poulenard et al., 2009; Rickson, 2014; Sun et al., 2015; Zhang et al., 2013; Zheng et al., 2012). Currently, we are unable to accurately predict SSCs in rivers over multiple timescales because we lack comprehensive understanding of how different drivers of SS transport interact over space and time.

Previous studies have used concepts such as ‘sediment coupling’, ‘sediment connectivity’, ‘jerky conveyor belt’ and ‘sediment cascade’ to describe the field-catchment-river sediment transfer system, all of which emphasise the variable, non-linear linkages across temporal and spatial scales that eventually determine

SS transport (Bracken et al., 2015; Croke et al., 2013; De Vente et al., 2007; Ferguson, 1981; Fryirs, 2013; Hollister et al., 2008; Koiter et al., 2013a). While these conceptual frameworks have helped researchers to better comprehend the dimensions of the sediment transfer system, important gaps remain in actually linking spatial and temporal scales of SS transport in rivers. A review study on scale independencies in geomorphic systems showed that, when the amount of scales in a system increases, it becomes more difficult to transfer knowledge and relationships from one scale to another (Phillips, 2016). In other words, the challenge lies in formulating conclusions about drivers and processes of SS transport both across spatial and temporal scales.

In this context, we argue that there are two key issues, already identified in previous studies, which need to be addressed in further detail. First, the choice of timescale in many sediment studies limits *a priori* our understanding of the potential explanatory factors driving SS transport (Cao et al., 2007; Dean et al., 2016; Harvey, 2002; Sun et al., 2015; Zhang et al., 2013). In general, studies of SS transport dynamics have focused predominantly at a specific temporal scale, e.g. short-term variations in SSC during flood events (i.e. hourly timescales) (De Girolamo et al., 2015; Fang et al., 2015; Francke et al., 2014) or decadal trends in SSLs (Belmont et al., 2011; Gao et al., 2015; Walling, 2009). As these studies are typically based on data collected at this single temporal scale, it is difficult, if not impossible, to interpret them in terms of processes and drivers over multiple timescales (Harvey, 2002; Zheng et al., 2012). When a river system is considered well or poorly connected (depending on its capacity to transmit the effects of environmental change through the system), the relative importance of drivers for geomorphic change is strongly influenced by different timescales (Harvey, 2002). Therefore, acknowledging the relative importance of these different timescales is essential to better understand and interpret SS transport dynamics.

A second and related issue is that common methods to analyse and quantify SS transport and sources are often applied without consideration of the different timescales at which SS transport occurs. Over the last few decades, a wide range of empirical approaches have been developed and applied, from single sediment

rating curves to complex multivariate analysis techniques (Asselman, 2000; Francke et al., 2014; Onderka et al., 2012; Poulenard et al., 2012). A review study on understanding catchment-scale SS transport showed that the appropriate method for sampling and calculating SSLs in rivers depends on the timescale considered (Gao, 2008). Therefore, it is essential to consider to what degree sediment dynamics (both spatial and temporal) should be captured to match the specific research question of a study (Gao, 2008) and how different methods are able to represent these dynamics (Cao et al., 2007).

This review will build further on these key issues by using previously published literature to highlight the importance of evaluating and interpreting SS transport dynamics over multiple temporal scales in order to elucidate the spatial and temporal process interactions driving these dynamics. The main objectives of the review are to: (i) briefly summarise the main drivers of variation in SS transport in rivers (Section 2); (ii) review the common empirical approaches that are used to analyse and quantify site-specific SS transport and sources, with special focus on the limitations of these methods in terms of capturing temporal variability (Section 3); (iii) apply these findings to recent case studies to illustrate how method and timescale affect the interpretation of SS transport dynamics (Section 4); and finally (iv) synthesise the findings of the review into a set of guidelines for a multi-timescale approach to characterise the sediment regime of a river (Section 5).

In addition to the review on SS monitoring and modelling by Gao (2008), other excellent reviews address different aspects of SS transport, including SS sampling and determining sediment fluxes (Horowitz, 2008); human legacy effects on sediment transport (Wohl, 2015); sediment delivery at the catchment scale (Fryirs, 2013); the influence of SS on water quality and ecology (Bilotta and Brazier, 2008); and sediments in urban river basins (Taylor and Owens, 2009). This review complements these earlier reviews by linking SS transport dynamics to various drivers across timescales. It provides both an up-to-date summary of the major drivers of SS transport in rivers and practical guidance on designing SS transport and sourcing studies, which in combination will aid future research

to better identify, characterise and model the scale-dependent temporal variations in SS transport in rivers.

2.2 Spatiotemporal complexity of suspended sediment transport

The field-catchment-river sediment transfer system is a continuum of erosion, transport and deposition. The amount of SS transport by rivers depends on the interaction of multiple drivers acting on different spatial and temporal scales (Bracken et al., 2015; Fryirs, 2013; Onderka et al., 2012; Poulenard et al., 2012; Rickson, 2014; Sear et al., 2003). In this section, we provide a concise summary of the main processes of fine sediment generation and transport on land (Section 2.1), and the factors driving spatial (Section 2.2) and temporal (Section 2.3) variability in SS transport within rivers. The total SSL in rivers generally consists of SS and bedload. This review focusses on SS, which is the fine-grained fraction of the sediment (generally < 63 µm), transported within the water column of a river. SS is the dominant type of sediment generated within catchments and accounts for approximately 70 percent of the annual sediment delivery by rivers to the oceans (Morgan, 2005).

2.2.1 Sediment generation and transport towards the river

One of the primary sources of SS in rivers is the erosion of soils. Soil erosion occurs in two phases. First, individual soil particles or small aggregates are detached from the 'in-situ' soil, as a result of various processes such as rainfall impact, running water, biological activity, geochemical and physical weathering, freeze-thaw cycling, wind and other processes that disturb the soil. Then the detached soil particles and aggregates are entrained by wind or water flow, which transports them away from their point of origin (Morgan, 2005). Soil erosion is mainly driven by: (i) the erosivity of the eroding agent; (ii) the erodibility of the soil (i.e. the susceptibility of the soil to detachment, entrainment and transport by the eroding agent), as determined by soil properties; (iii) the slope length and steepness of the land (i.e. the topography); and (iv) the nature of the surface cover, including land use and management practices (Morgan, 2005; Renard et

al., 1991). Besides the erosion of soils, sediment can also originate from mass movements (such as landslides), riverbank erosion and/or anthropogenic activities and interventions in the landscape (Fryirs, 2013; Morgan, 2005). Material eroded in the catchment may be transported (e.g. by overland flow or wind) directly to the nearest channel (natural or artificial) or deposited before it reaches the channel, where it may be remobilised by other processes at a later stage (i.e. when the transporting agent is more effective at carrying the sediment). The sequence of transport, deposition and remobilisation has also been described as a sediment cascade (Collins and Walling, 2004; Fryirs, 2013; Harvey, 2002). In the following sections, the spatial and temporal dimensions of the sediment cascade are further discussed.

2.2.2 Spatial variability in suspended sediment transport

SS transport in rivers is determined by the interaction between processes operating at multiple scales (Fryirs, 2013; Harvey, 2002). Therefore we need to understand how SS transport can vary spatially within a catchment and how these variations in turn affect temporal variations. The combination of geological, topographical, pedological, climatic and land cover features of a catchment determines the spatial distribution of soil erosion and sediment transfer that regulate the SSC at any particular point in the river (Figure 2-1). In this section, we briefly discuss how these catchment characteristics affect differences in (i) sediment generation, (ii) sediment transfer and (iii) sediment transport within the river.

First, the SSL of a river is primarily determined by the availability of sediment in the catchment and the transport capacity of the erosive agent. Sediment generation can vary immensely across a river catchment depending on differences in soil susceptibility to erosion, determined primarily by erodibility and land cover. For example, arable and horticultural lands are known to be more prone to soil erosion compared to grassland or forested catchments. The lack of a continuous vegetation cover exposes the soil to erosive agents, and field operations such as tillage disturb the natural structure and strength of the soil, which increases the vulnerability of the soil to erosion (Panagos et al., 2015;

Renard et al., 1991). In addition, surface sealing and crusting due to the redeposition of fine soil particles following erosion, leads to poor water infiltration, increasing the volume and velocity of overland flow and its capacity to erode and transport large quantities of soil particles (García-Ruiz et al., 2015). Contrary to arable areas, forested areas and grasslands generate less sediment because of their permanent vegetation cover, rooting systems and higher infiltration rates, which increase soil cohesion and reduce the risk of generating erosive runoff (De Baets et al., 2008; Ola et al., 2015). Topographical differences within the catchment add to this spatial variability in soil erosion by generating more water runoff (and erosion) on steep slopes compared to gentler gradients and concentrating flow paths at the field scale (e.g. leading to gully formation). Besides sediment originating from natural surfaces such as soils and bedrock, sediment can also originate from anthropogenic sources. Fine particulate material from road construction works, roads, car parks and atmospheric pollution (e.g. from vehicle combustion and industrial sources) as well as other particles originating from anthropogenic activities, are deposited on land. Large expanses of impervious surfaces in urban areas generate higher volumes of overland flow that will transport these particles to artificial drainage networks and rivers (Horowitz, 2009; Rossi et al., 2013; Taylor and Owens, 2009).

Secondly, the amount of sediment reaching the channel depends mainly on the catchment connectivity (Brosinsky et al., 2014a; Sear et al., 2003). Fryirs (2013) developed a conceptual framework, describing catchment connectivity in terms of three different types of linkages (longitudinal, lateral and vertical) and three types of blockages (buffers, barriers and blankets). The linkages represent the relationship between the catchment and the river network, while the blockages disrupt the linkages. The (dis)connectivity of the linkages determines the total SSL in the river. In other words, river catchments can be seen as nested hierarchies wherein subareas are connected to the river system to various degrees. Some areas within the catchment (sometimes of considerable size) can be ignored as sediment source areas because they are poorly connected to the river network, as a result of topographical blockages preventing sediment reaching the river (Fryirs and Brierley, 2013). Therefore, an analysis based only

on total catchment land cover and/or geology and their influence on erosion may overestimate SSLs (Figure 2-1).

Finally, once the fine sediment is delivered to the river, it will either be transported downstream as SS or deposited locally, mostly depending on the grain size of the sediment particles and the energy of the stream flow (i.e. the capacity of the river to transport fine sediments). SS can be deposited as a result of a drop in stream velocity and turbulence that both keep sediment suspended, resulting in a decrease in the capacity of the river to transport SS. Examples are the development of debris fans at a junction of a tributary with a high SS flux and the main river characterised by low stream velocities, or deposition in rivers where the channel morphology suddenly changes causing a drop in velocity (Harvey, 2002).

2.2.3 Temporal variability in suspended sediment transport

In this section, we outline how temporal variability in SS transport at a given location adds to the spatial complexity of SS transport described in Section 2.2 (Fryirs, 2013). The temporal variability in SS transport at a particular point in the river, otherwise called the sediment regime, is determined by the interaction of various catchment-scale drivers (Grove et al., 2015; Thompson et al., 2014), which can be classified into four main, but often strongly interlinked, categories: (i) hydro-meteorological factors (ii) sediment source variations; (iii) natural landscape disturbances; and (iv) human interventions (Figure 2-1).

First, hydro-meteorological conditions are dominant drivers of SS transport processes, both on long and short timescales (Horowitz et al., 2014). Precipitation and subsequent overland flow are the main agents of soil erosion and sediment transport (Perks et al., 2015; Yellen et al., 2014). Therefore, different parameters such as total discharge, peak discharge, water yield, time of rise and fall of hydrograph, total duration of a precipitation event, maximum 30-minute rainfall, mean rainfall intensity and antecedent rainfall are commonly included in models to estimate sediment transfer from the catchment to the river (e.g. Dominic et al., 2015; Duvert et al., 2010; Fang et al., 2015; Onderka et al., 2012; Seeger et al., 2004; Tena et al., 2014). In addition, snowmelt has been shown to be a dominant

driver for SS transport in many parts of the world (e.g. Lana-Renault et al., 2011; Le et al., 2006; López-Tarazón and Batalla, 2014; Praskievicz, 2014). For example, in a small catchment in the subalpine belt of the Central Spanish Pyrenees, discharge and SS transport during a snowmelt period accounted for up to 50% and 60% of the respective annual values, while precipitation during this period only represented 10-13% of the annual precipitation (Lana-Renault et al., 2011).

Second, SS transport will vary as a result of changes in the dominant sediment source(s). Sediment source variations are often the result of interactions between catchment characteristics and hydro-meteorological processes, causing complex feedback mechanisms and threshold behaviour (Onderka et al., 2012). Changes in vegetation cover (e.g. due to crop rotation or natural seasonal variations) can cause a shift in the dominant sediment source to the river (Belmont et al., 2011; Rovira et al., 2015; Sun et al., 2015). Furthermore, erosion hotspots such as gullies can form on fields during storm events, causing an increased contribution of sediment from a specific source. Finally, during individual precipitation events, the sediment supply from a particular source can become exhausted or diluted during persistent high discharges, or other sediment sources might become more connected to the river over time (Fan et al., 2012; Francke et al., 2014; Martínez-Carreras et al., 2010; Poulenard et al., 2012).

Third, large scale natural landscape disturbances such as mass movements and wildfires can have a significant impact on SS supply and transport in rivers over short and long term timescales. Similar to sediment source variations, complex feedback mechanisms are caused by interactions between landscape disturbances and other drivers (Owens et al., 2013). Changes in hillslope and/or river connectivity due to landslides can cause a shift in the dominant sediment source. Furthermore, landslides can either be the result of hydro-meteorological conditions (e.g. induced by typhoons (Chang et al., 2015)) or can induced by other landscape disturbances (e.g. earthquakes (Vanmaercke et al., 2016; Wang et al., 2015)). Likewise, wildfires are often considered as a factor causing an increase in SS transport. However, recent studies show that the effect of wildfires

strongly depends on the specific impact of the fire and often only creates the conditions for increased soil erosion, whereby the specific hydro-meteorological conditions during recovery of the vegetation are mainly driving any changes in SS transport (Owens et al., 2013; Prosser and Williams, 1998).

Finally, SSCs can also be affected by human intervention. Although human intervention can cause short-term variations in SSC (i.e. during road construction works), most of these interventions are manifest in the SSCs and SSLs over extended periods of time, which are called ‘legacy effects’ (Wohl, 2015). Reduction of sediment transport and deposition can occur when there is less sediment input caused by, for example, the construction of dams and reservoirs, changes to the channel dimensions due to flood alleviation schemes or by soil and water conservation measures. Increase in SSLs can result from a greater sediment supply, e.g. as a result of soil erosion due to intensification of land use, mining and mineral exploitation or construction works (Fan et al., 2012; Fuchs et al., 2011; Gao et al., 2015; Mohr et al., 2014; Sun et al., 2015; Zhang et al., 2009).

2.2.4 Conclusions: spatiotemporal complexity of suspended sediment transport

SS transport in rivers is highly non-linear in time and space, and is often characterised by threshold behaviour and feedback mechanisms (Bracken et al., 2015; Onderka et al., 2012). The non-linear nature of soil erosion and transport of sediment at the catchment-scale results in spatiotemporal variations in sediment generation, transfer to the channel and transport through the river network. A point upstream in the catchment may be characterised by entirely different SS dynamics compared to the catchment outlet. These differences are especially marked in catchments with variable erosion rates due to mixed land use (e.g. urban, agriculture, grassland and woodland) or a heterogeneous topography and lithology (Zeiger and Hubbart, 2016). Furthermore, a single point in the river is often characterised by a changing sediment regime over multiple timescales caused by variations in the sediment and/or water supply over time resulting in a sediment deficit or surplus. Due to complex interactions between the different factors driving SS transport, it is often difficult to identify the dominant

driver, especially when considering multiple timescales. To develop frameworks with improved spatiotemporal resolution that specify provenance and changes in SS transport along the sediment cascade (Fryirs, 2013, p. 31), comprehensive understanding is required of the capabilities and limitations of the common approaches to quantify SS transport and sources over multiple timescales.

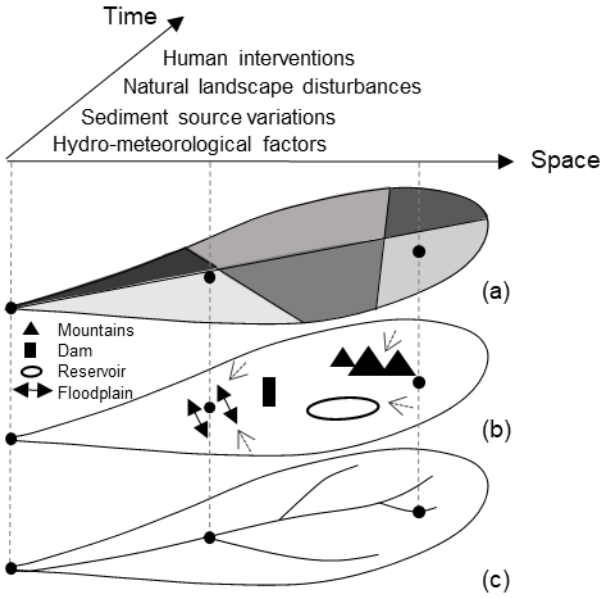

Figure 2-1: Visualisation of the driving factors underlying suspended sediment transport at the catchment-scale. Suspended sediment transport vary: (i) spatially depending on the interactions between (a) catchment characteristics (e.g. geology, land use, climate, topography), (b) catchment connectivity influenced by blockages, and (c) river transport capacity; and (ii) temporally depending on the interaction between hydro-meteorological factors, sediment source variations, natural landscape disturbances and human interventions.

2.3 Empirical approaches to analyse suspended sediment transport and sources

A range of empirical models are used to analyse and quantify SSLs and sources in rivers and evaluate the importance of different drivers (Bilotta et al., 2012; Collins and Walling, 2004; Gao, 2008). While individually these models are useful for expressing SS transport for the process and scale under question, they typically address specific parts of the sediment cascade and are relevant to particular timescales. Therefore the results of different methods are difficult to

interpret in terms of drivers and processes underlying SS transport operating over multiple timescales. In the following section, four main empirical approaches are discussed: (i) sediment rating curves; (ii) hysteresis models; (iii) multivariate data-mining techniques; and (iv) sediment fingerprinting. For each approach, the main limitations and challenges are discussed, with special focus on how each deals with temporal variability in SS transport.

2.3.1 Sediment rating curves

The approach

One of the most commonly used approaches to estimate SSLs over time is to establish a relationship between discharge and SSC, i.e. sediment rating curves. In this approach, discharge is considered a proxy variable that represents the sum of all processes controlling soil (and sediment) erosion and transport to and within the river (Asselman, 2000; Horowitz, 2003). Generally sediment rating curves are represented by a power function of the following form: $S = aQ^b$, where *S* is the SSC (mg/l) and *Q* the river discharge (m^3/s) and a and b are regression coefficients. Sediment rating curves from different rivers demonstrate varying relationships between discharge and SSC over different orders of magnitude, depending on the location, as indicated in Section 2.2 (Figure 2-2). Sediment rating curves are popular because they are fairly simple to construct and they can be established with a discrete and relatively small dataset (Horowitz et al., 2014). In the case where only a few sediment samples are available, turbidity (calibrated with SSC data) can be used as a proxy variable for SSC to develop sediment rating curves (Bilotta and Brazier, 2008; Gao, 2008).

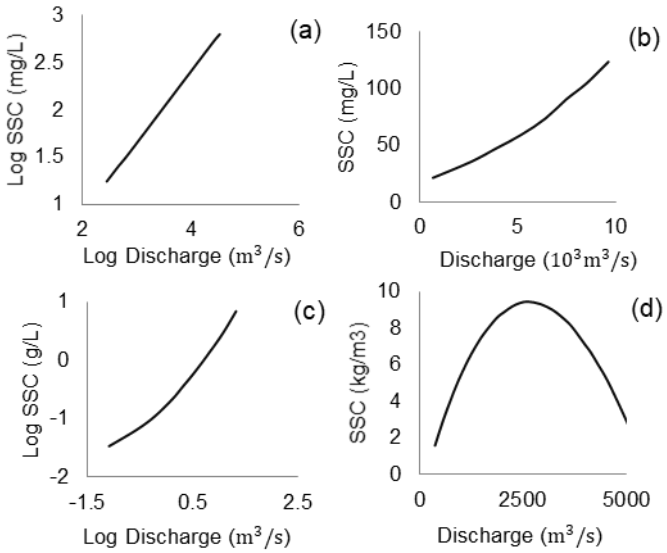

Figure 2-2: Examples of sediment rating curves between suspended sediment concentration (SSC) and discharge for (a) the Broad River, Georgia, USA, using linear regression (modified from Horowitz, 2003), (b) a tributary of the River Rhine, Germany, using nonlinear least squares regression (modified from Asselman, 2000) (c) the Celone River, Italy, using second-order polynomial regression (July 2010-July 2011) (modified from De Girolamo et al., 2015), (d) the Ningxia-Inner Mongolia reaches of the Yellow River using third-order polynomial regression (1969-1986) (modified from Fan et al., 2012)

Accounting for temporal variability

With the sediment rating curve approach, the relationship between SSC and discharge is represented by univariate mathematical formulations. However, univariate relationships do not account for the variable drivers behind SS transport (Dean et al., 2016; Kisi, 2004; Onderka et al., 2012). In other words, the method is not sufficient to explain the scatter around the relationship between SSC and discharge which is caused by the spatiotemporal complexity associated with erosion and sediment transport processes (Asselman, 2000; Horowitz, 2003; Kisi, 2004; Onderka et al., 2012; Smith and Blake, 2014).

Furthermore, the statistical approaches used in sediment rating curves can lead to considerable uncertainties with regards to time. For example, Horowitz (2008) showed that sediment rating curves tend to underestimate high and overestimate low SSCs because high flows are generally less common than low flows, while regression techniques tend to reduce the importance of outliers. Horowitz et al. (2014) evaluated the effects of sample numbers and sampling scheduling on the precision and accuracy of annual SSL estimations based on daily SS data from

monitoring stations in the USA. Their study demonstrates that instead of sampling at fixed points in time, hydrology-based sampling (i.e. sampling during high-flow events) is the most accurate method to estimate annual SSLs with the fewest number of samples. Asselman (2000) showed that rating curves fitted by least squares regression on logarithmically transformed data underestimate long-term sediment transport rates by 10-50%. This is because sediment rating curves do not account for the scatter along the regression line caused by events with high SSCs. Finally, as discussed in Section 2, the relationship between discharge and SSCs is dynamic in nature, depending on the interaction of multiple drivers across timescales (Horowitz 2008; Tena et al. 2014). These findings imply that previously established sediment rating curves may not be representative when major changes in the river and/or catchment characteristics occur, such as the construction of dams or changes in land cover. Sediment rating curves need to be updated regularly and interpreted with caution when estimating annual SSLs. Furthermore, they are only valid for a particular timescale, depending on the data used to construct the rating curve (Bezak et al., 2016; De Girolamo et al., 2015; Francke et al., 2014; Horowitz, 2008).

Methodological challenges

Although they are the most commonly used method to estimate SSLs at a specific location, sediment rating curves have some methodological limitations. An appropriate regression model needs to be chosen and fitted to the data. There is no consensus as to the most appropriate regression technique and the final choice mostly depends on the observed data. Most common methods are linear least squares regressions performed on log-transformed data (Figure 2-2 a). Several studies have developed alternative approaches to construct sediment rating curves such as nonlinear least squares regression (Asselman, 2000) (Figure 2-2 b-d) and generalised linear models (Cox et al., 2008). Furthermore, other studies subdivide calibration data into groups related to seasonality, hydrology or flood limbs to improve the outputs (Eder et al., 2010; Fang et al., 2015). As a result, studies are highly inconsistent (and difficult to interpret) in terms of the relationship between discharge and sediment dynamics (Sun et al., 2015).

2.3.2 Hysteresis models

The approach

Various interactions at the catchment scale between factors described in Section 2 often result in hysteresis patterns between SSC and discharge, as represented in the sediment rating curve (e.g. Duvert et al., 2010; Lloyd et al., 2016; Sun et al., 2015; Tananaev, 2015). The most common patterns are anti-clockwise and clock-wise loops (Figure 2-3) (Horowitz et al., 2014; Williams, 1989). More complex hysteresis patterns have also been observed, such as a single line plus a loop and figure-eight patterns (Sun et al., 2015). The analysis of hysteresis patterns can provide useful insights into the presence of feedback mechanisms and thresholds determining SS transport (Eder et al., 2010; Krueger et al., 2009). While hysteresis patterns are commonly used to express SS dynamics at the event-based scale, they can also be used to visualise seasonal variations in the relationship between SSC and discharge (Sun et al., 2015).

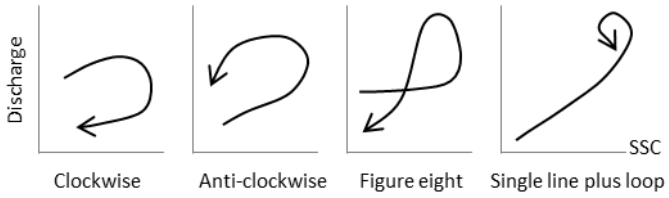

Figure 2-3: Hysteresis patterns between discharge and suspended sediment concentration (SSC)

Accounting for temporal variability

Hysteresis patterns express the temporal variability in SSC and emphasise the context-specificity of the observed processes. Krueger et al. (2009) developed empirical models of sediment event dynamics from observations at high temporal resolution in a drained and undrained, intensive grassland, field-scale experiment. Instead of a simple power law (as in the sediment ratings curve technique), an additional factor is added to account for the rate of change of river discharge: $S = aQ^b + c\ dQ/dt$, where S is the SSC, Q the river discharge and dQ/dt is the slope of the hydrograph. Their results showed that the model performed well in simulating small hysteresis loops, but could not account for the

exhaustion of sediment sources due to the variability in sediment transport dynamics (Krueger et al., 2009). Eder et al. (2010) tested four methods to calculate instantaneous SSC in an agricultural catchment in Austria. They conclude that both general rating curves and event-specific rating curves result in considerable scatter for event specific SSCs and total SSLs. The inclusion of parameters related to the rate of change of the discharge to account for hysteresis effects, resulted in improved estimations with 0-1% deviation from the measured SSCs. However, the model proved to be unsuitable for high numbers of data points and for complex hysteresis patterns comprising multiple discharge and sediment peaks (Eder et al., 2010).

Methodological challenges

The main challenge related to the analysis of hysteresis patterns is their interpretation, which is strongly context driven and not straightforward (i.e. two similar hysteresis patterns can be the result of the interaction of different drivers or different timescales) (Fan et al., 2012; Smith and Blake, 2014; Smith and Dragovich, 2009). To address these issues, Smith and Dragovich (2009) developed a quantitative method to compare hysteresis patterns between nested catchments (i.e. sub-catchment versus entire catchment). The aim was to facilitate the interpretation of these patterns in terms of erosion and sediment transport processes across spatial scales. It was reasoned that similarity in response to particular rainfall and flow events might reflect spatial uniformity in the observed hysteresis patterns and the corresponding erosion processes and/or proportional sediment source contributions. Towards this end, a dimensionless ‘similarity function’ was developed, based on individual line lengths and angles formed between SSCs and discharge data for each sampling time (Smith and Dragovich, 2009). Similarity in hysteresis patterns seemed to reflect uniform rainfall patterns, resulting in erosion and transport processes occurring both at the sub-catchment and catchment scale. In addition, the similarity function could also reflect consistency in the dominant sediment sources (Smith and Dragovich, 2009). Contrarily, small, local events appeared to result in less or no similarity between hysteresis patterns, indicating less uniformity in erosion and transport processes. Despite the possibilities this

approach offers, its applicability is spatially limited due to strong variability in the dominant erosion and transport processes and thus variations in sediment sources (Smith and Dragovich, 2009).

2.3.3 Multivariate data-mining techniques

The approach

The heterogeneity of sediment transport processes in time and space require other methods besides sediment rating curves and hysteresis models to represent SS dynamics and to identify the main factors controlling them (Francke et al., 2014; Onderka et al., 2012). The increasing volume of environmental data has created opportunities to develop alternative approaches based on data-mining techniques to estimate SSCs at a high temporal resolution. Data-mining techniques in this context represent a range of multivariate data-analysis methods to establish relationships between SSCs and a set of variables. For example, quantile regression forests (Francke et al., 2008; Zimmermann et al., 2012), fuzzy logic (Kisi, 2005; Lohani et al., 2007), M5′ model trees (Onderka et al., 2012), artificial neural networks (Cobaner et al., 2009), and Stepwise Multiple Discriminant Analysis (MDA) (Bilotta et al., 2012) have all been used successfully to estimate SSCs in various contexts. Other studies have performed more simple correlation matrices and principal component analyses (PCA) to examine the importance of different drivers that regulate SS transport (e.g. Dominic et al., 2015; Perks et al., 2015; Seeger et al., 2004; Tena et al., 2014).

Accounting for temporal variability

Over the last decade, a range of different studies have demonstrated the capability of data-mining techniques to account for the temporal variability in SSCs and SSLs, including the importance of multiple drivers of the processes involved. Numerous examples indicate that SS transport is often strongly driven by a set of catchment-specific drivers. For example, a data-driven model based on Quantile Regression Forests to estimate monthly SSLs was developed by Francke et al. (2014) for the Isabena catchment in Spain. The model included factors such as the rate of change of discharge, rainfall energy and the day of the year to account for sediment supply variations and antecedent conditions. Their

results demonstrate that the variables with the most predictive power depend on the time and location, indicating the importance of local processes. Onderka et al. (2012) developed a modular data-driven model (M5' model trees) to simulate intra-event SSCs in response to a range of controlling variables in a headwater catchment in Luxembourg. Hydro-meteorological variables were included in the model, as identified in Section 2.2, which defined conditions prior to and during events. Their results show that antecedent hydro-meteorological conditions are the main drivers for the amount of SS during storm events (Onderka et al., 2012). Grove et al (2015) used an MDA model based on a set of hydro-meteorological and catchment variables to predict mean annual SSCs based on 15 minute turbidity data collected over two years for ten reference-condition stream/river sites. They found that the mean annual SSCs was significantly different for all the sites between the two observed years, and that this variability could be predicted reasonably well using the MDA model. Perks et al. (2015) performed a factor analysis on a range of environmental variables representing the fluvial and wider catchment conditions prior to, and during, hydrological events for grassland dominated headwater catchments. Their results also show that complex hysteresis patterns are mainly driven by antecedent hydro-meteorological conditions. Zeiger and Hubbart (2016) performed multiple linear regression analyses on a four-year SS dataset in Hinkson Creek Watershed in the Lower Missouri Mississippi River Basin, USA. They conclude that annual SSLs are significantly correlated with total annual precipitation, but also with land use (Zeiger and Hubbart, 2016). Finally, Cobaner et al. (2009) used neuro-fuzzy computing techniques and artificial neural networks to predict SSCs in the River Mad catchment, USA. Similar to the conclusions in other studies, their study demonstrates that data-driven models containing hydro-meteorological data perform better in predicting SSCs compared to sediment rating curves.

Methodological challenges

The main limitation towards extensive use of data-mining techniques in the context of SS transport is the availability of sufficiently large (continuous) datasets of SSCs and other variables, over multiple timescales. Continuous sediment data (as well as data on catchment-scale variables that drive SS transport) in time and

space are often scarce and collected with a range of different methods, that may not be comparable or consistent (Kettner et al., 2007; Rovira et al., 2015; Vanmaercke et al., 2011). Furthermore, large datasets require the use of complex data management techniques and advanced computational skills. As a result, many computational techniques tend to be 'black-box' in approach, which makes them less transparent and flexible compared to simple sediment rating curves (Kisi, 2004).

2.3.4 Sediment fingerprinting

The approach

A final empirical approach to gain insights into SS dynamics is to compare temporal variations in sediment source contributions to the total SSL in the river (Brosinsky et al., 2014b; Carter et al., 2003; Cooper et al., 2014a; Fang et al., 2015; Poulenard et al., 2009). Fryirs (2013) noted that information on the preferential delivery of certain sources of sediment and the loss of other sources should be taken into account when assessing sediment delivery within a catchment, because sediment sources may vary between and during high flow events. Knowledge of sediment source variations can provide the necessary information to formulate more conclusive statements about factors driving the variations in SS transport. One approach to retrieve this kind of information is by sediment fingerprinting.

Generally, the interactions between geology, climate, hydrology, land cover, weathering processes and anthropogenic activities define the composition of soil and sediment (Koiter et al., 2013b). Sediment from a particular source can therefore be characterised by a "fingerprint", i.e. a combination of biogeochemical and/or physically-based properties specific to their origin within the river catchment. It is assumed that these properties behave conservatively (meaning that they do not change with time) and thus allow a direct comparison between the primary source material and the SS (Koiter et al., 2013b; Walling, 2013). The fingerprints are used to develop statistical models to estimate the relative contributions of sediment sources to the SS (Davis et al., 2009; Walling, 2013).

Accounting for temporal variability

Since the 1970s, sediment fingerprinting has been successfully applied as a tool to gain insights into sediment dynamics at a river basin scale in catchments all over the world (Mukundan et al., 2012). Despite its widespread use, most studies report the dominant sediment source, but do not consider possible source variations over time (e.g. Vale et al., 2016). However, recent sediment fingerprinting studies have demonstrated significant variations in sediment sources on a decadal scale (e.g. Belmont et al., 2011; Chen et al., 2016) and during individual events (e.g. Cooper et al., 2014a; Evrard et al., 2013; Poulenard et al., 2012). Therefore, applying sediment fingerprinting on multiple timescales can provide information on possible variations and shifts in the dominant sediment source over short to long term timescales, which can help to better understand the interactions between the factors underlying SS transport.

Methodological challenges

When applying sediment fingerprinting to provide insights into the spatial and temporal complexities of SS transport, there are three major challenges. The first one is accounting for sediment pathways from source to sink. As indicated in Section 2, materials can be eroded and subsequently deposited before they finally reach the river (Cooper et al., 2014a; Vale et al., 2016). In sediment fingerprinting, only the primary sediment source is identified, without providing information about sediment transport rates and the complexity of the pathways (i.e. locations and duration of intermediate sediment storage in the catchment and in the river) (Cooper et al., 2014a; Koiter et al., 2013b; Poulenard et al., 2009). This problem is clearly illustrated by a hydromorphological assessment study of the River Frome (UK) (Grabowski and Gurnell, 2016). Previous studies showed that erosion from agriculture was the dominant sediment source in the River Frome, while changes in the river planform over time suggest that this contribution could be dated back to the post-WWII agricultural expansion in the UK. While the use of fallout radionuclides in sediment fingerprinting has helped to assess the time passed since the sediment eroded (residence time) (e.g. Palazón et al., 2015; Smith and Blake, 2014; Wilkinson et al., 2015), it remains

a challenge to interpret patterns in sediment source contributions in terms of catchment erosion processes.

Second, some geochemical sediment properties (even though considered conservative) significantly change as a result of variability in particle size distribution and organic matter content, as well as biological, geochemical and physical transformations over multiple scales during sediment generation and transport in the catchment and in the river (Koiter et al., 2013b; Smith and Blake, 2014). Therefore, caution needs to be taken when identifying the sources of sediment based on geochemical properties.

Finally, traditional sediment fingerprinting approaches based on geochemical analysis techniques are very time- and cost-consuming, limiting the use of the technique at a high temporal resolution (Brosinsky et al., 2014a; Cooper et al., 2014a; Poulenard et al., 2012). Recently, studies have demonstrated the promise of spectral reflectance-based (visible and (near) infrared) fingerprinting methods as a quicker and less costly alternative for sediment source apportionment, with considerable potential to expand the temporal resolution of sediment fingerprinting analyses during high-flow events (e.g. Cooper et al., 2014a, 2014b; Evrard et al., 2013; Martínez-Carreras et al., 2010; Poulenard et al., 2009; Tiecher et al., 2015).

2.3.5 Conclusions: analysing and quantifying suspended sediment transport over multiple timescales

Different empirical methods exist to analyse and quantify sediment sources and SS transport dynamics over multiple timescales, ranging from simple sediment rating curves to more complex approaches that can assess the relative importance of various drivers. In summary, sediment rating curves are an appropriate method to provide a first explorative characterisation of the sediment regime of a river (i.e. to estimate SSLs over a certain period), but they are not sufficient to capture the temporal variation caused by the interactions of drivers and feedback mechanisms. By including additional catchment-scale variables, multivariate methods are better able to represent the multiple interactions between hydrological and geomorphological processes that drive temporal

variation in SS transport, especially at short to medium timescales (i.e. individual high flow events to seasonal). Sediment fingerprinting is a complementary method to provide information on sediment source variations over multiple timescales. However, given the high spatiotemporal complexity of SS dynamics, interpretation of the results of different methods in terms of drivers over multiple timescales and the selection of appropriate methods remains challenging.

2.4 Interpretation of suspended sediment transport dynamics

While a wide range of empirical techniques have been used to analyse and quantify SSCs and SSLs, the majority of studies have applied these techniques to a single timescale, generating a snapshot of sediment transport with which they deduce variations in the drivers of SS transport. The problem is that the quantification of SSCs and SSLs and their variability over time is dependent on the scale at which the system is studied (Horowitz et al., 2014). If data are collected at a resolution appropriate for analysis for a single timescale, it limits *a priori* the potential to identify the explanatory factors driving SS transport (Cao et al., 2007; Sun et al., 2015; Zheng et al., 2012). While this is not a problem if the study is interested in a single timescale (for example, land cover change at a decadal scale and the resultant changes in SSLs), it makes it difficult to investigate the process interactions and feedbacks between different drivers across timescales. A lack of understanding of these drivers and interactions makes the accurate prediction of SSCs or SSLs at management-relevant timescales an impossible goal at present (Cao et al., 2007; Harvey, 2002). To illustrate how timescale could affect our understanding of processes, examples of SS transport studies from around the world are presented and their results interpreted at three different timescales in this section (Figure 2-4). Furthermore, we demonstrate how the combination of different methods presented in Section 3 provides better insights into multiple drivers of SS transport and their mutual interactions.

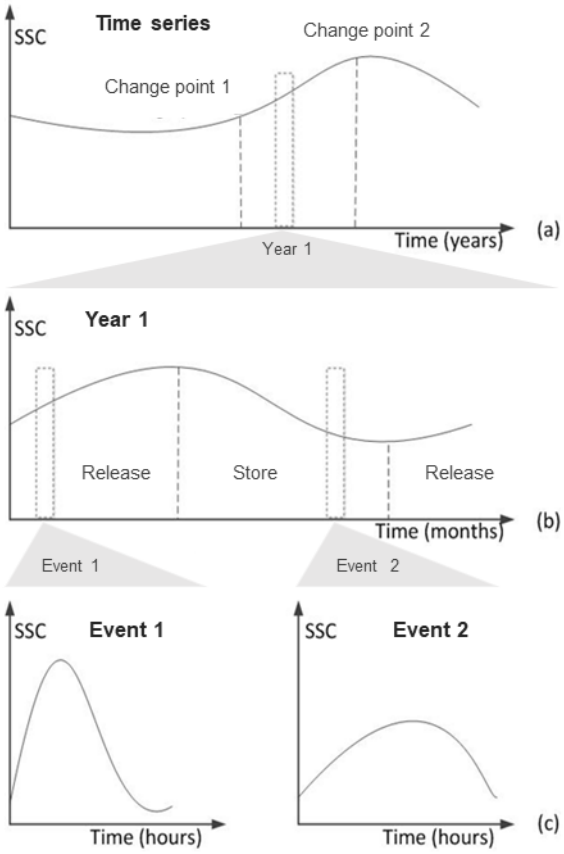

Figure 2-4: Temporal scales of suspended sediment concentration (SSC) in rivers; (a) inter-annual: indicating change points and/or trends defined as a result of drastic changes in one or more of the drivers, (b) seasonal: indicating the capacity of the catchment to store sediments, and (c) event-based dynamics: indicating the impact of individual events and feedback mechanisms.

2.4.1 Inter-annual variation

SSLs vary over long timescales (i.e. decades and centuries) due to natural and anthropogenic forces. Long term SS dynamics can therefore indicate change points and/or trends in water and/or sediment supply in the catchment. Change points are abrupt alterations in the sediment regime caused by drastic changes in one or more of the drivers that affect sediment production and transport (Huang et al., 2013; Wohl, 2015). Therefore, assessing long-term sediment regime alterations not only provides insights into the impact of climatic changes on discharge and corresponding SSLs, but also into the impact of human interventions (Fan et al., 2012; Francke et al., 2008; Horowitz, 2008; Smith and Blake, 2014; Stone et al., 2015; Sun et al., 2015).

Drivers

As discussed in Section 2.2, hydro-meteorological factors such as rainfall and river discharge are major drivers of SS transport. Over long timescales, discharge or water yield (i.e. amount of water per unit of time) is often a good predictor of mean SSLs (Horowitz, 2008; Rovira et al., 2015). Changes in rainfall patterns and amounts (e.g. as associated with climate change) can cause significant changes in long-term SSLs (Kettner et al., 2007; Rovira et al., 2015; Walling, 2009). Furthermore, a shift in sediment source(s) can cause variable SSLs under similar (constant) hydro-meteorological conditions. Land cover changes (e.g. conversion of forested land to arable agriculture) and catchment connectivity changes (e.g. as a result of tectonic activity or mass movements) can cause a (permanent) shift in the sediment supply (Bracken et al., 2015; Foerster et al., 2014; Fryirs, 2013). In addition, human interventions along the river network such as dam construction, flood alleviation schemes and soil and water conservation techniques can cause long-term legacy effects on the sediment supply to the river and/or the sediment transport capacity of the river (Chen et al., 2016; Rovira et al., 2015; Sun et al., 2015; Verstraeten et al., 2002; Wohl, 2015).

Interpretation

The impact of dam construction on SS transport has been well documented for several rivers, and provides a good example of legacy effects on long-term patterns. For example, Huang et al. (2013) assessed alterations in the SSL in the upper Yangtze River in China between 1950 and 2008. Two change points were identified in 1986 and 2003 (Figure 2-5 a). The decrease in the SSL after 1986 was attributed to a set of dams constructed in the tributaries and the Gezhouba Dam in the main river, upstream of the monitoring site. In addition, land cover changes may have played a contributing role in changing the sediment regime, as grassland areas increased to cover more than 50% of the catchment. The further decrease in SSL after 2003 was mainly attributed to the construction of the Three Gorges Reservoir, which traps large amounts of sediment in the reservoir (Huang et al., 2013). Similarly, Fan et al. (2012) showed that dam construction along the Ningxia-Inner Mongolia reaches of the Upper Yellow River

played an important role in the long-term decrease in SSCs between 1952 and 1968.

However, clear trends and/or change points are not always present, especially when different factors operate simultaneously, and the interpretation of the observed patterns becomes less straightforward. Sun et al. (2015) analysed SS dynamics in the Loushui River in South-Central China from 1966 to 1985 and 2007 to 2011. They found that the SS-discharge relationship changed considerably between decades, with no clear change points or trends (Figure 2-5 b). Instead, four stages were identified with a sharp rise in SSL between 1966 and 1970, a slow decrease in 1971-1978, a strong increase in 1979-1985 and again a decrease after 2007. No overall explanation was given, but the change was attributed to climate (rainfall pattern and intensity) and human interventions (mining, forest cutting and road construction works). A case where the effect of dam construction on the SSL is muted by other factors is given by Geeraert et al. (2015) for the Tana River (Kenya). Analysis of monitored SS data in combination with historical data suggests that upland dam construction in the 1960s and 1980s decreased the SSCs just downstream of the dams, but did not greatly affect the annual SSL in the lower Tana River. The authors hypothesise that autogenic processes, namely river bed dynamics and bank erosion downstream of the dams, mobilise large quantities of sediment stored in the alluvial plain, and thus overwhelm any possible changes caused by the dams in the lower reaches of the river (Geeraert et al., 2015).

In the previous examples, water yields and other hydro-meteorological variables are not always sufficient to explain the variation in SS transport. Additional information about the impact of different drivers is required to interpret the observed patterns correctly. One way of obtaining more information is by sediment fingerprinting as discussed in Section 3.4. Chen et al. (2016) used composite geochemical sediment fingerprinting to assess the impact of land use changes in the Green-for-Green Project in the Loess Plateau of China, a nationwide conservation program launched in 1999 involving reforestation to reduce soil erosion in cropland. Their results, based on deposited sediment

cores, showed that as the planted forest matured with time, the sediment contribution from those catchments steadily decreased. The gradual shift is attributed to changes in soil characteristics and surface hydrological response over time; the previously cultivated soils have developed vertical structure that facilitates infiltration and have become covered by several layers of leaves, protecting the soil against erosion (Chen et al., 2016). Another study by Belmont et al. (2011) used sediment fingerprinting (based on radiogenic tracers) and geomorphic change detection techniques to characterise the sediment regime in Lake Pepin on the Mississippi River over the previous 150 years. Other studies in the area have shown that the sediment supply increased 10-fold during this period, but the combination of approaches used in Belmont et al.'s study allowed the authors to identify the drivers that are likely to be responsible for this increase. The sediment fingerprinting analysis indicated that the dominant sediment source shifted from agricultural soil erosion to erosion of stream banks, and the geomorphic analysis linked the accelerated erosion of streambanks to a combination of changes in precipitation and large scale changes to the drainage network (e.g. installation of agricultural ditches and subsurface tile drains) (Belmont et al., 2011). In addition, by analysing sediment cores of deposited sediment, historic SS yields can be reconstructed and combined with sediment fingerprinting to assess the impact of different drivers. Walling et al. (2003) used sediment cores from small lakes and reservoirs to reconstruct SS yields and sources in the catchments of the Rivers Ouse and Tweed in the UK over the last 100-150 years. Their findings suggest that there was considerable temporal variability in the SSL throughout this period. The reconstructed SSL and sources were explained by major changes in land use and management (e.g. afforestation, conversion from pasture to arable), and the changes did not show a significant correlation with climate change (Walling et al., 2003). Similarly, a study from the Waipaoa River system in New Zealand used sediment cores in combination with a hydrological model to construct SS transport during the last 3000 years. The study shows that historic land use changes had a profound impact on the SSL in the rivers, inducing a permanent shift in the sediment

regime, while the climatic impact was more muted and restricted to individual events (Kettner et al., 2007).

In conclusion, long-term observations are essential to demonstrate the interactions between the catchment and the river (Gao et al., 2013). Long term data on SSLs can indicate change points and/or trends within the catchment. However, the interpretation of the patterns is not straightforward and requires additional information such as sediment source contributions and insights into the interactions of drivers to make definitive conclusions about the dominant factors driving SS transport on the long term.

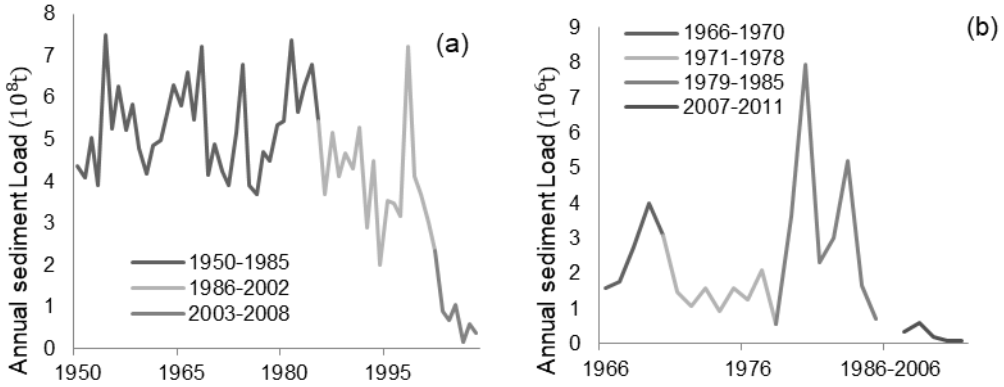

Figure 2-5: Annual sediment loads indicating (a) three change points in the upper Yangtze River, China (modified from Huang et al., 2013) and (b) more complex patterns in the Loushui River, China (modified from Sun et al., 2015)

2.4.2 Seasonal variation

In most regions of the world, SSLs vary significantly throughout the year. This variability is often related to seasonal patterns in rainfall, snowmelt and storm events, but precipitation events of similar magnitudes during different times of the year can also result in different sediment-discharge relationships, suggesting a more complex set of drivers and interactions (Lloyd et al., 2016). Therefore, understanding the behaviour of the catchment in terms of sediment generation and storage is crucial to assess the annual cycling of SS transport, which is especially important for the development of targeted soil and water conservation strategies.

Drivers

As discussed in Section 2, interactions between land use, rainfall patterns, soil moisture and hydrology cause variations in SS transport. Especially on a seasonal scale, changes in rainfall and hydrology across the year often cause marked variations in SS transport in rivers, for which the impact is often magnified by land cover changes in both natural (e.g. loss of leaf cover in a deciduous forest during winter) and agricultural systems (e.g. bare soil due to cropping patterns). For example in the lower Ebro River in Spain, a Pearson correlation matrix and PCA was performed on different variables to explain SS dynamics during flushing flows (i.e. controlled water releases). The results showed that the dominant drivers considerably varied according to season and the location within the catchment (Tena et al., 2014). Furthermore, in (sub)tropical catchments, there is often a marked difference between factors controlling SS transport in the dry seasons compared to the wet seasons (Dominic et al., 2015; Franz et al., 2014; Omengo et al., 2016). A PCA applied in two tropical sub-catchments of the Klang River (Malaysia) shows that total rainfall and rainfall intensity are strongly related to SS hysteresis patterns in the dry season, while soil moisture plays a more important role in determining SS hysteresis patterns during the wet season (Dominic et al., 2015). Finally, episodic events on a seasonal basis such as snowmelt are also important in causing variation in SS transport (Lana-Renault et al., 2011).

Interpretation

The interactions between drivers result in different patterns in SS transport, which have been visualised in changing hysteresis patterns over the course of the year. For example, Alexandrov et al. (2007) studied SSCs during flood events between 1991 and 2001 in the semi-arid northern Negev, Israel. The authors demonstrated that high intensity, convective rain storms during autumn and spring flush out sediment within the channel at the start of the event, resulting in clockwise hysteresis patterns. On the other hand, frontal storms common in winter generally produce anti-clockwise or no hysteresis patterns, with no signs of sediment flushing.

Besides different responses during individual events across the year, larger seasonal patterns in SS transport can also be observed that provide better insights into the cycling of sediment production and transport. Sun et al. (2015) showed that SSLs in the Loushui River in China are highest in summer, indicating that sediment produced by erosion, weathering and human activities is stored during the dry winter and spring, while the sediment is released during the summer and early autumn floods (Figure 2-6 a-b). A reverse pattern was demonstrated by another study on the Ebro River in Spain. It showed a clockwise loop in the SSLs at the seasonal scale, which demonstrates the flushing of sediment during the wetter months in autumn and the progressive exhaustion of the sediment supply within the catchment throughout the winter until the SSL is very low during the drier summer (Rovira et al., 2015) (Figure 2-6 a-c). Similar conclusions were drawn from a study by Park and Latrubesse (2014) who used field measurements of SSCs in the Amazon River to calibrate MODIS data to model SS distribution patterns over space and time. The results of this study showed clear seasonal variability in SSCs in the main channel, with low SSCs during the peak to falling water stages (May to October) and high SSCs during the first half of the rainy season (Park and Latrubesse, 2014).

These findings can also be supported by the results of sediment fingerprinting studies. For example, a fingerprinting study based on fallout radionuclides performed in an agricultural catchment in Wisconsin (USA) by Huisman et al. (2013) revealed that upland areas were the dominant source of SS, whereby the SS during spring was found to be generated (eroded) more recently prior to mobilisation compared to SS in the wetter autumn months. These results indicate the relative importance of bed sediment remobilisation during periods when rainfall and discharges are higher (Huisman et al., 2013).

The above examples suggest that seasonal SSLs are an indication of the presence of store-release processes within the catchment, i.e. periods when sediment is produced due to weathering and erosion, and stored within the catchment, and periods when this sediment is then transported towards and within the river (Harvey, 2002; Sun et al., 2015). These conclusions provide a

clear illustration of the interactions of drivers discussed in Section 2. Insights into seasonal SS dynamics are useful to assess the connectivity of the catchment and the capacity of the catchment to store sediments at different times of the year, which are both essential to develop adequate soil and water conservation strategies.

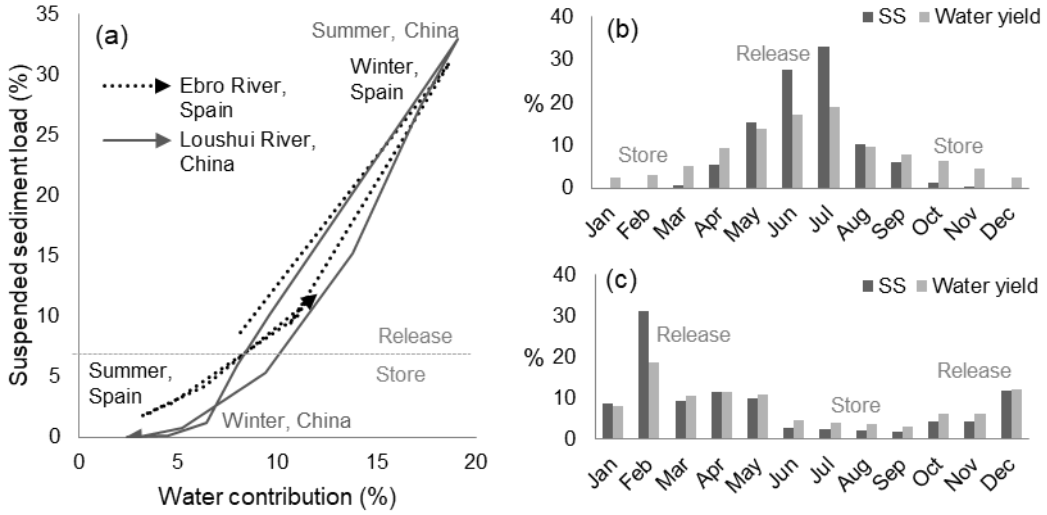

Figure 2-6: (a) Seasonal variation in suspended sediment and water contributions to the annual loads illustrating a phase of sediment build-up (storage) and a subsequent sediment release-phase for (b) the Loushui River in South-Central China (1966-2011) (modified from Sun et al., 2015); and (c) the Ebro River in Spain (modified from Rovira et al., 2015).

2.4.3 Event-based variation

In most cases, the sediment regime of a river is not characterised by a constant sediment supply, but rather by the episodic occurrence of rainfall events and/or snowmelt and subsequent high river flows. High-flow events generate a large proportion of the total annual SSL in rivers (Fang et al., 2015; Horowitz, 2009; Lloyd et al., 2016; Pulley et al., 2015). Consequently, disentangling the factors that drive event-based SS dynamics is essential to improve our understanding of longer term SS trends, the importance of episodic events on those trends, and the impact of SS on ecology, geomorphology and infrastructure.

Drivers

During a single rainfall event, there is considerable variation in SSCs in the river, and these variations have been associated with numerous drivers (Lloyd et al., 2016; Smith and Blake, 2014). Compared to long-term patterns in SS transport, more specific hydro-meteorological factors need to be taken into account to explain the variations in SS transport during events. In recent data-mining studies, a range of variables have been identified which represent changes in rainfall impact and soil characteristics (e.g. soil moisture), including antecedent rainfall, duration of the rainfall event, maximum rainfall over 30-minutes, mean rainfall intensity of the event, time of rise and fall of the hydrograph, runoff duration, peak discharge and total runoff (e.g. Dominic et al., 2015; Duvert et al., 2010; Fang et al., 2015; Perks et al., 2015; Seeger et al., 2004; Tena et al., 2014). Furthermore, the succession of multiple rainfall events has proved to be a good explaining factor for SSCs (Onderka et al., 2012; Perks et al., 2015).

In addition, sediment sources can also change over short timescales. Persistent high discharge in the river can for example cause banks to collapse, resulting in a sudden increase in sediment supply (Carter et al., 2003; De Girolamo et al., 2015; Onderka et al., 2012; Yellen et al., 2014). Sudden connectivity changes within the catchment (e.g. by landslides or gully formation) can act both as a blockage to sediment movement or as an additional sediment source. Contrarily, SSCs in the river can also decrease during an event when the sediment supply gets exhausted or when dilution occurs as a result of persistent high river discharges (Bracken et al., 2015; Croke et al., 2013; Fryirs, 2013). Finally, human activities can also have an impact on the SSCs during events, especially in urban areas. For example, it is argued that street sweeping or reducing air pollution can limit the contribution of street dust to the SSL in urban rivers (Marsalek and Viklander, 2010; Selbig et al., 2013; Taylor and Owens, 2009). However, little is known about the actual pathways of urban sediments to streams and the effect of mitigation strategies such as the frequency of street sweeping (Taylor and Owens, 2009).

Interpretation

Patterns in event-based SS transport are extremely difficult to interpret because of feedback mechanisms and interactions between multiple drivers. In general, clockwise hysteresis patterns are attributed to a fast response system (short distances between sediment source and receptor), because the peak in SSCs typically precedes the maximum discharge of the event. Fast response systems are characterised by rapid sediment flushing and depletion in the river network, because of a limited supply of readily-available material for transport (De Girolamo et al., 2015; Fan et al., 2012; Fang et al., 2015; Francke et al., 2014; Sun et al., 2015; Tena et al., 2014). In contrast, anti-clockwise hysteresis patterns, in which the increase in SSC is delayed, are typically explained by sediment being supplied from more distant sources (associated with extended travel times), channel bed erosion or prolonged erosion processes during extended storm events (De Girolamo et al., 2015; Fan et al., 2012; Fang et al., 2015; Francke et al., 2014; Sun et al., 2015; Tena et al., 2014). However, these general conclusions are by no means uniformly agreed upon.

Lag times between peak SSCs and discharge have also been explained by spatial differences in rainfall pattern and intensity within the catchment (Poulenard et al., 2012; Smith and Blake, 2014; Sun et al., 2015). High intensity events and corresponding runoff generation generally lead to a rapid increase in SSC (clockwise hysteresis patterns), while prolonged events result in the supply of more distant sources (anti-clockwise patterns) (De Girolamo et al., 2015). Furthermore, clockwise patterns have also been attributed to rainfall of long duration and low intensity, high total runoff and high initial soil moisture. In the latter case, the event is characterised by a first flush of nearby sediment sources, but then rainfall causes an increasing area of the catchment to contribute to the total SSL, while nearby sources are exhausted (Eder et al., 2010).

The interaction of drivers and the importance of antecedent conditions becomes apparent when attempting to explain SSCs during events with more complex hysteresis patterns (Fan et al., 2012; Francke et al., 2014; Onderka et al., 2012; Poulenard et al., 2012; Smith and Blake, 2014; Sun et al., 2015; Tena et al.,

2014). For example, a figure-eight pattern characterised by a clockwise loop at high discharges and an anti-clockwise loop at low discharges indicates that the SSC continues to be high after an initial drop, while the discharge decreases. This type of pattern has been attributed to a second pulse of sediment input caused by, for example, bank failure or river bed erosion (Fan et al., 2012). A pattern defined by an anti-clockwise loop at high discharges and a clockwise loop at low discharges means that the SSC decreases strongly when discharge decreases. Possible explanations for this pattern are (i) sediment exhaustion, (ii) delayed contribution of a sub-catchment (due to initial poor connectivity for example), (iii) storage in small basins and their subsequent connection after filling, or (iv) overbank flooding resulting in a drop of the streamflow velocity which causes a decrease of flow transport capacity (Eder et al., 2010; Fan et al., 2012). Patterns that consist of multiple figure-eight loops are usually caused by the succession of different events and peak flows.

The above examples illustrate that hysteresis patterns can be interpreted differently depending on the spatial and temporal scale and context. Therefore other information must be included to make more conclusive statements about the drivers of SS transport (Smith and Dragovich, 2009). Poulenard et al. (2012) used an infrared-based (Diffuse Reflectance Infrared Fourier Transform, DRIFTS) sediment fingerprinting technique to identify sediment contributions from three geological zones characterised by black marls, marly-limestone and molasses, during flood events in a mountainous catchment in the Southern French Alps. During a flood with an anti-clockwise hysteresis pattern recorded in August 2008, they found that black marls were the dominant source of the first sediment flush, while marly-limestones were the main supply of sediment during the peak discharge (Figure 2-7 a). These results were explained by the vicinity and high erodibility of the black marls and the distance of marly-limestone sources from the sampling point. However, an earlier anti-clockwise event in November 2007 had a different cause. In this event, molasses sediment was more dominant during the first stage of the event (Figure 2-7), even though it was the most distant sediment source in the catchment. The authors argue that this

material originated from sediment deposited on the riverbed, and which was resuspended during the first flush (Poulenard et al., 2012).

These different explanations for event-based SS patterns can be linked back to the findings in Section 4.2, and the seasonal differences in the amount of material available for mobilisation. A sediment fingerprinting study (based on visible diffuse reflectance spectrometry) in a rural catchment in Luxembourg found that during an event with a clockwise SS hysteresis pattern, the sediment source changed from cultivated topsoil at the beginning of the event, to grassland topsoil during the peak discharges. The findings show that the initially readily-available material from cultivated topsoil becomes supply-limited. The authors attribute the limited supply to the presence of artificial drains on the edges of the arable fields which disconnect the cultivated topsoils from the river network (Martínez-Carreras et al., 2010). A recent DRIFTS-based fingerprinting study by Cooper et al. (2014a) defined sediment sources by erosion processes (i.e. surface versus subsurface soils) in the catchment of the River Wensum (UK). The study shows that during precipitation events, the contribution of surface soils to the SS in the river is dominant, indicating surface erosion from arable fields. On the other hand, during lower river flows, SS originates mostly from subsurface erosion associated with channel banks and field drains characterised by Mid-Pleistocene chalky boulder clays, with limited contribution from surface sources (Cooper et al., 2014a).

The fingerprinting examples demonstrate that an analysis based on a single method (such as hysteresis patterns or rating curve) does not provide sufficient insights into the drivers of SS transport and might lead to oversimplified conclusions. In conclusion, event-based sediment dynamics provide insights into the conditions under which SS is transported in rivers. Knowing these conditions provides a better understanding of the importance of individual storm events in defining the longer term SS trends, and on catchment-scale SSLs in terms of location, magnitude, frequency and their sequencing over space and time (Gao, 2008; Smith and Blake, 2014).

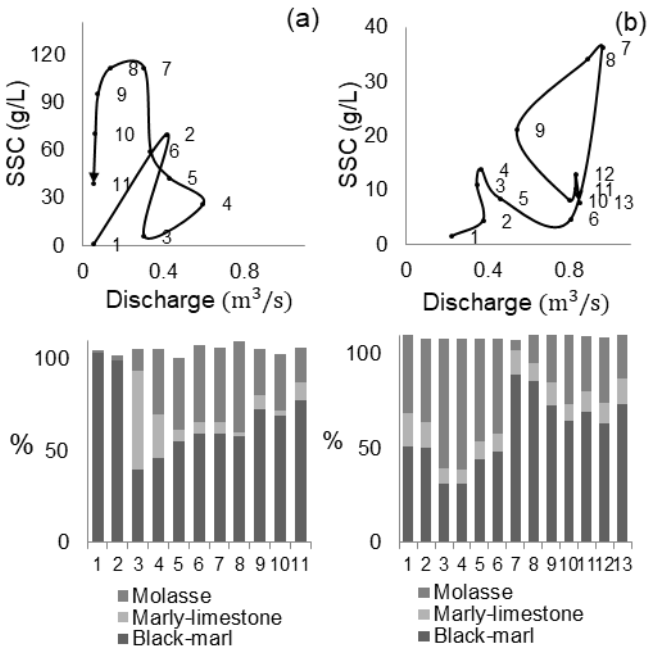

Figure 2-7: Discharge, suspended sediment concentration (SSC) and sediment source contributions for two flood events in the Calabre River catchment, Southern French Alps (a) 12/13 August 2008 and (b) 21/26 November 2007 (modified from Poulenard et al., 2012)

2.4.4 Conclusions: interpreting suspended sediment dynamics in terms of multi-timescale drivers

The interactions between hydro-meteorological factors, sediment sources, landscape disturbances and human interactions result in variable SSCs over short (high-flow events) and longer (monthly, annual) timescales (Sun et al., 2015; Zhang et al., 2013). The examples discussed in this section illustrate that sediment dynamics on one temporal scale are driven by a different set of processes to those at other temporal scales (Harvey, 2002). Long-term sediment transport variations are related to inter-annual climatic cycles, but also reveal change points caused by abrupt or steady changes in one or more of the catchment-scale drivers of SS transport. However, long-term SS dynamics give no information about the processes operating at smaller timescales and do not help to make conclusions about the episodic nature of SS transport. Seasonal sediment transport variations demonstrate the capacity of the catchment to store sediments and the subsequent transport of those sediments to and by the river system as a function of various drivers. Finally, event-based SS transport

variations demonstrate the impact of single high-flow events on the total SSL and the specific conditions and feedback mechanisms underlying SS transport. The case studies emphasise that a single hysteresis pattern or rating curve based on one temporal scale does not adequately represent the entire sediment regime and the corresponding geomorphic responses of a river catchment (Dean et al., 2016).

2.5 Guidelines for a multi-timescale approach to sediment regime characterisation

From both a scientific and a management perspective, it is often important to characterise the sediment regime of a river, i.e. to quantify the SSL in rivers and understand over which timescale and under which conditions most of the SS is actually transported. Towards this end, a thorough understanding of the processes and interactions underlying SS transport is essential. The findings of this review emphasise the importance of considering the spatial and temporal scales of SS transport in order to infer conclusions about dominant drivers and processes. A main outcome of this study is a call for future multi-timescale SS studies that structurally combine different analysis techniques to fully capture SS transport patterns, sources and underlying drivers.

SS transport dynamics can be expressed over multiple timescales, for which different dominant drivers are operating. This scale-dependency has important modelling and management implications. For example, when a catchment is characterised as having problematically high SSLs, annual SSLs will not provide the appropriate information to develop targeted management strategies if most sediment is transported during a specific part of the year (e.g. wet season or snowmelt). Furthermore, when assessing the SS dynamics of a river to assess possible changes in the sediment regime as a result of future dam construction, it is not sufficient to rely on long-term SSL data. While this type of data provides useful information about how SS transport interacts with certain changes within the catchment (e.g. land use change or climatic change), it does not provide in-depth information about the specific flow conditions of SS transport, and thus the potential impact of flow alterations on the SSL of a river (Geeraert et al., 2015).

Similarly, for ecological purposes and the establishment of water quality guidelines and thresholds of acceptable SSCs, it is important to understand how long-term SSLs and mean SSCs relate to the short-term episodic flushing of sediment during flood events at a specific location in the river (Grove et al., 2015). These considerations emphasise the importance of event-based sediment sampling, as already emphasised in more detailed review studies on SS sampling and modelling (e.g. Gao, 2008; Horowitz, 2008).

To assist in the design of future studies, we have summarised the main empirical methods described in the review, what type of information they can generally provide, and how this information can be interpreted in terms of underlying processes and drivers over multiple timescales at a single point in the river (Table 2-1). The aim of Table 2-1 is to serve as a guideline for scientists, practitioners and policy makers who are concerned about SS sediment transport in a particular river and want to better identify, characterise and model the scale-dependent variations in SS transport in rivers. The guidelines provided here will aid future research to structurally analyse existing SS datasets and/or develop time-integrated SS monitoring/assessment programs.

Table 2-1: Key aspects of an empirical multi-timescale approach to sediment regime characterisation

	Inter-annual data	Seasonal data	Event-based data
Resolution	Monthly to annual	Daily to monthly	Minutes to daily
Data type	SSC*/turbidity/cores	SSC*/turbidity	SSC*/turbidity
Method and output			
Sediment rating curves	Calculate annual SSLs, identify climatic cycling, trends and/or change points	Calculate seasonal SSLs, assess possible seasonal variation in SSLs	Calculate event-based SSLs, assess possible variation in event specific SSLs
Sediment fingerprinting	Identify possible shift in dominant sediment source	Identify possible seasonal variation in sediment sources	Identify possible event-based variation in sediment sources
Hysteresis analysis		Assess variable relationship between discharge and SS transport	Assess variable relationship between discharge and SS transport
Multivariate data-analysis			Assess importance of multiple factors as potential drivers
Drivers and processes	Impact of climatic and/or land use changes, major landscape disturbances and human interventions	Presence of store-release phases of sediment due to seasonal variations in hydro-meteorological conditions and sediment availability	Feedback-mechanisms between hydro-meteorological conditions, sediment availability, landscape disturbance and human factors
Management relevance	• Quantify mean SSCs and annual loads • Assess impact of historical changes	• Assess relative impact of natural/ anthropogenic vegetation changes and/or hydro-meteorological seasonality on sediment transport • Developing soil and water conservation strategies	• Identify conditions for sediment transport • Assess importance of events relative to annual SSC • Assess impact of future changes in flow conditions • Develop acceptable SSC thresholds for ecology

2.6 Conclusions

Linking SS transport dynamics to the underlying drivers across timescales and unravelling the process interactions between them is essential to the accurate prediction of SSCs and SLs in rivers and the development of sustainable solutions to sediment-related challenges such as soil erosion, sedimentation and pollution in streams. However, we are currently unable to fully capture the spatial and temporal dimensions of the factors and catchment scale sediment transport processes that drive SSCs in rivers. This review used previously published literature to highlight the importance of evaluating and interpreting SS transport dynamics in rivers across multiple temporal scales to gain better insights into the interactions of the factors driving these dynamics. The main objectives of the review were to: (i) briefly summarise the main drivers for variation in SS transport in rivers; (ii) review the common empirical approaches that are used to analyse and quantify SS transport and sources, with special focus on the limitations of these methods in terms of capturing temporal variability; a (iii) apply these findings to recent case studies to illustrate how method and timescale affect the interpretation of SS transport dynamics; and finally (iv) synthesise the findings of the review into a set of guidelines for a multi-timescale approach to characterise the sediment regime of a river.

Sediment transport processes in rivers are highly non-linear over time and space and are characterised by threshold behaviour and feedback mechanisms (Bracken et al., 2015; Onderka et al., 2012). These processes are driven by a wide range of factors which determine changes in sediment transport over short and long timescales. Over the past few decades, research on estimating and evaluating SS transport dynamics has shifted from single sediment rating curves to complex data-mining techniques and sediment fingerprinting methods. However, these methods have often been applied without consideration of the temporal scale of the processes. This has limited our capacity to interpret and fully understand sediment transport patterns and drivers over different timescales. The insights and guidelines provided in this review will hopefully contribute to a more consistent design of SS studies and a more comprehensive

understanding of SS dynamics and associated driving factors. By recognising *a priori* that study design and temporal scale have an impact on the interpretation of SS dynamics and employing methods that address these issues, future research will be better able to identify the drivers of SS transport in rivers, improve sediment transport modelling, and propose effective, sustainable solutions to sediment management problems.

2.7 Acknowledgements

This work was funded by an industrial PhD studentship supported by Cranfield University, Leeds City Council and Arup. We are very grateful for the comments made by the anonymous reviewers and we believe that they have helped us to significantly improve the manuscript.

2.8 References

Alexandrov, Y., Laronne, J.B., Reid, I., 2007. Intra-event and inter-seasonal behaviour of suspended sediment in flash floods of the semi-arid northern Negev, Israel. Geomorphology 85, 85–97. https://doi.org/10.1016/j.geomorph.2006.03.013

Asselman, N.E.M., 2000. Fitting and interpretation of sediment rating curves. J. Hydrol. 234, 228–248. https://doi.org/10.1016/S0022-1694(00)00253-5

Belmont, P., Gran, K.B., Schottler, S.P., Wilcock, P.R., Day, S.S., Jennings, C., Lauer, J.W., Viparelli, E., Willenbring, J.K., Engstrom, D.R., Parker, G., 2011. Large shift in source of fine sediment in the upper Mississippi River. Environ. Sci. Technol. 45, 8804–8810. https://doi.org/10.1021/es2019109

Bezak, N., Šraj, M., Mikoš, M., 2016. Analyses of suspended sediment loads in Slovenian rivers. Hydrol. Sci. J. 1–15. https://doi.org/10.1080/02626667.2015.1006230

Bilotta, G.S., Brazier, R.E., 2008. Understanding the influence of suspended solids on water quality and aquatic biota. Water Res. 42, 2849–2861. https://doi.org/10.1016/j.watres.2008.03.018

Bilotta, G.S., Burnside, N.G., Cheek, L., Dunbar, M.J., Grove, M.K., Harrison, C., Joyce, C., Peacock, C., Davy-Bowker, J., 2012. Developing environment-specific water quality guidelines for suspended particulate matter. Water Res. 46, 2324–2332. https://doi.org/10.1016/j.watres.2012.01.055

Bracken, L.J., Turnbull, L., Wainwright, J., Bogaart, P., 2015. Sediment connectivity: a framework

for understanding sediment transfer at multiple scales. Earth Surf. Process. Landforms 40, 177–188. https://doi.org/10.1002/esp.3635

Bridge, J., 2003. Rivers and Floodplains: Forms, Processes, and Sedimentary Record. Blackwell Science, Oxford.

Brosinsky, A., Foerster, S., Segl, K., Kaufmann, H., 2014a. Spectral fingerprinting: sediment source discrimination and contribution modelling of artificial mixtures based on VNIR-SWIR spectral properties. J. Soils Sediments 14, 1949–1964. https://doi.org/10.1007/s11368-014-0925-1

Brosinsky, A., Foerster, S., Segl, K., López-Tarazón, J.A., Piqué, G., Bronstert, A., 2014b. Spectral fingerprinting: characterizing suspended sediment sources by the use of VNIR-SWIR spectral information. J. Soils Sediments. https://doi.org/10.1007/s11368-014-0927-z

Cao, Z., Li, Y., Yue, Z., 2007. Multiple time scales of alluvial rivers carrying suspended sediment and their implications for mathematical modeling. Adv. Water Resour. 30, 715–729. https://doi.org/10.1016/j.advwatres.2006.06.007

Carter, J., Owens, P.N., Walling, D.E., Leeks, G.J.L., 2003. Fingerprinting suspended sediment sources in a large urban river system. Sci. Total Environ. 314–316, 513–534. https://doi.org/10.1016/S0048-9697(03)00071-8

Chang, C., Harrison, J.F., Huang, Y., 2015. Modeling Typhoon-Induced Alterations on River Sediment Transport and Turbidity Based on Dynamic Landslide Inventories: Gaoping River Basin, Taiwan. Water 7, 6910–6930. https://doi.org/10.3390/w7126666

Chen, F., Zhang, F., Fang, N., Shi, Z., 2016. Sediment source analysis using the fingerprinting method in a small catchment of the Loess Plateau, China. J. Soils Sediments. https://doi.org/10.1007/s11368-015-1336-7

Cobaner, M., Unal, B., Kisi, O., 2009. Suspended sediment concentration estimation by an adaptive neuro-fuzzy and neural network approaches using hydro-meteorological data. J. Hydrol. 367, 52–61. https://doi.org/10.1016/j.jhydrol.2008.12.024

Collins, A.L., Walling, D.E., 2004. Documenting catchment suspended sediment sources: problems, approaches and prospects. Prog. Phys. Geogr. 28, 159–196. https://doi.org/10.1191/0309133304pp409ra

Cooper, R.J., Krueger, T., Hiscock, K.M., Rawlins, B.G., 2014a. High-temporal resolution fluvial sediment source fingerprinting with uncertainty: A Bayesian approach. Earth Surf. Process. Landforms. https://doi.org/10.1002/esp.3621

Cooper, R.J., Rawlins, B.G., Lézé, B., Krueger, T., Hiscock, K.M., 2014b. Combining two filter

paper-based analytical methods to monitor temporal variations in the geochemical properties of fluvial suspended particulate matter. Hydrol. Process. 28, 4042–4056. https://doi.org/10.1002/hyp.9945

Cox, N.J., Warburton, J., Armstrong, A., Holliday, V.J., 2008. Fitting concentration and load rating curves with generalized linear models. Earth Surf. Process. Landforms 33, 25–39. https://doi.org/10.1002/esp

Croke, J., Fryirs, K.A., Thompson, C., 2013. Channel-floodplain connectivity during an extreme flood event: Implications for sediment erosion, deposition, and delivery. Earth Surf. Process. Landforms 38, 1444–1456. https://doi.org/10.1002/esp.3430

Davis, C.M., Fox, J.F., 2009. Sediment Fingerprinting : review of the method and future improvements for allocating nonpoint source pollution. J. Environ. Eng. 137, 490–505.

De Baets, S., Torri, D., Poesen, J., Salvador, M.P., Meersmans, J., 2008. Modelling increased soil cohesion due to roots with EUROSEM. Earth Surf. Process. Landforms 33, 1948–1963. https://doi.org/10.1002/esp

De Girolamo, A.M., Pappagallo, G., Lo Porto, A., 2015. Temporal variability of suspended sediment transport and rating curves in a Mediterranean river basin: The Celone (SE Italy). Catena 128, 135–143. https://doi.org/10.1016/j.catena.2014.09.020

Dean, D.J., Topping, D.J., Schmidt, J.C., Griffiths, R.E., Sabol, T.A., 2016. Sediment supply versus local hydraulic controls on sediment transport and storage in a river with large sediment loads. J. Geophys. Res. Earth Surf. 182–110. https://doi.org/10.1002/2015JF003436

De Vente, J., Poesen, J., Arabkhedri, M., Verstraeten, G., 2007. The sediment delivery problem revisited. Prog. Phys. Geogr. 31, 155–178. https://doi.org/10.1177/0309133307076485

Dominic, J.A., Aris, A.Z., Sulaiman, W.N.A., 2015. Factors controlling the suspended sediment yield during rainfall events of dry and wet weather conditions in a tropical urban catchment. Water Resour. Manag. 29, 4519–4538.

Duvert, C., Gratiot, N., Evrard, O., Navratil, O., Némery, J., Prat, C., Esteves, M., 2010. Drivers of erosion and suspended sediment transport in three headwater catchments of the Mexican Central Highlands. Geomorphology 123, 243–256. https://doi.org/10.1016/j.geomorph.2010.07.016

Eder, A., Strauss, P., Krueger, T., Quinton, J.N., 2010. Comparative calculation of suspended sediment loads with respect to hysteresis effects (in the Petzenkirchen catchment, Austria). J. Hydrol. 389, 168–176. https://doi.org/10.1016/j.jhydrol.2010.05.043

Evrard, O., Poulenard, J., Némery, J., Ayrault, S., Gratiot, N., Duvert, C., Prat, C., Lefèvre, I., Bonté, P., Esteves, M., 2013. Tracing sediment sources in a tropical highland catchment of central Mexico by using conventional and alternative fingerprinting methods. Hydrol. Process. 27, 911–922. https://doi.org/10.1002/hyp.9421

Fan, X., Shi, C., Zhou, Y., Shao, W., 2012. Sediment rating curves in the Ningxia-Inner Mongolia reaches of the upper Yellow River and their implications. Quat. Int. 282, 152–162. https://doi.org/10.1016/j.quaint.2012.04.044

Fang, N.F., Shi, Z.H., Chen, F.X., Zhang, H.Y., Wang, Y.X., 2015. Discharge and suspended sediment patterns in a small mountainous watershed with widely distributed rock fragments. J. Hydrol. 528, 238–248. https://doi.org/10.1016/j.jhydrol.2015.06.046

Ferguson, R.I., 1981. Channel forms and channel changes, in: Lewin, J. (Ed.), British Rivers. Allen and Unwin, London, pp. 90–125.

Foerster, S., Wilczok, C., Brosinsky, A., Segl, K., 2014. Assessment of sediment connectivity from vegetation cover and topography using remotely sensed data in a dryland catchment in the Spanish Pyrenees. J. Soils Sediments 14, 1982–2000. https://doi.org/10.1007/s11368-014-0992-3

Francke, T., Lopez-Tarazon, J.A., Vericat, D., Bronstert, A., Batalla, R.J., 2008. Flood-based analysis of high-magnitude sediment transport using a non-parametric method. Earth Surf. Process. Landforms 33, 2064–2077. https://doi.org/10.1002/esp. 1654

Francke, T., Werb, S., Sommerer, E., López-Tarazón, J.A., 2014. Analysis of runoff, sediment dynamics and sediment yield of subcatchments in the highly erodible Isábena catchment, Central Pyrenees. J. Soils Sediments 14, 1909–1920. https://doi.org/10.1007/s11368-014-0990-5

Franz, C., Makeschin, F., Weiß, H., Lorz, C., 2014. Sediments in urban river basins: identification of sediment sources within the Lago Paranoá catchment, Brasilia DF, Brazil - using the fingerprint approach. Sci. Total Environ. 466–467, 513–23. https://doi.org/10.1016/j.scitotenv.2013.07.056

Fryirs, K.A., 2013. (Dis)Connectivity in catchment sediment cascades: A fresh look at the sediment delivery problem. Earth Surf. Process. Landforms 38, 30–46. https://doi.org/10.1002/esp.3242

Fryirs, K.A., Brierley, G.J., 2013. Geomorphic analysis of river systems: An approach to reading the landscape. Wiley-Blackwell, West Sussex.

Fuchs, M., Will, M., Kunert, E., Kreutzer, S., Fischer, M., Reverman, R., 2011. The temporal and spatial quantification of Holocene sediment dynamics in a meso-scale catchment in northern

Bavaria , Germany. The Holocene 21, 1093–1104. https://doi.org/10.1177/0959683611400459

Gao, J.H., Xu, X., Jia, J., Kettner, A.J., Xing, F., Wang, Y.P., Yang, Y., Qi, S., Liao, F., Li, J., Bai, F., Zou, X., Gao, S., 2015. A numerical investigation of freshwater and sediment discharge variations of Poyang Lake catchment , China over the last 1000 years. The Holocene. https://doi.org/10.1177/0959683615585843

Gao, P., 2008. Understanding watershed suspended sediment transport. Prog. Phys. Geogr. 32, 243–263. https://doi.org/10.1177/0309133308094849

Gao, P., Nearing, M. a., Commons, M., 2013. Suspended sediment transport at the instantaneous and event time scales in semiarid watersheds of southeastern Arizona, USA. Water Resour. Res. 49, 6857–6870. https://doi.org/10.1002/wrcr.20549

García-Ruiz, J.M., Beguería, S., Nadal-Romero, E., González-Hidalgo, J.C., Lana-Renault, N., Sanjuán, Y., 2015. A Meta-Analysis of soil erosion rates across the world. Geomorphology 239, 160–173. https://doi.org/10.1016/j.geomorph.2015.03.008

Geeraert, N., Omengo, F.O., Tamooh, F., Paron, P., Bouillon, S., Govers, G., 2015. Sediment yield of the lower Tana River, Kenya, is insensitive to dam construction: Sediment mobilization processes in a semi-arid tropical river system. Earth Surf. Process. Landforms 40, 1827–1838. https://doi.org/10.1002/esp.3763

Grabowski, R.C., Gurnell, A.M., 2016. Diagnosing problems of fine sediment delivery and transfer in a lowland catchment. Aquat. Sci. 78, 95–106. https://doi.org/10.1007/s00027-015-0426-3

Grove, M.K., Bilotta, G.S., Woockman, R.R., Schwartz, J.S., 2015. Suspended sediment regimes in contrasting reference-condition freshwater ecosystems: Implications for water quality guidelines and management. Sci. Total Environ. 502, 481–492. https://doi.org/10.1016/j.scitotenv.2014.09.054

Harvey, A.M., 2002. Effective timescales of coupling within fluvial systems. Geomorphology 44, 175–201. https://doi.org/10.1016/S0169-555X(01)00174-X

Hollister, J.W., August, P. V., Paul, J.F., 2008. Effects of spatial extent on landscape structure and sediment metal concentration relationships in small estuarine systems of the United States' Mid-Atlantic Coast. Landsc. Ecol. 23, 91–106. https://doi.org/10.1007/s10980-007-9143-1

Horowitz, A.J., 2009. Monitoring suspended sediments and associated chemical constituents in urban environments: lessons from the city of Atlanta, Georgia, USA Water Quality Monitoring Program. J. Soils Sediments 9, 342–363. https://doi.org/10.1007/s11368-009-

0092-y

Horowitz, A.J., 2008. Determining annual suspended sediment and sediment-associated trace element and nutrient fluxes. Sci. Total Environ. 400, 315–43. https://doi.org/10.1016/j.scitotenv.2008.04.022

Horowitz, A.J., 2003. An evaluation of sediment rating curves for estimating suspended sediment concentrations for subsequent flux calculations. Hydrol. Process. 17, 3387–3409. https://doi.org/10.1002/hyp.1299

Horowitz, A.J., Clarke, R.T., Merten, G.H., 2014. The effects of sample scheduling and sample numbers on estimates of the annual fl uxes of suspended sediment in fl uvial systems. Hydrol. Process. https://doi.org/10.1002/hyp

Huang, F., Xia, Z., Li, F., Wu, T., 2013. Assessing sediment regime alteration of the upper Yangtze River. Environ. Earth Sci. 70, 2349–2357. https://doi.org/10.1007/s12665-013-2381-4

Huisman, N.L.H., Karthikeyan, K.G., Lamba, J., Thompson, A.M., Peaslee, G., 2013. Quantification of seasonal sediment and phosphorus transport dynamics in an agricultural watershed using radiometric fingerprinting techniques. J. Soils Sediments 13, 1724–1734. https://doi.org/10.1007/s11368-013-0769-0

Kettner, A.J., Gomez, B., Syvitski, J.P.M., 2007. Modeling suspended sediment discharge from the Waipaoa River system, New Zealand: The last 3000 years. Water Resour. Res. 43, 1–15. https://doi.org/10.1029/2006WR005570

Kisi, O., 2005. Suspended sediment estimation using neuro-fuzzy and neural network approaches. Hydrol. Sci. J. 50, 683–696. https://doi.org/10.1623/hysj.2005.50.4.683

Kisi, O., 2004. Daily suspended sediment modelling using a fuzzy differential evolution approach. Hydrol. Sci. J. 49, 183–197. https://doi.org/10.1623/hysj.49.1.183.54001

Koiter, A.J., Lobb, D.A., Owens, P.N., Petticrew, E.L., Tiessen, K.H.D., Li, S., 2013a. Investigating the role of connectivity and scale in assessing the sources of sediment in an agricultural watershed in the Canadian prairies using sediment source fingerprinting. J. Soils Sediments 13, 1676–1691. https://doi.org/10.1007/s11368-013-0762-7

Koiter, A.J., Owens, P.N., Petticrew, E.L., Lobb, D.A., 2013b. The behavioural characteristics of sediment properties and their implications for sediment fingerprinting as an approach for identifying sediment sources in river basins. Earth-Science Rev. 125, 24–42. https://doi.org/10.1016/j.earscirev.2013.05.009

Krueger, T., Quinton, J.N., Freer, J.E., Macleod, C.J.A., Bilotta, G.S., Brazier, R.E., Butler, P.,

Haygarth, P.M., 2009. Uncertainties in data and models to describe event dynamics of agricultural sediment and phosphorus transfer. J. Environ. Qual. 38, 1137–1148. https://doi.org/10.2134/jeq2008.0179

Lana-Renault, N., Alvera, B., García-Ruiz, J.M., 2011. Runoff and Sediment Transport during the Snowmelt Period in a Mediterranean High-Mountain Catchment. Arctic, Antarct. Alp. Res. 43, 213–222. https://doi.org/10.1657/1938-4246-43.2.213

Le, V.S., Yamashita, T., Okunishi, T., Shinohara, R., Miyatake, M., 2006. Characteristics of suspended sediment material transport in the Ishikari Bay in snowmelt season. Appl. Ocean Res. 28, 275–289. https://doi.org/10.1016/j.apor.2006.11.001

Lloyd, C.E.M., Freer, J.E., Johnes, P.J., Collins, A.L., 2016. Using hysteresis analysis of high-resolution water quality monitoring data, including uncertainty, to infer controls on nutrient and sediment transfer in catchments. Sci. Total Environ. 543, 388–404. https://doi.org/10.1016/j.scitotenv.2015.11.028

Lohani, A.K., Goel, N.K., Bhatia, K.K.S., 2007. Deriving stage–discharge–sediment concentration relationships using fuzzy logic. Hydrol. Sci. J. 52, 793–807. https://doi.org/10.1623/hysj.52.4.793

López-Tarazón, J.A., Batalla, R.J., 2014. Dominant discharges for suspended sediment transport in a highly active Pyrenean river. J. Soils Sediments 14, 2019–2030. https://doi.org/10.1007/s11368-014-0961-x

Marsalek, J., Viklander, M., 2010. Controlling contaminants in urban stormwater: Linking environmental science and policy, in: Jan Lundqvist (Ed.), On the Water Front. World Water Week 2010, Stockholm.

Martínez-Carreras, N., Krein, A., Udelhoven, T., Gallart, F., Iffly, J.F., Hoffmann, L., Pfister, L., Walling, D.E., 2010. A rapid spectral-reflectance-based fingerprinting approach for documenting suspended sediment sources during storm runoff events. J. Soils Sediments 10, 400–413. https://doi.org/10.1007/s11368-009-0162-1

Mohr, C.H., Zimmermann, A., Korup, O., Iroumé, A., Francke, T., Bronstert, A., 2014. Seasonal logging, process response, and geomorphic work. Earth Surf. Dynamucs 2, 117–125. https://doi.org/10.5194/esurf-2-117-2014

Morgan, R.P.C., 2005. Soil Erosion & Conservation. Blackwell Publishing Ltd, Oxford.

Mukundan, R., Walling, D.E., Gellis, A.C., Slattery, M.C., Radcliffe, D.E., 2012. Sediment source fingerprinting: transforming from a research tool to a management tool. J. Am. Water Resour. Assoc. 48, 1241–1257. https://doi.org/10.1111/j.1752-1688.2012.00685.x

Ola, A., Dodd, I.C., Quinton, J.N., 2015. Can we manipulate root system architecture to control soil erosion? Soil 1, 603–612. https://doi.org/10.5194/soil-1-603-2015

Omengo, F.O., Alleman, T., Geeraert, N., Bouillon, S., Govers, G., 2016. Sediment deposition patterns in a tropical floodplain, Tana River, Kenya. Catena 143, 57–69. https://doi.org/10.1016/j.catena.2016.03.024

Onderka, M., Krein, A., Wrede, S., Martínez-Carreras, N., Hoffmann, L., 2012. Dynamics of storm-driven suspended sediments in a headwater catchment described by multivariable modeling. J. Soils Sediments 12, 620–635. https://doi.org/10.1007/s11368-012-0480-6

Owens, P.N., Giles, T.R., Petticrew, E.L., Leggat, M.S., Moore, R.D., Eaton, B.C., 2013. Muted responses of streamflow and suspended sediment flux in a wildfire-affected watershed. Geomorphology 202, 128–139. https://doi.org/10.1016/j.geomorph.2013.01.001

Palazón, L., Latorre, B., Gaspar, L., Blake, W.H., Smith, H.G., Navas, A., 2015. Comparing catchment sediment fingerprinting procedures using an auto-evaluation approach with virtual sample mixtures. Sci. Total Environ. 532, 456–466. https://doi.org/10.1016/j.scitotenv.2015.05.003

Panagos, P., Borrelli, P., Meusburger, K., Alewell, C., Lugato, E., Montanarella, L., 2015. Estimating the soil erosion cover-management factor at the European scale. Land use policy 48, 38–50. https://doi.org/10.1016/j.landusepol.2015.05.021

Park, E., Latrubesse, E.M., 2014. Modeling suspended sediment distribution patterns of the Amazon River using MODIS data. Remote Sens. Environ. 147, 232–242. https://doi.org/10.1016/j.rse.2014.03.013

Perks, M.T., Owen, G.J., Benskin, C.M.H., Jonczyk, J., Deasy, C., Burke, S., Reaney, S.M., Haygarth, P.M., 2015. Dominant mechanisms for the delivery of fine sediment and phosphorus to fluvial networks draining grassland dominated headwater catchments. Sci. Total Environ. 523, 178–190. https://doi.org/10.1016/j.scitotenv.2015.03.008

Phillips, J.D., 2016. Vanishing point: Scale independence in geomorphological hierarchies. Geomorphology 266, 66–74. https://doi.org/10.1016/j.geomorph.2016.05.012

Phillips, J.D., 2003. Sources of nonlinearity and complexity in geomorphic systems. Prog. Phys. Geogr. 27, 1–23. https://doi.org/10.1191/0309133303pp340ra

Poulenard, J., Legout, C., Némery, J., Bramorski, J., Navratil, O., Douchin, A., Fanget, B., Perrette, Y., Evrard, O., Esteves, M., 2012. Tracing sediment sources during floods using Diffuse Reflectance Infrared Fourier Transform Spectrometry (DRIFTS): A case study in a highly erosive mountainous catchment (Southern French Alps). J. Hydrol. 414–415, 452–462. https://doi.org/10.1016/j.jhydrol.2011.11.022

Poulenard, J., Perrette, Y., Fanget, B., Quetin, P., Trevisan, D., Dorioz, J.M., 2009. Infrared spectroscopy tracing of sediment sources in a small rural watershed (French Alps). Sci. Total Environ. 407, 2808–19. https://doi.org/10.1016/j.scitotenv.2008.12.049

Praskievicz, S., 2014. Impacts of Projected Climate Changes on Streamflow and Sediment Transport for Three Snowmelt-Dominated Rivers in the Interior Pacific Northwest. River Res. Appl. n/a-n/a. https://doi.org/10.1002/rra.2841

Prosser, I.P., Williams, L., 1998. The effect of wildfire on runoff and erosion in native Eucalyptus forest. Hydrol. Process. 12, 251–265. https://doi.org/10.1002/(SICI)1099-1085(199802)12:2<251::AID-HYP574>3.0.CO;2-4

Pulley, S., Foster, I., Antunes, P., 2015. The uncertainties associated with sediment fingerprinting suspended and recently deposited fluvial sediment in the Nene river basin. Geomorphology 228, 303–319. https://doi.org/10.1016/j.geomorph.2014.09.016

Renard, K.G., Foster, G.R., Weesies, G. a., Porter, J.P., 1991. RUSLE: Revised universal soil loss equation. J. Soil Water Conserv. 46, 30–33.

Rickson, R.J., 2014. Can control of soil erosion mitigate water pollution by sediments? Sci. Total Environ. 468–469, 1187–1197. https://doi.org/10.1016/j.scitotenv.2013.05.057

Rossi, L., Chèvre, N., Fankhauser, R., Margot, J., Curdy, R., Babut, M., Barry, D.A., 2013. Sediment contamination assessment in urban areas based on total suspended solids. Water Res. 47, 339–50. https://doi.org/10.1016/j.watres.2012.10.011

Rovira, A., Ibáñez, C., Martín-Vide, J.P., 2015. Suspended sediment load at the lowermost Ebro River (Catalonia, Spain). Quat. Int. 388, 188–198. https://doi.org/10.1016/j.quaint.2015.05.035

Sear, D.A., Malcolm, D.N., Thorne, C.R., 2003. Guidebook for Applied Fluvial Geomorphology, R&D Technical Report FD1914. London.

Seeger, M., Errea, M.P., Beguería, S., Arnáez, J., Martí, C., García-Ruiz, J.M., 2004. Catchment soil moisture and rainfall characteristics as determinant factors for discharge/suspended sediment hysteretic loops in a small headwater catchment in the Spanish pyrenees. J. Hydrol. 288, 299–311. https://doi.org/10.1016/j.jhydrol.2003.10.012

Selbig, W.R., Bannerman, R., Corsi, S.R., 2013. From streets to streams: assessing the toxicity potential of urban sediment by particle size. Sci. Total Environ. 444, 381–91. https://doi.org/10.1016/j.scitotenv.2012.11.094

Smith, H.G., Blake, W.H., 2014. Sediment fingerprinting in agricultural catchments: A critical re-examination of source discrimination and data corrections. Geomorphology 204, 177–191.

https://doi.org/10.1016/j.geomorph.2013.08.003

Smith, H.G., Dragovich, D., 2009. Interpreting sediment delivery processes using suspended sediment-discharge hysteresis patterns from nested upland catchments, south-eastern Australia. Hydrol. Process. 23, 2416–2426. https://doi.org/10.1002/hyp

Stone, M.L., Juracek, K.E., Graham, J.L., Foster, G.M., 2015. Quantifying suspended sediment loads delivered to Cheney Reservoir, Kansas: Temporal patterns and management implications. J. Soil Water Conserv. 70, 91–100. https://doi.org/10.2489/jswc.70.2.91

Sun, L., Yan, M., Cai, Q., Fang, H., 2015. Suspended sediment dynamics at different time scales in the Loushui River, south-central China. Catena Published. https://doi.org/10.1016/j.catena.2015.02.014

Tananaev, N.I., 2015. Hysteresis effects of suspended sediment transport in relation to geomorphic conditions and dominant sediment sources in medium and large rivers of the Russian Arctic. Hydrol. Res. 46, 232. https://doi.org/10.2166/nh.2013.199

Taylor, K.G., Owens, P.N., 2009. Sediments in urban river basins: a review of sediment–contaminant dynamics in an environmental system conditioned by human activities. J. Soils Sediments 9, 281–303. https://doi.org/10.1007/s11368-009-0103-z

Tena, A., Vericat, D., Batalla, R.J., 2014. Suspended sediment dynamics during flushing flows in a large impounded river (the lower River Ebro). J. Soils Sediments 14, 2057–2069. https://doi.org/10.1007/s11368-014-0987-0

Thompson, J., Cassidy, R., Doody, D.G., Flynn, R., 2014. Assessing suspended sediment dynamics in relation to ecological thresholds and sampling strategies in two Irish headwater catchments. Sci. Total Environ. 468–469, 345–357. https://doi.org/10.1016/j.scitotenv.2013.08.069

Tiecher, T., Caner, L., Minella, J.P.G., Bender, M.A., dos Santos, D.R., 2015. Tracing sediment sources in a subtropical rural catchment of southern Brazil by using geochemical tracers and near-infrared spectroscopy. Soil Tillage Res. https://doi.org/10.1016/j.still.2015.03.001

Vale, S.S., Fuller, I.C., Procter, J.N., Basher, L.R., Smith, I.E., 2016. Characterization and quantification of suspended sediment sources to the Manawatu River, New Zealand. Sci. Total Environ. 543, 171–186. https://doi.org/10.1016/j.scitotenv.2015.11.003

Vanmaercke, M., Ardizzone, F., Rossi, M., Guzzetti, F., 2016. Exploring the effects of seismicity on landslides and catchment sediment yield: An Italian case study. Geomorphology. https://doi.org/10.1016/j.geomorph.2016.11.010

Vanmaercke, M., Poesen, J., Verstraeten, G., de Vente, J., Ocakoglu, F., 2011. Sediment yield

in Europe: Spatial patterns and scale dependency. Geomorphology 130, 142–161. https://doi.org/10.1016/j.geomorph.2011.03.010

Verstraeten, G., Van Oost, K., Van Rompaey, A., Poesen, J., Govers, G., 2002. Evaluating an integrated approach to catchment management to reduce soil loss and sediment pollution through modelling. Soil Use Manag. 18, 386–394. https://doi.org/10.1079/SUM2002150

Walling, D.E., 2013. The evolution of sediment source fingerprinting investigations in fluvial systems. J. Soils Sediments 13, 1658–1675. https://doi.org/10.1007/s11368-013-0767-2

Walling, D.E., 2009. The impact of global change on erosion and sediment transport by rivers: Current progress and future challenges, The United Nations World Water Development Report 3. Paris.

Walling, Owens, P.N., Foster, I.D.L., Lees, J.A., 2003. Changes in the fine sediment dynamics of the Ouse and Tweed basins in the UK over the last 100-150 years. Hydrol. Process. 17, 3245–3269. https://doi.org/10.1002/hyp.1385

Wang, J., Jin, Z., Hilton, R.G., Zhang, F., Densmore, A.L., Li, G., Joshua West, A., 2015. Controls on fluvial evacuation of sediment from earthquake-triggered landslides. Geology 43, 115–118. https://doi.org/10.1130/G36157.1

Wilkinson, S.N., Olley, J.M., Furuichi, T., Burton, J., Kinsey-Henderson, A.E., 2015. Sediment source tracing with stratified sampling and weightings based on spatial gradients in soil erosion. J. Soils Sediments. https://doi.org/10.1007/s11368-015-1134-2

Williams, G.P., 1989. Sediment concentration versus water discharge during single hydrologic events in rivers. J. Hydrol. https://doi.org/10.1016/0022-1694(89)90254-0

Wohl, E., 2015. Legacy effects on sediments in river corridors. Earth-Science Rev. 147, 30–53. https://doi.org/10.1016/j.earscirev.2015.05.001

Yellen, B., Woodruff, J.D., Kratz, L.N., Mabee, S.B., Morrison, J., Martini, A.M., 2014. Source, conveyance and fate of suspended sediments following Hurricane Irene. New England, USA. Geomorphology 226, 124–134. https://doi.org/10.1016/j.geomorph.2014.07.028

Zeiger, S., Hubbart, J.A., 2016. Quantifying suspended sediment flux in a mixed-land-use urbanizing watershed using a nested-scale study design. Sci. Total Environ. 542, 315–323. https://doi.org/10.1016/j.scitotenv.2015.10.096

Zhang, W., Yan, Y., Zheng, J., Li, L., Dong, X., Cai, H., 2009. Temporal and spatial variability of annual extreme water level in the Pearl River Delta region, China. Glob. Planet. Change 69, 35–47. https://doi.org/10.1016/j.gloplacha.2009.07.003

Zhang, Y.Y., Zhong, D.Y., Wu, B.S., 2013. Multiple temporal scale relationships of bankfull

discharge with streamflow and sediment transport in the Yellow River in China. Int. J. Sediment Res. 28, 496–510. https://doi.org/10.1016/S1001-6279(14)60008-1

Zheng, M., Yang, J., Qi, D., Sun, L., Cai, Q., 2012. Flow-sediment relationship as functions of spatial and temporal scales in hilly areas of the Chinese Loess Plateau. Catena 98, 29–40. https://doi.org/10.1016/j.catena.2012.05.013

Zimmermann, A., Francke, T., Elsenbeer, H., 2012. Forests and erosion: Insights from a study of suspended-sediment dynamics in an overland flow-prone rainforest catchment. J. Hydrol. 428–429, 170–181. https://doi.org/10.1016/j.jhydrol.2012.01.039

CHAPTER 3: MULTI-TIMESCALE APPROACH TO PREDICT SUSPENDED SEDIMENT TRANSPORT IN RIVERS

Abstract

SS transport in rivers is highly variable in time and space, making it challenging to develop predictive models that are applicable across timescales and river systems. Previous studies have developed a range of approaches to estimate SLs, and to identify catchment and hydro-meteorological variables controlling SSCs at different temporal scales, but these have not been unified across scales in process-based models because of the difficulty of identifying underlying mechanisms. This study investigated the scale-specific processes and process interactions that control temporal variation in SS transport, which are central to selecting the most appropriate predictive model and developing more holistic predictive models. The River Aire, UK, was used as a case study to: (i) identify the dominant factors and mechanisms driving SS transport over inter-annual, intra-annual and event scales by comparing the performance of different approaches (univariate, sediment rating curve versus multivariate, partial least squares regression) to estimate SLs based on two datasets (monthly, long-term data and hydrology-based, short-term data), and (ii) develop a framework to link SS transport dynamics and mechanisms across timescales. The estimated sediment yield ranged from 6 to 52 t km^{-2} $year^{-1}$, depending on the timescale of the data used. The processes underlying temporal variability in SS transport were found to be highly scale-dependent, with inter-annual variation mainly driven by land use change, but strongly influenced by the interplay of catchment characteristics and hydro-meteorological variables over shorter scales. This scale dependency stresses the need for an approach to connect mechanisms controlling SSCs at the event scale and dynamics over longer timescales. The fractal power of a SS transport system could be an appropriate starting point in developing transferrable process-based approaches to quantify and predict SSCs, as well as to develop targeted management policies.

3.1 Introduction

SS transport in rivers is extremely variable in space and time. The amount of SS in a river is controlled by a complex system of processes and process interactions over multiple scales (Bracken et al., 2015; McDonnell et al., 2007; Onderka et al., 2012; Vercruysse et al., 2017). This complexity makes it challenging to adequately quantify and predict SS transport (Ahn et al., 2017; Gao, 2008; Phillips, 2003; Raven et al., 2010; Rickson, 2014). Yet, quantifying and predicting SSCs in rivers has become a necessity, because, despite being a fundamental part of river systems, anthropogenic activities have altered sediment transport processes in most rivers leading to significant management problems. Excess fine sediment in rivers causes ecological degradation, water quality decline (with higher associated water treatment costs), increased flood risk, and infrastructural damage (Bilotta et al., 2012; Bilotta and Brazier, 2008; Horowitz, 2009; Owens et al., 2005; Taylor and Owens, 2009). Therefore, it is essential to quantify and predict SS transport in order to develop well-informed management policies.

In general, SS in rivers originates from soil erosion on land, and is therefore strongly determined by the topographical, pedological, geological, climatic and/or land cover characteristics of a catchment (Vanmaercke et al., 2011; Vercruysse et al., 2017). Sediment transfer towards and within the river also varies across spatial scales, as a result of repeated soil erosion, sediment deposition and remobilisation (Bracken et al., 2015; De Vente et al., 2007; Ferguson, 1981; Fryirs, 2013; Fryirs and Brierley, 2013; Hollister et al., 2008; Perks et al., 2017; Smith and Dragovich, 2009; Tetzlaff et al., 2008). Further, the temporal variability in SS transport is controlled by the interaction of hydro-meteorological factors, sediment source variations, natural landscape disturbances, and human interventions (Vercruysse et al., 2017). River discharge is generally considered to be a dominant driver for SS transport, but analysis of detailed environmental data have identified other significant hydro-meteorological factors, such as antecedent soil moisture, rainfall intensity and duration, and air temperature (McDowell and Sharpley, 2002; Onderka et al., 2012; Seeger et al., 2004; Smith and Dragovich, 2009; Tena et al., 2014). These hydro-meteorological factors form the basis of multiple catchment-specific empirical models that have been

used to estimate SSCs at high temporal resolutions (Cobaner et al., 2009; Francke et al., 2008; Kisi, 2005; Lohani et al., 2007; Onderka et al., 2012; Zimmermann et al., 2012).

However, the prediction of SSCs over multiple timescales is further complicated by short- and long-term changes in the dominant sediment sources (e.g. due to sediment supply exhaustion or vegetation changes), and by natural (e.g. mass movements) and human (e.g. land cover change or dam construction) landscape disturbances (Belmont et al., 2011; Grabowski and Gurnell, 2016; Rovira et al., 2015; Sun et al., 2015; Vanmaercke et al., 2016). As a result, the prediction of SSC has generally been very empirically-based and scale-dependent; predictive models often do not account for changes caused by processes and feedback mechanisms over various timescales (Ahn et al., 2017; Vercruysse et al., 2017). This is a well-known problem in many natural sciences, such as hydrology (Blöschl and Sivapalan, 1995), ecology (Wheatley and Johnson, 2009), and geography (Dark and Bram, 2007), which has driven the development of process-based approaches and models that can be applied to different scales. Towards this end, many studies stress the need to identify and synthesise driving factors and underlying processes across multiple scales (Blöschl, 2006; Blöschl and Sivapalan, 1995; Evans and Brazier, 2005; McDonnell et al., 2007; Raven et al., 2010; Tetzlaff et al., 2008; Troch et al., 2009; Van Nieuwenhuyse et al., 2011).

The dominant processes underlying soil erosion and sediment transport over multiple spatial scales have been identified in conceptual frameworks of sediment transport (e.g. sediment connectivity, expressed as the degree to which the efficiency of spatial sediment transfer is limited due to catchment characteristics and transport processes (Bracken et al., 2015; Fryirs, 2013)), or through investigations into landscape metrics controlling hydrological processes (Van Nieuwenhuyse et al., 2011). At the temporal level, the idea of “effective timescales of connectivity” (Fryirs, 2013; Harvey, 2002) has been used to define the timeframe over which sediment (dis)connectivity occurs, whereby parts of the catchment are “switched on and off” as a response of events with varying frequency-magnitude relationships (e.g. rare storm events versus land use

change) (Fryirs, 2013). Similarly, “characteristic timescales” are used in different scientific disciplines to address variability across different scales, which involves identifying lengths of time that are representative for particular processes (Skøien et al., 2003). However, while these concepts provide excellent frameworks to understand temporal variability and identify relevant timescales for sediment transport, it remains a challenge to identify and synthesise the underlying mechanisms for variability in SS transport across different timescales (Blöschl, 2006; Vercruysse et al., 2017).

Better understanding of the mechanisms driving variation in SS transport and how these mechanisms link across temporal scales, is essential to develop transferable process-based approaches to quantify and predict SSCs, and develop target management strategies. Therefore, this study aims to investigate SS transport at multiple timescales to uncover the scale-specific processes and process interactions that determine temporal variations in SS transport. The mixed urban-rural catchment of the River Aire, UK is used as a case study to: (i) identify the dominant factors and mechanisms driving SS transport over inter-annual, intra-annual, and event scales by comparing the performance of different approaches (univariate, sediment rating curve versus multivariate, partial least squares regression) to estimate SLs based on two datasets (monthly, long-term data and hydrology-based, short-term data), and (ii) develop a framework to link SS transport dynamics across multiple timescales.

3.2 Materials and methods

3.2.1 Study area

The River Aire rises in North Yorkshire (200 m AOD) and continues for 70 km until it reaches the city of Leeds (26 m AOD) (Figure 3-1), before it flows into the River Ouse. It has a total catchment area of 879 km^2 (upstream on Leeds: 690km^2) and consists of three main Carboniferous geologies: limestone and shale in the upper part, millstone grit in the middle part, and coal measures in the lower part (Morton et al., 2011). The upper part of the catchment is mainly characterised by grassland and heath with peat bogs (59% and 12% of the entire catchment respectively). The middle and lower reaches of the catchment are

strongly urbanised (25%) including the major cities Bradford and Leeds, with some arable land (4%) (Figure 3-1). The dominantly loamy to clayey soils in the catchment consist of raw oligo-fibrous peats, and stagnohumic and stagnogley soils in the upper part, and brown earths and pelo-stagnogley soils in the middle and lower parts (Carter et al., 2006).

3.2.2 Data

Suspended sediment data

To capture SS transport dynamics at inter- and intra-annual, and event scales, two data sources of SSC were used. First, monthly SSCs (1989-2014) were obtained from three monitoring stations within the city of Leeds from the Environment Agency (EA) of England (Figure 3-1). Second, SS samples were collected with a depth-integrating SS sampler during 14 precipitation events (200 samples) between June 2015 and March 2017 at a single location within the city center, 300 m from the most upstream EA SS monitoring station (Figure 3-1). In both cases, sediment samples were obtained by filtration of a measured volume of water (between 1 and 0.4 L depending on the turbidity) on pre-dried and pre-weighted glass/quartz fibre filters. All filters were dried for 2 hours at 105°C before being weighed. The measured SSC varied between 1 and 1000 mg L^{-1}, with a mean of 29.15 mg L^{-1} (± 64.8 mg L^{-1} SE) between 1989 and 2017.

Hydro-meteorological data

River discharge time series were obtained from the closest monitoring station (Figure 3-1) to the manual SS sampling point: mean daily discharge were downloaded from the National River Flow Archive (NRFA) (1961-2015) (Centre for Ecology and Hydrology, 2017), and instantaneous discharge (15 min) was provided by the EA (2007-2017). From the same location, monthly precipitation measurements were obtained from NRFA (1961-2015). Additionally, instantaneous precipitation data (15 min) were obtained (2015-2017) from 10 EA loggers across the catchment (Figure 3-1).

Based on the flow duration curve of the discharge data, the median daily flow (Q_{50}) of the River Aire in Leeds is 10 m^3 s^{-1}, while there is a 10% probability of

discharges exceeding 40 m^3 s^{-1} (Q_{10}). Annual precipitation rates vary between 637 and 1470 mm $year^{-1}$, with a mean of 1054 mm $year^{-1}$.

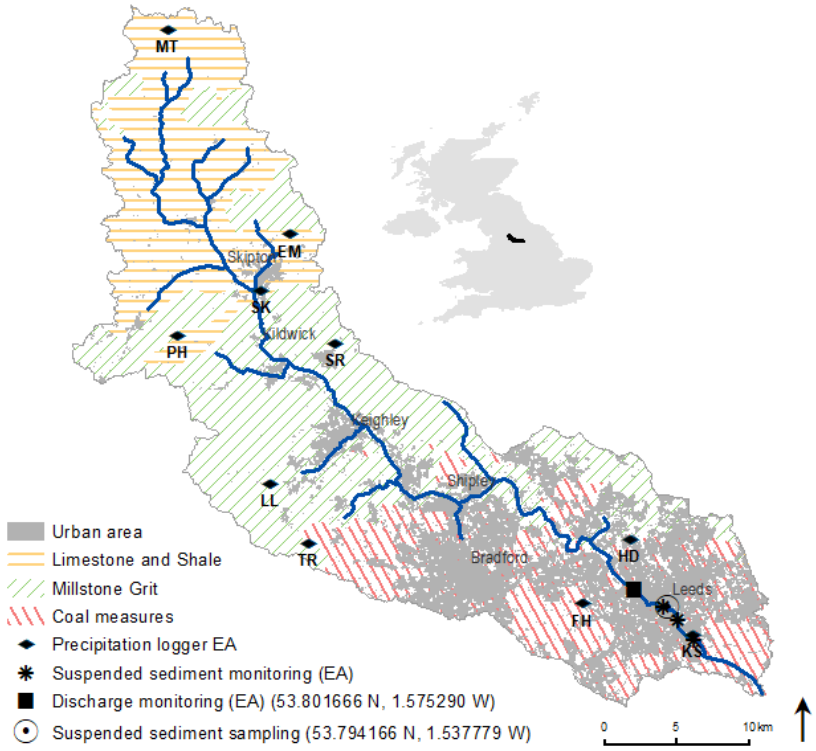

Figure 3-1: The River Aire catchment (UK): geology, urban land cover, and locations of monitoring and sampling (MT: Malham Tarn, EM: Embsay, PH: Proctor Heigts, SK: Skipton, SR: Silsden Reservoir, LL: Lower Laithe, TR: Thornton Reservoir, FH: Farnley Hall, HD: Headingley, KS: Knotstrop) (land cover data derived from LCM 2007 (Morton et al., 2011)).

3.2.3 Data analysis

The SSC and hydro-meteorological data were analysed over three timescales (i.e. inter-, intra-annual and event) to quantify temporal variation and identify scale-dependent factors controlling SSC. Additionally, SLs and sediment yields were estimated. The SL (t) in a river is the amount of sediment transport per unit of time, and sediment yield (t km^{-2}) is the SL divided by the catchment area per unit of time.

Inter-annual suspended sediment transport

Mean annual SSC and discharge, and total annual precipitation were calculated based on the EA data (Table 3-1). The SSC datasets of the three EA monitoring stations contain gaps in the time series (irregular samples and missing years, see

Appendix B) and were therefore averaged over the three stations to construct a single SSC time series for further statistical analysis.

To identify trends, and to assess whether similar trends are present in both the annual hydro-meteorological data and the SSC, the annual time series (Table 3-1) were analysed using (i) a Pettitt's change point analysis to detect abrupt changes (Pohlert, 2015; Sun et al., 2015); and (ii) a non-parametric Mann-Kendall test to detect the presence of gradual, monotonic trends (Fan et al., 2012; Sun et al., 2015; Zhang and Lu, 2009; Zhang and Mao, 2015; Zhang et al., 2009).

At the inter-annual scale, limited hydro-meteorological information is available. Therefore, LSs were estimated based on the standard approach using a sediment rating curve (SRC) that describes the relationship between discharge and SSC (Asselman, 2000; Horowitz et al., 2014). All available discharge-SSC data were log transformed to reduce the effect of outliers, and regression equations were fitted on the transformed data. The regression equation from the SRC was then used to estimate SSCs based on daily discharges between 1961 and 2016, which were subsequently used to estimate annual SLs (Horowitz, 2003; Old et al., 2003).

Intra-annual suspended sediment transport

Both the EA and sampled SSC data were used for the intra-annual analysis (Table 3-1): average monthly SSCs were calculated and compared with average monthly discharges, as well as average monthly precipitation. To identify possible annual cycling in sediment transport and storage, the relationships between discharge and SSC, and precipitation and SSC, were assessed by examining the monthly hysteresis pattern between both variables (Sun et al., 2015). Finally, seasonal SRCs were constructed following the SRC approach described in the previous section.

Event suspended sediment transport

At the event-scale, high temporal resolution hydro-meteorological and sediment data are available which allows to investigate the relation between different hydro-meteorological variables and SSC in more detail. A multivariate dataset

was constructed, including instantaneous and antecedent discharge (1 hour; 1, 7 and 21 days) and precipitation (1, 7 and 21 days) for 10 monitoring stations across the catchment (Table 3-1) (Dominic et al., 2015; Lawler et al., 2006; Lloyd et al., 2016; Perks et al., 2015; Tena et al., 2014; Zeiger and Hubbart, 2016).

The event-based multivariate dataset was used to (i) identify hydro-meteorological variables that are significantly correlated to the SSC, and (ii) establish a significant relationship between those variables and SSC. However, the precipitation data from different locations and the discharge data are highly collinear, making a multiple linear regression unsuitable without an initial variable selection step. An alternative approach is partial least squares regression (PLSR), which is better able to handle data with strongly collinear variables, while also providing additional statistics on variable importance (Karaman et al., 2013; Martens and Martens, 2000; Wold et al., 2001). The data are projected onto a new set of variables (components) similarly to principal component analysis (PCA), but instead of maximising the variance within one dataset as in PCA, PLSR maximises the covariance between two datasets based on the respective scores (Stevens and Lopez, 2015). The multivariate dataset was divided into two parts: 75% for calibration and 25% for validation, randomly selected by a Kennard-Stone sampling algorithm. Leave-one-out cross validation in the calibration phase was applied to determine the optimal number of components based on the amount of components with the lowest root mean squared error (RMSE) (Martens and Martens, 2000; Poulenard et al., 2009; Wold et al., 2001). The PLSR scores and loadings were subsequently used to examine the components of the model. Observations with a high score on a particular component are better explained by that component, while variables with large loadings (between -1 and 1) on a component are more correlated to that component (Karaman et al., 2013; Martens and Martens, 2000; Wold et al., 2001).

The PLSR model was also used to estimate SSCs at a 15 min resolution for the period 2015-2017. Additionally, event-specific SLs were estimated. To detect a wide range of high-flow events (i.e. not only the highest flows defined by peak

over threshold), the events were identified based on visual inspection of individual hydrographs (Sun et al., 2015): a rising hydrograph was detected whenever the difference in discharge ≥ 0.5 $m^3 s^{-1}$ at a 15 min resolution, whereby the start of the event was set 12 hours before the rise, and the end at 48 hours after the rise. On this basis, 362 high-flow events based on discharge were identified between January 2007 and February 2017.

Table 3-1: Sediment and hydro-meteorological variables per temporal scale

Scale	Data	Variable	Unit	Description
Inter-annual	NRFA+EA (1961-2014)	Q	$m^3 s^{-1}$	Mean daily discharge per year
	NRFA+EA (1961-2014)	P	mm	Total annual precipitation
	EA (1989-2014)	SSC	Mg L^{-1}	Mean annual SSC
Intra-annual	NRFA+EA (1961-2014)	Q	$m^3 s^{-1}$	Mean daily discharge per month
	NRFA+EA (1961-2014)	P	mm	Total monthly precipitation
	EA (1989-2014)	SSC	Mg L^{-1}	Mean monthly SSC (averaged for 3 stations)
	Sampled (2015-2017)	SSC	Mg L^{-1}	Mean monthly SSC
Event	EA (2015-2017)	Q	$m^3 s^{-1}$	Instantaneous discharge (time of sampling)
		Q_{1h}	$m^3 s^{-1}$	Discharge one hour prior to time of sampling
		Q_{1d}	$m^3 s^{-1}$	Discharge 1 day prior to time of sampling
		Q_{7d}	$m^3 s^{-1}$	Discharge 7 days prior to time of sampling
		Q_{21d}	$m^3 s^{-1}$	Discharge 21 days prior to time of sampling
		P	mm	Instantaneous precipitation (time of sampling) (*)
		P_{1d}	mm	Precipitation 1 day prior to event (*)
		P_{7d}	mm	Precipitation 7 days prior to event (*)
		P_{21d}	mm	Precipitation 21 days prior to event (*)
	Sampled (2015-2017)	SSC	Mg L^{-1}	Instantaneous SSC

(*) Variables calculated for each precipitation logger (10)

3.3 Results

3.3.1 Inter-annual suspended sediment transport

Discharge and precipitation exhibited strong inter-annual variation between 1961 and 2017 (Figure 3-2). A significant change point in discharge was identified in 1980 ($p = 0.039$), marking a shift to a higher discharge period (1980-2017) in which the annual mean, maximum, and minimum discharge increased by 8%, 5%, and 25%, respectively, compared to 1961-1980. No change points were

observed in the precipitation time series data, and no monotonic trends were detected in the annual discharge or precipitation data.

The SSC time series also shows strong inter-annual variation between 1989 and 2014. However, no correlation was found between the mean annual SSC and discharge or precipitation. A significant change point is present in the SSC time series in 2006 (p = 0.006), whereby the mean SSC decreased by 14% between the pre- and post-2006 period (Figure 3-2). The Mann-Kendall test showed a significant decreasing trend in SSC (p = 0.05).

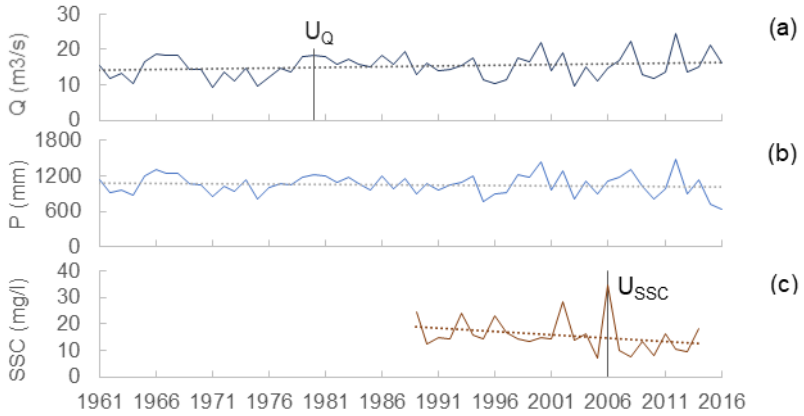

Figure 3-2: Annual time series of (a) discharge (Q), (b) precipitation (P) and (c) suspended sediment concentration (SSC). Grey doted lines represent a linear regression and the vertical lines the Pettitt's change points in Q (U_Q) and SSC (U_{SSC}).

3.3.2 Intra-annual suspended sediment transport

Considerable intra-annual variation was observed in mean monthly discharge, precipitation, and SSC (Figure 3-3 a). In general, the mean monthly SSC fluctuates around 12-16 mg L^{-1}, while the highest mean SSCs are observed in October, November and December (mean 23 mg L^{-1}). Similarly, mean monthly discharges are around 10 m^3 s^{-1} from May to September and highest from October to March (on average 20 m^3 s^{-1}).

The relationship between mean monthly discharge and SSC is expressed as a clockwise hysteresis pattern, while a figure-eight patterns was observed between the mean monthly precipitation and SSC (Figure 3-3 b-c). The SSC increases with increasing discharge and precipitation from August to December, while from

January SSCs and precipitation drop, and discharges remain high until March. From March to May, both SSC and discharge further decrease until July, while precipitations remains relatively constant. Based on this discharge-SSC hysteresis pattern, four periods can be identified: (i) October - December with high discharge and SSC; (ii) January - March with similar discharges, but decreasing SSCs; (iii) April - June with low discharges and low SSCs; and (iv) July - September with low discharges, but increasing SSCs.

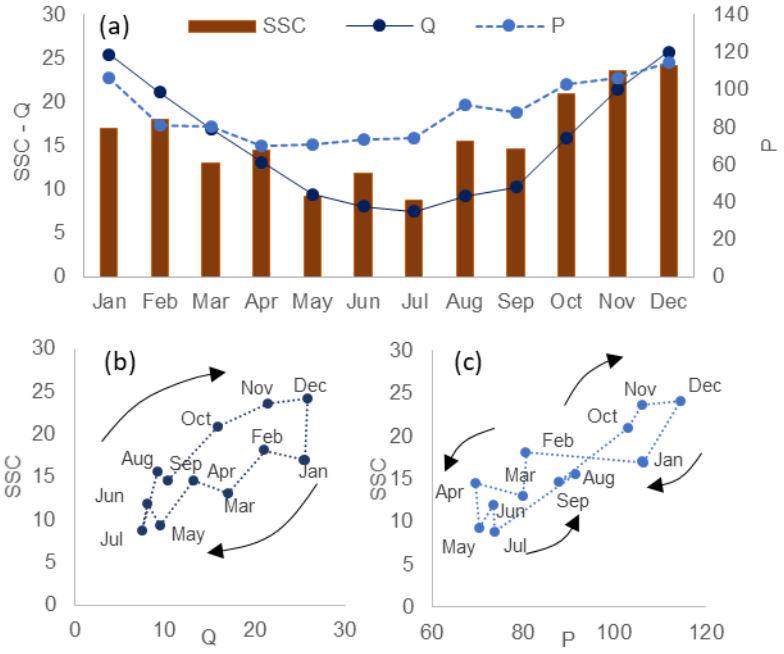

Figure 3-3: Monthly sediment and water dynamics: (a) mean discharge (m^3 s^{-1}) (Q), mean suspended sediment concentration (mg L^{-1}) (SSC) and precipitation (mm) (P); relationship between (b) mean monthly Q and SSC, and (c) mean monthly P and SSC

3.3.3 Event suspended sediment transport

The sampled events ranged in mean discharges (9.4 - 72.3 m^3 s^{-1}) and SSCs (15.9 to 179.4 mg L^{-1}), and were characterised by different hysteresis patterns between discharge and SSC, as illustrated for three events in Figure 3-4. The events in June 2015 and September 2016 had a similar hydrograph with peak discharges of around 40 m^3 s^{-1} and both were characterised by counter-clockwise hysteresis between discharge and SSC. However, SSCs were significantly different between both events; the September event reached an exceptionally

high SSC peak of 1007.5 mg L^{-1}. Similarly, the events in June 2015 and November 2016 had similar SSCs, while the peak discharge in November was double that of June and showed a clockwise hysteresis pattern.

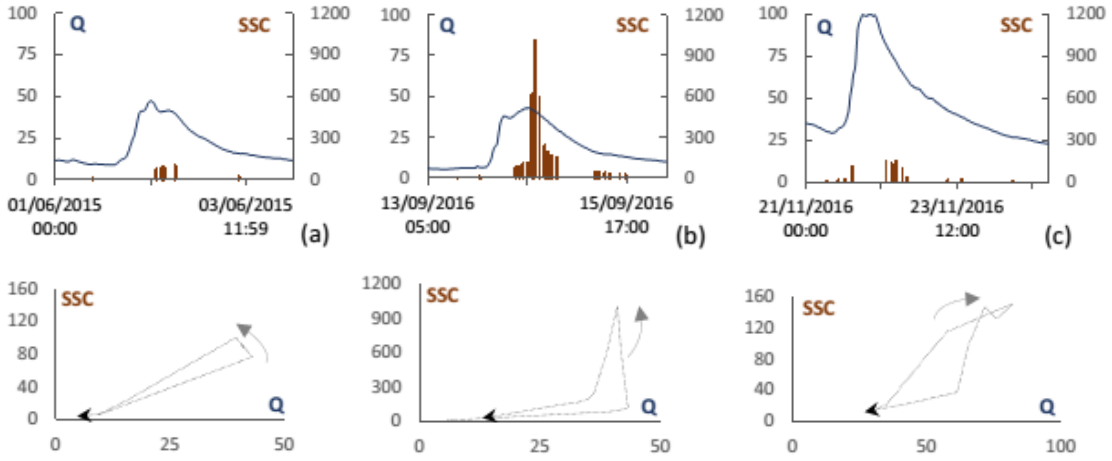

Figure 3-4: Discharge (Q in m^3 s^{-1}) and SSC (in mg L^{-1}) of selected high-flow events in (a) June 2015, (b) September 2016 and (c) November 2016

The PLSR analysis performed on the event-based hydro-meteorological and SSCs dataset, resulted in a regression model consisting of four components (RMSE = 70 mg L^{-1}, R^2 = 0.41; Figure 3-5). The high RMSE was influenced by outliers caused by exceptionally high SSCs during an event in September 2016 (Figure 3-4 b). The four components explain 43% of the total variance in the SSC (15.5%, 14%, 8%, and 5.5% respectively).

The squared PLSR loadings provide insights into which variables are most important in defining the PLSR components (Figure 3-5 a). The first component is mainly determined by P_{1d}, Q and Q_{1h}, while the second component is related to P_{21d}, Q_{1d} and Q_{7d}. The instantaneous precipitation variables (P) are generally included into the third component, and the fourth component is characterised by P_{7d} and P_{21d}. Furthermore, the scores of the individual observations on the components quantify which component explains the most variation for a particular observation (Figure 3-5 b-d). In general, peak SSCs correspond with high scores on the first component (P_{1d} and Q). The second component (P_{21d}) appears to be important throughout events, but especially at the start and end. The third

component (P) is generally more important at the start of the events. Trends throughout the sequence of events are also observed. At the start of the first event in June 2016, the second and third components are most important in explaining the SSCs, while gradually the first component becomes dominant. In the Nov-16 series of events, the third component becomes more important towards the third SSC peak. Finally in February 17, the first component is dominant during the first event, while the second component becomes more important afterwards.

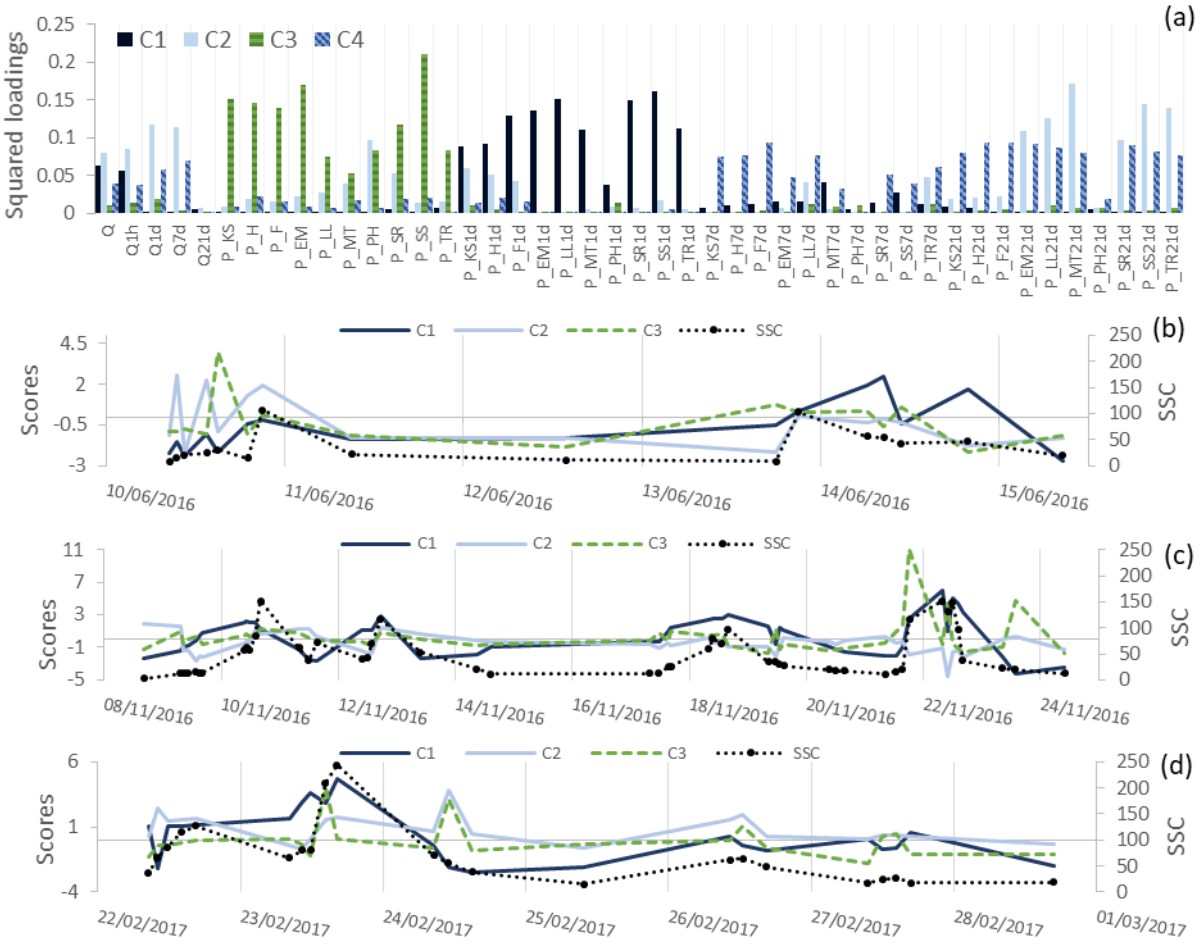

Figure 3-5: PLS regression statistics: (a) squared PLS loadings for four components (C1 to C4); Observed SSCs and associated PLS scores on the first four components for a sequence of events (b) June 2016, (b) November 2016, (d) February 2017

3.3.4 Suspended sediment loads and yields

As no significant temporal trends in both the annual discharge and SSC data (1989-2014) were observed, a single SRC was developed to estimate annual SLs (Horowitz, 2008; Tena et al., 2014). A linear relationship between the log transformed discharge and SSC was established (R^2 = 0.40, p-value = 5.9 x 10^{-41}; Figure 3-6 a). The estimated annual sediment yields (1961-2016) vary between 6 and 29 t km^{-2} $year^{-1}$ (4,142 to 19,835 t $year^{-1}$), with a mean of 14 t km^{-2} $year^{-1}$ (Figure 3-7 a).

However, the relationship between discharge and SSC varied at the intra-annual scale according to the four periods identified based on the monthly hysteresis pattern (Figure 3-3). Therefore seasonal SRCs were developed for these four periods. Based on the EA data alone (i.e. monthly random sampling), the seasonal SRCs do not differ significantly from the general SRC. However, when the event-based data was added to the dataset, a clear seasonal signal in the SRCs was observed, in which SSCs are higher in July-September compared to January-March for the same discharges (i.e. slope of the regression is higher in July-September) (Figure 3-6 b). When the annual SL is estimated using these seasonal SRCs, the average SL is 13,600 t $year^{-1}$ (20 t km^{-2}), which is 29% higher than the average SL based on the standard SRC (9,641 t). SLs in April-June and July-September averaged 1,642 t and 1,652 t (~ 2.5 t km^{-2}) respectively, and 5,614 t (8 t km^{-2}) and 4,698 t (6.8 t km^{-2}) for October-December and January-March (Figure 3-7 b). Furthermore, considerable variation was observed in the relative importance of the seasonal sediment yield to the annual sediment yield (Figure 3-7 b). For example, the January-March 2016 period was exceptionally wet resulting in high sediment yields (13 t km^{-2}), which mainly determined the total SL in 2016 (14.8 t km^{-2}), while in 2012, the July-September and October-December sediment yields were comparable around 15 t km^{-2}.

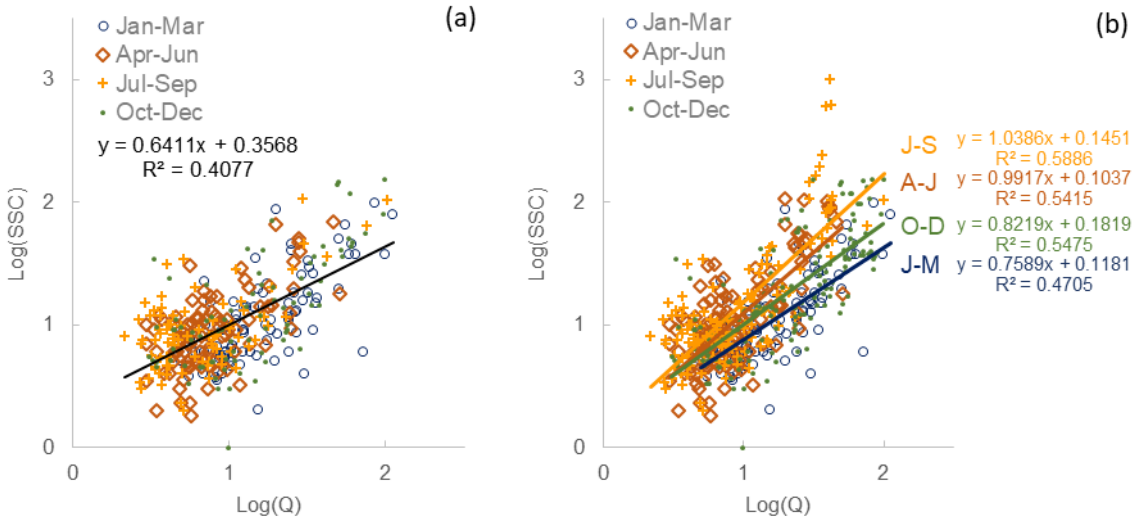

Figure 3-6: Discharge-sediment rating curves: (a) general (data: EA 1989-2014), and (b) per seasonal period (data: EA + sampled 1989-2017). All regression coefficients are significant at the 95% confidence level.

Finally, SLs were estimated based on the PLSR model. Applying the PLSR model to 15 min discharge and precipitation data for 2016 results in an annual SL of 35,632 t (51 t km^{-2}), compared to 10,219 t (15 t km^{-2}) based on the standard SRC, and 13160 t (19 t km^{-2}) with the seasonal SRCs. In other words, the annual SL estimated based on more detailed hydro-meteorological data is 70% higher compared the SL estimated based on a single SRC with monthly SSC values. Additionally, event-specific SLs were estimated. An extreme flood event in December 2015 (with peak discharges of 400 m^3 s^{-1}) accounted for 10% of the total water yield (741 x 10^6 m^3), and 47% of the total SL (129,767 t) between July 2015 and June 2016. Furthermore, the event in September 2016 (Figure 3-4 b) had an estimated SL of 916 t, and the event in November 2016 (Figure 3-4 c) a SL of 1020 t, which both contributed around 3% to the annual SL in 2016 (35,632 t) (Figure 3-7 c).

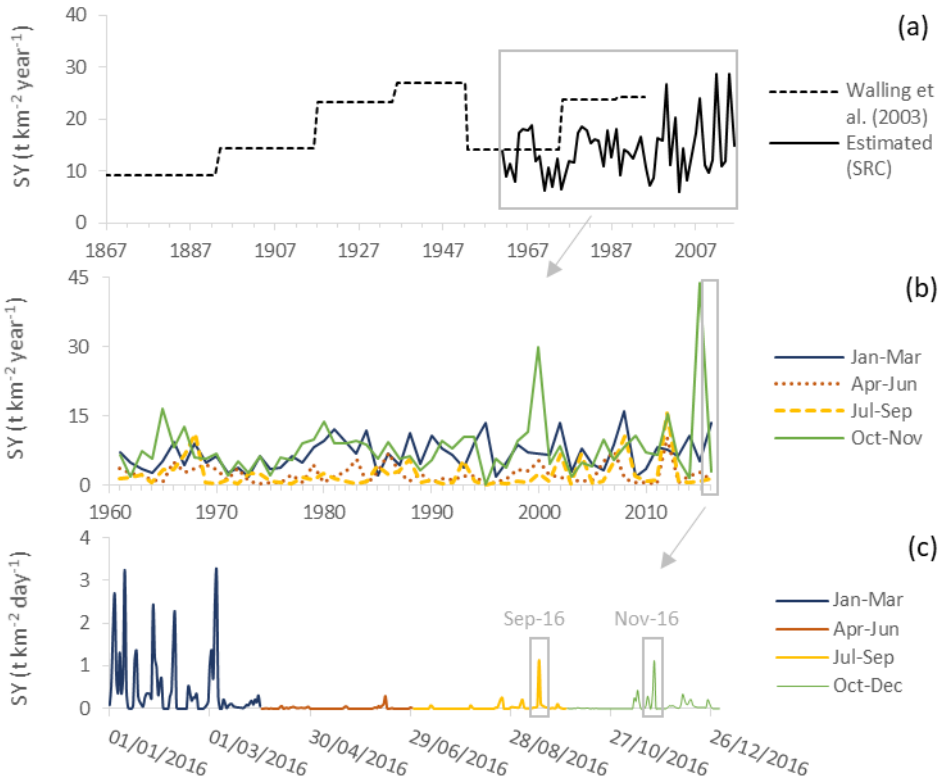

Figure 3-7: Sediment yields in the River Aire based on: (a) standard SRC (1961-2016), (b) seasonal SCR's (1961-2016), and (c) PLSR (2016)

3.4 Discussion

This study investigated the scale-specific processes and process interactions that determine SSCs in rivers through statistical analysis of empirical SS data for the River Aire. The multi-timescale analysis of SSC and potential explanatory variables of SSC revealed that the estimation of sediment yield and the identification of dominant factors and underlying mechanisms controlling SSCs differ at inter-annual, intra-annual, and seasonal scales.

3.4.1 Mechanisms for temporal variation in suspended sediment transport

Inter-annual variation

At the inter-annual scale, a significant decreasing trend in mean annual SSC was observed between 1989 and 2014, yet sediment yields during the same period did not decrease due to an increase in discharge, especially in the period after

1980 (Figure 3-7 a). The SSC is also not significantly correlated to discharge or precipitation, which suggests that climatic factors are not the dominant driving force for long-term SS transport, and stresses the importance of other factors (e.g. land use change or natural landscape disturbances) in controlling inter-annual variability in SSCs in the River Aire.

The importance of land use change on SLs has been demonstrated in previous studies in the River Aire catchment (Foster and Lees, 1999; Walling et al., 2003). The observed increase in sediment yield between 1930 and 1950 was attributed to the conversion of pasture to arable land during and shortly after World War II, while the increase since the mid-1970s was attributed to the conversion of moorland to grassland for pasture (Walling et al., 2003). Those land use changes would have made the soil more vulnerable to erosion due to agricultural practices (e.g. tillage), the removal of a permanent vegetation cover, and soil compaction by livestock (Collins et al., 2010; Franz et al., 2014; Janes et al., 2017).

Furthermore, studies report increasingly on the significant contribution of particles from “urban” origin to the SL in rivers (Marsalek and Viklander, 2010; Taylor and Owens, 2009; Zeiger and Hubbart, 2016) which could be an additional/alternative explanation for the increase in sediment yield since the mid-1970s (Figure 3-7 a). The urban area expanded with 9% (or 62 km^2) between 1990 and 2007 (decreased heath (6%) and grassland (3%)) (Morton et al., 2011; Wyatt et al., 1993), A sediment fingerprinting study in 2003 found that 33-40% of the SS originates from street dust and solids from sewage treatment works (Carter et al., 2003), while another study reported heavy metal pollution associated to SS coming from combined sewage overflows, industrial discharges, and road runoff (D. E. Walling et al., 2003). The likely contribution of fine sediment from urban street dust is also supported by a study on Bradford Beck, a major tributary of the River Aire, which observed an increase in SLs associated to urban street dust and combined sewage overflows as the river flows through an urbanised area (Old et al., 2006).

Despite the increase in total annual SL, the observed decrease in mean annual SSCs (with a change point in 2006) could possibly be linked to major

improvement works which were carried out at the Esholt sewage treatment plant upstream of the city of Leeds between 2006 and 2010 (Feather and Caldwell, 2007) (Figure 3-2). However, average annual SSCs can be strongly influenced by outliers at the intra-annual scale. Therefore, it is important to recognize that land use change cannot explain all the inter-annual variation in SS transport (e.g. change point in SSC in 2006; Figure 3-2 or SL peaks in 2012 and 2015; Figure 3-7 a), suggesting that other factors are also controlling the SL, which only become apparent at finer timescales.

Intra-annual variation

At the intra-annual scale, the varying SSC-discharge relationship (i.e. hysteresis; Figure 3-3 b) uncovers the interplay of natural and anthropogenic processes that control changes in catchment sediment supply and transport.

The seasonality in the SSC-discharge relationship, marked by high discharges and SSCs in October-December and decreasing SSCs towards the end of winter (Figure 3-3 b), suggests a store-release system of sediment throughout the year driven by factors other than discharge (Dominic et al., 2015; Huisman et al., 2013; Park and Latrubesse, 2014; Rovira et al., 2015; Sun et al., 2015). From April to July, SSCs and precipitation are at their lowest, indicating that surface runoff and discharge are not sufficient to transport the eroded material from the catchment towards and within the river. As a result, the readily available sediment (i.e. eroded material) is temporarily stored within the catchment and river system. Additionally, this period also coincides with an increase in vegetation density (Boyd et al., 2011; Ogunbadewa, 2012), limiting the detachment and supply of particles. When precipitation (and discharge) increase, the available material is (re)mobilised, resulting in high SSCs. However, from January to March, SSCs decrease while discharges remain high, suggesting that the sediment supply becomes exhausted as the winter progresses into spring (Rovira et al., 2015; Sun et al., 2015). Furthermore, the store-release mechanism also provides an explanation for the difference in the slope of the regression lines in the seasonal SRCs (Figure 3-6 b): for similar discharges, the estimated SSC will be higher in

July-September compared to January-March due to exhaustion of the sediment supply during the latter period.

Additionally, sediment exhaustion in January-March may be enhanced by changes in the sediment supply and connectivity of the catchment (Bracken et al., 2015; Fryirs, 2013), due to the growth of vegetation in spring in both agricultural and natural systems (i.e. protecting the soil from rainfall impact and enhancing infiltration) (Fryirs, 2013). Furthermore, considerable variation is observed in the relative importance of the seasonal periods to the total annual sediment yields, e.g. for several years the January-March sediment yields is higher than the preceding October-November sediment yield (Figure 3-7 b). This suggests that the presence (or absence) of a sediment-exhaustion effect is also driven by factors acting at shorter temporal scales.

Event-scale variation

The detailed hydro-meteorological data available at the event scale allowed to identify specific variables that are correlated to the SSC, which emphasise the importance of timing, frequency, and magnitude of precipitation events in controlling both the short- and long-term SSC in the river.

The results of the PLSR model indicate that antecedent precipitation explains the most variance in the SSC, in particular P_{1d} and P_{21d} (Figure 3-5). This supports the findings of other studies that demonstrate the importance of antecedent soil moisture conditions in controlling SSC (McDowell and Sharpley, 2002; Onderka et al., 2012; Seeger et al., 2004; Smith and Dragovich, 2009; Tena et al., 2014). Generally, soil moisture conditions regulate the generation of surface runoff by influencing infiltration and water storage capacity of the soils, which in turn controls erosion and sediment transport (Rickson, 2014; Seeger et al., 2004; Smith and Dragovich, 2009). Therefore, the effect of antecedent moisture conditions on SSCs is determined by the interplay with catchment characteristics, and characterised by threshold behaviour (Onderka et al., 2012), which is clearly illustrated by the temporal variability in the importance of PLSR components throughout events.

The events in June 2016 were characterised by moderate peak discharges, but relatively high SSCs (Figure 3-5 b). The drier period prior to the events in June 2016 would have led to dry soils which generally tend to repel water and crust (surface sealing) at the first rainfall impact. Soil crusting reduces infiltration and leads to the generation of overland flow, which can (re)mobilise the sediment stored within the catchment, as well as increase the likelihood of interrill and gully erosion (Onderka et al., 2012), and is reflected in the importance of P_{21d} in controlling the SSC at the start of the first event. As the month progressed, P_{1d} became the dominant factor controlling SSCs, suggesting that soils became increasingly saturated, so that saturation excess overland flow became the dominant process for erosion and sediment transport to and in the river. Similarly, prolonged precipitation in November 2016 (Figure 3-5 c), and associated saturation excess overland flow, may have caused more soil erosion, as well as connected more distant sediment sources to the river (Bracken et al., 2015). However, threshold behaviour appears to be present, whereby increasing antecedent moisture conditions do not lead to increasing SSCs. In February 2017 (Figure 3-5 d), SSCs decrease towards the second event (while discharges remain similar), which coincides with an increase in the importance of P_{21d}. Similar to the observations at the monthly scale, this indicates exhaustion of the sediment supply (on the river bed and within the catchment) with increasing antecedent precipitation (Krueger et al., 2009; Onderka et al., 2012).

3.4.2 Linking temporal scales of suspended sediment transport

The high temporal variability in SS transport makes it essential to develop transferable process-based approaches to quantify and predict SSCs. However, this study clearly indicates that SS transport is driven by different processes and process interactions over multiple timescales, resulting in a complex system that is difficult to model.

This complexity and scale-dependency of processes driving SS transport stress the need to decipher how different timescales are linked, i.e. to assess how short-scale variability influences long-term variability in SS transport (Vercruysse et al., 2017). Ahn et al. (2017) addressed this by developing time-varying SS-discharge

rating curves, which proved very useful to show the effect of individual events on long-term dynamics in SS transport. However, a limitation of their approach is that it cannot account for the non-linearity in the relationship between discharge and SSC, while this study especially indicates the importance of antecedent moisture conditions and threshold behaviour in controlling SSCs.

Therefore, a more holistic approach is proposed here that aims to first identify the dominant processes for SS transport, whereby the SS transport system is described as a fractal system (Halley et al., 2004). Fractals are used to describe and predict patterns over different spatial or temporal scales in a wide range of disciplines, including catchment hydrology, (fluvial) geomorphology, geography, and ecology (Halley et al., 2004; Jiang and Brandt, 2016; Medina-Cobo et al., 2016; Rodriguez-Iturbe and Rinaldo, 2001; Sivakumar, 2001; Skøien et al., 2003; Van Nieuwenhuyse et al., 2011). By approaching SS transport dynamics as a fractal system, it is assumed that patterns of variation in SS transport exist over different timescales (e.g. Figure 3-7), while linkages across those temporal scales are expressed as fractal power. Fractal power represents the ratio of large-scale variability and small-scale variability, and implies that if the small-scale variability in time is very high, it overwhelms the effect of the large-scale variability (Skøien et al., 2003). The SS transport system in the River Aire is characterised by high fractal power. In the long term, variation in SS transport is dominantly driven by land use. However, SSCs at the intra-annual and event scale are strongly driven by interactions and feedback mechanisms between catchment characteristics and hydro-meteorological conditions, which overwhelms variation caused by processes at longer timescales. For example, the exceptionally wet period between January and March 2016 largely determined the total annual SL in 2016. Similarly, the single flood event in December 2015 generated almost half of the total SL between July 2015 and June 2016, while events with relatively low discharges (e.g. September 2016; Figure 3-4 b) can also generate significant SLs depending on the antecedent moisture conditions (Figure 3-7).

The fractal approach provides a useful framework to characterise the dominant mechanisms controlling SSCs in rivers (Figure 3-8). In systems with low fractal

power, the long-term driving processes are dominant and are visible at smaller scales (e.g. overall higher SSCs as a result of deforestation (Walling, 2009)), while in systems with high fractal power long-term variation is overwhelmed by processes over shorter timescales (e.g. River Aire) (Figure 3-8). Therefore, the fractal power of a SS transport system has important implications for predictive modelling. For example, the range of SS yields in the River Aire estimated based on the standard SRC, the seasonal SRCs, and the PLSR model (6 - 52 t km^{-2} $year^{-1}$) are all comparable to yields estimated in other studies based on sediment cores from around the study area (7 - 86 t km^{-2} $year^{-1}$) (Foster and Lees, 1999; Walling et al., 2003). However, important differences in SL estimations between the different approaches were observed which can be explained by the high fractal power of the SS transport system in the River Aire; a single regression (SRC) does not take into account the scatter around the regression line caused by temporal variability, and thus ignores the high fractal power of the system. This observation supports previous studies that have shown that SRCs based on least squares regression and monthly data underestimate SLs by 10–70% (Asselman, 2000; Ferguson, 1985; Horowitz, 2008; Skarbøvik et al., 2012). Similarly, Perks et al.(2017) tested the impact of sampling frequency on the calculation on mean monthly SSCs. They found that single, random monthly samples significantly underestimate the mean monthly SSCs based on 15 min monitoring records. Moreover, it was observed that as sample frequency decreased, the deviation from the reference SSC increased non-linearly (Perks et al., 2017). Therefore, insights into the degree of fractal power can form a useful basis to evaluate and develop the most appropriate predictive models and management strategies.

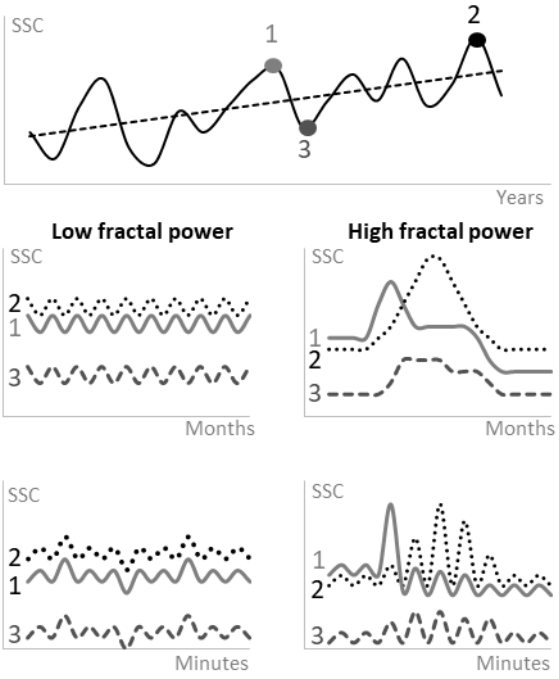

Figure 3-8: Temporal variability in suspended sediment transport exhibits different degrees of fractal power: low fractal power means that processes at the intra-annual and event timescales do not overwhelm the long-term processes; high fractal power means that seasonal and event dynamics significantly impact variations at the inter-annual scale. Numbers 1, 2, 3 represent individual years.

3.5 Conclusion

The sediment yield in the River Aire has been estimated between 6 - 52 t km^{-2} $year^{-1}$, and exhibits considerable inter- and intra-annual variation. By systematically comparing the variation in SS transport over multiple timescales with hydro-meteorological data, the scale dependency of temporal variability in SS transport, in terms of controlling variables and mechanisms, was demonstrated. Long-term variation in annual sediment yields appeared to be driven by land use change. However, land use change could not explain all the inter-annual variation in SSC, which was strongly influenced by the interplay of catchment characteristics and hydro-meteorological variables over shorter (i.e. intra-annual and event) scales.

The SS transport in rivers should be considered as a fractal system, consisting of different timescales controlled by a set of interacting processes. A fractal approach would provide a useful framework to identify the dominant mechanisms

controlling SSCs in rivers, and to characterise the connection between processes controlling SSC at the event scale and SS dynamics over longer timescales. Identifying the fractal power of a SS transport system could therefore be an appropriate starting point in developing transferrable process-based approaches to quantify and predict SSCs, as well as to develop targeted management policies. Towards this purpose, a possible road for future research would be to develop a classification system for SS transport dynamics in river systems in terms fractal power based on the dominant processes underlying SS transport.

3.6 Acknowledgements and data statement

This research was funded by an industrial PhD studentship supported by Cranfield University, Leeds City Council and Ove Arup and Partners Limited.

3.7 References

Ahn, K.-H., Yellen, B., Steinscheider, S., 2017. Dynamic linearmodels to explore time-varying suspended sediment-discharge rating curves. Water Resour. Res. 53, 5375–5377. doi:10.1002/2013WR014979.Reply

Asselman, N.E.M., 2000. Fitting and interpretation of sediment rating curves. J. Hydrol. 234, 228–248. doi:10.1016/S0022-1694(00)00253-5

Belmont, P., Gran, K.B., Schottler, S.P., Wilcock, P.R., Day, S.S., Jennings, C., Lauer, J.W., Viparelli, E., Willenbring, J.K., Engstrom, D.R., Parker, G., 2011. Large shift in source of fine sediment in the upper Mississippi River. Environ. Sci. Technol. 45, 8804–8810. doi:10.1021/es2019109

Bilotta, G.S., Brazier, R.E., 2008. Understanding the influence of suspended solids on water quality and aquatic biota. Water Res. 42, 2849–2861. doi:10.1016/j.watres.2008.03.018

Bilotta, G.S., Burnside, N.G., Cheek, L., Dunbar, M.J., Grove, M.K., Harrison, C., Joyce, C., Peacock, C., Davy-Bowker, J., 2012. Developing environment-specific water quality guidelines for suspended particulate matter. Water Res. 46, 2324–2332. doi:10.1016/j.watres.2012.01.055

Blöschl, G., 2006. Hydrologic synthesis: Across processes, places, and scales. Water Resour. Res. 42, 2–4. doi:10.1029/2005WR004319

Blöschl, G., Sivapalan, M., 1995. Scale issues in hydrological modelling: A review. Hydrol. Process. 9, 251–290. doi:10.1002/hyp.3360090305

Boyd, D.S., Almond, S., Dash, J., Curran, P.J., Hill, R.A., 2011. Phenology of vegetation in southern england from envisat meris terrestrial chlorophyll index (MTCI) data. Int. J. Remote Sens. 32, 8421–8447. doi:10.1080/01431161.2010.542194

Bracken, L.J., Turnbull, L., Wainwright, J., Bogaart, P., 2015. Sediment connectivity: a framework for understanding sediment transfer at multiple scales. Earth Surf. Process. Landforms 40, 177–188. doi:10.1002/esp.3635

Carter, J., Owens, P.N., Walling, D.E., Leeks, G.J.L., 2003. Fingerprinting suspended sediment sources in a large urban river system. Sci. Total Environ. 314–316, 513–534. doi:10.1016/S0048-9697(03)00071-8

Carter, J., Walling, D.E., Owens, P.N., Leeks, G.J.L., 2006. Spatial and temporal variability in the concentration and speciation of metals in suspended sediment transported by the River Aire, Yorkshire, UK. Hydrol. Process. 20, 3007–3027. doi:10.1002/hyp.6156

Centre for Ecology and Hydrology, 2017. Daily Flow Data Aire at Armley [WWW Document]. URL http://nrfa.ceh.ac.uk/data/station/info/27028

Cobaner, M., Unal, B., Kisi, O., 2009. Suspended sediment concentration estimation by an adaptive neuro-fuzzy and neural network approaches using hydro-meteorological data. J. Hydrol. 367, 52–61. doi:10.1016/j.jhydrol.2008.12.024

Collins, A.L., Walling, D.E., Webb, L., King, P.L., 2010. Apportioning catchment scale sediment sources using a modified composite fingerprinting technique incorporating property weightings and prior information. Geoderma 155, 249–261. doi:10.1016/j.geoderma.2009.12.008

Dark, S.J., Bram, D., 2007. The modifiable areal unit problem (MAUP) in physical geography. Prog. Phys. Geogr. 31, 471–479. doi:10.1177/0309133307083294

De Vente, J., Poesen, J., Arabkhedri, M., Verstraeten, G., 2007. The sediment delivery problem revisited. Prog. Phys. Geogr. 31, 155–178. doi:10.1177/0309133307076485

Dominic, J.A., Aris, A.Z., Sulaiman, W.N.A., 2015. Factors controlling the suspended sediment yield during rainfall events of dry and wet weather conditions in a tropical urban catchment. Water Resour. Manag. 29, 4519–4538.

Evans, R., Brazier, R., 2005. Evaluation of modelled spatially distributed predictions of soil erosion by water versus field-based assessments. Environ. Sci. Policy 8, 493–501. doi:10.1016/j.envsci.2005.04.009

Fan, X., Shi, C., Zhou, Y., Shao, W., 2012. Sediment rating curves in the Ningxia-Inner Mongolia reaches of the upper Yellow River and their implications. Quat. Int. 282, 152–162. doi:10.1016/j.quaint.2012.04.044

Feather, N., Caldwell, P., 2007. Yorkshire Water's Large FFD Scheme Introduction to £ 220m Freshwater Fish Directive Programme.

Ferguson, R.I., 1985. River Loads Underestimated by Rating Curves. Water Resour. Res. 22, 0043–1397.

Ferguson, R.I., 1981. Channel forms and channel changes, in: Lewin, J. (Ed.), British Rivers. Allen and Unwin, London, pp. 90–125.

Foster, I.D.L., Lees, J.A., 1999. Changing headwater suspended sediment yields in the LOIS catchments over the last century: A paleolimnological approach. Hydrol. Process. 13, 1137–1153. doi:10.1002/(SICI)1099-1085(199905)13:7<1137::AID-HYP794>3.0.CO;2-M

Francke, T., Lopez-Tarazon, J.A., Vericat, D., Bronstert, A., Batalla, R.J., 2008. Flood-based analysis of high-magnitude sediment transport using a non-parametric method. Earth Surf.

Process. Landforms 33, 2064–2077. doi:10.1002/esp. 1654

Franz, C., Makeschin, F., Weiß, H., Lorz, C., 2014. Sediments in urban river basins: identification of sediment sources within the Lago Paranoá catchment, Brasilia DF, Brazil - using the fingerprint approach. Sci. Total Environ. 466–467, 513–23. doi:10.1016/j.scitotenv.2013.07.056

Fryirs, K.A., 2013. (Dis)Connectivity in catchment sediment cascades: A fresh look at the sediment delivery problem. Earth Surf. Process. Landforms 38, 30–46. doi:10.1002/esp.3242

Fryirs, K.A., Brierley, G.J., 2013. Geomorphic analysis of river systems: An approach to reading the landscape. Wiley-Blackwell, West Sussex.

Gao, P., 2008. Understanding watershed suspended sediment transport. Prog. Phys. Geogr. 32, 243–263. doi:10.1177/0309133308094849

Grabowski, R.C., Gurnell, A.M., 2016. Diagnosing problems of fine sediment delivery and transfer in a lowland catchment. Aquat. Sci. 78, 95–106. doi:10.1007/s00027-015-0426-3

Halley, J.M., Hartley, S., Kallimanis, A.S., Kunin, W.E., Lennon, J.J., Sgardelis, S.P., 2004. Uses and abuses of fractal methodology in ecology. Ecol. Lett. 7, 254–271. doi:10.1111/j.1461-0248.2004.00568.x

Harvey, A.M., 2002. Effective timescales of coupling within fluvial systems. Geomorphology 44, 175–201. doi:10.1016/S0169-555X(01)00174-X

Hollister, J.W., August, P. V., Paul, J.F., 2008. Effects of spatial extent on landscape structure and sediment metal concentration relationships in small estuarine systems of the United States' Mid-Atlantic Coast. Landsc. Ecol. 23, 91–106. doi:10.1007/s10980-007-9143-1

Horowitz, A.J., 2009. Monitoring suspended sediments and associated chemical constituents in urban environments: lessons from the city of Atlanta, Georgia, USA Water Quality Monitoring Program. J. Soils Sediments 9, 342–363. doi:10.1007/s11368-009-0092-y

Horowitz, A.J., 2008. Determining annual suspended sediment and sediment-associated trace element and nutrient fluxes. Sci. Total Environ. 400, 315–43. doi:10.1016/j.scitotenv.2008.04.022

Horowitz, A.J., 2003. An evaluation of sediment rating curves for estimating suspended sediment concentrations for subsequent flux calculations. Hydrol. Process. 17, 3387–3409. doi:10.1002/hyp.1299

Horowitz, A.J., Clarke, R.T., Merten, G.H., 2014. The effects of sample scheduling and sample numbers on estimates of the annual fl uxes of suspended sediment in fl uvial systems.

Hydrol. Process. doi:10.1002/hyp

Huisman, N.L.H., Karthikeyan, K.G., Lamba, J., Thompson, A.M., Peaslee, G., 2013. Quantification of seasonal sediment and phosphorus transport dynamics in an agricultural watershed using radiometric fingerprinting techniques. J. Soils Sediments 13, 1724–1734. doi:10.1007/s11368-013-0769-0

Janes, V., Nicholas, A., Collins, A., Quine, T., 2017. Analysis of fundamental physical factors influencing channel bank erosion: results for contrasting catchments in England and Wales. Environ. Earth Sci. 76. doi:10.1007/s12665-017-6593-x

Jiang, B., Brandt, S., 2016. A Fractal Perspective on Scale in Geography. ISPRS Int. J. Geo-Information 5, 95. doi:10.3390/ijgi5060095

Karaman, I., Qannari, E.M., Martens, H., Hedemann, M.S., Knudsen, K.E.B., Kohler, A., 2013. Comparison of Sparse and Jack-knife partial least squares regression methods for variable selection. Chemom. Intell. Lab. Syst. 122, 65–77. doi:10.1016/j.chemolab.2012.12.005

Kisi, O., 2005. Suspended sediment estimation using neuro-fuzzy and neural network approaches. Hydrol. Sci. J. 50, 683–696. doi:10.1623/hysj.2005.50.4.683

Krueger, T., Quinton, J.N., Freer, J.E., Macleod, C.J.A., Bilotta, G.S., Brazier, R.E., Butler, P., Haygarth, P.M., 2009. Uncertainties in data and models to describe event dynamics of agricultural sediment and phosphorus transfer. J. Environ. Qual. 38, 1137–1148. doi:10.2134/jeq2008.0179

Lawler, D.M., Petts, G.E., Foster, I., Harper, S., 2006. Turbidity dynamics during spring storm events in an urban headwater river system: the Upper Tame, West Midlands, UK. Sci. Total Environ. 360, 109–26. doi:10.1016/j.scitotenv.2005.08.032

Lloyd, C.E.M., Freer, J.E., Johnes, P.J., Collins, A.L., 2016. Using hysteresis analysis of high-resolution water quality monitoring data, including uncertainty, to infer controls on nutrient and sediment transfer in catchments. Sci. Total Environ. 543, 388–404. doi:10.1016/j.scitotenv.2015.11.028

Lohani, A.K., Goel, N.K., Bhatia, K.K.S., 2007. Deriving stage–discharge–sediment concentration relationships using fuzzy logic. Hydrol. Sci. J. 52, 793–807. doi:10.1623/hysj.52.4.793

Marsalek, J., Viklander, M., 2010. Controlling contaminants in urban stormwater: Linking environmental science and policy, in: Jan Lundqvist (Ed.), On the Water Front. World Water Week 2010, Stockholm.

Martens, H., Martens, M., 2000. Modified Jack-knife estimation of parameter uncertainty in bilinear modelling by partial least squares regression (PLSR). Food Qual. Prefer. 11, 5–16.

doi:10.1016/S0950-3293(99)00039-7

McDonnell, J.J., Sivapalan, M., Vache, K., Dunn, S., Grant, G., Haggerty, R., Hinz, C., Hooper, R., Kirchner, J., Roderick, M.L., Selker, J., Weiler, M., 2007. Moving beyond heterogeneity and process complexity: A new vision for watershed hydrology. Water Resour. Res. 43, 1–6. doi:10.1029/2006WR005467

McDowell, R.W., Sharpley, A.N., 2002. The effect of antecedent moisture conditions on sediment and phosphorus loss during overland flow: Mahantango Creek catchment, Pennsylvania, USA. Hydrol. Process. 16, 3037–3050. doi:10.1002/hyp.1087

Medina-Cobo, M.T., Garcia-Marin, A.P., Estevez, J., Ayuso-Munoz, J.L., 2016. The identification of an appropriate Minimum Inter-event Time (MIT) based on multifractal characterization of rainfall data series. Hydrol. Process. 30, 3507–3517. doi:10.1002/hyp.10875

Morton, D., Rowland, C., Wood, C., Meek, L., Marston, C., Smith, G., Wadsworth, R., Simpson, I.C., 2011. Final Report for LCM2007 - the new UK Land Cover Map. Countryside Survey Technical Report No. 11/07.

Ogunbadewa, E.Y., 2012. Tracking seasonal changes in vegetation phenology with a SunScan canopy analyzer in northwestern England. Forest Sci. Technol. 8, 161–172. doi:10.1080/21580103.2012.704971

Old, G.H., Leeks, G.J.L., Packman, J.C., Smith, B.P.G., Lewis, S., Hewitt, E.J., 2006. River flow and associated transport of sediments and solutes through a highly urbanised catchment, Bradford, West Yorkshire. Sci. Total Environ. 360, 98–108. doi:10.1016/j.scitotenv.2005.08.028

Old, G.H., Leeks, G.J.L., Packman, J.C., Smith, B.P.G., Lewis, S., Hewitt, E.J., Holmes, M., Young, A., 2003. The impact of a convectional summer rainfall event on river flow and fine sediment transport in a highly urbanised catchment: Bradford, West Yorkshire. Sci. Total Environ. 314–316, 495–512. doi:10.1016/S0048-9697(03)00070-6

Onderka, M., Krein, A., Wrede, S., Martínez-Carreras, N., Hoffmann, L., 2012. Dynamics of storm-driven suspended sediments in a headwater catchment described by multivariable modeling. J. Soils Sediments 12, 620–635. doi:10.1007/s11368-012-0480-6

Owens, P.N., Batalla, R.J., Collins, A.J., Gomez, B., Hicks, D.M., Horowitz, A.J., Kondolf, G.M., Marden, M., Page, M.J., Peacock, D.H., Petticrew, E.L., Salomons, W., Trustrum, N.A., 2005. Fine-grained sediment in river systems: environmental significance and management issues. River Res. Appl. 21, 693–717. doi:10.1002/rra.878

Park, E., Latrubesse, E.M., 2014. Modeling suspended sediment distribution patterns of the Amazon River using MODIS data. Remote Sens. Environ. 147, 232–242.

doi:10.1016/j.rse.2014.03.013

Perks, M.T., Owen, G.J., Benskin, C.M.H., Jonczyk, J., Deasy, C., Burke, S., Reaney, S.M., Haygarth, P.M., 2015. Dominant mechanisms for the delivery of fine sediment and phosphorus to fluvial networks draining grassland dominated headwater catchments. Sci. Total Environ. 523, 178–190. doi:10.1016/j.scitotenv.2015.03.008

Perks, M.T., Warburton, J., Bracken, L.J., Reaney, S.M., Emery, S.B., Hirst, S., 2017. Use of spatially distributed time-integrated sediment sampling networks and distributed fine sediment modelling to inform catchment management. J. Environ. Manage. 1–10. doi:10.1016/j.jenvman.2017.01.045

Phillips, J.D., 2003. Sources of nonlinearity and complexity in geomorphic systems. Prog. Phys. Geogr. 27, 1–23. doi:10.1191/0309133303pp340ra

Pohlert, T., 2015. Non-Parametric Trend Tests and Change-Point Detection 1–8.

Poulenard, J., Perrette, Y., Fanget, B., Quetin, P., Trevisan, D., Dorioz, J.M., 2009. Infrared spectroscopy tracing of sediment sources in a small rural watershed (French Alps). Sci. Total Environ. 407, 2808–19. doi:10.1016/j.scitotenv.2008.12.049

Raven, E.K., Lane, S.N., Bracken, L.J., 2010. Understanding sediment transfer and morphological change for managing upland gravel-bed rivers. Prog. Phys. Geogr. 34, 23–45. doi:10.1177/0309133309355631

Rickson, R.J., 2014. Can control of soil erosion mitigate water pollution by sediments? Sci. Total Environ. 468–469, 1187–1197. doi:10.1016/j.scitotenv.2013.05.057

Rodriguez-Iturbe, I., Rinaldo, A., 2001. Fractal river basins: Chance and self-organization. Cambridge University Press, Cambridge.

Rovira, A., Ibáñez, C., Martín-Vide, J.P., 2015. Suspended sediment load at the lowermost Ebro River (Catalonia, Spain). Quat. Int. 388, 188–198. doi:10.1016/j.quaint.2015.05.035

Seeger, M., Errea, M.P., Beguería, S., Arnáez, J., Martí, C., García-Ruiz, J.M., 2004. Catchment soil moisture and rainfall characteristics as determinant factors for discharge/suspended sediment hysteretic loops in a small headwater catchment in the Spanish pyrenees. J. Hydrol. 288, 299–311. doi:10.1016/j.jhydrol.2003.10.012

Sivakumar, B., 2001. Is a chaotic multi-fractal approach for rainfall possible? Hydrol. Process. 15, 943–955. doi:10.1002/hyp.260

Skarbøvik, E., Stålnacke, P., Bogen, J., Bønsnes, T.E., 2012. Impact of sampling frequency on mean concentrations and estimated loads of suspended sediment in a Norwegian river: Implications for water management. Sci. Total Environ. 433, 462–471.

doi:10.1016/j.scitotenv.2012.06.072

Skøien, J.O., Blöschl, G., Western, A.W., 2003. Characteristic space scales and timescales in hydrology. Water Resour. Res. 39. doi:10.1029/2002WR001736

Smith, H.G., Dragovich, D., 2009. Interpreting sediment delivery processes using suspended sediment-discharge hysteresis patterns from nested upland catchments, south-eastern Australia. Hydrol. Process. 23, 2416–2426. doi:10.1002/hyp

Stevens, A., Lopez, L.R., 2015. A Guide to Diffuse Reflectance Spectroscopy & Multivariate Calibration with the R Statistical Software.

Sun, L., Yan, M., Cai, Q., Fang, H., 2015. Suspended sediment dynamics at different time scales in the Loushui River, south-central China. Catena Published. doi:10.1016/j.catena.2015.02.014

Taylor, K.G., Owens, P.N., 2009. Sediments in urban river basins: a review of sediment–contaminant dynamics in an environmental system conditioned by human activities. J. Soils Sediments 9, 281–303. doi:10.1007/s11368-009-0103-z

Tena, A., Vericat, D., Batalla, R.J., 2014. Suspended sediment dynamics during flushing flows in a large impounded river (the lower River Ebro). J. Soils Sediments 14, 2057–2069. doi:10.1007/s11368-014-0987-0

Tetzlaff, D., McDonnell, J.J., Uhlenbrook, S., McGuire, K.J., Bogaart, P.W., Naef, F., Baird, A.J., Dunn, S.M., Soulsby, C., 2008. Conceptualizing catchment processes: Simply too complex? Hydrol. Process. 22, 1727–1730. doi:10.1002/hyp.7069

Troch, P.A., Carrillo, G.A., Heidbüchel, I., Rajagopal, S., Switanek, M., Volkmann, T.H.M., Yaeger, M., 2009. Dealing with landscape heterogeneity in watershed hydrology: A review of recent progress toward new hydrological theory. Geogr. Compass 3, 375–392. doi:10.1111/j.1749-8198.2008.00186.x

Van Nieuwenhuyse, B.H.J., Antoine, M., Wyseure, G., Govers, G., 2011. Pattern-process relationships in surface hydrology: Hydrological connectivity expressed in landscape metrics. Hydrol. Process. 25, 3760–3773. doi:10.1002/hyp.8101

Vanmaercke, M., Ardizzone, F., Rossi, M., Guzzetti, F., 2016. Exploring the effects of seismicity on landslides and catchment sediment yield: An Italian case study. Geomorphology. doi:10.1016/j.geomorph.2016.11.010

Vanmaercke, M., Poesen, J., Verstraeten, G., de Vente, J., Ocakoglu, F., 2011. Sediment yield in Europe: Spatial patterns and scale dependency. Geomorphology 130, 142–161. doi:10.1016/j.geomorph.2011.03.010

Vercruysse, K., Grabowski, R.C., Rickson, R.J., 2017. Suspended sediment transport dynamics in rivers: Multi-scale drivers of temporal variation. Earth-Science Rev. 166, 38–52. doi:10.1016/j.earscirev.2016.12.016

Walling, D.E., 2009. The impact of global change on erosion and sediment transport by rivers: Current progress and future challenges, The United Nations World Water Development Report 3. Paris.

Walling, D.E., Owens, P.N., Carter, J., Leeks, G.J.L., Lewis, S., Meharg, A.A., Wright, J., 2003. Storage of sediment-associated nutrients and contaminants in river channel and floodplain systems. Appl. Geochemistry 18, 195–220. doi:10.1016/S0883-2927(02)00121-X

Walling, Owens, P.N., Foster, I.D.L., Lees, J.A., 2003. Changes in the fine sediment dynamics of the Ouse and Tweed basins in the UK over the last 100-150 years. Hydrol. Process. 17, 3245–3269. doi:10.1002/hyp.1385

Wheatley, M., Johnson, C., 2009. Factors limiting our understanding of ecological scale. Ecol. Complex. 6, 150–159. doi:10.1016/j.ecocom.2008.10.011

Wold, S., Sjostrom, M., Eriksson, L., 2001. PLS-regression : a basic tool of chemometrics. Chemom. Intell. Lab. Syst. 58, 109–130.

Wyatt, B.K., Greatorex-Davies, N.G., Bunce, R.G.H., Fuller, R.M., Hill, M.O., 1993. Comparison of land cover definitions. Countryside 1990 Series: Volume 3. London.

Zeiger, S., Hubbart, J.A., 2016. Quantifying suspended sediment flux in a mixed-land-use urbanizing watershed using a nested-scale study design. Sci. Total Environ. 542, 315–323. doi:10.1016/j.scitotenv.2015.10.096

Zhang, S., Lu, X.X., 2009. Hydrological responses to precipitation variation and diverse human activities in a mountainous tributary of the lower Xijiang, China. Catena 77, 130–142. doi:10.1016/j.catena.2008.09.001

Zhang, S., Mao, X., 2015. Hydrology, sediment circulation and long-term morphological changes in highly urbanized Shenzhen River estuary, China: A combined field experimental and modeling approach [WWW Document]. URL http://www.scopus.com/alert/results/record.url?AID=4225684&ATP=search&eid=2-s2.0-84940099673&origin=SingleRecordEmailAlert

Zhang, W., Yan, Y., Zheng, J., Li, L., Dong, X., Cai, H., 2009. Temporal and spatial variability of annual extreme water level in the Pearl River Delta region, China. Glob. Planet. Change 69, 35–47. doi:10.1016/j.gloplacha.2009.07.003

Zimmermann, A., Francke, T., Elsenbeer, H., 2012. Forests and erosion: Insights from a study of

suspended-sediment dynamics in an overland flow-prone rainforest catchment. J. Hydrol. 428–429, 170–181. doi:10.1016/j.jhydrol.2012.01.039

CHAPTER 4: IMPACT OF SEDIMENT SOURCE CLASSIFICATION ON SOURCE APPORTIONMENT WITH DRIFTS-BASED SEDIMENT FINGERPRINTING

Abstract

Sediment fingerprinting is a statistical method to estimate contributions of dominant sediment sources to river sediment based on source-specific sediment properties. Classification of potential sediment sources within the studied area is critical to the representativeness and usefulness of sediment fingerprinting results. Yet, there is still considerable uncertainty around how source classification impacts source apportionment. Sediment fingerprinting approaches using independent models for each source individually, are potentially very valuable in this context. If all independently estimated source contributions sum up to approximately 100%, it can theoretically indicate that all dominant sediment sources were classified. However, because independent models also have different confidence intervals, it is impossible to confirm the representativeness of the source classification based on this assumption. This study aimed to improve the application of sediment fingerprinting by investigating how the reliability and interpretation of the source apportionment is influenced by a priori sediment source classification using sediment fingerprinting based on Diffuse Reflectance Infrared Fourier Transform spectrometry. To this end, a study design was developed to assess how source classification affects the precision of source apportionment by systematically excluding individual sediment sources from the classification and model calibration. The approach was applied to the catchment of the River Aire, UK. Five potential sediment source were classified: grassland topsoil in three lithological areas (limestone, millstone grit and coal measures), eroding riverbanks and urban street dust. Dominant sediment sources were topsoil from the limestone area (45 ± 12 %) and urban street dust (43 ± 10 %). Topsoil from the millstone and coals area contributed on average 19 ± 13 % and 14 ± 10 % respectively, and eroding riverbanks 16 ± 18%. Model testing showed that for multiple classifications, the sum of source contributions fluctuated around 100%. Omitting redundant sediment sources (e.g. coals grassland) have a limited impact on source apportionment (i.e. no change in other source contributions). Removing dominant, well-discriminated sources (e.g. limestone grassland) increased the contribution of poorly-discriminated sources (i.e. riverbank), while removing important, but poorly-discriminated sources (e.g. riverbank) increased contributions of all sources. The findings demonstrate that using independent models is not sufficient to evaluate the representativeness of source classification. The findings also confirm previous research that call for the development of standard approaches for sediment source classification and discrimination to accurately represent the sediment sources in the river.

4.1 Introduction

Despite being a natural part of rivers, SS (< 63 µm) in rivers can have a detrimental impact by degrading the ecological, biochemical and physical state of river systems, while also causing increased costs related to water treatment and infrastructural maintenance (Bilotta and Brazier, 2008; Horowitz, 2009; Taylor and Owens, 2009). Therefore, monitoring SS transport and sources is essential to improve scientific understanding on sediment transfer at the catchment scale, and to develop appropriate management strategies.

Sediment fingerprinting is an approach to estimate sediment source contributions to the river sediment, based on sediment properties associated to the different origins of sediment particles (Davis et al., 2009; Walling, 2013). SS particles in rivers mainly originate from soil erosion on land, but particles from other sources can also enter the river, e.g. street dust, solids from sewer overflows, and road construction works (Mukundan et al., 2012; Taylor and Owens, 2009). Therefore, the composition of sediment particles is defined by their origin, i.e. controlled by geology, climate, hydrology, land cover, and anthropogenic activities (e.g. particle size distribution, clay mineralogy, organic matter content) (Koiter et al., 2013). As a result, a sediment sample from a river represents a mixture of particles with different characteristics depending on their origin, and sediment from a particular source can be characterised by a "fingerprint", i.e. a combination of biogeochemical and/or physically-based properties specific to their origin within the river catchment. These fingerprints are used to develop statistical models to estimate contributions of sediment sources, i.e. to un-mix a sediment sample from the river in the contribution of its sources.

Sediment fingerprinting approaches have been developed using various sediment properties (e.g. geochemical elements, fallout radionuclides, magnetic properties, compound-specific stable isotopes) which have been described and discussed in multiple review studies (Collins et al., 2017; Collins and Walling, 2004; Haddadchi et al., 2013; Koiter et al., 2013; Mukundan et al., 2012). Common techniques to identify sediment properties are loss-on-ignition (LOI), colorimetry, acid digestion, inductively coupled plasma-optical emission

spectrometry (ICP-OAS) and atomic absorption spectrometry (AAS) (Cooper et al., 2014a; Laceby and Olley, 2015; Legout et al., 2013; Martínez-Carreras et al., 2010b; Poulenard et al., 2009). However, these techniques requiere relatively large sample volumes (> 100 mg) which are often not available when working with SS, involves extensive sample preparation (e.g. acid digestion and packing), and tend to be expensive to run (Cooper et al., 2014b). More recently, Diffuse Reflectance Infrared Fourier Transform Spectrometry (DRIFTS) based sediment fingerprinting has been developed and proved to be a cost- and time-efficient alternative to gain sediment source information at a high temporal resolution because it requires smaller sample volumes (~15 mg) with very little preparation, and measurements are done in seconds (Cooper et al., 2014b; Poulenard et al., 2009).

However, important challenges remain towards widespread application of sediment fingerprinting for scientific and management purposes. Previous studies have stressed the need to establish standardised procedures to increase the repeatability of the approach and to increase the reliability of the source apportionment (Collins et al., 2017; Davis and Fox, 2009; Haddadchi et al., 2013; Mukundan et al., 2012; Owens et al., 2016). There is a need to thoroughly understand the uncertainties related to sediment fingerprinting and how those uncertainties influence the precision of the sediment source apportionment. Only when all sources of uncertainty are considered, it is possible to reliably use the source information to improve scientific understanding of sediment transport processes (Fryirs and Brierley, 2013), and develop targeted sediment management solutions (Collins et al., 2017).

To this end, statistical model uncertainty associated with sediment fingerprinting has been reduced significantly through advancements in statistical un-mixing models (Koiter et al., 2013), for example by using Bayesian uncertainty estimation frameworks (e.g. Cooper et al., 2014a; Moore and Semmens, 2008; Nosrati et al., 2014) or Markov Chain Monte Carlo algorithms (e.g. Collins et al., 2010; Palazón et al., 2015; Wilkinson et al., 2015). Other studies have investigated the impact of sediment properties variations (e.g. particle size distributions) on

sediment fingerprinting results (Koiter et al., 2013; Laceby et al., 2017), and compared different measuring techniques (e.g. DRIFTS versus ICP) (Legout et al., 2013; Martínez-Carreras et al., 2010b; Tiecher et al., 2016; Verheyen et al., 2014). However, little attention has been given to source classification and its subsequent effect on the reliability of the source apportionment. A study testing the impact of sediment source group classification on the accuracy of geochemically-based sediment fingerprinting, demonstrated that small differences in the degree of discrimination between sediment source groups and a high within-source variability can result in significant uncertainty associated with the source apportionment (Pulley et al., 2017a). It is therefore necessary to determine if the sediment source groups are likely to be representative of the actual sediment sources (Collins et al., 2017; Pulley et al., 2017b). This need is especially important in sediment fingerprinting based on experimental mixtures of the potential sediment sources to calibrate the un-mixing models (e.g. in DRIFTS-based sediment fingerprinting) (Martínez-Carreras et al., 2010a; Poulenard et al., 2009; Tiecher et al., 2016). By doing so, it is assumed that the mixtures are an accurate representation of the sediment samples from the river. However, as with many classification systems, the mixtures are inevitably a simplification of reality and may lead to misinterpretation of the observed patterns (Collins and Walling, 2004; Dark and Bram, 2007).

To the author's knowledge, no study has explicitly tested the impact of the source classification on source apportionment in the context of sediment fingerprinting with experimental mixtures. Therefore, this study aims to improve the application of sediment fingerprinting by investigating how the reliability and interpretation of the source apportionment is influenced by *a priori* sediment source classification using DRIFTS-based sediment fingerprinting with experimental mixtures. To this end, a study design was developed to assess how source classification affects the precision of source apportionment by systematically excluding individual sediment sources from the classification and model calibration. The approach was applied to the catchment of the River Aire, UK.

4.2 Methods

4.2.1 Study area

The River Aire has a catchment area of 879 km^2 (upstream on Leeds: 690km^2) with a mean annual water discharge of 15 (± 3.3 SE) m^3 s^{-1} and a mean rainfall of 1018 (± 210 SE) mm $year^{-1}$ (1960-2017). The geology of the catchment is entirely Carboniferous with a large area in the lower reaches defined by the Coal Measures (272 km^2; mixture of siltstone, mudstone and sandstone); an area in the middle with Millstone Grit (402 km^2; sandstone); and the higher part of the catchment is mainly characterised by limestone and shale formations (205 km^2) (British Geological Survey, 2016) (Figure 4-1). The upper part of the catchment is characterised by stagnohumic and stagnogley soils, while brown earths and pelo-stagnogley soils are dominant in the middle and lower parts (Carter et al., 2003). Land cover in the catchment is predominantly grassland (59%) and urbanised area (25%), and the rest of the catchment is covered with moorland (12%) and scattered arable land (4%).

4.2.2 Sediment data and sampling

River sediment

Between June 2015 and March 2017, SS samples (200) were collected with a depth-integrating SS sampler during individual precipitation events at a single location in the river (Figure 4-1). The median particle size of SS in the River Aire ranges between 5.2 and 13.3 µm (Carter et al., 2006; Walling et al., 2003). Additionally, to investigate the contribution of sediment sources to the fine sediment along the profile of the river, five grab samples were taken (between 16-18/06/2016) with a metal bucket from the channel bed (bed sediment, BS) (Figure 4-1).

Sediment source material

In line with a previous sediment fingerprinting study in the upper reaches of the River Aire based on geochemical properties (Carter et al., 2003), five potential sediment sources were classified: uncultivated grassland topsoils from the limestone and shale area (“limestone”, L), the Millstone Grit area (“millstone”, M)

and the Coal Measures area (“coals”, C), eroding riverbanks (“riverbank”, R) and urban street dust (“urban”, U).

Locations for source material sampling were identified based on accessibility and targeted to the areas most prone to erosion based on the Revised Universal Soil Loss Equation (RUSLE) (Renard et al., 1991). A total of 117 source samples (around 200 g for each sample) was taken. From each soil sampling location, three subsamples within one square meter were taken. Samples from grassland topsoils (21 locations) and subsoil samples from eroding riverbanks (12 locations) were collected using a non-metallic trowel (Figure 4-1). For the topsoil samples, only the top 5 cm of the topsoil was sampled to ensure that only material likely to be eroded and transported to the river was collected (Carter et al., 2003; Cooper et al., 2014a; Martínez-Carreras et al., 2010b; Pulley et al., 2015). Street dust samples (18 locations) were collected along road drains using a dustpan and brush (or trowel when wet) (Cooper et al., 2014a; Pulley et al., 2015).

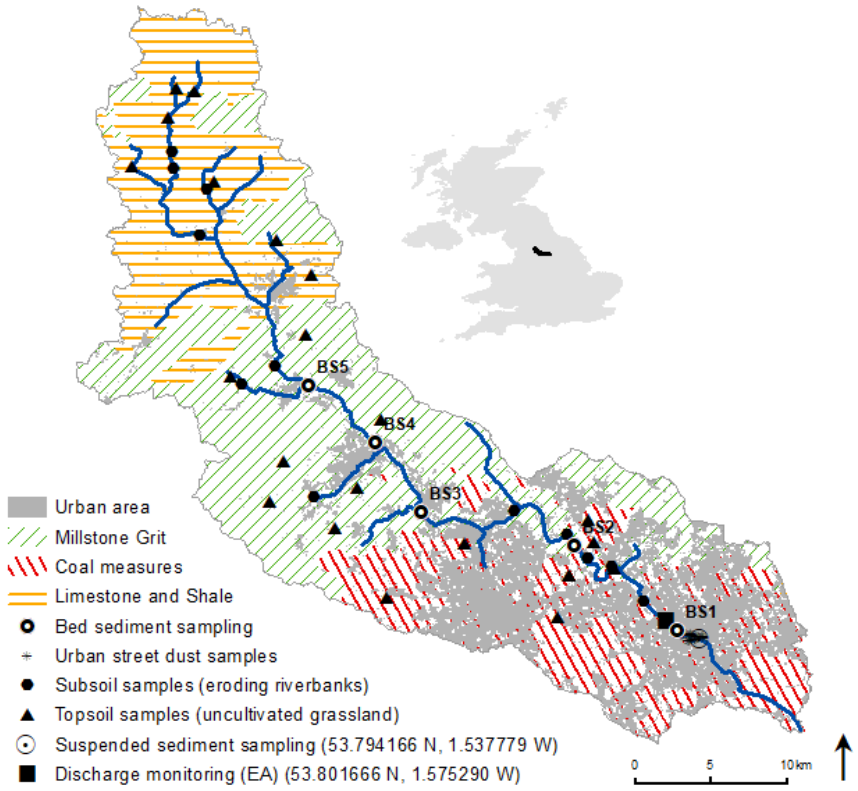

Figure 4-1: Aire Catchment (UK), including locations for suspended sediment, channel bed sediment, and sediment source sampling (land cover data: Morton et al. (2011)).

4.2.3 DRIFTS-based sediment fingerprinting

The sediment fingerprinting technique applied in this study is largely based on the approach developed by Poulenard et al. (2009) and consists of three steps: (i) analysis of sediment samples with DRIFTS; (ii) sediment source discrimination; and (iii) development of statistical un-mixing models to estimate source contributions to the SS.

DRFITS analysis of sediment samples

BS and sediment source samples were wet sieved to retain the < 63 µm fraction to reduce the effect of particle size variations on source attribution and spectral distortion (Laceby et al., 2017; Poulenard et al., 2009). All sediment samples (SS, BS and sources) were then filtered on quartz fibre filters and oven-dried for two hours at 105˚C (Cooper et al., 2014a; Pulley et al., 2015). The filters containing sediment were scanned with DRIFTS using a Bruker Vector 22 and a Perkin Elmer Spectrum Spotlight 200 spectrometer at a 4 cm^{-1} resolution across the 4000-400 cm^{-1} spectrum with 32 co-added scans per spectrum. The data was processed using the software provided by the manufacturer of the spectrometers. A minimum of 20 mg of sediment was required on the filters to exclude interference of the filter.

The average spectra of the three subsamples of the source material were used for further analysis (Brosinsky et al., 2014; Evrard et al., 2013; Poulenard et al., 2012, 2009). Pre-processing techniques were applied on the DRIFTS spectra to reduce additional noise. Mean-centering and filtering using a Savitzky-Golay algorithm were applied, as a combination of those techniques has been shown to improve results in similar studies (Cooper et al., 2014b; Martínez-Carreras et al., 2010a). To avoid CO_2 interference in the area between 2400 and 2300 cm^{-1}, only the ranges 3800–2400 cm^{-1} and 2300–650 cm^{-1} where used for further statistical analysis (Poulenard et al., 2009).

Sediment source discrimination

Visual interpretation

The DRIFTS spectra were examined visually to assess any major differences between the source samples. DRIFTS spectra of soils are controlled by the differential reflectance and absorbance characteristics of sediment properties, and especially characterised by absorption peaks caused by inorganic fractions such as clays, silica and carbonates in combination with organic matter (Reeves III, 2012). However, due to spectral distortions and overlapping of absorption peaks, the absorption peaks of the spectra cannot be used directly to quantify the sediment composition without calibration with quantitative geochemical data (which was not available in this study). Therefore, inspection of the spectra was only used to provide semi-quantitative information on the sediment composition (Poulenard et al., 2012; Reeves III, 2010).

Discriminant analysis

Statistical techniques were applied to test whether the source samples can be discriminated based on their respective DRIFTS spectra. First, a principal component analysis (PCA) was performed on the processed DRIFTS spectra to determine the natural clustering of the samples. Secondly, a discriminant analysis (DA) based on Mahalanobis Distances (MD) was performed using the PCA scores as input data (Poulenard et al., 2009; Stevens and Lopez, 2015). MDs are expressed in standard deviations and therefore provide a statistical measure to assess whether the DRIFTS spectra of source samples are significantly different from each other. Based on the results of the DA, a set of sediment sources is retained for analysis.

Un-mixing model development and evaluation

To estimate sediment source contributions directly from the DRIFTS spectra of SS and BS samples, statistical un-mixing models were calibrated with experimental mixtures.

A total of 54 experimental mixtures was prepared containing variable, known quantities of soil from the sediment sources (Table 4-1). This results in a

multivariate regression problem between the processed DRIFTS spectra (X predictors) of the experimental mixtures and the weight contributions of the sediment sources (dependent Y variables). Spectral data are highly correlated and noisy, containing much more variables than samples, hence a simple multivariate regression is not suitable. Therefore, partial least squares regression (PLSR) was used because it is better able to handle this type of data (Karaman et al., 2013; Martens and Martens, 2000; Wold et al., 2001).

PLSR works by maximising the covariance between two datasets based on the respective scores (Stevens and Lopez, 2015). X-scores ($\boldsymbol{U}$) are computed as linear combinations of the original X variables with a set of weights $\boldsymbol{W}$ so that $\boldsymbol{X}$ can be expressed in terms of scores, loadings and residuals. The Y dataset is also decomposed in scores ($\boldsymbol{T}$) and loadings ($\boldsymbol{F}$), but in such a way that the covariance between the X-scores $\boldsymbol{U}$ and the Y-scores $\boldsymbol{T}$ is maximised. As a result, X-scores can serve as good predictors of Y, so that a multivariate regression can be approached with $\mathbf{W} * \mathbf{F}$ as regression coefficients (Wold et al., 2001).

The mixture dataset was divided into two parts: 75% for calibration and 25% for validation. To randomly select the calibration set, a Kennard-Stone sampling algorithm was used (Poulenard et al., 2009). To avoid under- or overfitting of the model, the best compromise between the description of the calibration set and the model predictive power was determined by identifying the appropriate number of PLSR components based on leave-one-out cross validation in the calibration phase (Evrard et al., 2013; Poulenard et al., 2012, 2009; Wold et al., 2001). The optimal number of components is the number with the lowest root mean squared error (RMSE) of cross validation (Martens and Martens, 2000; Poulenard et al., 2009; Wold et al., 2001). Five separate PLSR models were developed (i.e. one for each source): $PLSR_L$ (limestone), $PLSR_M$ (millstone), $PLSR_C$ (coals), $PLSR_R$ (riverbank), and $PLSR_U$ (urban street dust). Standard errors of prediction (RMSEP) associated with the model estimates were calculated and expressed as 95% confidence intervals (Legout et al., 2013; Martínez-Carreras et al., 2010a; Poulenard et al., 2012).

Table 4-1: Set of experimental mixtures for mixing-model calibration

	Limestone	Millstone	Coals	Riverbank	Street dust
Mix1	25 %	25 %	25 %	25 %	
Mix2	25 %	25 %	25 %		25 %
Mix3	33 %	33 %	33 %		
Mix4	10 %	20 %	40 %	30 %	
Mix5	40 %	10 %	20 %	30 %	
Mix6	20 %	40 %	25 %		15 %
Mix7	10 %	40 %	20 %		30 %
Mix8	40 %	10 %	20 %		30 %
Mix9	20 %	40 %	25 %		15 %
Mix10	25 %	25 %		25 %	25 %
Mix11		25 %	25 %	25 %	25 %
Mix12	25 %		25 %	25 %	25 %
Mix13	20 %	30 %		30 %	20 %
Mix14		20 %	30 %	30 %	20 %
Mix15		60 %		20 %	20 %
Mix16		30 %	30 %	40 %	
Mix17	50 %	25 %		25 %	
Mix18	20 %	20 %			60 %
Mix19		20 %	40 %	40 %	
Mix20		40 %	50 %		10 %
Mix21		80 %	20 %		
Mix22	80 %	20 %			
Mix23	10 %	90 %			
Mix24		10 %	90 %		
Mix25				75 %	25 %
Mix26				25 %	75 %
Mix27	100 %				
Mix28	10 %			50 %	40 %
Mix29	80 %			15 %	5 %
Mix30	60 %			10 %	30 %
Mix31	10 %			90 %	
Mix32	90 %			10 %	
Mix33	10 %				90 %
Mix34	90 %				10 %
Mix35		100 %			
Mix36		10 %		50 %	40 %
Mix37		85 %		15 %	
Mix38		60 %		15 %	25 %
Mix39		10 %		90 %	
Mix40		90 %		10 %	
Mix41		10 %			90 %
Mix42		90 %			10 %
Mix43		100 %			
Mix44		50 %		40 %	10 %
Mix45		80 %		10 %	10 %
Mix46		30 %		40 %	30 %
Mix47			100 %		
Mix48			10 %	50 %	40 %
Mix49			80 %	10 %	10 %
Mix50			60 %	10 %	30 %
Mix51			10 %	90 %	
Mix52			90 %	10 %	
Mix53			10 %		90 %
Mix54			90 %		10 %

4.2.4 Assessment of sediment source classification

If measurement errors and the intra-source variability of the DRIFTS spectra are minimal, the model RMSEP can be considered as a good estimate of the final uncertainty on the model output. However, this is only valid when the experimental mixtures are a good representation of the actual river sediment samples, i.e. when all dominant sediment sources were correctly identified and included into the model calibration (Collins and Walling, 2004; Davis and Fox, 2009; Haddadchi et al., 2013; Koiter et al., 2013).

The DRIFTS-PLSR models independently estimate source contributions (i.e. individual regression models for all sources). Therefore, a sum close to 100% of all estimated contributions is usually considered as an indication that all dominant sediment sources were correctly identified (Legout et al., 2013; Poulenard et al., 2012). However, variable confidence intervals are associated with the models, so that it remains unclear to what extent the deviation from 100% is caused by model uncertainties or the classification of sediment sources (i.e. whether a source is missing or redundant).

To test the impact of the *a priori* sediment source classification on the final model estimates, PLSR model-sets were developed, whereby individual sources were systematically excluded from the model calibration (Table 4-2). Subsequently, the output of the reference PLSR models was compared with the output of the PLSR models in the partial model-sets by calculating the average RMSE between both: $RMSE = \sqrt{\sum_{i=1}^{n}\left(X_{Refi} - X_{NYi}\right)^2 / n}$ with X_{Refi} the contribution of source X with the reference model, X_{NYi} the contribution of source X with the model without source Y, *i* the observation, and *n* the amount of observations.

Table 4-2: PLSR model-sets

Model-set	Source removed	n mixtures	PLSR models
Reference	/	54	$PLSR_L$, $PLSR_M$, $PLSR_C$, $PLSR_R$, $PLSR_U$
NL	Limestone	24	$PLSR_M$, $PLSR_C$, $PLSR_R$, $PLSR_U$
NM	Millstone	35	$PLSR_L$, $PLSR_C$, $PLSR_R$, $PLSR_U$
NC	Coals	29	$PLSR_L$, $PLSR_M$, $PLSR_R$, $PLSR_U$
NR	Riverbank	21	$PLSR_L$, $PLSR_M$, $PLSR_C$, $PLSR_U$
NU	Urban	31	$PLSR_L$, $PLSR_M$, $PLSR_C$, $PLSR_R$

4.3 Results

4.3.1 Sediment source discrimination

Visual interpretation

Based on the DRIFTS spectra of the sediment source samples, 17 characteristic absorption peaks were identified that are typical for soil samples (Figure 4-2) (Tiecher et al., 2016). The 3695 and 3620 cm^{-1} peaks are characteristic for aluminosilicates (kaolinite and micas), which are typically present in clays (Parikh et al., 2014; Poulenard et al., 2012; Tiecher et al., 2016; Yang and Mouazen, 2012). The peaks around 2920 and 2850 cm^{-1} are generally attributed to organic matter (Poulenard et al., 2009; Reeves III, 2012; Tiecher et al., 2016), while the peak at 2505 cm^{-1} is attributed to carbonates (inorganic carbon) (Poulenard et al., 2012; Reeves III et al., 2001; Viscarra Rossel et al., 2016). The 1990, 1870 and 1785 cm^{-1} peaks are generally related to quartz (Qz), and 1630 cm^{-1} to Qz and clay minerals. The peaks around 1530 and 1360 cm^{-1} are attributed to Qz and organic matter, while 1160 cm^{-1} relates to clay minerals and organic matter (Tiecher et al., 2016). Finally, the 1115 to 698 cm^{-1} peaks are attributed to the combination of clay minerals and Qz (Ge et al., 2014; Parikh et al., 2014; Reeves III, 2012; Viscarra Rossel et al., 2006).

In general, the spectra of SS and BS are comparable to the spectra of the source material and the experimental mixtures, especially for wavelengths > 2000 cm^{-1}. The spectra of BS had a more pronounced trough at 1020 cm^{-1} compared to the SS, and the peak at 1160 cm^{-1} (clay + OM) in the spectra of SS and BS is not as pronounced in the spectra of the source material. Furthermore, the grassland and riverbank sources appeared to have a higher clay content compared to urban street dust, while urban street dust had a relatively higher OM and Qz content (Figure 4-2 b-c). The urban street dust also appeared to be enriched in Qz and inorganic carbon. Topsoil from the coals area had the highest clay content and relatively high Qz peaks, while topsoil from the millstone area appeared to be characterised by the lowest clay content.

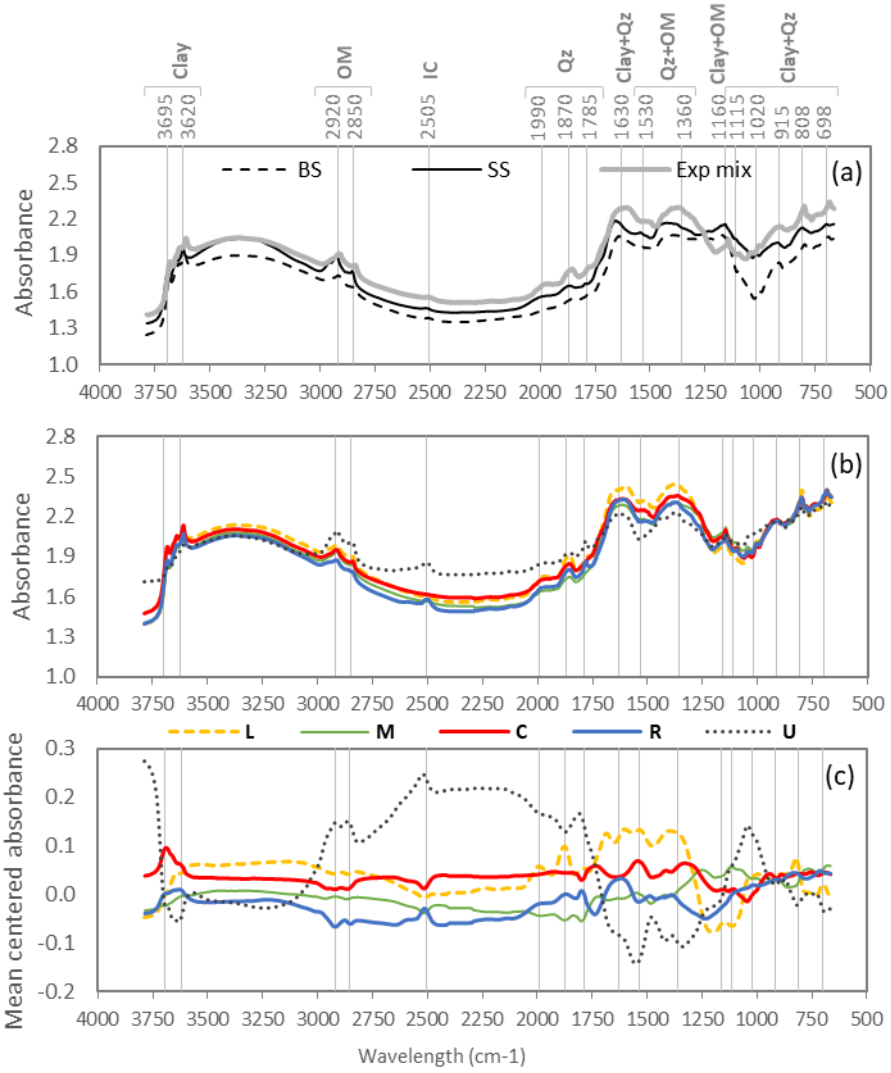

Figure 4-2: Mean DRIFTS spectra of (a) suspended sediment (SS), bed sediment (BS), and experimental mixtures (Exp. mix); (b) unprocessed and (c) processed sediment source samples. Vertical lines represent absorption peaks ascribed to clay minerals, organic matter (OM), inorganic carbon (IC), quartz (Qz).

Discriminant analysis

The processed DRIFTS spectra (Figure 4-2 c) were used as input for the PCA. The results of the PCA indicated that nine components describe 99% of the variation in the data. Therefore, the first nine components were retained for the DA. Most samples were consistently closer (standard deviations < 3) to the mean of their own group compared to the other group (Figure 4-3). Urban street dust samples are most strongly discriminated from the other sources (standard deviations up to 40), while the samples from riverbanks were less strongly defined

by their DRIFTS spectra (i.e. high intra-source variability). Despite the relatively weak discriminative power of riverbank sources, it was decided to take into account all classes as potential sediment sources to evaluate the effect of the discriminative power on the final sediment source estimates.

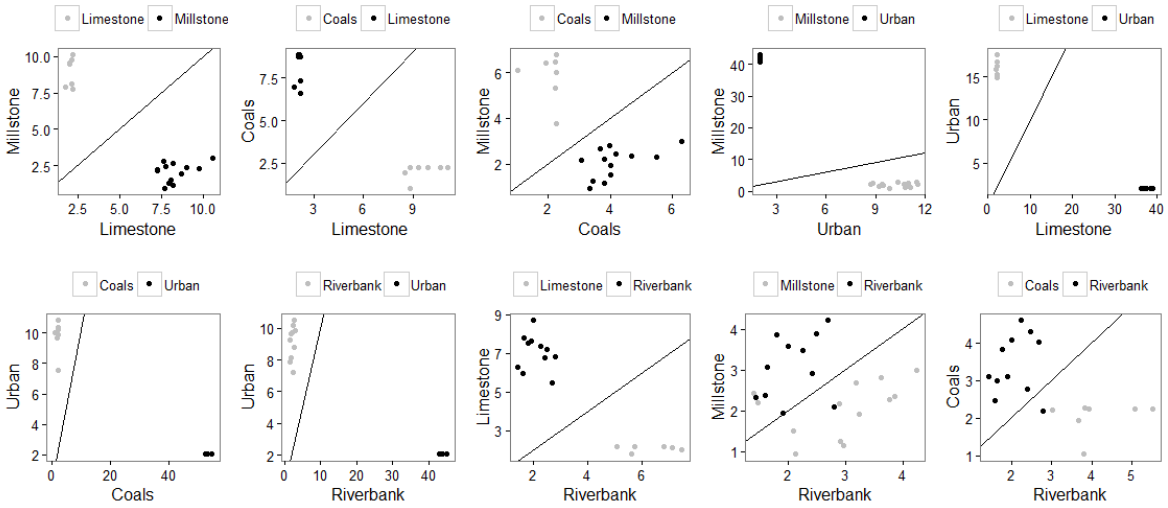

Figure 4-3: Pairwise comparison of Mahalanobis Distances between sediment source classes

4.3.2 Sediment source apportionment

Reference models

Five PLSR models were developed to estimate sediment contributions from each source. Model calibration indicated that eight components minimises the RMSE in all models, and thus is the optimal number of components. The PLSR models had a RMSEP ranging between 4 and 6%, with exception of the riverbank model (9%), resulting in 95% confidence intervals between ±10 and ±18% (Table 4-3). The PLSR models were applied on the DRIFTS spectra of the SS to estimate average sediment source contributions. The dominant sediment sources in the River Aire appeared to be topsoil from the limestone area (45 ± 12 %) and urban street dust (43 ± 10 %). Topsoil from the millstone and coals area contributed on average 19 ± 13 % and 14 ± 10 %, respectively, and eroding riverbanks 16 ± 18% (Figure 4-4).

The mean sum of the source contributions estimated based on the reference models amounted 137 ± 28%. Taken into account the confidence intervals associated to the PLSR models, the total sum can be considered close to 100%. This observation could be interpreted as an indication that all major sediment sources were included into the model calibration (Cooper et al., 2014a; Martínez-Carreras et al., 2010a; Poulenard et al., 2009; Tiecher et al., 2016). However, the effect of source classification on the source apportionment is further examined in the next section.

Table 4-3: Reference PLSR model uncertainty statistics

Model	R^2	RMSEC	RMSEP	95% CI	Explained variance
$PLSR_L$	0.884	0.053	0.059	± 12	99.09
$PLSR_M$	0.877	0.148	0.065	± 13	93.78
$PLSR_C$	0.929	0.151	0.053	± 10	85.57
$PLSR_R$	0.790	0.156	0.092	± 18	88.92
$PLSR_U$	0.772	0.091	0.045	± 10	96.19

Partial models

The partial models were also applied to the SS samples to estimate source contributions and associated confidence intervals (Figure 4-4). With the model-sets without coals (NC in Figure 4-4), the sediment source contributions were very similar to the reference model estimations, whereby limestone and urban street dust are the dominant sediment sources. Contrarily, when limestone (NL), millstone (NM) or urban (NU) were excluded as sources, the riverbank contributions became very high (80 to 180%), and when riverbank was excluded as a source, most of the sediment was attributed to millstone (140%). Furthermore, the sum of the average contributions per model-set varied between 108 % (NL) and 233 % (NL). Based on these numbers, it is difficult, if not impossible, to evaluate how well the source classification accurately represents the actual sediment sources.

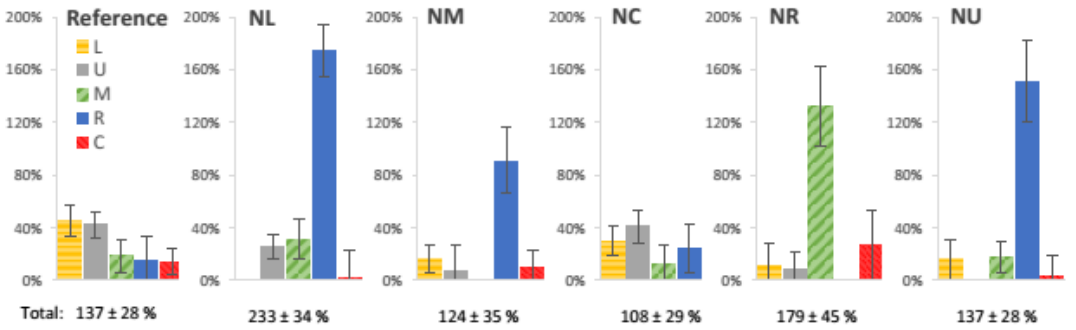

Figure 4-4: Average source contributions to the suspended sediment in the River Aire based on different model calibrations.

The variation in the source estimates between model-sets was further quantified by calculating the RMSE between the estimations of the reference models and the partial models (Table 4-4). Source contributions from the coals area varied the least between model-sets (14% on average), while estimations for riverbank contributions varied considerably (up to 155%). Furthermore, when coals was removed as a source (NC), the deviations from the reference models were within the confidence intervals associated to the reference models (Table 4-3). However, when other sources were removed, the effect was more pronounced: removing limestone and urban (NL and NU) most strongly influenced the riverbank contribution (155% and 133% respectively), while removing millstone (NM) both influenced the urban (37%) and riverbank (74%) contribution. Finally, when riverbank was removed as a source (NR), the estimated millstone contribution changed most significantly (112%).

Table 4-4: RMSE between source estimates of the partial and reference models.

Model	Contribution	Ref-NL	Ref-NM	Ref-NC	Ref-NU	Ref-NR
$PLSR_L$	Limestone	/	28%	15%	29%	32%
$PLSR_M$	Millstone	15%	/	11%	11%	112%
$PLSR_C$	Coals	11%	9%	/	10%	25%
$PLSR_U$	Urban	22%	37%	5%	/	36%
$PLSR_R$	Riverbank	155%	74%	17%	133%	/

The above observations are also illustrated with two concrete examples (Figure 4-5). First, based on the reference model (ALL), there was no coals contribution to the BS (Figure 4-5 a). Given that the first three locations of BS samples (BS5 to 3) are located in the millstone area, no contribution of the coals area is indeed expected. However, with the partial models, high coals contributions (up to 80%) were estimated even where it was geographically not possible (Figure 4-5 a). Furthermore, when coals was removed as a source (NC), the other source contributions did not change significantly compared to the reference model, while removing riverbank (NR) had a pronounced effect on the millstone contribution.

Second, similar observations were made for the estimated SS source contributions during an individual high-flow event in September 2016 (Figure 4-5 b): coals appeared to be an important sediment source during the peak in SSC, but when coals was removed as a source, the other source contributions remain relatively constant compared to the reference model. Furthermore, millstone became more important when riverbank was removed as a source, while the riverbank contributions increased with removal of limestone.

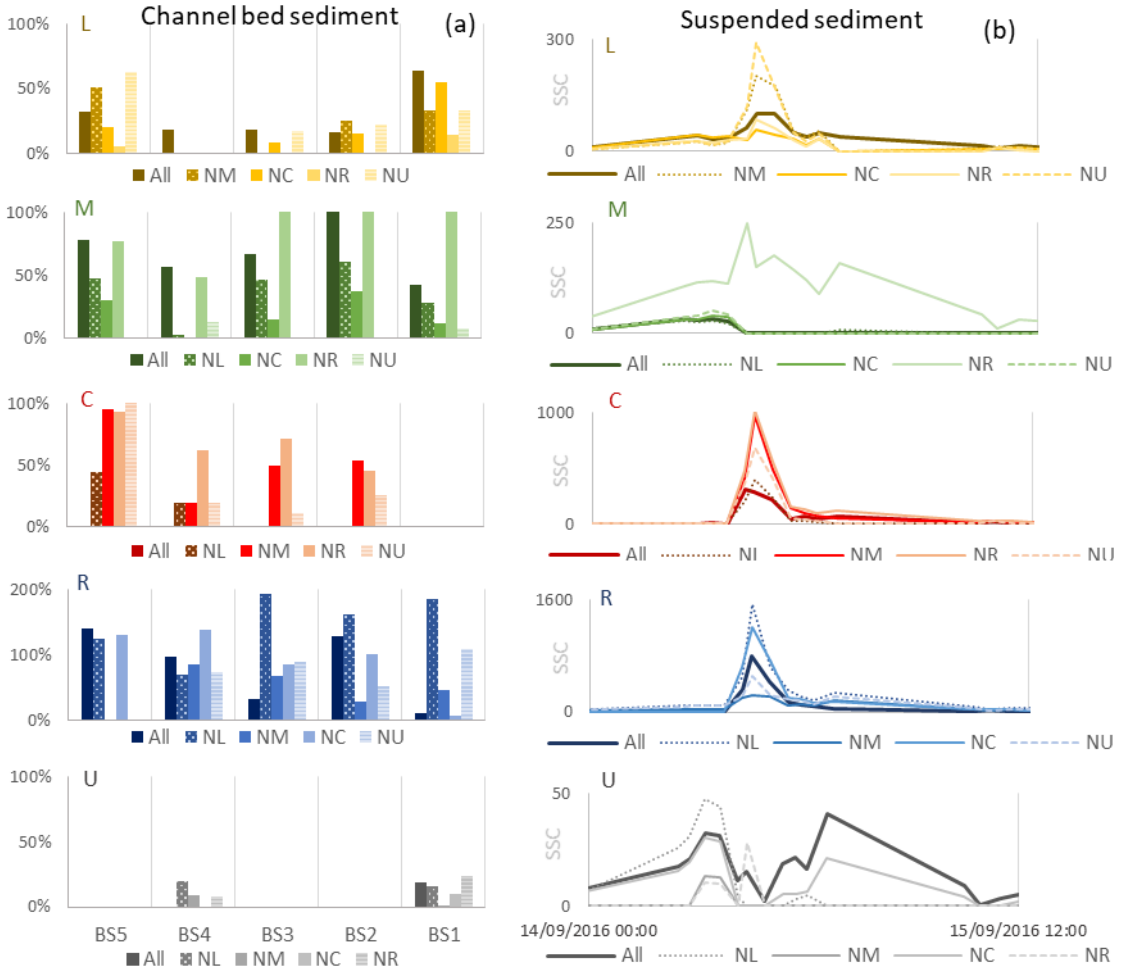

Figure 4-5: Examples of sediment source contributions estimated by different model-sets for (a) bed sediment samples; and (b) suspended sediment (SSC, mg L^{-1}) during a high-flow event in September 2016

4.4 Discussion

The results in this study confirm that DRIFTS spectra can serve as fingerprints to discriminate between the classified sediment sources, which can be used to develop PLSR models to estimate SS source contributions. The associated model uncertainties are of the same order as other spectral-based (visible, near-infrared and infrared with experimental mixtures) fingerprinting studies (i.e. between 5% and 20%) (Brosinsky et al., 2014; Evrard et al., 2013; Poulenard et al., 2012, 2009; Verheyen et al., 2014). However, the study also demonstrates that the source apportionment is strongly influenced by the initial sediment source classification, which can be related to the degree of discrimination between the sources.

4.4.1 Source discrimination

The sediment sources are characterised by a different degree of discrimination, whereby riverbank sources appeared to be the least well discriminated from all sources, while urban street dust is most strongly discriminated (Figure 4-3; Table 4-3). This variability in discrimination can be linked back to the primary origin of the source material (Koiter et al., 2013).

First, the urban street dust is most distinct of all other sources (Figure 4-3), which is in line with previous observations that street dust is characterised by the least within-source variability and highest discrimination based on geochemistry (Pulley et al., 2015). The mean DRIFTS spectrum of street dust suggests that street dust samples were depleted in clay minerals, and enriched in OM and quartz, which reflects the primary origin of street dust as a mixture of particles from urban runoff, sewage and atmospheric deposition, and soils and sand from construction works (Franz et al., 2014; Shilton et al., 2005; Taylor and Owens, 2009).

Secondly, the grassland samples are generally also characterized by a low intra-source variability (Figure 4-3). The difference between the grassland sources is mainly defined by the parent mineral material of the lithological areas. Grassland topsoil from the limestone area was defined by a combination of peak areas corresponding to clay, OM, carbonates and quartz (Figure 4-2), which is linked to the limestone (carbonates) and shale (quartz) bed rock of the area (British Geological Survey, 2016). Topsoil from the coals area had the highest clay content and was mainly defined by quartz peaks, which is also in agreement with the main lithology (mixture of siltstone, mudstone and sandstone) (British Geological Survey, 2016). Contrarily, topsoil from the millstone area (sandstone) appeared to be characterised by the lowest clay content of the topsoils and an average mineral content compared to the other sources (Figure 4-2).

Finally, the within-source variability of riverbank samples was higher compared to the other sources, and the discrimination from especially millstone and coals samples was less pronounced (Figure 4-3). This observation is in agreement with the fact that riverbank material generally represents a mixture of floodplain

deposits consisting of various primary sediment sources (Vale et al., 2016), so that its discrimination from topsoil sources is strongly influenced by different degrees of weathering since deposition (Pulley et al., 2015; Vale et al., 2016).

4.4.2 Model sensitivity to source classification

The findings suggest that the degree of discrimination of the source classes, in combination with the importance of the source classes as actual sediment sources, determines the sensitivity of the model to the exclusion of a particular source. These observations are synthesised in five scenarios (Figure 4-6).

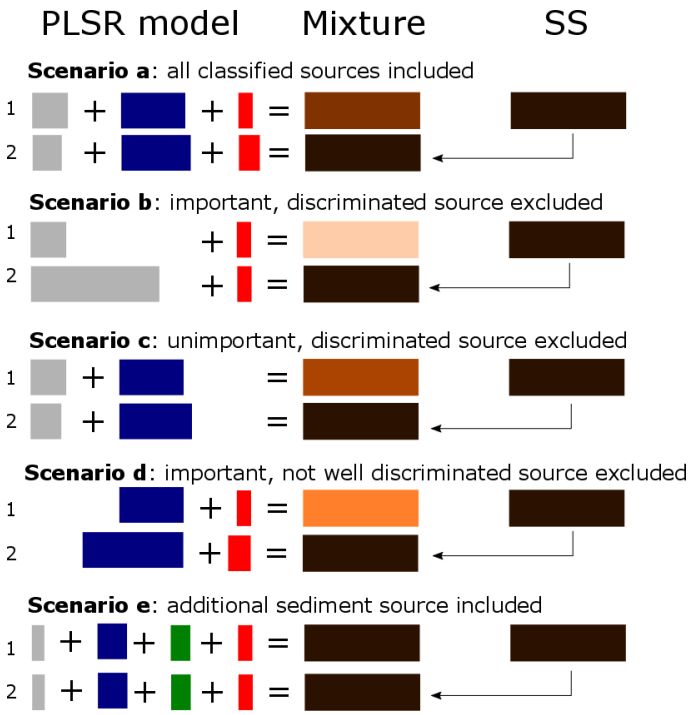

Figure 4-6: Visualisation of different scenario's in PLSR fingerprinting model calibration (1) and application (2) (sediment sources: grey is poorly discriminated, blue and red are well discriminated, green is additional, unknown source)

The first scenario (a) represents the reference model-setup in this study where all classified sources are included in the model calibration. It is assumed that all important sediment sources were identified, and thus that the mixtures used to calibrate the models are a close representation of the SS. Therefore, the exclusion of a dominant, well-defined sediment source has a pronounced impact on the apportionment of other sources (scenario b). For example, limestone-grassland and urban street dust are well-discriminated and also dominant

sources to the SS (Figure 4-4). Removing these sources results in mixtures that are not comparable with the SS, so that part of the SS remains unclassified. Consequently, when applying this model to the actual SS, a higher contribution is attributed to the least well discriminated source (i.e. riverbank) to compensate for the unclassified part.

Contrarily, when coals is excluded as a source, the estimated contributions of the other sources do not change significantly compared to the reference estimations (scenario c). The apparent insensitivity of the models to the exclusion of coals as a source, suggests that topsoil from the coals area may not be a significant sediment source. In other words, without coals as a source, there is little part of the SS that remains un-identified and is being attributed to other sources. This corresponds well to what would be expected based on land use in the Aire catchment. The amount of grassland in the coal area upstream of the point of SS sampling is limited (~85 km^2); most of the area is strongly urbanised with scattered patches of grassland which are not directly connected to the river system. However, during the high-flow event in September 2016 (Figure 4-5 b), the coals contribution reaches high levels up until being the second largest sediment source during the peak SSC. For this reason, it can be argued that coals may generally not be a dominant sediment source, but its importance varies over time which can be driven by changes in the connectivity of the catchment to transfer sediment to the river system (e.g. as a result of precipitation) (Bracken et al., 2015; Wethered et al., 2015).

Furthermore, while riverbank appears to be an important sediment source (especially to the BS, Figure 4-5 b) which would be in agreement with previous research in the catchment (Carter et al., 2003), it is also the least well discriminated source based on DRIFTS (scenario d). Consequently, removing riverbank as a source results in a significant impact on the other source contributions (e.g. coals contribution where no is expected, Figure 4-5 a).

Finally, these observations also suggest that it is possible that too few sediment sources were classified which are currently attributed to the riverbank source (scenario e). This hypothesis is also supported by the small differences between

the DRIFTS spectra of BS, SS and the source material, especially at 1160 and 1020 cm^{-1} (Figure 4-2). A possibly additional source could be solids from sewage treatment works (STW), which was estimated to contribute 14-18% of the SS in the fingerprinting study by Carter et al. (2003).

4.5 Conclusion

A DRIFTS-based sediment fingerprinting approach has been successfully tested and applied to identify the sediment source contributions to the SS in the River Aire. The potential sediment sources could be discriminated based on their respective DRIFTS spectra and statistical un-mixing models were developed that can estimate sediment source contributions with acceptable model uncertainties. However, while model uncertainties were acceptable and the model appeared to be insensitive to redundant sediment sources, the source apportionment appeared to be very sensitive to the initial degree of discrimination between the sources classes. This type of model testing has not been performed previously on DRIFTS-based sediment fingerprinting with experimental mixtures, and it clearly demonstrates that the sum of the individual sediment source estimates is not an appropriate measure to assess how well the source classification represents the actual sediment sources.

The findings provide important empirical evidence that highlights the need to clearly define when a source class has a sufficiently high degree of discrimination from the other classes in order to reliably interpret sediment fingerprinting results based on DRIFTS. When a source class has low degree of discrimination, it is recommended to use other fingerprinting techniques to better characterise the specific fingerprint (Collins et al., 2017). Additionally, the potential of objective sediment source classification based on the similarity between source material and river sediment (Pulley et al., 2017a), in combination with DRIFTS-based fingerprinting should be further investigated.

4.6 References

Bilotta, G.S., Brazier, R.E., 2008. Understanding the influence of suspended solids on water quality and aquatic biota. Water Res. 42, 2849–2861. doi:10.1016/j.watres.2008.03.018

Bracken, L.J., Turnbull, L., Wainwright, J., Bogaart, P., 2015. Sediment connectivity: a framework for understanding sediment transfer at multiple scales. Earth Surf. Process. Landforms 40, 177–188. doi:10.1002/esp.3635

British Geological Survey, 2016. The BGS Lexicon of Named Rock Units [WWW Document]. URL http://www.bgs.ac.uk/lexicon/home.html

Brosinsky, A., Foerster, S., Segl, K., Kaufmann, H., 2014. Spectral fingerprinting: sediment source discrimination and contribution modelling of artificial mixtures based on VNIR-SWIR spectral properties. J. Soils Sediments 14, 1949–1964. doi:10.1007/s11368-014-0925-1

Carter, J., Owens, P.N., Walling, D.E., Leeks, G.J.L., 2003. Fingerprinting suspended sediment sources in a large urban river system. Sci. Total Environ. 314–316, 513–534. doi:10.1016/S0048-9697(03)00071-8

Carter, J., Walling, D.E., Owens, P.N., Leeks, G.J.L., 2006. Spatial and temporal variability in the concentration and speciation of metals in suspended sediment transported by the River Aire, Yorkshire, UK. Hydrol. Process. 20, 3007–3027. doi:10.1002/hyp.6156

Collins, A.L., Pulley, S., Foster, I.D.L., Gellis, A., Porto, P., Horowitz, A.J., 2017. Sediment source fingerprinting as an aid to catchment management: A review of the current state of knowledge and a methodological decision-tree for end-users. J. Environ. Manage. 194, 86–108. doi:10.1016/j.jenvman.2016.09.075

Collins, A.L., Walling, D.E., 2004. Documenting catchment suspended sediment sources: problems, approaches and prospects. Prog. Phys. Geogr. 28, 159–196. doi:10.1191/0309133304pp409ra

Collins, A.L., Walling, D.E., Webb, L., King, P.L., 2010. Apportioning catchment scale sediment sources using a modified composite fingerprinting technique incorporating property weightings and prior information. Geoderma 155, 249–261. doi:10.1016/j.geoderma.2009.12.008

Cooper, R.J., Krueger, T., Hiscock, K.M., Rawlins, B.G., 2014a. High-temporal resolution fluvial sediment source fingerprinting with uncertainty: A Bayesian approach. Earth Surf. Process. Landforms. doi:10.1002/esp.3621

Cooper, R.J., Rawlins, B.G., Lézé, B., Krueger, T., Hiscock, K.M., 2014b. Combining two filter paper-based analytical methods to monitor temporal variations in the geochemical properties of fluvial suspended particulate matter. Hydrol. Process. 28, 4042–4056. doi:10.1002/hyp.9945

Dark, S.J., Bram, D., 2007. The modifiable areal unit problem (MAUP) in physical geography. Prog. Phys. Geogr. 31, 471–479. doi:10.1177/0309133307083294

Davis, C.M., Fox, J.F., 2009. Sediment Fingerprinting : review of the method and future improvements for allocating nonpoint source pollution. J. Environ. Eng. 137, 490–505.

Evrard, O., Poulenard, J., Némery, J., Ayrault, S., Gratiot, N., Duvert, C., Prat, C., Lefèvre, I., Bonté, P., Esteves, M., 2013. Tracing sediment sources in a tropical highland catchment of central Mexico by using conventional and alternative fingerprinting methods. Hydrol. Process. 27, 911–922. doi:10.1002/hyp.9421

Franz, C., Makeschin, F., Weiß, H., Lorz, C., 2014. Sediments in urban river basins: identification of sediment sources within the Lago Paranoá catchment, Brasilia DF, Brazil - using the fingerprint approach. Sci. Total Environ. 466–467, 513–23. doi:10.1016/j.scitotenv.2013.07.056

Fryirs, K.A., Brierley, G.J., 2013. Geomorphic analysis of river systems: An approach to reading the landscape. Wiley-Blackwell, West Sussex.

Ge, Y., Thomasson, J.A., Morgan, C.L.S., 2014. Mid-infrared attenuated total reflectance spectroscopy for soil carbon and particle size determination. Geoderma 213, 57–63. doi:10.1016/j.geoderma.2013.07.017

Haddadchi, A., Ryder, D.S., Evrard, O., Olley, J.M., 2013. Sediment fingerprinting in fluvial systems: Review of tracers, sediment sources and mixing models. Int. J. Sediment Res. 28, 560–578. doi:10.1016/S1001-6279(14)60013-5

Horowitz, A.J., 2009. Monitoring suspended sediments and associated chemical constituents in urban environments: lessons from the city of Atlanta, Georgia, USA Water Quality Monitoring Program. J. Soils Sediments 9, 342–363. doi:10.1007/s11368-009-0092-y

Karaman, I., Qannari, E.M., Martens, H., Hedemann, M.S., Knudsen, K.E.B., Kohler, A., 2013. Comparison of Sparse and Jack-knife partial least squares regression methods for variable selection. Chemom. Intell. Lab. Syst. 122, 65–77. doi:10.1016/j.chemolab.2012.12.005

Koiter, A.J., Owens, P.N., Petticrew, E.L., Lobb, D.A., 2013. The behavioural characteristics of sediment properties and their implications for sediment fingerprinting as an approach for identifying sediment sources in river basins. Earth-Science Rev. 125, 24–42. doi:10.1016/j.earscirev.2013.05.009

Laceby, J.P., Evrard, O., Smith, H.G., Blake, W.H., Olley, J.M., Minella, J.P.G., Owens, P.N., 2017. The challenges and opportunities of addressing particle size effects in sediment source fingerprinting: A review. Earth-Science Rev. 169, 85–103. doi:10.1016/j.earscirev.2017.04.009

Laceby, J.P., Olley, J., 2015. An examination of geochemical modelling approaches to tracing sediment sources incorporating distribution mixing and elemental correlations. Hydrol.

Process. 29, 1669–1685. doi:10.1002/hyp.10287

Legout, C., Poulenard, J., Nemery, J., Navratil, O., Grangeon, T., Evrard, O., Esteves, M., 2013. Quantifying suspended sediment sources during runoff events in headwater catchments using spectrocolorimetry. J. Soils Sediments 13, 1478–1492. doi:10.1007/s11368-013-0728-9

Martens, H., Martens, M., 2000. Modified Jack-knife estimation of parameter uncertainty in bilinear modelling by partial least squares regression (PLSR). Food Qual. Prefer. 11, 5–16. doi:10.1016/S0950-3293(99)00039-7

Martínez-Carreras, N., Krein, A., Udelhoven, T., Gallart, F., Iffly, J.F., Hoffmann, L., Pfister, L., Walling, D.E., 2010a. A rapid spectral-reflectance-based fingerprinting approach for documenting suspended sediment sources during storm runoff events. J. Soils Sediments 10, 400–413. doi:10.1007/s11368-009-0162-1

Martínez-Carreras, N., Udelhoven, T., Krein, A., Gallart, F., Iffly, J.F., Ziebel, J., Hoffmann, L., Pfister, L., Walling, D.E., 2010b. The use of sediment colour measured by diffuse reflectance spectrometry to determine sediment sources: Application to the Attert River catchment (Luxembourg). J. Hydrol. 382, 49–63. doi:10.1016/j.jhydrol.2009.12.017

Moore, J.W., Semmens, B.X., 2008. Incorporating uncertainty and prior information into stable isotope mixing models. Ecol. Lett. 11, 470–80. doi:10.1111/j.1461-0248.2008.01163.x

Morton, D., Rowland, C., Wood, C., Meek, L., Marston, C., Smith, G., Wadsworth, R., Simpson, I.C., 2011. Final Report for LCM2007 - the new UK Land Cover Map. Countryside Survey Technical Report No. 11/07.

Mukundan, R., Walling, D.E., Gellis, A.C., Slattery, M.C., Radcliffe, D.E., 2012. Sediment source fingerprinting: transforming from a research tool to a management tool. J. Am. Water Resour. Assoc. 48, 1241–1257. doi:10.1111/j.1752-1688.2012.00685.x

Nosrati, K., Govers, G., Semmens, B.X., Ward, E.J., 2014. A mixing model to incorporate uncertainty in sediment fingerprinting. Geoderma 217–218, 173–180. doi:10.1016/j.geoderma.2013.12.002

Owens, P.N., Blake, W.H., Gaspar, L., Gateuille, D., Koiter, A.J., Lobb, D.A., Petticrew, E.L., Reiffarth, D.G., Smith, H.G., Woodward, J.C., 2016. Fingerprinting and tracing the sources of soils and sediments: Earth and ocean science, geoarchaeological, forensic, and human health applications. Earth-Science Rev. 162, 1–23. doi:10.1016/j.earscirev.2016.08.012

Palazón, L., Gaspar, L., Latorre, B., Blake, W.H., Navas, A., 2015. Identifying sediment sources by applying a fingerprinting mixing model in a Pyrenean drainage catchment. J. Soils Sediments 15, 2067–2085. doi:10.1007/s11368-015-1175-6

Parikh, S.J., Goyne, K.W., Margenot, A.J., Mukome, F.N.D., Calderón, F.J., 2014. Soil chemical insights provided through vibrational spectroscopy, Advances in Agronomy. doi:10.1016/B978-0-12-800132-5.00001-8

Poulenard, J., Legout, C., Némery, J., Bramorski, J., Navratil, O., Douchin, A., Fanget, B., Perrette, Y., Evrard, O., Esteves, M., 2012. Tracing sediment sources during floods using Diffuse Reflectance Infrared Fourier Transform Spectrometry (DRIFTS): A case study in a highly erosive mountainous catchment (Southern French Alps). J. Hydrol. 414–415, 452–462. doi:10.1016/j.jhydrol.2011.11.022

Poulenard, J., Perrette, Y., Fanget, B., Quetin, P., Trevisan, D., Dorioz, J.M., 2009. Infrared spectroscopy tracing of sediment sources in a small rural watershed (French Alps). Sci. Total Environ. 407, 2808–19. doi:10.1016/j.scitotenv.2008.12.049

Pulley, S., Foster, I., Antunes, P., 2015. The uncertainties associated with sediment fingerprinting suspended and recently deposited fluvial sediment in the Nene river basin. Geomorphology 228, 303–319. doi:10.1016/j.geomorph.2014.09.016

Pulley, S., Foster, I., Collins, A.L., 2017a. The impact of catchment source group classification on the accuracy of sediment fingerprinting outputs. J. Environ. Manage. 194, 16–26. doi:10.1016/j.jenvman.2016.04.048

Pulley, S., Van Der Waal, B., Collins, A.L., Foster, I.D.L., Rowntree, K., 2017b. Are source groups always appropriate when sediment fingerprinting? The direct comparison of source and sediment samples as a methodological step. River Res. Appl. 1–11. doi:10.1002/rra.3192

Reeves III, J.B., 2012. Mid-infrared spectral interpretation of soils: Is it practical or accurate? Geoderma 189–190, 508–513. doi:10.1016/j.geoderma.2012.06.008

Reeves III, J.B., 2010. Near- versus mid-infrared diffuse reflectance spectroscopy for soil analysis emphasizing carbon and laboratory versus on-site analysis: Where are we and what needs to be done? Geoderma 158, 3–14. doi:10.1016/j.geoderma.2009.04.005

Reeves III, J.B., Mccarty, G.W., Reeves, V.B., 2001. Mid-infrared diffuse reflectance spectroscopy for the quantitative analysis of agricultural soils. J. Agric. Food Chem. 49, 766–772. doi:10.1021/jf0011283

Renard, K.G., Foster, G.R., Weesies, G. a., Porter, J.P., 1991. RUSLE: Revised universal soil loss equation. J. Soil Water Conserv. 46, 30–33.

Shilton, V.F., Booth, C.A., Smith, J.P., Giess, P., Mitchell, D.J., Williams, C.D., 2005. Magnetic properties of urban street dust and their relationship with organic matter content in the West Midlands, UK. Atmos. Environ. 39, 3651–3659. doi:10.1016/j.atmosenv.2005.03.005

Stevens, A., Lopez, L.R., 2015. A Guide to Diffuse Reflectance Spectroscopy & Multivariate Calibration with the R Statistical Software.

Taylor, K.G., Owens, P.N., 2009. Sediments in urban river basins: a review of sediment–contaminant dynamics in an environmental system conditioned by human activities. J. Soils Sediments 9, 281–303. doi:10.1007/s11368-009-0103-z

Tiecher, T., Caner, L., Minella, J.P.G., Evrard, O., Mondamert, L., Labanowski, J., Rheinheimer dos Santos, D., 2016. Tracing Sediment Sources using Mid-Infrared Spectroscopy in Arvorezinha Catchment, Southern Brazil. L. Degrad. Dev. doi:10.1002/ldr.2690

Vale, S.S., Fuller, I.C., Procter, J.N., Basher, L.R., Smith, I.E., 2016. Characterization and quantification of suspended sediment sources to the Manawatu River, New Zealand. Sci. Total Environ. 543, 171–186. doi:10.1016/j.scitotenv.2015.11.003

Verheyen, D., Diels, J., Kissi, E., Poesen, J., 2014. The use of visible and near-infrared reflectance measurements for identifying the source of suspended sediment in rivers and comparison with geochemical fingerprinting. J. Soils Sediments 14, 1869–1885. doi:10.1007/s11368-014-0938-9

Viscarra Rossel, R.A., Behrens, T., Ben-Dor, E., Brown, D.J., Demattê, J.A.M., Shepherd, K.D., Shi, Z., Stenberg, B., Stevens, A., Adamchuk, V., Aïchi, H., Barthès, B.G., Bartholomeus, H.M., Bayer, A.D., Bernoux, M., Böttcher, K., Brodský, L., Du, C.W., Chappell, A., Fouad, Y., Genot, V., Gomez, C., Grunwald, S., Gubler, A., Guerrero, C., Hedley, C.B., Knadel, M., Morrás, H.J.M., Nocita, M., Ramirez-Lopez, L., Roudier, P., Campos, E.M.R., Sanborn, P., Sellitto, V.M., Sudduth, K.A., Rawlins, B.G., Walter, C., Winowiecki, L.A., Hong, S.Y., Ji, W., 2016. A global spectral library to characterize the world's soil. Earth-Science Rev. 155, 198–230. doi:10.1016/j.earscirev.2016.01.012

Viscarra Rossel, R. a., Walvoort, D.J.J., McBratney, A.B., Janik, L.J., Skjemstad, J.O., 2006. Visible, near infrared, mid infrared or combined diffuse reflectance spectroscopy for simultaneous assessment of various soil properties. Geoderma 131, 59–75. doi:10.1016/j.geoderma.2005.03.007

Walling, D.E., 2013. The evolution of sediment source fingerprinting investigations in fluvial systems. J. Soils Sediments 13, 1658–1675. doi:10.1007/s11368-013-0767-2

Walling, D.E., Owens, P.N., Carter, J., Leeks, G.J.L., Lewis, S., Meharg, A.A., Wright, J., 2003. Storage of sediment-associated nutrients and contaminants in river channel and floodplain systems. Appl. Geochemistry 18, 195–220. doi:10.1016/S0883-2927(02)00121-X

Wethered, A.S., Ralph, T.J., Smith, H.G., Fryirs, K.A., Heijnis, H., 2015. Quantifying fluvial (dis)connectivity in an agricultural catchment using a geomorphic approach and sediment

source tracing. J. Soils Sediments 15, 2052–2066. doi:10.1007/s11368-015-1202-7

Wilkinson, S.N., Olley, J.M., Furuichi, T., Burton, J., Kinsey-Henderson, A.E., 2015. Sediment source tracing with stratified sampling and weightings based on spatial gradients in soil erosion. J. Soils Sediments. doi:10.1007/s11368-015-1134-2

Wold, S., Sjostrom, M., Eriksson, L., 2001. PLS-regression : a basic tool of chemometrics. Chemom. Intell. Lab. Syst. 58, 109–130.

Yang, H., Mouazen, A.M., 2012. Vis / Near- and Mid- Infrared Spectroscopy for Predicting Soil N and C at a Farm Scale. Infrared Spectrosc. Biomed. Sci. 185–211. doi:10.1016/j.proenv.2011.09.108

CHAPTER 5: USING SEDIMENT SOURCE INFORMATION TO IDENTIFY PROCESSES CONTROLLING TEMPORAL VARIABILITY IN SUSPENDED SEDIMENT TRANSPORT

Abstract

The natural SS transport dynamics in rivers are often strongly disturbed, especially when the degree of human intervention in a river catchment is high, leading to problems such as excessive siltation, water pollution and ecosystem degradation. However, our understanding of SS transport is not yet sufficient to fully explain the spatial and temporal variability in sediment concentrations in rivers, which hinders the development of targeted management strategies. To this end, the study investigated how variations in SS sources during individual high-flow events control the total SSC in rivers in response to hydro-meteorological and catchment processes. A sediment fingerprinting technique based on Diffuse Reflectance Infrared Fourier Transform spectrometry was applied in the River Aire, UK. Five potential sediment sources were classified: grassland topsoil in three lithological areas (limestone, millstone grit and coal measures), eroding riverbanks and urban street dust. A total of 200 SS samples were collected during 14 high-flow events between 2015 and 2017, which exhibited different hysteresis patterns between SSC and river discharge. Grassland from the limestone area and urban street dust were the dominant sources of fine sediment, but, significant variations in source contributions during and between events were observed. By combining source information with a multivariate statistical analysis of detailed hydro-meteorological data, mechanisms for SS transport could be derived. While SSCs were generally hydrologically driven, catchment sediment connectivity also appeared to play an important role in controlling sediment source contributions and the total sediment supply. The findings in this study show that the combination of innovative statistical methods for sediment source apportionment and the estimation of SSC based on hydro-meteorological data, allows the identification of underlying processes for temporal variation in SS transport, which can serve as a basis for process-based modelling and management decisions.

5.1 Introduction

The natural SS transport dynamics in rivers are often strongly disturbed, especially when the degree of human intervention in a river catchment is high (Lexartza-Artza and Wainwright, 2011; Taylor and Owens, 2009; Walling et al., 2003; Wohl, 2015), leading to problems such as diffuse pollution and ecosystem degradation (Bilotta and Brazier, 2008; Mauad et al., 2015). Yet the application of effective sediment management solutions is partly hindered by the difficulty in accurately quantifying and predicting SSCs due to the high variability in SS transport over short to medium timescales (Vercruysse et al., 2017). While research has demonstrated the importance of interactions between a range of hydro-meteorological variables to explain this temporal variability (Francke et al., 2014; Onderka et al., 2012; Perks et al., 2015; Zeiger and Hubbart, 2016), these variables can only be used to infer conclusions about the underlying processes without consideration of the continuum of sediment sources and stores and how sediment is transferred (Bracken et al., 2015). The lack of sediment source information associated with the SS complicates our ability to identify the underlying processes and process interactions controlling SS transport. Therefore, there is a need to combine the analysis of controlling variables with detailed information on the sediment sources in order to fully understand SS transport dynamics (Fryirs, 2013).

For example, while hysteresis patterns between SSC and river discharge are commonly used to extrapolate information about the processes controlling SS availability, transport and sources (e.g. Aich et al., 2014; Eder et al., 2010; Francke et al., 2008; Lloyd et al., 2016; Pietroń et al., 2015; Sherriff et al., 2016; Smith and Dragovich, 2009; Sun et al., 2015; Williams, 1989), the interpretation of hysteresis patterns is highly context-specific and often relies on assumptions about the role of sediment sources in controlling SSCs (Smith and Dragovich, 2009; Vercruysse et al., 2017). Clockwise hysteresis patterns during a high-flow event, i.e. peak SSCs precede peak discharges, are typically attributed to the contribution of sediment sources located close the river (Aich et al., 2014; Eder et al., 2010). Conversely, counter-clockwise patterns, characterised by a delayed peak SSC relative to discharge, are attributed generally to the contribution of

more distant sediment sources becoming connected to the river system, or the sudden influx of sediment to the river (e.g. bank collapse) (De Girolamo et al., 2015; Fan et al., 2012; Fang et al., 2015; Francke et al., 2014; Tena et al., 2014). Hysteresis patterns have also been attributed to antecedent soil moisture conditions within the catchment, as well as precipitation patterns, duration and intensity (Francke et al., 2014; Onderka et al., 2012; Poulenard et al., 2012; Sherriff et al., 2016; Smith and Blake, 2014). For example, when a flow event has a second discharge peak that results in similar hysteresis behaviour compared to the first peak, this is often attributed to connectivity changes during the event, linking other sediment sources to the river system (Aich et al., 2014). Moreover, a study comparing hysteresis patterns between catchments with different soil drainage classes found that clockwise patterns were dominant in the poorly drained catchment and were correlated to discharge and precipitation variables, while in the moderately drained catchment, counter-clockwise patterns were dominant and only correlated to precipitation variables. Therefore, sediment in the poorly drained catchment was attributed to the channel system (i.e. bank erosion and channel storage), and in the moderately drained catchment, the dominant sediment source was linked to superficially derived sediment due to soil erosion by water (i.e. detachment, entrainment, transport and deposition) (Sherriff et al., 2016). These examples demonstrate that the interpretation of hysteresis patterns in terms of underlying processes is not straightforward and strongly depends on the specific context of the study. More detailed information on sediment source variations during individual high-flow events is needed to improve scientific understandings on the role of SS sources in controlling the total SS transport in rivers.

To gain information on SS sources, sediment fingerprinting can be applied, which links physical and/or geochemical characteristics of the SS to soil samples from the catchment to develop statistical un-mixing models to determine the relative contributions of sources to the SS (Mukundan et al., 2012). However, most sediment fingerprinting studies report the average SS source contributions based on a selected number of samples, and few capture actual variations in SS sources over short to medium timescales (i.e. events) (Cooper et al., 2014a). The

paucity of high frequency sediment source data is mainly due to methodological constraints, such as the lack of a standardised procedures for sediment fingerprinting (e.g. sediment source identification and discrimination) (Collins et al., 2017; Collins and Walling, 2004; Davis and Fox, 2009; Fox and Papanicolaou, 2008; Haddadchi et al., 2013; Koiter et al., 2013; Mukundan et al., 2012; Smith et al., 2015), and the cost- and time intensive nature of most approaches (e.g. loss-on-ignition (LOI), colorimetry, inductively coupled plasma-optical emission spectrometry (ICP-OAS) and atomic absorption spectrometry (AAS)). These techniques tend to be expensive to run, require relatively large sample volumes (> 100 mg; which are often not available for SS), and involve extensive sample preparation (e.g. acid digestion) (Cooper et al., 2014a; Sherriff et al., 2016; Walling, 2013). To address these issues, sediment fingerprinting based on Diffuse Reflectance Infrared Fourier Transform spectrometry (DRIFTS) was developed as a more resource efficient alternative, because it requires almost no sample preparation, and measurements can be done in seconds on small sampling volumes (~15 mg). These features enable DRIFTS-sediment fingerprinting to be applied at a much a finer temporal resolution to retrieve detailed information on variations in SS sources (Poulenard et al., 2009; Tiecher et al., 2016).

Therefore, this study investigates how variations in SS sources during high-flow events control the total SSC in rivers in response to hydro-meteorological and catchment processes. To this end, DRIFTS-based sediment fingerprinting is applied on an extensive SSC dataset from the River Aire, UK, and combined with a multivariate analysis of detailed hydro-meteorological data to identify controlling factors for source-specific SS transport dynamics.

5.2 Materials and methods

5.2.1 Study area

The River Aire has a catchment area of 879 km^2 (690km^2 upstream of Leeds), a mean annual rainfall of 1018 (± 210 SE) mm $year^{-1}$, and a mean discharge of 15 (± 3.3 SE) $m^3 s^{-1}$ (1961-2017) Based on random monthly SS measurements from the Environment Agency (EA) of England (1990-2014), the average SSC in the

River Aire within the city centre of Leeds is 15.8 mg L^{-1}, ranging between 0 and 100 mg L^{-1} (SE of 20 mg L^{-1}). The median particle size of the SS ranges between 5.2 and 13.3 µm (Carter et al., 2006; D. E. Walling et al., 2003).

The dominant land use is grassland (59%), followed by urbanised area (25%). The remaining land is covered in moorland in the highest parts (12%) and scattered arable land (4%). The catchment mainly consists of poorly draining loamy and clayey soils, with raw oligo-fibrous peats, and stagnohumic and stagnogley soils in the upper part, and brown earths and pelo-stagnogley soils in the middle and lower parts (Carter et al., 2003). The geology of the catchment dates from the Carboniferous Period and consists of three main zones: Coal Measures in the lower (272 km^2), Millstone Grit in the middle (402 km^2), and limestone and shale formations in the upper catchment (205 km^2) (British Geological Survey, 2016) (Figure 5-1).

5.2.2 Data collection

Hydro-meteorological data and suspended sediment sampling

Discharge and precipitation data were obtained from the EA at a 15 min resolution. Discharge measurements originate from a monitoring station at Armley located at 3 km from the SS sampling site. Precipitation data were obtained from three data loggers located at the upstream edge of each geological zone at Malham Tarn (MT), Thornton Reservoir (TR), and Proctor Heights (PH) (Figure 5-1).

SS samples were collected with a depth-integrating SS sampler during individual high-flow events between June 2015 and March 2017. In total, 14 high-flow events were sampled with a total of 200 individual samples, covering a range of peak discharges (23 to 120 m^3 s^{-1}) and peak SSCs (18 to 1000 mg L^{-1}). Additionally, five grab sediment samples were taken from the middle of the channel bed with a metal bucket (between 16-18/06/2016) (bed sediment, BS) to investigate the source contributions to fine sediment deposited along the profile of the river (Figure 5-1).

Sediment source sampling

Based on land use in the River Aire catchment and a previous sediment fingerprinting study (Carter et al., 2003), five potential SS sources were classified: soil from grassland in three geological zones (limestone (“L”), millstone grit (“M”) and coal (“C”) measures), eroding riverbanks (“R”) and urban street dust (“U”).

An erosion map based on the Revised Universal Soil Loss Equation (RUSLE) was used as a guideline during sampling, to target zones within the catchment that are most prone to soil erosion. A total of 117 sediment source samples (around 200 g for each sample) was taken. Source materials from uncultivated topsoil (21 locations) and subsoil from eroding channel banks (12 locations) were collected using a trowel (Figure 5-1). At each soil sampling location three subsamples were taken within one square meter. Only the top 5 cm of the topsoil was sampled to ensure that only material likely to be eroded and transported to the river was collected (Carter et al., 2003; Cooper et al., 2014a; Martínez-Carreras et al., 2010b; Pulley et al., 2015). Street dust samples (18) were collected along road drains using a dustpan and brush (Cooper et al., 2014a; Pulley et al., 2015).

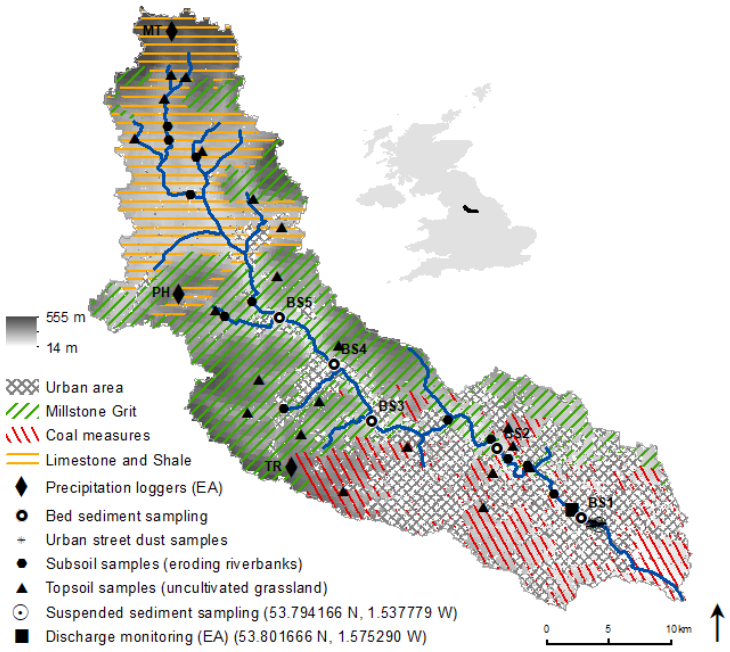

Figure 5-1: Catchment of the River Aire with sediment source areas and sampling locations (TR: Thornton Reservoir, PH: Proctor Heights, MT: Malham Tarn)

5.2.3 Sediment fingerprinting

DRIFTS measurements

SS source samples were prepared for analysis following the method developed by Poulenard et al. (2009), in which only the < 63 µm fraction of the sediment is analysed to limit the effect of particle size on spectral distortion and source apportionment (Laceby et al., 2017). The sediment source, BS, and SS samples were filtered on quartz fibre filters and oven-dried for two hours at 105˚C (Cooper et al., 2014a; Pulley et al., 2015). All samples were measured directly on the filters with DRIFTS (Cooper et al., 2014a; Poulenard et al., 2009). Samples were scanned at a 4 cm^{-1} resolution across the 4000-400 cm^{-1} spectrum with 32 co-added scans per spectrum. Only the ranges 3800–2400 cm^{-1} and 2300–650 cm^{-1} were used for further analysis to avoid interference of CO_2 absorption (Poulenard et al., 2009). Mean-centering and filtering using a Savitzky-Golay algorithm were applied on the DRIFTS spectra to reduce additional noise (Cooper et al., 2014b; Martínez-Carreras et al., 2010a).

Sediment source discrimination

Statistical techniques were applied to test whether the sources can be discriminated based on their respective DRIFT spectra. First, a principal component analysis (PCA) was performed on the processed spectra to determine the natural clustering of the samples. Secondly, a discriminant analysis based on Mahalanobis Distances was applied using the PCA scores as input data (Poulenard et al., 2009). The analysis showed that all identified sources could be discriminated based on their respective DRIFTS spectra and were therefore all considered as potential sediment sources.

Un-mixing model development

To develop models to estimate source contributions directly from the DRIFTS spectra of the SS, a set of 54 experimental mixtures was prepared using different ratios of the pure sediment source samples. Statistical regression models between the known quantities and the DRIFTS spectra of the experimental mixtures were then developed for each sediment source separately (i.e. five regression models) (Poulenard et al., 2009). To this end, Partial Least Squares

regression (PLSR) was used to address statistical problems related to the highly correlated and noisy spectral data (Karaman et al., 2013; Martens and Martens, 2000; Poulenard et al., 2009; Wold et al., 2001). In PLSR, the data are projected onto a new set of variables (PLSR components) by maximising the covariance between two datasets based on the respective scores (Stevens and Lopez, 2015). The experimental mixture dataset was divided into two parts: 75% for calibration and 25% for validation, randomly selected by a Kennard-Stone sampling algorithm. Leave-one-out cross validation in the calibration phase was applied to determine the optimal number of components (i.e. minimal root mean squared error (RMSE) between observed and predicted values) (Martens and Martens, 2000; Poulenard et al., 2009; Wold et al., 2001). Finally, the RMSE of prediction in the validation phase of each model was used to calculate 95% confidence intervals on the SS source contribution estimations.

5.2.4 Inter- and intra-event variation in suspended sediment sources

Besides calculating average sediment source contributions, variations in the total SSCs and the source contributions were assessed to evaluate how SSCs relate to hydro-meteorological variables and sediment sources. At the inter-event scale, a PCA was performed on average event variables to assess the natural clustering of events based on sediment and hydro-metrological variables. The event variables included the total and source-specific SSCs (SSC_t (total), SSC_L (limestone), SSC_M (millstone), SSC_C (coals), SSC_R (riverbank) and SSC_U (urban)) together with discharge (Q) and antecedent precipitation totals for one day, 7 days and 21 days prior to the event (P_{1d}, P_{7d}, P_{21d}). Similar to previous studies, antecedent precipitation is used in this study as a proxy variable for the antecedent soil moisture conditions (Krueger et al., 2009; Onderka et al., 2012). At the intra-event scale, hysteresis patterns between discharge and (source-specific) SSCs were visually examined to investigate possible changes in the dominant SS source throughout individual events, and to assess the consistency of source-specific hysteresis patterns, i.e. to assess whether the source-specific SSCs vary simultaneously throughout events.

5.2.5 Hydro-meteorological controlling factors

A multivariate analysis approach was preformed to investigate the correlation between the total SSCs and source-specific SSCs with a range of hydro-meteorological variables in order to substantiate hypotheses about the role of SS source variations in controlling hysteresis patterns (Aich et al., 2014; Francke et al., 2014; Onderka et al., 2012; Perks et al., 2015; Sherriff et al., 2016; Zeiger and Hubbart, 2016). The multivariate dataset included all sampled SSCs, the estimated source-specific SSCs, discharge and precipitation at the time of sampling (Q and P), as well as 1, 7 and 21 day antecedent discharge (Q_{1d}, Q_{7d}, Q_{21d}) and precipitation (P_{1d}, P_{7d}, P_{21d}) for the 3 monitoring stations (MT, PH and TR).

Two types of multivariate analyses were done, each aimed at investigating a different level of correlation between the variables. First, a Pearson correlation analysis was performed to investigate the pairwise correlation between the SSCs, the source specific SSCs and the hydro-meteorological variables. Secondly, relationships were established between the SSCs and source-specific SSCs (Y_i) and the hydro-meteorological variables (X). To avoid problems related to multicollinearity of variables and associated variable selection in a multiple linear regression, PLSR was again used following the same methodological steps as described previously. In total, six SSC-PLSR models (i.e. one for the total SSC and five for the source-specific SSCs) were developed. The PLSR scores and loadings were used to examine the components in the model (Karaman et al., 2013; Martens and Martens, 2000; Wold et al., 2001). SS samples that have high scores on a component are better explained by that component, while the sum of squared loadings (SSL) is a measure to evaluate which hydro-meteorological variables define the model components.

5.2.6 Source-specific sediment loads

The SSC-PLSR models between the source-specific SSCs and the hydro-meteorological variables were applied to estimate SSCs at a 15 min resolution between June 2015 and February 2017. The estimated SSCs were subsequently used to calculate the amount of sediment transported over time per source, i.e.

source-specific SSL (t) per unit of time (15 min or year). The sediment yield (t km^{-2}) was expressed as the SSL per unit of time divided by the catchment area.

5.3 Results

5.3.1 Average sediment source contributions

Limestone-grassland (45% ± 12%) was identified as the dominant SS source in the River Aire, followed by urban street dust (43% ± 10%) (Figure 5-2 a). Millstone- and coals-grassland contributed on average 19% (± 13%) and 14% (±10%) respectively, while eroding riverbanks accounted for 16% (± 18%) of the total SSC.

Furthermore, source contributions to the BS varied considerably along the profile of the river (Figure 5-2 b). Contrary to the SS, riverbanks (up to 140% ± 18%) and millstone-grassland (up to 78% ± 13%) appeared to be major sediment sources to the BS in the upper part of the catchment. The limestone-grassland contribution was only dominant at the most downstream sampling location (BS1), while no coals-grassland contribution to the BS was observed.

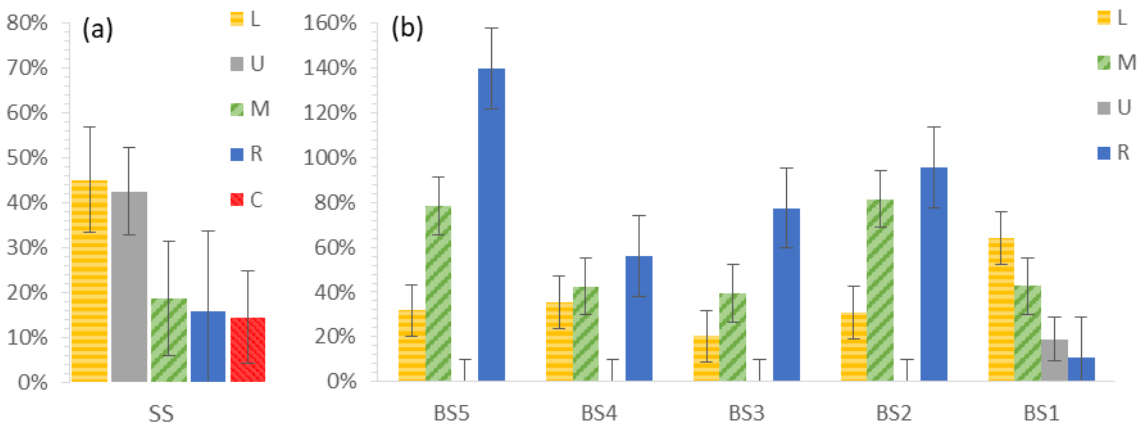

Figure 5-2: Average relative sediment source contributions (%): (a) suspended sediment and (b) bed sediment (BS1 to 5 locations indicated in Figure 5-1). Error bars represent the 95% confidence intervals.

5.3.2 Inter- and intra-event variation in suspended sediment sources

Considerable seasonal variation in the relative source contributions was observed, even with consideration of the 95% confidence intervals. The relative urban street dust contribution was highest in summer (68% ± 10%) and lowest in autumn (35% ± 10%), while the riverbank contribution was lowest in summer (11% ± 18%). In autumn and winter, the combination of sediment sources appeared to be well-mixed with all sources more equally represented compared to spring and summer (Figure 5-3).

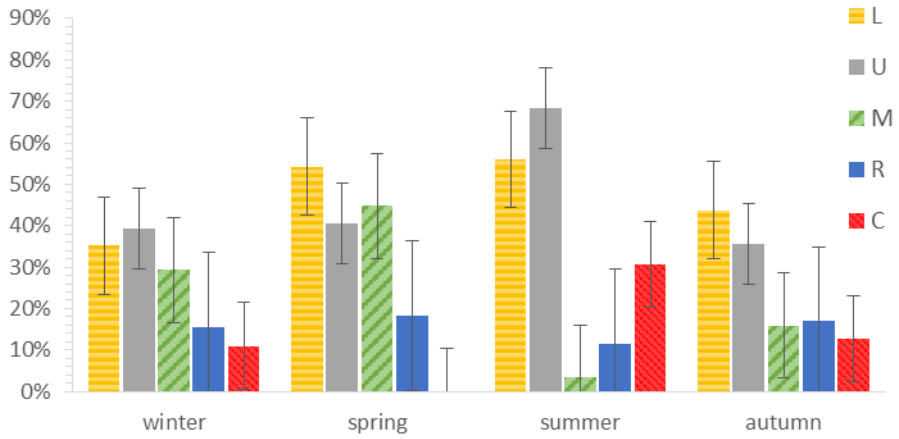

Figure 5-3: Average relative suspended sediment source contributions (%) per season. Error bars represent the 95% confidence intervals.

The seasonal variation in relative SS source contributions suggests that there is substantial temporal variability in the dominant sediment sources, which becomes especially apparent at the event scale (Table 5-1). While the events in November 2016 were generally characterised by the highest discharges and SSCs, smaller events, in terms of discharge, were observed with compared high SSCs that were linked to different sources. For example, compared to other events, Jun-16 (1) was characterised by a low Q_{max} (31 m^3 s^{-1}) and P_{7d} (12 mm), but relatively high SSCs (107 mg L^{-1}) with a dominant contribution from urban street dust.

Table 5-1: Hydro-meteorological and sediment variables per event ($SSC_{mean, max, min, L, M, C, U, R}$: suspended sediment concentration (mg L^{-1}) mean, maximum, minimum, mean L, M, C, U and R; $Q_{mean, max}$: discharge (m^3 s^{-1}) mean and maximum; $P_{1d, 7d, 21d}$: precipitation (mm) 1-7-21day antecedent totals)

	SSC_{mean}	SSC_{max}	SSC_{min}	SSC_L	SSC_M	SSC_C	SSC_U	SSC_R	Q_{mean}	Q_{max}	P_{1d}	P_{7d}	P_{21d}
Aug-15	29.1	90.6	7.0	24.7	2.5	2.9	13.3	11.9	21.5	74.1	13.1	28.2	69.3
Nov-15	33.9	46.7	14.7	16.8	0.0	1.6	14.1	6.1	72.3	122.0	5.3	16.0	158.6
Mar-16	19.8	27.4	12.5	12.4	4.3	0.0	15.5	0.0	26.7	40.9	0.5	53.8	81.9
Jun-16(1)	28.2	107.3	8.7	21.1	0.0	13.5	31.8	0.0	9.4	31.1	7.2	11.9	44.2
Jun-16(2)	47.1	103.4	8.3	19.2	0.0	33.5	31.9	0.0	16.5	30.7	10.6	33.2	49.0
Aug-16	15.9	18.7	13.0	7.7	2.3	0.0	7.0	4.9	13.5	23.2	15.0	54.2	81.4
Sep-16	179.4	1007.5	7.4	39.4	7.3	66.0	15.1	115.8	18.8	43.3	14.2	20.1	64.8
Nov-16(1)	42.8	151.0	3.3	31.6	20.9	1.9	17.9	2.1	18.2	37.6	2.7	8.4	22.2
Nov-16(2)	51.7	116.0	11.7	24.4	13.4	3.8	15.7	3.9	28.4	53.4	0.3	27.4	34.0
Nov-16(3)	37.6	97.8	12.3	18.1	3.3	5.6	15.9	0.7	47.0	72.0	4.8	44.7	57.7
Nov-16(4)	65.6	152.0	11.2	20.9	7.0	18.7	22.5	7.4	48.4	101.0	3.1	47.3	88.7
Jan-17	12.0	21.6	3.7	5.3	3.6	0.0	3.7	4.8	18.5	29.5	0.6	15.8	37.8
Feb-17(1)	98.3	243.5	36	34.2	33.3	14.9	46.3	1.7	37.8	88.2	6.24	12.82	50.42
Feb-17(2)	33.0	64.8	15.9	8.6	3.8	7.1	9.4	5.1	34.4	54.5	6.62	35.64	61.36

Principal component analysis

The complex relationship between discharge and SSC is demonstrated by the PCA results, in which two components explained 59.4% of the total variance. The first component (36.4%) was determined predominantly by the total and source-specific SSCs, and the second component (23%) by Q, SSC_M and SSC_U (Figure 5-4). The events Sep-16 and Feb-17(1) were both characterised by higher SSCs (first component) compared to the other events (Table 5-1; Figure 5-4). However, the SSC_{max} was significantly higher in Sep-16 than in Feb-17(1) (1000 mg L^{-1} compared to 243 mg L^{-1}), while Q_{max} in Sep-16 was less than half the one of Feb-17(1) (43 m^3 s^{-1} compared to 88 m^3 s^{-1}) (second component). The difference between both events was also expressed in the dominant sediment source, which was urban street dust in Feb-17 (1), and riverbank in Sep-16. Contrarily, Jun-16(2) and Aug-16 were both characterised by comparable Q_{max} (second component), while the events differed strongly in SSC_{max} and SSC_C (second component).

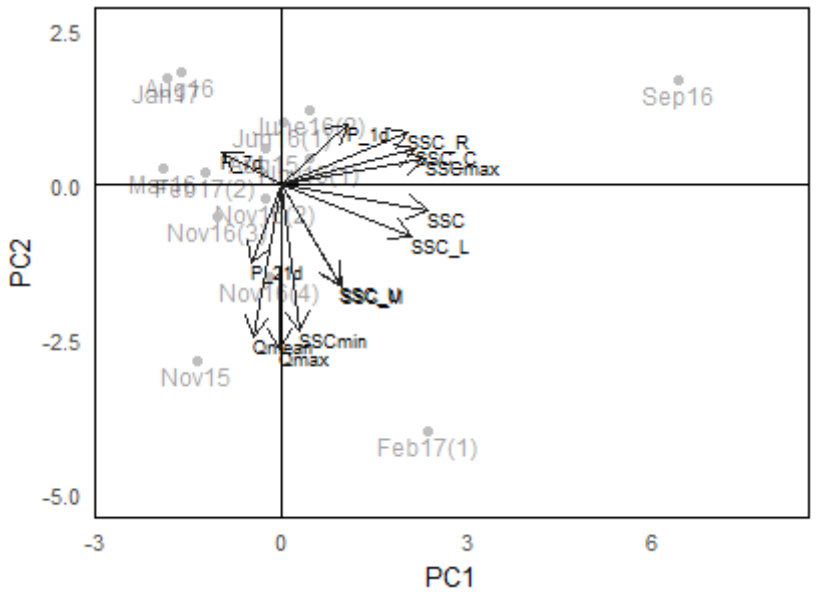

Figure 5-4: Biplot of the scores (grey) and loading vectors (black) on the first and second principal component (PC1 and PC2) of the principal component analysis (PCA) applied on the data in Table 5-1

Hysteresis analysis

The results of the PCA illustrated that the relationship between discharge and SSC is complex, and that events with high discharges can be characterised by both low and high SSCs. This complexity is clearly illustrated by the discharge-SSC hysteresis patterns at the intra-event scale (Figure 5-5). The most important observation is that the source-specific SSCs do not always follow the same hysteresis pattern, i.e. the source contributions are not constant and not equally important throughout events.

In Jun-16(1) a slight counter-clockwise pattern was observed, with urban street dust as the dominant SS source (Figure 5-5 a). Furthermore, the hysteresis patterns of the SSC, SSC_L, SSC_C and SSC_U exhibited a consistent counter-clockwise pattern, while SSC_R and SSC_M were close to zero. Contrarily, the counter-clockwise hysteresis pattern in Sep-16 was characterised by slightly higher discharges and a very high SSC peak (Figure 5-5 b). During the first half of the event, the SSC_R, SSC_L and SSC_C increased consistently with the SSC, and riverbank became the dominant SS source. However, the SSC_R decreased rapidly towards the end of the event, while the SSC_C decreased more gradually,

which coincided with a slight increase of the SSC_U. Furthermore, the Nov-16(4) event exhibited a clockwise-pattern whereby the dominant sediment source changed from urban street dust during the rise of the hydrograph, to coals-grassland at peak discharges, and limestone-grassland during the falling limb (Figure 5-5 c). The SSC_L, SSC_C and SSC_U hysteresis patterns were consistent with the SSC, all showing a second SSC peak during the falling limb of the hydrograph, while in the SSC_R a double peak was present before and after the second SSC peak. Finally, Feb-17(2) was characterised by a complex hysteresis pattern with a counter-clockwise loop during the first peak, and a smaller clockwise during the second peak (Figure 5-5 d). The first peak was mainly characterised by SSC_C (clockwise) and SSC_R (counter-clockwise). During the second peak, SSC_L and SSC_U became dominant, both displaying a clockwise pattern.

The complex relationship between SSC, discharge and source contributions is also illustrated in the time series of multiple discharge peaks in November 2016 and February 2017 (Figure 5-6). As the discharge peaks in November 2016 progressed, SSC_L appeared to decrease, while the SSC_C increased. Furthermore, SSC_U appeared to be highest during the rising limb of the hydrographs, remaining an important source throughout the events, while the SSC_R was higher during the second half of the discharge peaks (Figure 5-6 a). Similar trends in SSC_L, SSC_C and SSC_R were evident in discharge peaks in February 2017, while the total SSC appeared to decrease despite similar discharge peaks (Figure 5-6 b).

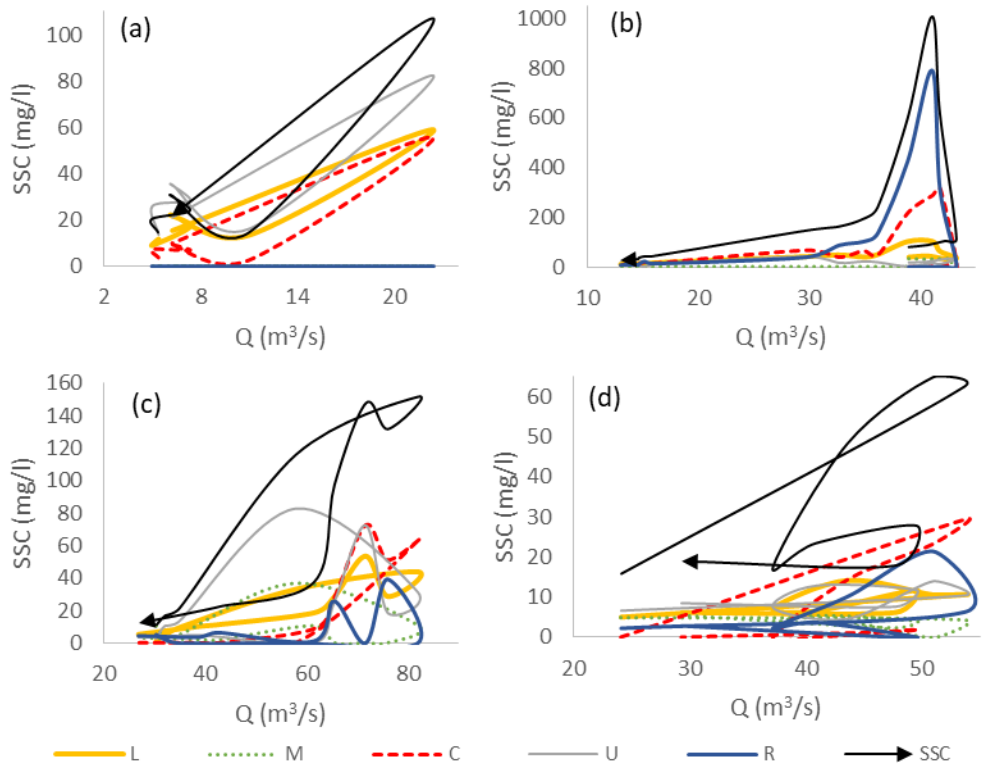

Figure 5-5: Hysteresis patterns between suspended sediment concentration (SSC) and discharge (Q) with estimated source-specific SSCs during high-flow events in (a) Jun-16(1), (b) Sep-16, (c) Nov-16(4), and (d) Feb-17(2)

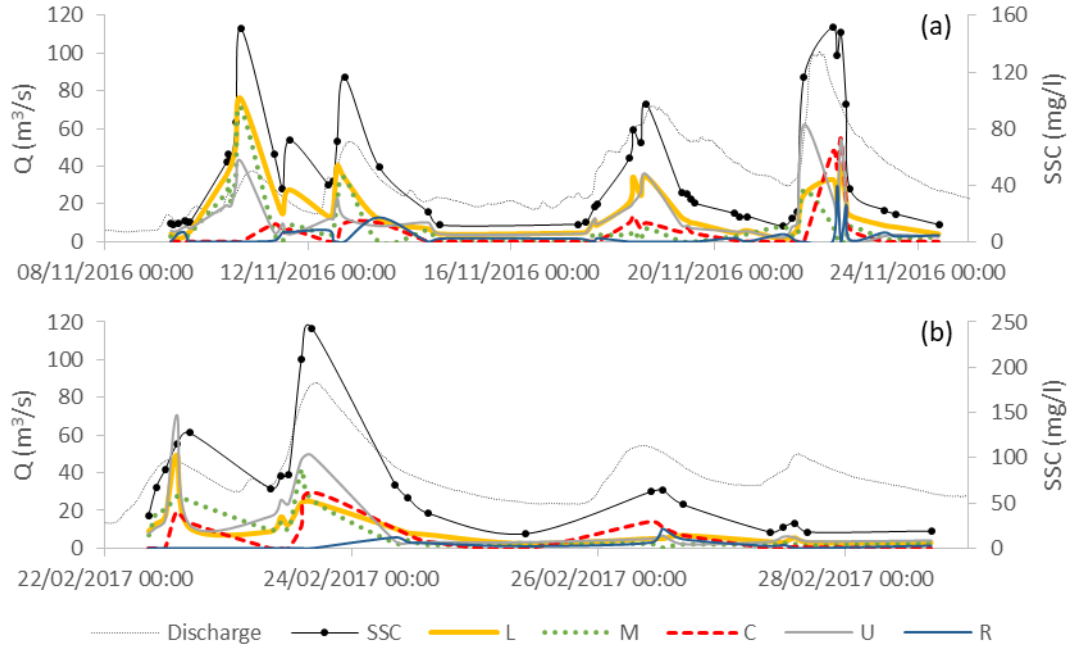

Figure 5-6: Discharge (Q) and sampled suspended sediment concentration (SSC) with estimated sediment source-specific SSCs in (a) November 2016 and (b) February 2017.

5.3.3 Hydro-meteorological controlling factors

Pearson correlation analysis

The Pearson Correlation analysis confirmed significant correlations between the sediment and hydro-meteorological variables (Table 5-2). Correlations existed between the types of SSC: the total SSC (SSC_t) was positively correlated with SSC_L, SSC_C, and SSC_R, while negatively correlated with SSC_U. Most discharge variables were also significantly correlated with precipitation variables, and strong correlations existed between the precipitation variables at different monitoring stations.

Furthermore, SSCs were correlated to various hydro-meteorological variables (Table 5-2). The SSC_t was correlated to Q, P_{1d} and P_{7d} (mainly from PH). The SSC_L and SSC_u were positively correlated with instantaneous P, while negatively correlated with Q and antecedent P. A similar correlation was present for SSC_C, mostly with precipitation variables at MT. Contrarily, SSC_M was positively correlated with antecedent discharge (Q_{21d}) and the SSC_R was positively correlated to antecedent P at PH.

Table 5-2: Pearson correlation analysis between SSC, Source-specific SSCs and hydro-meteorological variables (Q: discharge, P: precipitation, 1, 7 and 21 days antecedent Q and P). Bold numbers are significant at the 95% confidence level.

	SSC	SSC_L	SSC_M	SSC_C	SSC_U	SSC_R	Q	Q_{1d}	Q_{7d}	Q_{21d}	P_{TR}	P_{TR1d}	P_{TR7d}	P_{TR21d}	P_{PH}	P_{PH1d}	P_{PH7d}	P_{PH21d}	P_{MT}	P_{MT1d}	P_{MT7d}	P_{MT21d}
SSC	1.00																					
SSC_L	**-0.36**	1.00																				
SSC_M	-0.08	0.10	1.00																			
SSC_C	**0.24**	-0.16	**-0.46**	1.00																		
SSC_U	**-0.32**	**0.52**	0.06	0.07	1.00																	
SSC_R	**0.41**	**-0.52**	**-0.22**	0.00	**-0.51**	1.00																
Q	**0.19**	**-0.23**	-0.10	-0.07	**-0.30**	-0.09	1.00															
Q_{1d}	**-0.20**	-0.05	**-0.22**	**-0.21**	**-0.21**	-0.02	**0.59**	1.00														
Q_{7d}	-0.11	0.06	-0.16	**-0.21**	0.00	0.00	**0.62**	**0.73**	1.00													
Q_{21d}	0.07	0.07	**0.24**	**-0.25**	0.09	0.01	-0.16	-0.02	0.06	1.00												
P_{TR}	-0.06	0.16	-0.05	0.00	**0.27**	-0.12	-0.09	0.01	0.07	0.01	1.00											
P_{TR1d}	**0.30**	0.12	**0.19**	0.04	0.05	**-0.23**	**0.51**	0.02	**0.19**	-0.04	0.06	1.00										
P_{TR7d}	-0.10	-0.04	**-0.34**	0.08	-0.07	-0.08	**0.64**	**0.68**	**0.58**	-0.15	-0.01	**0.27**	1.00									
P_{TR21d}	-0.09	0.08	**-0.31**	-0.14	-0.06	0.11	**0.56**	**0.68**	**0.84**	-0.05	0.00	0.16	**0.76**	1.00								
P_{PH}	-0.09	**0.21**	0.03	0.00	**0.29**	**-0.20**	-0.09	-0.02	0.09	-0.01	**0.20**	0.15	0.03	0.00	1.00							
P_{PH1d}	**0.60**	-0.13	0.05	0.10	**-0.23**	**0.21**	0.12	**-0.33**	-0.16	0.08	-0.06	**0.52**	-0.04	-0.04	0.00	1.00						
P_{PH7d}	**0.25**	-0.07	**-0.28**	0.11	**-0.33**	**0.31**	-0.14	**-0.23**	**-0.34**	**-0.19**	-0.11	0.09	0.10	0.00	-0.08	0.46	1.00					
P_{PH21d}	0.14	-0.02	-0.11	-0.16	**-0.42**	**0.28**	0.11	0.04	0.01	**-0.19**	-0.10	0.08	0.17	**0.23**	0.06	**0.32**	0.73	1.00				
P_{MT}	-0.10	**0.24**	0.08	-0.15	**0.18**	**-0.22**	0.14	**0.27**	**0.39**	0.07	**0.21**	**0.20**	**0.20**	**0.26**	**0.57**	-0.05	**-0.19**	0.08	1.00			
P_{MT1d}	**0.45**	-0.12	0.13	**0.18**	-0.14	-0.11	**0.51**	-0.15	0.00	**-0.21**	-0.05	**0.74**	**0.20**	0.06	0.04	**0.66**	0.12	0.11	0.03	1.00		
P_{MT7d}	-0.04	**-0.25**	-0.03	**-0.32**	**-0.42**	0.04	**0.60**	**0.45**	**0.22**	**-0.18**	-0.14	0.06	**0.52**	**0.29**	-0.05	-0.03	**0.19**	**0.41**	0.09	**0.19**	1.00	
P_{MT21d}	0.00	-0.07	**-0.22**	**-0.29**	**-0.28**	**0.22**	**0.64**	**0.66**	**0.81**	-0.05	-0.06	0.10	**0.63**	**0.91**	-0.05	0.03	0.06	**0.38**	**0.23**	0.11	**0.52**	1.00

Partial Least Squares regression

Overall, the results of the Pearson Correlation analysis demonstrated the high degree of covariation between the different variables, which justifies the use of PLSR. PLSR models were developed to estimate the total SSC and the source-specific SSCs as a function of hydro-meteorological variables (Table 5-3). The SSC_L-PLSR model had the highest goodness of fit (R^2 = 56.2%) , while the root mean squared error of prediction (RMSEP) was highest for SSC_t (56.6 mg L^{-1}), which could be attributed to the exceptionally high total SSCs during the event in September 2016. Generally, the models consisted of 4 to 6 components with a varying explained variance between 42% and 57%. In all models, the first component explained significantly more variance than the second component.

Table 5-3: Partial Least Squares regression model statistics (RMSEP: root mean squared error of prediction)

	SSC_t	SSC_L	SSC_M	SSC_C	SSC_U	SSC_R
R^2 (%)	36.4	56.2	29.7	48.5	28.7	32.3
RMSEP (mg L^{-1})	56.6	10.7	10.4	27	12.8	42.8
Number of components	5	5	6	4	4	5
Explained variance 1st component (%)	32.57	41.51	26.98	20.99	33.09	15.13
Explained variance 2nd component (%)	5.07	6.33	8.95	8.69	2.91	3.92
Explained variance all components (%)	56.2	57.53	41.88	48.51	49.93	31.08

Further examination of the sum of squared PLSR loadings allowed the identification of hydro-meteorological variables that define the model components (Figure 5-7). In the SSC_t model, the first component was determined by P_{1d} and Q, and the second component by P_{7d}, P_{21}d, Q_{1d} and Q_{7d}. Similar combinations of variables represented the first and second components of the SSC_L model. However, the other sediment sources appeared to be controlled by other sets of variables, suggesting the presence of different mechanisms controlling the source-specific SSCs. In general, SSC_M, SSC_C and SSC_U were more correlated to precipitation variables at MT and TR and less to precipitation at PH. Specifically, both in the SSC_M and SSC_C models, the first component was generally determined by P_{7d} and P_{21d} and Q_{7d}, and the second component by Q and P_{1d}. The SSC_U model was determined by P_{1d} in the first component, and Q,

P_{7d} and P_{21d} in the second component. Contrarily, the SSC_R model was mainly determined by precipitation at PH (first component), while discharge variables together with P_{7d} and P_{21d} at MT and TR defined the second component.

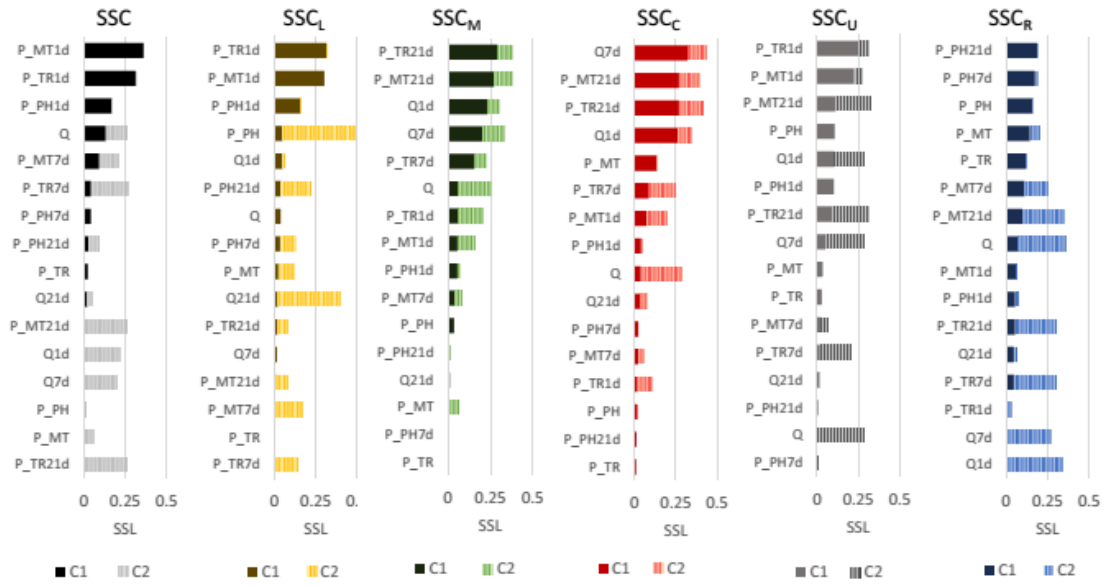

Figure 5-7: Sum of squared loadings (SSL) of the first two components (C1 and C2) of the SSC-PLSR models.

The interaction of controlling factors on the SSCs is also expressed in the varying importance of the components in explaining the estimated SSCs (i.e. the variable scores of the observations on the components) (Figure 5-8). The PLSR scores on the first two components for each PLSR model are shown for SS samples in November 2016 (same as in Figure 5-6 a). In the SSC_L model, both components were equally important at the start, while as the events progressed the first component (P_{1d}) became dominant in explaining the SSC_L. Similarly, the second component (P_{1d}) became more important in explaining the SSC_M and SSCc as the events progressed (Figure 5-8). The SSC_U model also showed an increasing importance of the second component (P_{7d} and P_{21d}) towards the end of the month, while in the riverbank model both components remained equally important throughout the events.

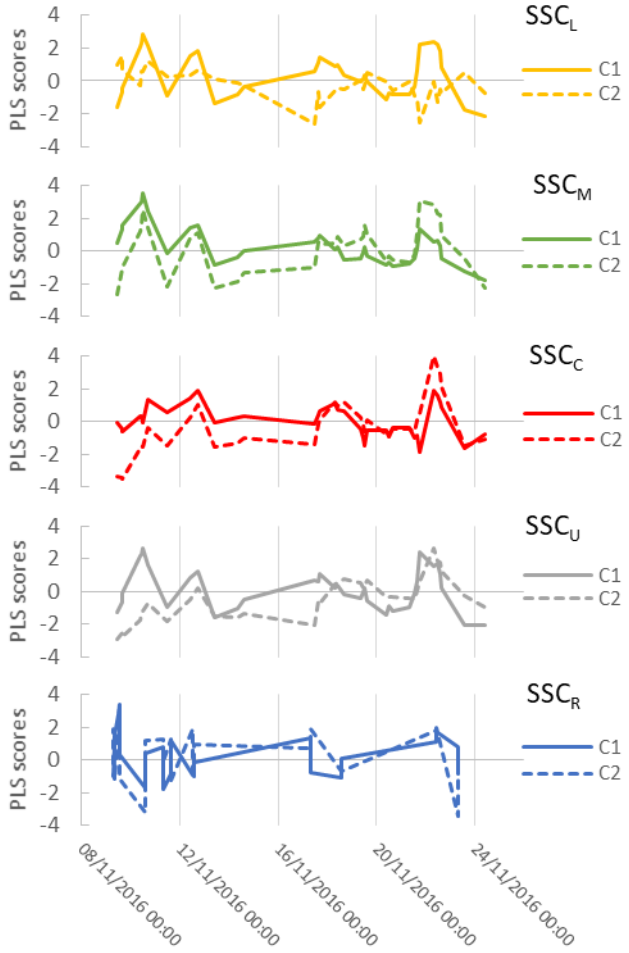

Figure 5-8: Scores on the first (C1) and second (C2) components of the SSC-PLSR models for SS samples collected in November 2016.

5.3.4 Source-specific sediment loads

The SSC-PLSR models were applied to the entire available dataset of hydro-meteorological variables to estimate the total and source-specific SSCs at a 15-min resolution. For the November 2016 and February 2017 events the estimated SSCs correspond well with the observed SSCs (Figure 5-9). For example, the exhaustion effect during the progression of multiple events as observed in Figure 5-6 was also visible in the estimated SSCs. Furthermore, it was also observed that the estimated urban street dust contribution remains high at low flows (Figure 5-9).

The estimated SSCs were subsequently used to calculate the total and source-specific SSLs. In 2016, the total SSL was estimated to be 35,750 t, while the source-specific SSLs ranged from 12,908 t and 12,222 t for urban street dust and limestone-grassland respectively, to 9,246 t for coals-grassland, 8,047 t for millstone-grassland, and 6,431 t for riverbanks. It has to be noted that these SSLs should be interpreted with caution because the cumulative uncertainties associated with the initial estimation of the source contributions and the subsequent estimation of source-specific SSCs are not taken into account.

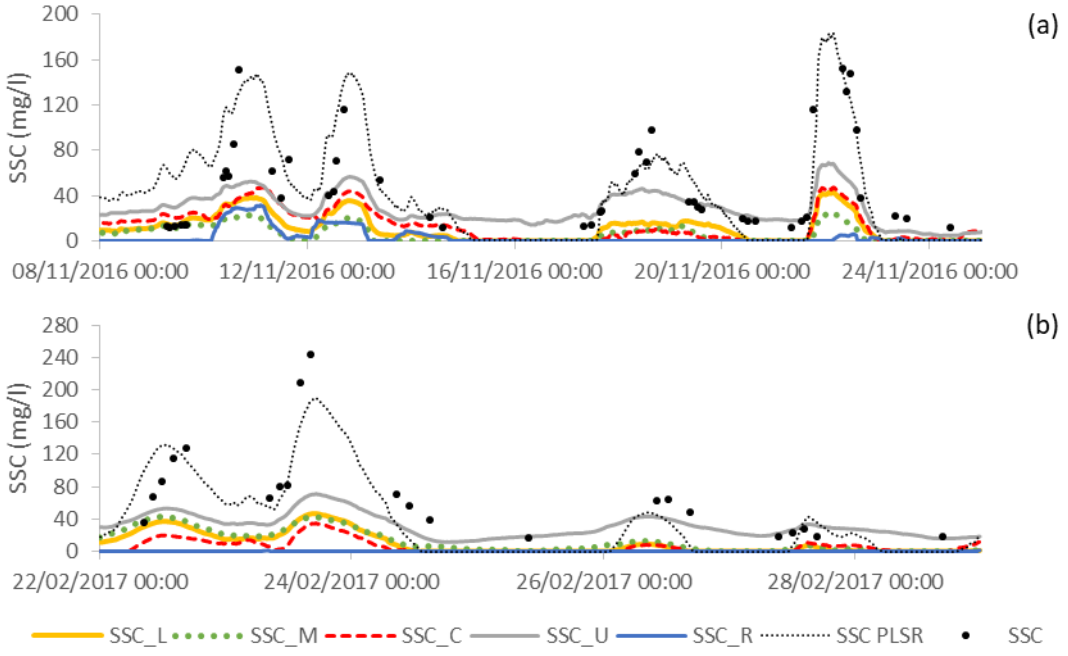

Figure 5-9: Observed suspended sediment concentration (SSC) (black dots) and estimated total and source-specific SSC in (a) November 2016 and (b) February 2017 based on SSC-PLSR models.

5.4 Discussion

This study combined high frequency SSC monitoring with DRIFTS-based sediment fingerprinting to investigate the mechanisms controlling source-specific SSCs at the intra-annual and event timescales. The results illustrate that while dominant sediment sources were identified, considerable temporal variability in the SSC and sources was also observed, confirming the difficulty in generalising hysteresis patterns in terms of underlying processes and sediment sources.

5.4.1 Dominant sediment sources

The fingerprinting results identified grassland from the limestone area as the dominant SS source in the River Aire (average 45% ± 12%), followed by urban street dust (average 43% ± 10%). The high urban contribution is in agreement with a previous sediment fingerprinting study in the catchment that estimated a relative urban street dust contribution of 20% to the SS (Carter et al., 2003). Other studies also observed that the urban environment had a significant impact on the total SSL in Bradford Beck, a major tributary of the River Aire (Old et al., 2006), and that the SS-associated contaminants increased downstream which was linked to increasing urban area (D. E. Walling et al., 2003).

Nevertheless, important differences between the results in this study and previous studies were also observed. In the study by Carter et al. (2003), riverbank was estimated to be the dominant SS source (43–84%, compared to 16% in this study), and the contribution of limestone- and millstone grassland were 13% and 87% respectively (compared to 45% and 19% in this study). The difference in results can be attributed to a number of factors. First, the studies used different fingerprinting approaches each with their specific assumptions and uncertainties. Carter et al. (2003) used geochemical fingerprinting based on two separate types of source classification: one based on geology (limestone and millstone) and one based on land use (uncultivated topsoil, riverbanks, and urban). In this study, the two classification-types were merged, allowing the discrimination between topsoil based on geology and riverbank material based on DRIFTS and experimental mixtures. Second, part of the difference may also be related to the SS sampling method, location and timing. Carter et al. (2003) used submersible pumps to collect 70 bulk SS samples between November 1997 and January 1999 (mostly) during high-flow events at five locations within the catchment (upstream of Leeds city centre). Contrarily, this study is based on a more extensive dataset of 200 SS samples taken during 14 high-flow events between June 2015 and March 2017 at a single location within Leeds city centre with a depth-integrating sampler. Due to their spatially distributed study design, Carter et al. (2003) demonstrated that the dominant SS sources varied considerably along the profile of the river, which is also suggested by the variable

source contributions to the BS in this study (Figure 5-2 b). Therefore, the spatial variability could be an important reason for the discrepancy between both studies. Furthermore, it was mentioned that precipitation between 1997 and 1999 was above average resulting in higher discharges, which may have contributed to increased bank collapse and channel scour (Carter et al., 2003). The possible impact of the latter aspect also supports the findings in this study showing that timing of sampling has a significant effect on the source apportionment.

5.4.2 Suspended sediment transport mechanisms

The analysis of the temporal variability in the total SSC along with hydro-metrological variables, suggests the presence of a fast-response, hydrology-driven SS transport system (correlation of the total SSC to P_{1d} and Q) (Bracken et al., 2015). Furthermore, the decrease in SSCs after multiple discharge peaks of the same magnitude towards the end of winter (e.g. Figure 5-6 b), may be an indication that the system is supply-limited, characterised by the exhaustion of the readily available sediment supply and/or the growth of a protective vegetation cover as the winter progresses into spring (Carter et al., 2003; Dominic et al., 2015; Foerster et al., 2014; Huisman et al., 2013; Park and Latrubesse, 2014; Rovira et al., 2015; Sun et al., 2015). However, by combining SS source information with detailed hydro-meteorological data, more specific mechanisms for SS transport can be identified controlling the sediment contribution from (i) grassland areas, (ii) urbanisation, and (iii) eroding riverbanks (Figure 5-10).

Erosion in grassland areas

The results demonstrate the differential erosion and sediment delivery rates from the grassland source areas, which appears to be controlled by antecedent moisture conditions and sediment connectivity, i.e. the capacity of the catchment to effectively transfer material towards the river determined by the presence/absence of physical blockages (e.g. hills, ditches, walls, plains) (Fryirs, 2013).

The SSC_L appeared to be most strongly correlated to the total SSC and showed a similar correlation to P_{1d} and Q. This corresponds well with the observation that

limestone-grassland is the dominant sediment source in the River Aire (Figure 5-2) and that the limestone-grassland contribution was significant throughout events (e.g. Figure 5-5). However, the limestone area is the most distant source area from the point of sampling (40 to 45 km), which suggests that a ready supply of limestone-grassland sediment must be available within the river system, for example stored on the river bed (Poulenard et al., 2012; Sherriff et al., 2016). The presence of a high limestone-sediment supply could possibly be explained by higher erosion rates in the upper part of the catchment due to the steeper topography (Figure 5-1; reflected in the predicted soil loss calculated by the RUSLE) and the higher connectivity of the landscape to the river (i.e. predominantly grassland directly alongside the river with few urbanised areas) compared to the other grassland areas (Fryirs, 2013) (Figure 5-10). This hypothesis is supported by the observation that precipitation from PH (located in a steep part of the catchment; Figure 5-1) was especially correlated to the SSC_L, and that the relative limestone-grassland contribution to the BS was dominant in the lower part of the catchment (BS1 in Figure 5-3).

Contrarily, the contributions of the millstone-grassland and coals-grassland were mainly correlated to antecedent precipitation (especially from MT and TR) and discharge, which can also be linked to sediment connectivity. The middle and, especially, the lower parts of the catchment are characterised by more gentle slopes, and the sediment connectivity in the landscape strongly decreases due to urbanisation (Figure 5-10). The coals-grassland area is very scattered within predominant urban area and is not well connected to the river system, which is reflected in the absence of sediment from this area in the BS samples (Figure 5-2 b). This observation suggests that more prolonged precipitation (i.e. antecedent precipitation) is required to connect the eroded material to the river system (Fryirs, 2013), and could explain the lag-time in the coals-grassland contribution during events (Figure 5-6).

Grassland is generally considered to be less prone to soil erosion compared to arable land. Yet, the presence of considerable stocks of sediment from the grassland areas might be the result of extensive cattle grazing in the Aire

catchment (Bilotta et al., 2007; James and Alexander, 1998; Meyles et al., 2006; Peukert et al., 2014; Trimble and Mendel, 1995). Livestock and farm vehicles disturb the soil surface through compaction and trampling, which can detach and mobilise sediment particles (Brazier et al., 2007). Furthermore, grazing can also cause flow paths (e.g. along sheep tracks) which connect hillslopes to the lower areas, leading to increased delivery of overland flow and associated erosion and sediment transport during high-flow events (Meyles et al., 2006). These processes can result in more sediment being delivered to the river, especially during autumn, when average precipitation increases and the vegetation cover decreases (seasonality of plant growth and/or or end grazing season), (Bilotta et al., 2007).

Urbanisation

As mentioned in the previous section, the strong degree of urbanisation at the point of SS sampling is clearly reflected in the significant contribution of urban street dust to the SS. The average street dust contribution during individual events was most strongly correlated to the event discharge and precipitation (Figure 5-4, Figure 5-5 and Figure 5-7). These results suggest that the street dust contribution responds fast to precipitation, which demonstrates the proximity of the urban area to the sampling location. Furthermore, the supply of urban street dust appears to be less controlled by hydrological processes (i.e. no exhaustion) (Bracken et al., 2015), which is also reflected in the high estimated street dust load during low flows (Figure 5-9). A possible explanation for this could be that high antecedent precipitation can connect more distant locations to the river, transporting additional street dust to the river system (i.e. particles from more distant locations reaching the river due to persistent rainfall and runoff) (Carter et al., 2003; Taylor and Owens, 2009).

Riverbank erosion

Riverbank erosion was not found to be a dominant source of SSC at the point of sampling. Riverbank contributions were the least well correlated to hydro-meteorological factors. While this lack of correlation can be partially linked to the low degree of discrimination of the riverbank class from the other source classes

and the associated high confidence intervals, it can also be linked to the nature of riverbank erosion.

In general, an increase in the riverbank contribution was observed towards the second-half of events (i.e. lag-time). This finding is consistent with previous studies suggesting that the majority of bank material is entrained at higher discharges (Janes et al., 2017; Rügner et al., 2014; Sear et al., 2003; Zeiger and Hubbart, 2016). For example, based solely on the total SSC, the counter-clockwise hysteresis pattern in Sep-16 (Figure 5-5 b) could indicate that a sediment source entered the river suddenly as the event progressed. This observation corresponded to a significant increase in riverbank sediment (e.g. as a result of bank collapse). Furthermore, in the upper part of the catchment (especially near Kildwick), riverbanks are strongly incised and visibly eroding (Figure 5-10), which can explain the correlation of riverbank sources to precipitation at PH and the high relative contribution of riverbanks to the BS in the upper part (Figure 5-3). These observations are in agreement with the findings from Carter et al. (2003), who observed a high relative contribution of riverbank in the upper part of the catchment. Contrarily, in the lower, more urbanised parts of the catchment, riverbanks are more protected by embankments (Figure 5-10), which can explain the low contribution of riverbank sediment to the BS in Leeds (BS 1 Figure 5-2 b) and could present an alternative explanation for the lag time in the riverbank contribution during events. Furthermore, the relative riverbank contribution to the SS was lowest in summer. This seasonal variation has also been observed in other rivers (Collins and Walling, 2004; Lawler et al., 1999) and could be linked to the presence of a protective vegetation cover in summer, and/or the combination of higher discharges, freeze-thaw processes and antecedent moisture conditions during winter (Carter et al., 2003; Foerster et al., 2014; Lawler et al., 1999).

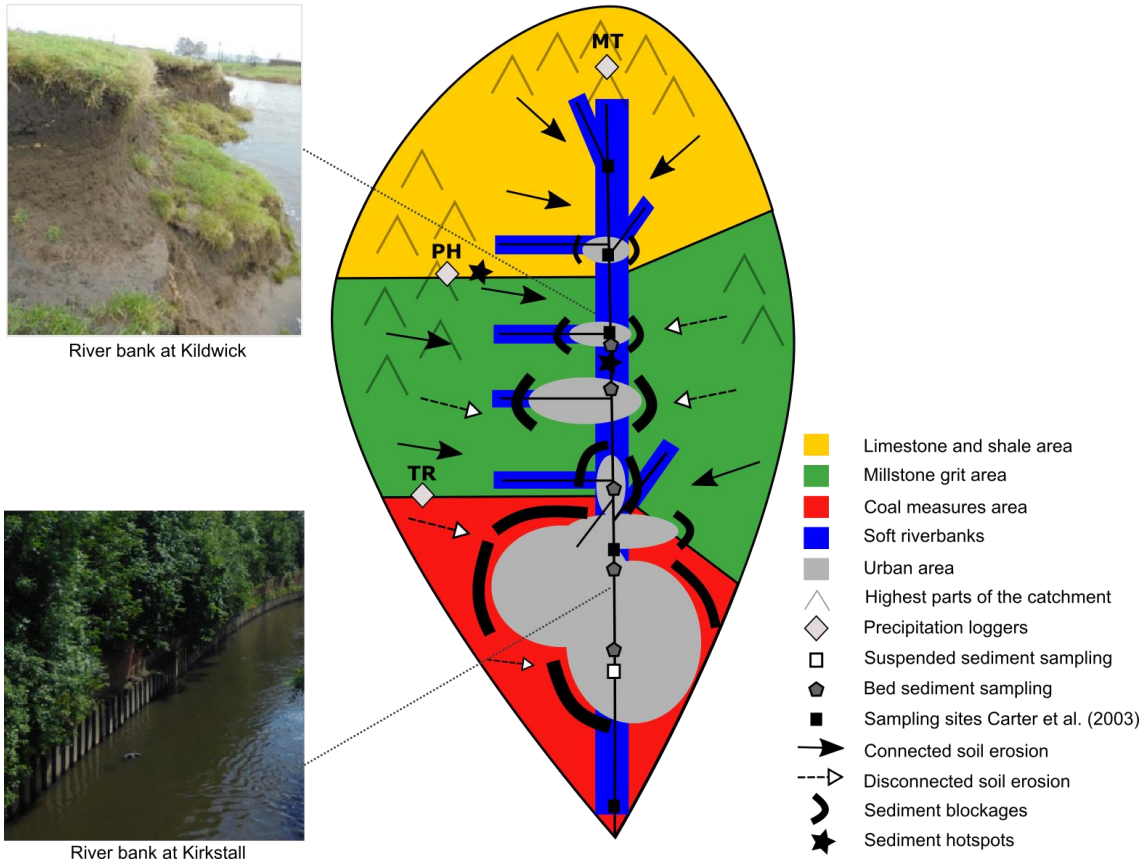

Figure 5-10: Conceptual illustration of the suspended sediment transport system in the River Aire catchment

5.5 Conclusion

This study demonstrated the potential of DRIFTS-based sediment fingerprinting in combination with statistical analysis of hydro-meteorological data to investigate variations in SS sources during individual high-flow events and to quantify how variations in SS sources control the total SSC in rivers in response to hydro-meteorological and catchment processes.

By taking into account sediment source information, the importance of the proximity of sediment sources in controlling hysteresis behaviour was nuanced and the effect of variations in source contributions can be better identified. Source-specific hydro-meteorological drivers could be identified that provide more detailed insights into the underlying mechanisms for SS transport. The total SSC was dominantly driven by to recent antecedent precipitation and discharge,

suggesting a fast-response, hydrology controlled SS transport system. However, antecedent conditions were also important and appeared to play a dual role: on the one hand, it controlled the total SSC by connecting more sources to the river system, while on the other it appeared to cause exhaustion of the sediment supply after persistent precipitation. The study also presented a first attempt to estimate source-specific SSLs as function of hydro-meteorological factors and emphasize that more research is required to reduce the uncertainty on the estimates (e.g. better source discrimination and statistical modelling).

The findings in this study show that by combining innovative statistical methods for sediment source apportionment and the estimation of SSCs, we are better able to identify underlying processes for temporal variation in SS transport, which can serve as a basis for process-based modelling and management decisions.

5.6 References

Aich, V., Zimmermann, A., Elsenbeer, H., 2014. Quantification and interpretation of suspended-sediment discharge hysteresis patterns: How much data do we need? Catena 122, 120–129. doi:10.1016/j.catena.2014.06.020

Bilotta, G.S., Brazier, R.E., 2008. Understanding the influence of suspended solids on water quality and aquatic biota. Water Res. 42, 2849–2861. doi:10.1016/j.watres.2008.03.018

Bilotta, G.S., Brazier, R.E., Haygarth, P.M., 2007. The Impacts of Grazing Animals on the Quality of Soils, Vegetation, and Surface Waters in Intensively Managed Grasslands. Adv. Agron. 94, 237–280. doi:10.1016/S0065-2113(06)94006-1

Bracken, L.J., Turnbull, L., Wainwright, J., Bogaart, P., 2015. Sediment connectivity: a framework for understanding sediment transfer at multiple scales. Earth Surf. Process. Landforms 40, 177–188. doi:10.1002/esp.3635

Brazier, R.E., Bilotta, G.S., Haygarth, P.M., 2007. A perspective on the role of lowland, agricultural grasslands in contributing to erosion and water quality problems in the UK. Earth Surf. Process. Landforms 32, 964–967. doi:10.1002/esp

British Geological Survey, 2016. The BGS Lexicon of Named Rock Units [WWW Document]. URL http://www.bgs.ac.uk/lexicon/home.html

Carter, J., Owens, P.N., Walling, D.E., Leeks, G.J.L., 2003. Fingerprinting suspended sediment sources in a large urban river system. Sci. Total Environ. 314–316, 513–534. doi:10.1016/S0048-9697(03)00071-8

Carter, J., Walling, D.E., Owens, P.N., Leeks, G.J.L., 2006. Spatial and temporal variability in the concentration and speciation of metals in suspended sediment transported by the River Aire, Yorkshire, UK. Hydrol. Process. 20, 3007–3027. doi:10.1002/hyp.6156

Collins, A.L., Pulley, S., Foster, I.D.L., Gellis, A., Porto, P., Horowitz, A.J., 2017. Sediment source fingerprinting as an aid to catchment management: A review of the current state of knowledge and a methodological decision-tree for end-users. J. Environ. Manage. 194, 86–108. doi:10.1016/j.jenvman.2016.09.075

Collins, A.L., Walling, D.E., 2004. Documenting catchment suspended sediment sources: problems, approaches and prospects. Prog. Phys. Geogr. 28, 159–196. doi:10.1191/0309133304pp409ra

Cooper, R.J., Krueger, T., Hiscock, K.M., Rawlins, B.G., 2014a. High-temporal resolution fluvial sediment source fingerprinting with uncertainty: A Bayesian approach. Earth Surf. Process. Landforms. doi:10.1002/esp.3621

Cooper, R.J., Rawlins, B.G., Lézé, B., Krueger, T., Hiscock, K.M., 2014b. Combining two filter paper-based analytical methods to monitor temporal variations in the geochemical properties of fluvial suspended particulate matter. Hydrol. Process. 28, 4042–4056. doi:10.1002/hyp.9945

Davis, C.M., Fox, J.F., 2009. Sediment Fingerprinting : review of the method and future improvements for allocating nonpoint source pollution. J. Environ. Eng. 137, 490–505.

De Girolamo, A.M., Pappagallo, G., Lo Porto, A., 2015. Temporal variability of suspended sediment transport and rating curves in a Mediterranean river basin: The Celone (SE Italy). Catena 128, 135–143. doi:10.1016/j.catena.2014.09.020

Dominic, J.A., Aris, A.Z., Sulaiman, W.N.A., 2015. Factors controlling the suspended sediment yield during rainfall events of dry and wet weather conditions in a tropical urban catchment. Water Resour. Manag. 29, 4519–4538.

Eder, A., Strauss, P., Krueger, T., Quinton, J.N., 2010. Comparative calculation of suspended sediment loads with respect to hysteresis effects (in the Petzenkirchen catchment, Austria). J. Hydrol. 389, 168–176. doi:10.1016/j.jhydrol.2010.05.043

Fan, X., Shi, C., Zhou, Y., Shao, W., 2012. Sediment rating curves in the Ningxia-Inner Mongolia reaches of the upper Yellow River and their implications. Quat. Int. 282, 152–162. doi:10.1016/j.quaint.2012.04.044

Fang, N.F., Shi, Z.H., Chen, F.X., Zhang, H.Y., Wang, Y.X., 2015. Discharge and suspended sediment patterns in a small mountainous watershed with widely distributed rock fragments. J. Hydrol. 528, 238–248. doi:10.1016/j.jhydrol.2015.06.046

Foerster, S., Wilczok, C., Brosinsky, A., Segl, K., 2014. Assessment of sediment connectivity from vegetation cover and topography using remotely sensed data in a dryland catchment in the Spanish Pyrenees. J. Soils Sediments 14, 1982–2000. doi:10.1007/s11368-014-0992-3

Fox, J.F., Papanicolaou, A.N., 2008. An un-mixing model to study watershed erosion processes. Adv. Water Resour. 31, 96–108. doi:10.1016/j.advwatres.2007.06.008

Francke, T., Lopez-Tarazon, J.A., Vericat, D., Bronstert, A., Batalla, R.J., 2008. Flood-based analysis of high-magnitude sediment transport using a non-parametric method. Earth Surf. Process. Landforms 33, 2064–2077. doi:10.1002/esp. 1654

Francke, T., Werb, S., Sommerer, E., López-Tarazón, J.A., 2014. Analysis of runoff, sediment dynamics and sediment yield of subcatchments in the highly erodible Isábena catchment, Central Pyrenees. J. Soils Sediments 14, 1909–1920. doi:10.1007/s11368-014-0990-5

Fryirs, K.A., 2013. (Dis)Connectivity in catchment sediment cascades: A fresh look at the sediment delivery problem. Earth Surf. Process. Landforms 38, 30–46. doi:10.1002/esp.3242

Haddadchi, A., Ryder, D.S., Evrard, O., Olley, J.M., 2013. Sediment fingerprinting in fluvial systems: Review of tracers, sediment sources and mixing models. Int. J. Sediment Res. 28, 560–578. doi:10.1016/S1001-6279(14)60013-5

Huisman, N.L.H., Karthikeyan, K.G., Lamba, J., Thompson, A.M., Peaslee, G., 2013. Quantification of seasonal sediment and phosphorus transport dynamics in an agricultural

watershed using radiometric fingerprinting techniques. J. Soils Sediments 13, 1724–1734. doi:10.1007/s11368-013-0769-0

James, P.A., Alexander, R.W., 1998. Soil erosion and runoff in improved pastures of the Clwydian Range, North Wales. J. Agric. Sci. 130, 473–488. doi:10.1017/S0021859698005425

Janes, V., Nicholas, A., Collins, A., Quine, T., 2017. Analysis of fundamental physical factors influencing channel bank erosion: results for contrasting catchments in England and Wales. Environ. Earth Sci. 76. doi:10.1007/s12665-017-6593-x

Karaman, I., Qannari, E.M., Martens, H., Hedemann, M.S., Knudsen, K.E.B., Kohler, A., 2013. Comparison of Sparse and Jack-knife partial least squares regression methods for variable selection. Chemom. Intell. Lab. Syst. 122, 65–77. doi:10.1016/j.chemolab.2012.12.005

Koiter, A.J., Owens, P.N., Petticrew, E.L., Lobb, D.A., 2013. The behavioural characteristics of sediment properties and their implications for sediment fingerprinting as an approach for identifying sediment sources in river basins. Earth-Science Rev. 125, 24–42. doi:10.1016/j.earscirev.2013.05.009

Krueger, T., Quinton, J.N., Freer, J.E., Macleod, C.J.A., Bilotta, G.S., Brazier, R.E., Butler, P., Haygarth, P.M., 2009. Uncertainties in data and models to describe event dynamics of agricultural sediment and phosphorus transfer. J. Environ. Qual. 38, 1137–1148. doi:10.2134/jeq2008.0179

Laceby, J.P., Evrard, O., Smith, H.G., Blake, W.H., Olley, J.M., Minella, J.P.G., Owens, P.N., 2017. The challenges and opportunities of addressing particle size effects in sediment source fingerprinting: A review. Earth-Science Rev. 169, 85–103. doi:10.1016/j.earscirev.2017.04.009

Lawler, D.M., Grove, J.R., Couperthwaite, J.., Leeks, G.J.L., 1999. Downstream Change in River Bank Erosion Rates in the Swale-Ouse System , Northern Downstream change in river bank erosion rates in the Swale ± Ouse system , northern England. Hydrol. Process. 13, 977–992. doi:10.1002/(SICI)1099-1085(199905)13

Lexartza-Artza, I., Wainwright, J., 2011. Making connections: Changing sediment sources and sinks in an upland catchment. Earth Surf. Process. Landforms 36, 1090–1104. doi:10.1002/esp.2134

Lloyd, C.E.M., Freer, J.E., Johnes, P.J., Collins, A.L., 2016. Using hysteresis analysis of high-resolution water quality monitoring data, including uncertainty, to infer controls on nutrient and sediment transfer in catchments. Sci. Total Environ. 543, 388–404. doi:10.1016/j.scitotenv.2015.11.028

Martens, H., Martens, M., 2000. Modified Jack-knife estimation of parameter uncertainty in bilinear modelling by partial least squares regression (PLSR). Food Qual. Prefer. 11, 5–16. doi:10.1016/S0950-3293(99)00039-7

Martínez-Carreras, N., Krein, A., Udelhoven, T., Gallart, F., Iffly, J.F., Hoffmann, L., Pfister, L., Walling, D.E., 2010a. A rapid spectral-reflectance-based fingerprinting approach for documenting suspended sediment sources during storm runoff events. J. Soils Sediments 10, 400–413. doi:10.1007/s11368-009-0162-1

Martínez-Carreras, N., Udelhoven, T., Krein, A., Gallart, F., Iffly, J.F., Ziebel, J., Hoffmann, L., Pfister, L., Walling, D.E., 2010b. The use of sediment colour measured by diffuse reflectance spectrometry to determine sediment sources: Application to the Attert River catchment (Luxembourg). J. Hydrol. 382, 49–63. doi:10.1016/j.jhydrol.2009.12.017

Mauad, C.R., Wagener, A.D.L.R., Massone, C.G., Aniceto, M.D.S., Lazzari, L., Carreira, R.S., Farias, C.D.O., 2015. Urban rivers as conveyors of hydrocarbons to sediments of estuarine areas: Source characterization, flow rates and mass accumulation. Sci. Total Environ. 506–507, 656–666. doi:10.1016/j.scitotenv.2014.11.033

Meyles, E.W., Williams, A.G., Ternan, J.L., Anderson, J.M., Dowd, J.F., 2006. The influence of grazing on vegetation, soil properties and stream discharge in a small Dartmoor catchment, southwest England, UK. Earth Surf. Process. Landforms 31, 622–631. doi:10.1002/esp.1352

Mukundan, R., Walling, D.E., Gellis, A.C., Slattery, M.C., Radcliffe, D.E., 2012. Sediment source fingerprinting: transforming from a research tool to a management tool. J. Am. Water Resour. Assoc. 48, 1241–1257. doi:10.1111/j.1752-1688.2012.00685.x

Old, G.H., Leeks, G.J.L., Packman, J.C., Smith, B.P.G., Lewis, S., Hewitt, E.J., 2006. River flow and associated transport of sediments and solutes through a highly urbanised catchment, Bradford, West Yorkshire. Sci. Total Environ. 360, 98–108. doi:10.1016/j.scitotenv.2005.08.028

Onderka, M., Krein, A., Wrede, S., Martínez-Carreras, N., Hoffmann, L., 2012. Dynamics of storm-driven suspended sediments in a headwater catchment described by multivariable modeling. J. Soils Sediments 12, 620–635. doi:10.1007/s11368-012-0480-6

Park, E., Latrubesse, E.M., 2014. Modeling suspended sediment distribution patterns of the Amazon River using MODIS data. Remote Sens. Environ. 147, 232–242. doi:10.1016/j.rse.2014.03.013

Perks, M.T., Owen, G.J., Benskin, C.M.H., Jonczyk, J., Deasy, C., Burke, S., Reaney, S.M., Haygarth, P.M., 2015. Dominant mechanisms for the delivery of fine sediment and phosphorus to fluvial networks draining grassland dominated headwater catchments. Sci. Total Environ. 523, 178–190. doi:10.1016/j.scitotenv.2015.03.008

Peukert, S., Griffith, B.A., Murray, P.J., Macleod, C.J.A., Brazier, R.E., 2014. Intensive management in grasslands causes diffuse water pollution at the farm scale. J. Environ. Qual. 43, 2009–23. doi:10.2134/jeq2014.04.0193

Pietroń, J., Jarsjö, J., Romanchenko, A.O., Chalov, S.R., 2015. Model analyses of the contribution of in-channel processes to sediment concentration hysteresis loops. J. Hydrol. 527, 576–589. doi:10.1016/j.jhydrol.2015.05.009

Poulenard, J., Legout, C., Némery, J., Bramorski, J., Navratil, O., Douchin, A., Fanget, B., Perrette, Y., Evrard, O., Esteves, M., 2012. Tracing sediment sources during floods using Diffuse Reflectance Infrared Fourier Transform Spectrometry (DRIFTS): A case study in a highly erosive mountainous catchment (Southern French Alps). J. Hydrol. 414–415, 452–462. doi:10.1016/j.jhydrol.2011.11.022

Poulenard, J., Perrette, Y., Fanget, B., Quetin, P., Trevisan, D., Dorioz, J.M., 2009. Infrared spectroscopy tracing of sediment sources in a small rural watershed (French Alps). Sci. Total Environ. 407, 2808–19. doi:10.1016/j.scitotenv.2008.12.049

Pulley, S., Foster, I., Antunes, P., 2015. The uncertainties associated with sediment fingerprinting suspended and recently deposited fluvial sediment in the Nene river basin. Geomorphology 228, 303–319. doi:10.1016/j.geomorph.2014.09.016

Rovira, A., Ibáñez, C., Martín-Vide, J.P., 2015. Suspended sediment load at the lowermost Ebro River (Catalonia, Spain). Quat. Int. 388, 188–198. doi:10.1016/j.quaint.2015.05.035

Rügner, H., Schwientek, M., Egner, M., Grathwohl, P., 2014. Monitoring of event-based mobilization of hydrophobic pollutants in rivers: calibration of turbidity as a proxy for particle facilitated transport in field and laboratory. Sci. Total Environ. 490, 191–8. doi:10.1016/j.scitotenv.2014.04.110

Sear, D.A., Malcolm, D.N., Thorne, C.R., 2003. Guidebook for Applied Fluvial Geomorphology, R&D Technical Report FD1914. London.

Sherriff, S.C., Rowan, J.S., Fenton, O., Jordan, P., Melland, A.R., Mellander, P.E., Huallacháin,

D., 2016. Storm Event Suspended Sediment-Discharge Hysteresis and Controls in Agricultural Watersheds: Implications for Watershed Scale Sediment Management. Environ. Sci. Technol. 50, 1769–1778. doi:10.1021/acs.est.5b04573

Smith, H.G., Blake, W.H., 2014. Sediment fingerprinting in agricultural catchments: A critical re-examination of source discrimination and data corrections. Geomorphology 204, 177–191. doi:10.1016/j.geomorph.2013.08.003

Smith, H.G., Dragovich, D., 2009. Interpreting sediment delivery processes using suspended sediment-discharge hysteresis patterns from nested upland catchments, south-eastern Australia. Hydrol. Process. 23, 2416–2426. doi:10.1002/hyp

Smith, H.G., Evrard, O., Blake, W.H., Owens, P.N., 2015. Preface—Addressing challenges to advance sediment fingerprinting research. J. Soils Sediments 15, 2033–2037. doi:10.1007/s11368-015-1231-2

Stevens, A., Lopez, L.R., 2015. A Guide to Diffuse Reflectance Spectroscopy & Multivariate Calibration with the R Statistical Software.

Sun, L., Yan, M., Cai, Q., Fang, H., 2015. Suspended sediment dynamics at different time scales in the Loushui River, south-central China. Catena Published. doi:10.1016/j.catena.2015.02.014

Taylor, K.G., Owens, P.N., 2009. Sediments in urban river basins: a review of sediment–contaminant dynamics in an environmental system conditioned by human activities. J. Soils Sediments 9, 281–303. doi:10.1007/s11368-009-0103-z

Tena, A., Vericat, D., Batalla, R.J., 2014. Suspended sediment dynamics during flushing flows in a large impounded river (the lower River Ebro). J. Soils Sediments 14, 2057–2069. doi:10.1007/s11368-014-0987-0

Tiecher, T., Caner, L., Minella, J.P.G., Evrard, O., Mondamert, L., Labanowski, J., Rheinheimer dos Santos, D., 2016. Tracing Sediment Sources using Mid-Infrared Spectroscopy in Arvorezinha Catchment, Southern Brazil. L. Degrad. Dev. doi:10.1002/ldr.2690

Trimble, S.W., Mendel, A.C., 1995. The cow as a geomorphic agent--a critical review. Geomorphology 13, 233–253.

Vercruysse, K., Grabowski, R.C., Rickson, R.J., 2017. Suspended sediment transport dynamics in rivers: Multi-scale drivers of temporal variation. Earth-Science Rev. 166, 38–52. doi:10.1016/j.earscirev.2016.12.016

Walling, D.E., 2013. The evolution of sediment source fingerprinting investigations in fluvial systems. J. Soils Sediments 13, 1658–1675. doi:10.1007/s11368-013-0767-2

Walling, D.E., Owens, P.N., Carter, J., Leeks, G.J.L., Lewis, S., Meharg, A.A., Wright, J., 2003. Storage of sediment-associated nutrients and contaminants in river channel and floodplain systems. Appl. Geochemistry 18, 195–220. doi:10.1016/S0883-2927(02)00121-X

Walling, Owens, P.N., Foster, I.D.L., Lees, J.A., 2003. Changes in the fine sediment dynamics of the Ouse and Tweed basins in the UK over the last 100-150 years. Hydrol. Process. 17, 3245–3269. doi:10.1002/hyp.1385

Williams, G.P., 1989. Sediment concentration versus water discharge during single hydrologic events in rivers. J. Hydrol. doi:10.1016/0022-1694(89)90254-0

Wohl, E., 2015. Legacy effects on sediments in river corridors. Earth-Science Rev. 147, 30–53. doi:10.1016/j.earscirev.2015.05.001

Wold, S., Sjostrom, M., Eriksson, L., 2001. PLS-regression : a basic tool of chemometrics. Chemom. Intell. Lab. Syst. 58, 109–130.

Zeiger, S., Hubbart, J.A., 2016. Quantifying suspended sediment flux in a mixed-land-use urbanizing watershed using a nested-scale study design. Sci. Total Environ. 542, 315–323. doi:10.1016/j.scitotenv.2015.10.096

CHAPTER 6: DISCUSSION

6.1 Introduction

The opening lines of the previous chapters stated that SS is a natural part of river systems, but extremely variable in time and space, and strongly disturbed by human activity. SS can be harmful for the ecological, biochemical and physical status of rivers, but because of its fundamental nature, SS should not simply be removed from the river system. Instead, SS in rivers must be managed. Yet, to develop and apply targeted management strategies, understanding and prediction of SSC variations and sources over multiple timescales is required.

To this end, the variation in SS transport in the River Aire was assessed over three timescales (inter-annual, intra-annual, and event) to uncover the scale-specific processes and process interactions that determine temporal variation in SS transport (Obj. 1), and a novel sediment fingerprinting approach was applied and tested (Obj. 2) to identify factors and processes controlling SS source contributions (Obj. 3). The final part of this thesis will therefore reflect on how process-based understanding of SS transport can contribute to improving quantification and prediction of SS transport in rivers, and support targeted sediment management strategies.

6.2 Quantifying and predicting suspended sediment transport

Chapter 2 showed how SSCs and associated sources can be estimated through multiple empirical approaches, each able to represent different scales of temporal variation in SS transport. It was also argued that consideration of different timescales is essential to deciphering the underlying processes and process interactions controlling SS transport, which was clearly illustrated in Chapter 3 and 5. In what follows, these insights are further explored in terms of their implications for (i) selecting appropriate models to predict SSCs based on the sediment transport dynamics, and (ii) improving existing process-based models to predict temporal variability in SS transport.

6.2.1 Classification of sediment transport systems

The multi-timescale study of SS transport presented in Chapter 3 demonstrated that controlling factors can be identified over multiple timescales, which can be expressed as fractal power: the higher the fractal power, the more difficult it is to decipher the underlying drivers and processes for SS transport. The higher the variability in SS transport at multiple timescales, more processes are likely at play, which complicates our ability to estimate SSCs over these different timescales. When processes control SS transport at several timescales, SRCs will likely underestimate the SSCs by not incorporating the impact of process interactions and feedback mechanisms. Instead, more complex, multi-variate models are recommended to predict SSLs. Therefore, the fractal concept is used here as a basis to develop a methodology to classify SS transport systems in terms of the degree of temporal variability, which can serve as a process-based evaluation and selection tool for models to predict SSCs (Figure 6-1).

When there is no dominant timescale of temporal variation in SS transport it is likely that the SS transport is driven by a single dominant process (type 1a, Figure 6-1). For example, a study in the Isábena River (Spain) showed that SSCs in the river are (quasi)constantly high, even at low flows, and do not show a distinct seasonal pattern, which is linked to the river being permanently at transport capacity, while the badland landscape provides a well-connected, unlimited supply of sediment (López-Tarazón and Batalla, 2014). However, when the variability in the SS transport over various timescales is higher, more processes should be taken into account. The SS transport in the River Aire (type 4b) is characterised by an event-driven, supply-limited SS transport system as a result of the interaction between hydro-meteorological and catchment processes showing a seasonal pattern, while also being influenced by long term land cover changes (Figure 3-7). Similarly, the SS transport system in the Loushui River (China), is event-driven with changing sediment sources throughout events, while also showing both inter-annual and seasonal variation in the SSL due to climatic variability and human intervention (Figure 2-5, 2-6) (Sun et al., 2015). Furthermore, SS transport can also vary over a single timescale. For example,

strong inter-annual changes in the SSL in the Chenyoulan River (China) have been observed, which was linked to landslides (type 3a) (Lin et al., 2008), while SSCs in the Izas Catchments (Spain) appear to be mainly controlled by seasonal snowmelt and individual rainfall events, both generating other sediment sources (Lana-Renault et al., 2011).

Based on this classification system, the choice of predictive model for SSCs can be evaluated in terms of how well it considers the SS transport processes and thus how appropriate the model is. For example, a study in the Tana River (Kenya) showed that the inter-annual SSLs have changed due to dam construction, and while most SS in the pre-dams period was transported during the wet seasons, a higher portion in now transported during the dry seasons due to a change in baseflow (type 4a) (Geeraert et al., 2017). Therefore, seasonal SRCs are most appropriate, but should also be updated after dam construction to estimate reliable SSLs. Similarly, in the case of a wildfire-affected, event-driven SS transport system, as observed in the East Kiewa catchments (Australia) (type 3b), a single SRC did not account for the observed exhaustion effect after multiple events and for the impact of the wildfire on the SSL (Sheridan et al., 2011). Therefore, a sequence of SRCs was generated by passing a 90-day window over the sampled storm events for a period of three years after the fire. This approach demonstrated the impact of events on the linearity of the SRC, while also showing a shift after the wildfire due to changes in the dominant erosion processes from hillslope erosion immediately after the fire, to channel processes as the vegetation recovered (Sheridan et al., 2011).

This research demonstrated the importance of recognising different timescales of SS transport to identify the underlying processes, so that the choice of predictive model can be better adjusted to these processes. However, the above examples are based on site-specific empirical models to estimate SSLs, which require extensive monitoring data for calibration and validation, as also illustrated with the case study of the River Aire. To avoid the need for extensive SSC datasets, existing process-based models can also be applied, which will be discussed in the following part.

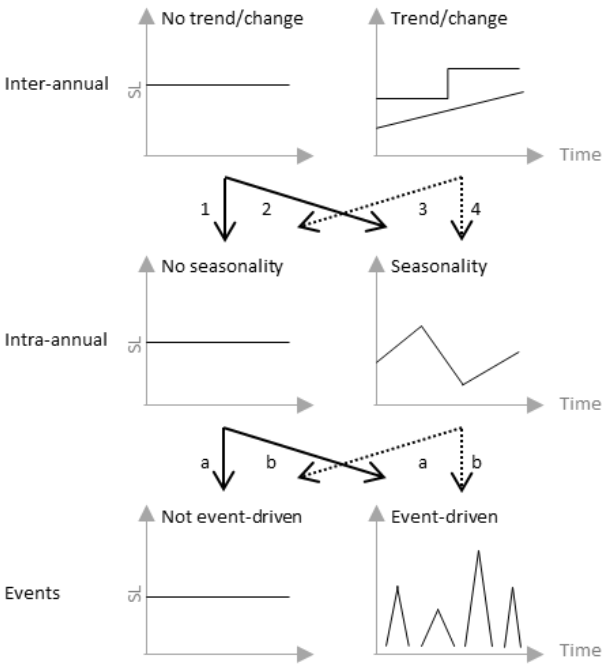

	Temporal variability	Examples
1a	No dominant timescale for variability	Isábena River, Spain, in badland catchment (López-Tarazón and Batalla, 2014)
2a	Intra-annual variability is dominant	Tropical upper Niger River basin, West Africa (Picouet et al. 2001)
3a	Inter-annual variability is dominant	Chenyoulan River, China, in catchment prone to landslides (Lin et al., 2008)
4a	Inter- and intra- annual variability	Tropical, dammed Tana River, Kenya (Geeraert et al., 2015)
1b	Event-driven variability is dominant	Wadi Abd (dryland river) catchment area, Algeria (Achite et al., 2007)
2b	Intra-annual and event-driven variability	Mountainous Izas catchment with snowmelt, Spain (Lana-Renault et al., 2011)
3b	Inter-annual and event-driven variability	East Kiewa Catchments after wildfires, Australia (Sheridan et al., 2011)
4b	Inter- and intra- annual, and event-driven variability	Subtropical, disturbed catchment of Loushui River, China (Sun et al. 2015)

Dominant process
low fractal power

Multiple interacting processes
high fractal power

Figure 6-1: Classification of suspended sediment transport systems according to temporal variability at three timescales (inter-annual, intra-annual, event).

6.2.2 Process-based modelling of sediment transport

Based on the multivariate analysis presented in Chapter 3, the temporal variability in SSCs in the River Aire was attributed to variation in the hydro-meteorological conditions and vegetation cover. By combining this information with detailed SS source information as presented in Chapter 5, more detailed hypotheses about the underlying processes could be developed. The SS source contributions appear to be driven by a different combination of processes and process-interactions, resulting in a varying importance of sediment source areas over time. Sediment originating from the grassland areas was estimated to be the dominant source of SS, especially the highly connected limestone area, while the other grassland areas were more dependent on the antecedent precipitation to become connected to the river system. Exhaustion of the sediment supply towards the end of winter was also mainly linked to sediment from the grassland areas, while the urban contributions to the SS appeared to be more supply-unlimited. Additionally, event-driven contributions of eroding riverbanks were also observed which were mainly attributed to riverbank erosion in the upper part of the catchment, especially during autumn and winter.

This temporal variability in the processes and process interactions for source-specific SS transport is generally not accounted for in models that simulate soil erosion and sediment transfer at the catchment scale. Many models, e.g. SCIMAP (Perks et al., 2017), PESERA, WATEM/SEDEM (De Vente et al., 2013), represent a selection of erosion and sediment transport processes at a particular spatial and temporal scale, so that they only provide reliable results when these processes are indeed dominant and when the models are applied to the scale for which they were calibrated (De Vente et al., 2013; Govers, 2011; Pandey et al., 2016).

This problem can be illustrated with the SCIMAP model, which estimates areas within the catchment where SS transport is likely to be highest based on stream power and hydraulic connectivity (Perks et al., 2017; Reaney et al., 2011). In general, the SCIPMAP SS risk map for the River Aire catchment (Figure 6-2) is

comparable to the conceptual scheme of sediment source areas and processes developed in Chapter 5 (Figure 5-9); both approaches identify the area around PH as a sediment hotspot because of the steep topography and connectivity to the river. However, the observed temporal variability in the relative importance of sediment source areas is not represented by SCIMAP, which has important implications for the implementation of soil conservation and pollution prevention strategies. Therefore, Perks et al. (2017) recommended the combination of SCIMAP modelling with a spatially distributed time-integrated SS sampling network. The authors showed that this approach enables the capture of spatial and temporal patterns of sediment fluxes and to identify key contributing sub-catchments.

Alternatively, more detailed models have been developed that represent a wider range of processes, e.g. infiltration, runoff, raindrop and flow detachment, sediment transport, deposition, and plant growth. A review of existing erosion and sediment yield models revealed that the AGNPS, SHETRAN, SWAT and WEPP models are some of the best models to simulate erosion and sediment transport processes at different spatial (hillslope to catchment) and temporal (day to years) scales (Pandey et al., 2016). Especially the SWAT model appears suitable in the case of the River Aire catchment, because it can be used on large catchments (including grassland), and it operates on a daily time step so that antecedent soil moisture conditions are also considered. Due to the inclusion of multiple processes, SWAT can be applied to assess the impact of various processes on the SSL over different timescales, e.g. climate change, pollutant cycling, land use change, plant parameters, hydropower projects, and urban areas (Neitsch et al., 2011; Pandey et al., 2016). Furthermore, specific packages were also developed to improve model calibration. For example, SWAT-CUP was developed as a decision-making framework that incorporates both manual and automated calibration, so that users can manually calibrate the modes according to their understanding of the processes and management practices occurring catchment (Arnold et al., 2012). However, sediment sources and sinks on land (e.g. intermediate storage) are also not well represented in SWAT due to a lack of

sediment source data (Arnold et al., 2012; Pandey et al., 2016), while this research has demonstrated the importance of sediment source information to better understand the processes and process interactions controlling SS transport.

Therefore, both in the case of popular models like SCIMAP and SWAT, there is a need to include information on how different processes and process interactions control the variable contribution of sediment sources to the total SSL. However, by including a wide range of processes, detailed process-based models often require a lot of input data on catchment characteristics, which is a limiting factor to widespread application of a model for scientific and especially management purposes, and risks additional uncertainty propagation due errors associated with the different data inputs (Arnold et al., 2012; Govers, 2011; Pandey et al., 2016). Therefore, we need better empirical data on the temporal variation in sediment sources and sinks to strengthen our capacity to not only calibrate models, but also to select and evaluate their suitability in particular cases.

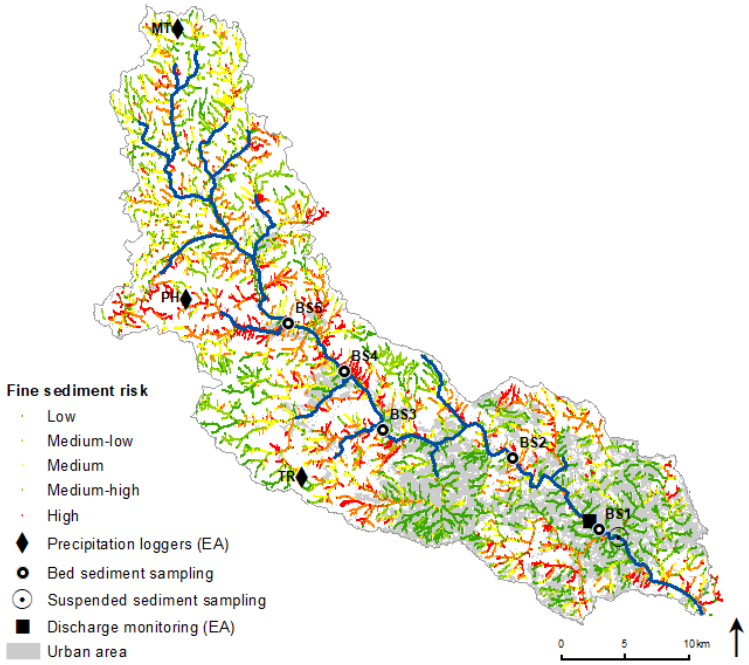

Figure 6-2: Fine sediment risk map for the River Aire catchment produced with SCIMAP

6.2.3 Implications for further research

It is important to acknowledge that the results of this research and associated interpretation in terms of underlying processes, are constrained by methodological limitations. Therefore, implications and recommendations for further research are formulated here in terms of (i) sediment monitoring and data availability; and (ii) sediment source information.

Suspended sediment monitoring and data availability

More long-term and high-temporal resolution SSC data, from the event to the inter-annual scale, is required to systematically test, compare, and calibrate predictive models at multiple spatial and temporal scales. Furthermore, besides the use of automated samplers, more research should explore alternative possibilities to increase the temporal and spatial resolution of SS monitoring, e.g. working with citizen technicians (Bannatyne et al., 2017).

While technological advancements have made it easier to collect large amounts of samples using automatic water samplers, implementation of specific measuring techniques are often constrained. For example in this study, due to the need for physical samples for sediment fingerprinting (i.e. continuous turbidity measurements were inappropriate) and the urban environment (i.e. automated samplers could not be deployed without significant infrastructure investment), sample frequency was limited to daylight hours due to health and safety and physical presence in Leeds. Consequently, not all flood events were sampled and gaps exists in the dataset. Furthermore, SS samples were only taken at a single location in the river and correlation analysis with hydro-meteorological data was constrained by the location of the available monitoring data.

Sediment source information

More studies are required that apply sediment fingerprinting at a high temporal and spatial resolution to improve scientific understandings on how changes in

sediment source contributions relate to hydro-meteorological processes and catchment connectivity.

However, towards application of DRIFTS-based sediment fingerprinting, and reliably quantify contributions of sediment sources, it is recommended to develop a methodology to better classify all potential sediment sources that are relevant for the aim of the study, and assess when a sediment source has a sufficiently high degree of discrimination (Pulley et al., 2017). For example, the model testing in Chapter 4 suggested that other sediment sources might be present. Due to time constraints, it was not possible to sample more sources and produce a new set of experimental mixtures of source samples. Additionally, sampling solids for sewer overflows was also constrained by health and safety issues.

Furthermore, alternative statistical approaches for uncertainty quantification (e.g. Bayesian modelling) in combination with DRIFTS-based fingerprinting should be further explored. This research presented a new way to estimate source-specific SSCs based on PLSR with hydro-meteorological data (Chapter 5). While associated model uncertainties were estimated, it should be acknowledged that no final uncertainty estimate could be given due to the propagation of uncertainties associated with the methods (fingerprinting and regression).

Finally, it is also important to note that the sediment source apportionment through sediment fingerprinting in this study are only valid for fine sediment (i.e. < 63 µm).

6.3 Sediment management in the River Aire catchment

6.3.1 Identifying sediment management needs

Despite extensive research demonstrating the detrimental impacts of fine sediment in river catchments and coastal zones, both in terms of quality and quantity, few comprehensive national and international sediment management guidelines exist (Owens et al., 2005). A main reason for this is the high spatiotemporal variability in SS transport, complicating our ability to formulate general guidelines. Only when we are able to capture the processes controlling

SS transport, it is possible to effectively allocate resources for conservation and pollution prevention (Owens et al., 2005; Perks et al., 2017; SedNet, 2009). By assessing SS transport and the associated processes over different timescales, potential sediment-related issues can be identified that require management intervention.

In general, the sediment yield of a catchment provides an indication of the order of magnitude of erosion within the catchment (García-Ruiz et al., 2015; Morgan, 2005; Vanmaercke et al., 2011). The average sediment yield in the River Aire (14 t km^{-2} yr^{-1}) is lower than the average sediment yield in a similar climate (Atlantic) and the rest of the European climates (Figure 6-3). The range of annual sediment yields in the River Aire (6 to 52 t km^{-2} yr^{-1}) is also situated among the lower end of the range of sediment yields in similar climates (0.4 to 2834 t km^{-2} yr^{-1}) (Vanmaercke et al., 2011). Furthermore, as discussed in Chapter 3, the estimated sediment yields in the River Aire are also comparable to other sediment yields observed in northern England (7 to 86 t km^{-2} yr^{-1}) (Foster and Lees, 1999; Walling et al., 2003).

These numbers suggest that the total SL in the River Aire is not alarmingly high compared to other catchments. However, the study has also showed the significant impact of human activity on the SSLs and composition at different timescales (e.g. land cover change and street dust), which suggest that the SSCs could still be higher compared to conditions with no human disturbances, posing potential risks for (i) ecology, (ii) pollution, and (iii) sedimentation.

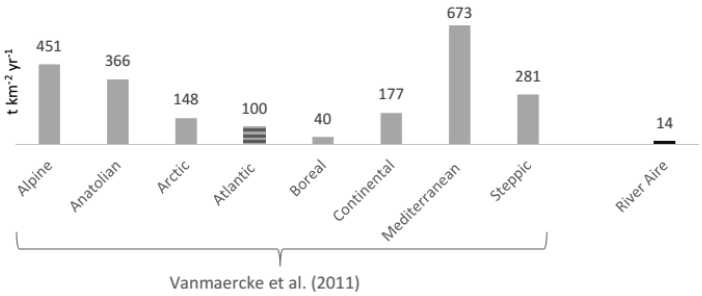

Figure 6-3: Comparison of average sediment yield in the River Aire with average sediment yields per European climatic zones. Atlantic climate corresponds to the climate of the River Aire catchment.

Ecological status

The SSC in the River Aire may have a negative impact on the ecological status of the river. In the former EU Freshwater Fisheries Directive (78/659/EEC), the threshold for acceptable SSC was set at 25mg/l (Grove et al., 2015). However, research has demonstrated that background SSCs (i.e. with minimal human disturbance) can be significantly lower or higher than 25 mg/L, so that guidelines for acceptable SSC levels should be based upon individual catchment characteristics (APEM, 2007; Bilotta et al., 2012). Therefore, a statistical model was developed by Bilotta et al. (2012) to estimate mean background SSCs, and the authors found that reference sites in the Yorkshire Dales National Park (source region of the River Aire) are mostly within the ranges 0-5.99 and 5.99-11.99 mg L^{-1}. The mean SSC in the River Aire is 15 mg L^{-1}, which is therefore slightly higher than what would be expected with limited human disturbance. Furthermore, based on the PLSR models developed in Chapter 3, the SSCs in the River Aire were estimated to exceed 25 mg L^{-1} around 32% of the time, and exceed 12 mg L^{-1} around 41% of the time between 2015 and 2017 (Table 6-1). Similarly, the models developed in Chapter 5 indicated that the estimated source-specific SSCs regularly exceed 25 mg L^{-1} and 12 mg L^{-1}, especially the urban contribution (80% of the time > 12 mg L^{-1}) (Table 6-1).

Table 6-1: Threshold exceedance of the estimated total and source-specific SSCs (% of time between June 2015 and February 2017)

	SSC_{Total}	SSC_L	SSC_M	SSC_C	SSC_U	SSC_R
> 12 mg L^{-1}	41%	59%	25%	59%	80%	22%
> 25 mg L^{-1}	32%	16%	9%	17%	36%	11%

Pollution

Pollution through fine sediment from urban and rural areas can also pose a significant hazard (Peukert et al., 2014; Taylor and Owens, 2009). The River Aire is classified as Heavily Modified Water Body under the Basin Management Plan, characterised by a poor ecological potential and a bad chemical status (Nicholson, 2015). As with many rivers in the UK, the industrial revolution had a

severe impact on the River Aire and its surroundings. Literature from 1860 to 1990 report the river being “abused”, “obstructed” and “polluted” with solids from industrial waste, streets and sewage, making the river “unfit for any ordinary use” from Skipton onwards (City Architect Department, 1994; Maclean, 1904; Royal Commission, 1866).

Also in more recent times, in the middle and lower reaches of the River Aire, pollution associated to the SS has been observed though the contribution of solids from sewage treatment works, combined sewer overflows, industrial discharges, and road runoff, which is reflected in lead, copper and chromium associated to SS (Carter et al., 2006, 2003; D. E. Walling et al., 2003). These earlier observations are in line with the high urban street dust contribution observed in this study, and has important implications for the quality of the river system as the contaminated sediments can be stored on the river bed and floodplain soils for extended periods of time (Lloyd et al., 2016; Rossi et al., 2013).

Furthermore, the high degree of sediment from grazing areas can also pose a potential threat through diffuse pollution causing eutrophication and bacterial infections associated with livestock faeces (Bilotta et al., 2007; Brazier et al., 2007; Peukert et al., 2014).

Sedimentation

Sedimentation of fine sediment in the River Aire may increase flood risk by reducing the capacity of the river channel to convey runoff (Slater et al., 2015; Wallerstein, 2006). As early as 1866, flooding along the River Aire was reported that was partially attributed to sediments coming from soil erosion and industrial waste raising the beds of the river channels and the construction of dams and culverts obstructing the flow (Royal Commission, 1866). This role of fine sediment in flood risk is especially relevant in the context of the Flood Alleviation Scheme, which is currently being finalized in Leeds. The scheme was developed to prevent flooding of the city from river flows up to the 1 in 100 year floods. It includes linear landscape flood defences along the river and the installation of movable weirs at Crown Point and Knostrop Cut. At Knostrop Cut the river and the canal were

merged and the riverbed was re-profiled to improve flood conveyance. These measurements were designed to reduce peak flows of the river while reducing the height of new defences needed within the city. Similar to the historical link between sedimentation in the river channel and flood frequency, future sedimentation in the river sections included in the scheme can reduce the capacity of the river to convey runoff.

An earlier assessment to investigate the deposition risk of fine sediment in the sections of the river included in the scheme, suggested that the risk of deposition would generally be low, arguing that at low flows little sediment will be present in the river (Nicholson, 2015). Based on the data collected in this study, the effective discharge, i.e. the discharge that transports most of the river's SSL in the long term (Crowder and Knapp, 2005; López-Tarazón and Batalla, 2014), in the River Aire is 13 m^3/s (Armley), which is equalled or exceeded 60% of the time. However, the results in this study also demonstrated that stream flow is not the only driver of SS transport, as illustrated in Chapter 3 and 5. The average monthly discharges in the River Aire from May to September are < 13 $m^3\ s^{-1}$, while some events during that period were characterised by very high SSCs (up to 1000 mg L^{-1}). As a result, these months might be periods with higher sedimentation risk, as well as other periods that are preceded by drier periods (i.e. larger sediment supply available for transport).

6.3.2 Sediment management recommendations

SS transport in the River Aire is not alarmingly high and the risk of high SS deposition can be considered relatively low under the current conditions. However, reducing the SS in the River Aire would be beneficial for soil and water conservation, and especially to aqueous habitats and ecology. Therefore, specific management recommendation are formulated for the River Aire catchment:

- In terms of reducing sediment quantity, the catchment would benefit most from **reducing soil erosion in grassland areas**. Given the likely role of grazing animals in soil erosion, possible remedies are to reduce the length of the grazing season, move the grazing animals to areas less prone to

erosion, and/or reducing the grazing period to those periods when the soil is below field capacity to avoid poaching issues, especially in Limestone area (Bilotta et al., 2007).

- Furthermore, the sporadic high contributions of riverbanks indicate that **channel bank protection measures** could also be beneficial to reduce the sediment quantity in the river, especially in the upper part of the catchment (SEPA, 2008).
- To **reduce the high amount of urban street dust** in the river, it is recommended to increase the frequency of street sweeping, especially during dry periods. Additionally, installing storm water ponds, and/or developing sustainable urban drainage systems within the city would also be potential mitigation strategies (Allen et al., 2017; Marsalek and Viklander, 2010; Taylor and Owens, 2009).
- Finally, it is recommended to **monitor the discharges of the river**, especially before and after flood events in spring and summer, to evaluate the risk of sediment deposition and the possible use of the weir system to flush down sediments.

6.4 References

Allen, D., Haynes, H., Arthur, S., 2017. Contamination of detained sediment in sustainable urban drainage systems. Water (Switzerland) 9. doi:10.3390/w9050355

APEM, 2007. Review of UKTAG proposed standard for suspended solids.

Arnold, J., Moriasi, D., Gassman, P., White, M., 2012. SWAT : Model use, calibration, and validation. Biol. Syst. Eng. 55, 1491–1508.

Bannatyne, L.J., Rowntree, K.M., Waal, B.W. Van Der, Nyamela, N., 2017. Design and implementation of a citizen technician – based suspended sediment monitoring network : Lessons from the Tsitsa River catchment , South Africa. WaterSA 43, 365–377.

Bilotta, G.S., Brazier, R.E., Haygarth, P.M., 2007. The Impacts of Grazing Animals on the Quality of Soils, Vegetation, and Surface Waters in Intensively Managed Grasslands. Adv. Agron. 94, 237–280. doi:10.1016/S0065-2113(06)94006-1

Bilotta, G.S., Burnside, N.G., Cheek, L., Dunbar, M.J., Grove, M.K., Harrison, C., Joyce, C., Peacock, C., Davy-Bowker, J., 2012. Developing environment-specific water quality

guidelines for suspended particulate matter. Water Res. 46, 2324–2332. doi:10.1016/j.watres.2012.01.055

Brazier, R.E., Bilotta, G.S., Haygarth, P.M., 2007. A perspective on the role of lowland, agricultural grasslands in contributing to erosion and water quality problems in the UK. Earth Surf. Process. Landforms 32, 964–967. doi:10.1002/esp

Carter, J., Owens, P.N., Walling, D.E., Leeks, G.J.L., 2003. Fingerprinting suspended sediment sources in a large urban river system. Sci. Total Environ. 314–316, 513–534. doi:10.1016/S0048-9697(03)00071-8

Carter, J., Walling, D.E., Owens, P.N., Leeks, G.J.L., 2006. Spatial and temporal variability in the concentration and speciation of metals in suspended sediment transported by the River Aire, Yorkshire, UK. Hydrol. Process. 20, 3007–3027. doi:10.1002/hyp.6156

City Architect Department, 1994. River Aire and Canals Study. Leeds.

Crowder, D.W., Knapp, H.V., 2005. Effective discharge recurrence intervals of Illinois streams. Geomorphology 64, 167–184. doi:10.1016/j.geomorph.2004.06.006

De Vente, J., Poesen, J., Verstraeten, G., Govers, G., Vanmaercke, M., Van Rompaey, A., Arabkhedri, M., Boix-Fayos, C., 2013. Predicting soil erosion and sediment yield at regional scales: Where do we stand? Earth-Science Rev. 127, 16–29. doi:10.1016/j.earscirev.2013.08.014

Foster, I.D.L., Lees, J.A., 1999. Changing headwater suspended sediment yields in the LOIS catchments over the last century: A paleolimnological approach. Hydrol. Process. 13, 1137–1153. doi:10.1002/(SICI)1099-1085(199905)13:7<1137::AID-HYP794>3.0.CO;2-M

García-Ruiz, J.M., Beguería, S., Nadal-Romero, E., González-Hidalgo, J.C., Lana-Renault, N., Sanjuán, Y., 2015. A Meta-Analysis of soil erosion rates across the world. Geomorphology 239, 160–173. doi:10.1016/j.geomorph.2015.03.008

Geeraert, N., Omengo, F.O., Tamooh, F., Marwick, T.R., Borges, A. V., Govers, G., Bouillon, S., 2017. Intra- and inter-annual variations in carbon fluxes in a tropical river system (Tana River, Kenya). Biogeosciences. doi:10.5194/bg-2017-31

Govers, G., 2011. Misapplications and Misconceptions of Erosion Models, in: Morgan, R.P.C., Nearing, M.A. (Eds.), Handbook of Erosion Modelling. Blackwell Publishing Ltd, pp. 117–134. doi:10.1002/9781444328455.ch7

Grove, M.K., Bilotta, G.S., Woockman, R.R., Schwartz, J.S., 2015. Suspended sediment regimes in contrasting reference-condition freshwater ecosystems: Implications for water quality

guidelines and management. Sci. Total Environ. 502, 481–492. doi:10.1016/j.scitotenv.2014.09.054

Lana-Renault, N., Alvera, B., García-Ruiz, J.M., 2011. Runoff and Sediment Transport during the Snowmelt Period in a Mediterranean High-Mountain Catchment. Arctic, Antarct. Alp. Res. 43, 213–222. doi:10.1657/1938-4246-43.2.213

Lin, G.W., Chen, H., Chen, Y.H., Horng, M.J., 2008. Influence of typhoons and earthquakes on rainfall-induced landslides and suspended sediments discharge. Eng. Geol. 97, 32–41. doi:10.1016/j.enggeo.2007.12.001

Lloyd, C.E.M., Freer, J.E., Johnes, P.J., Collins, A.L., 2016. Using hysteresis analysis of high-resolution water quality monitoring data, including uncertainty, to infer controls on nutrient and sediment transfer in catchments. Sci. Total Environ. 543, 388–404. doi:10.1016/j.scitotenv.2015.11.028

López-Tarazón, J.A., Batalla, R.J., 2014. Dominant discharges for suspended sediment transport in a highly active Pyrenean river. J. Soils Sediments 14, 2019–2030. doi:10.1007/s11368-014-0961-x

Maclean, W., 1904. Report Upon River Aire (non-tidal portion of main stream). Wakefield.

Marsalek, J., Viklander, M., 2010. Controlling contaminants in urban stormwater: Linking environmental science and policy, in: Jan Lundqvist (Ed.), On the Water Front. World Water Week 2010, Stockholm.

Morgan, R.P.C., 2005. Soil Erosion & Conservation. Blackwell Publishing Ltd, Oxford.

Neitsch, S.., Arnold, J.., Kiniry, J.., Williams, J.., 2011. Soil & Water Assessment Tool Theoretical Documentation Version 2009, Texas Water Resources Institute. doi:10.1016/j.scitotenv.2015.11.063

Nicholson, A., 2015. WFD Compliance Assessment: Leeds Flood Alleviation Scheme. Leeds.

Owens, P.N., Batalla, R.J., Collins, A.J., Gomez, B., Hicks, D.M., Horowitz, A.J., Kondolf, G.M., Marden, M., Page, M.J., Peacock, D.H., Petticrew, E.L., Salomons, W., Trustrum, N.A., 2005. Fine-grained sediment in river systems: environmental significance and management issues. River Res. Appl. 21, 693–717. doi:10.1002/rra.878

Pandey, A., Himanshu, S.K., Mishra, S.K., Singh, V.P., 2016. Physically based soil erosion and sediment yield models revisited. Catena 147, 595–620. doi:10.1016/j.catena.2016.08.002

Perks, M.T., Warburton, J., Bracken, L.J., Reaney, S.M., Emery, S.B., Hirst, S., 2017. Use of spatially distributed time-integrated sediment sampling networks and distributed fine

sediment modelling to inform catchment management. J. Environ. Manage. 1–10. doi:10.1016/j.jenvman.2017.01.045

Peukert, S., Griffith, B.A., Murray, P.J., Macleod, C.J.A., Brazier, R.E., 2014. Intensive management in grasslands causes diffuse water pollution at the farm scale. J. Environ. Qual. 43, 2009–23. doi:10.2134/jeq2014.04.0193

Pulley, S., Van Der Waal, B., Collins, A.L., Foster, I.D.L., Rowntree, K., 2017. Are source groups always appropriate when sediment fingerprinting? The direct comparison of source and sediment samples as a methodological step. River Res. Appl. 1–11. doi:10.1002/rra.3192

Reaney, S.M., Lane, S.N., Heathwaite, A.L., Dugdale, L.J., 2011. Risk-based modelling of diffuse land use impacts from rural landscapes upon salmonid fry abundance. Ecol. Modell. 222, 1016–1029. doi:10.1016/j.ecolmodel.2010.08.022

Rossi, L., Chèvre, N., Fankhauser, R., Margot, J., Curdy, R., Babut, M., Barry, D.A., 2013. Sediment contamination assessment in urban areas based on total suspended solids. Water Res. 47, 339–50. doi:10.1016/j.watres.2012.10.011

Royal Commission, 1866. Report of the Commissioners on the Best Means of Preventing The Pollution of Rivers (River Aire and Calder). George Edward Eyre and William Spottiswoode, London.

SedNet, 2009. Integration of Sediment in River Basin Management, Report on the 2nd SedNet Round Table Discussion, 6-7 October. Hamburg.

SEPA, 2008. Bank Protection Rivers and Lochs. Good Pract. Guid. 47.

Sheridan, G.J., Lane, P.N.J., Sherwin, C.B., Noske, P.J., 2011. Post-fire changes in sediment rating curves in a wet Eucalyptus forest in SE Australia. J. Hydrol. 409, 183–195. doi:10.1016/j.jhydrol.2011.08.016

Slater, L.J., Singer, M.B., Kirchner, J.W., 2015. Hydrologic versus geomorphic drivers of trends in flood hazard. Geophys. Res. Lett. 42.

Sun, L., Yan, M., Cai, Q., Fang, H., 2015. Suspended sediment dynamics at different time scales in the Loushui River, south-central China. Catena Published. doi:10.1016/j.catena.2015.02.014

Taylor, K.G., Owens, P.N., 2009. Sediments in urban river basins: a review of sediment–contaminant dynamics in an environmental system conditioned by human activities. J. Soils Sediments 9, 281–303. doi:10.1007/s11368-009-0103-z

Vanmaercke, M., Poesen, J., Verstraeten, G., de Vente, J., Ocakoglu, F., 2011. Sediment yield

in Europe: Spatial patterns and scale dependency. Geomorphology 130, 142–161. doi:10.1016/j.geomorph.2011.03.010

Wallerstein, N., 2006. Accounting for sediment in rivers. FRMRC Research Report UR9.

Walling, D.E., Owens, P.N., Carter, J., Leeks, G.J.L., Lewis, S., Meharg, A.A., Wright, J., 2003. Storage of sediment-associated nutrients and contaminants in river channel and floodplain systems. Appl. Geochemistry 18, 195–220. doi:10.1016/S0883-2927(02)00121-X

Walling, Owens, P.N., Foster, I.D.L., Lees, J.A., 2003. Changes in the fine sediment dynamics of the Ouse and Tweed basins in the UK over the last 100-150 years. Hydrol. Process. 17, 3245–3269. doi:10.1002/hyp.1385

CHAPTER 7: CONCLUSION

This research aimed to improve the quantification and prediction of SS transport in rivers, and to support the development of targeted sediment management strategies, by investigating the hydro-meteorological and catchment processes driving temporal variation in SS transport in a case-study catchment of the River Aire, UK.

By combining extensive empirical data on SSCs, with detailed hydro-meteorological data and sediment source information, there are three main ways in which this research will improve methodologies to quantify and predict SSCs and sources, and support the development of new theoretical knowledge on SS sources and transport dynamics.

First, a multi-timescale, statistical investigation based on empirical evidence on SS transport dynamics demonstrated the importance of identifying underlying transport mechanisms in order to evaluate and select models to predict SS transport. The SS transport in the River Aire is highly event-driven, fast-responding, and supply-limited at the intra-annual scale, while also being influenced by long-term changes in land use (Section 3.4.1). The SL was estimated to vary between 6 and 52 t km^{-2} yr^{-1}, depending on the timescale of the data used. The results of the case study confirm that common methods to quantify and predict SSCs (e.g. SRCs) generally do not account for processes and process interactions controlling SS transport, which limits their capacity to be applied across timescales (Section 3.4.2). These findings form the basis to conceptualising different timescales of SS transport in terms of underlying processes and process interactions for different catchments, which is essential towards better evaluation and selection of predictive models for SS transport (Section 6.2.1).

Second, while DRIFTS-based fingerprinting can be used to estimate SS source contributions with acceptable model errors, systematic testing of the approach demonstrated that the sediment apportionment based on experimental mixtures

is strongly influenced by the degree of discrimination between source classes (Section 4.4). This type of model testing has not been performed previously on DRIFTS-based sediment fingerprinting with experimental mixtures, and it clearly demonstrates that the sum of the individual sediment source estimates is not an appropriate measure to assess how well the source classification represents the actual sediment sources. The findings provide important empirical evidence that highlights the need to further develop approaches for sediment source classification and discrimination to accurately represent the sediment sources in the river.

Finally, by statistically linking a new and unique dataset on event-based sediment source information to hydro-meteorological data, source-specific SS transport dynamics and associated controlling processes for the River Aire catchment could be identified (Section 5.4.2). The findings substantiate hypotheses made in previous research which state that SLs at the event and intra-annual scale are strongly driven by the interaction of catchment and hydro-meteorological processes which result in variations in the dominant sediment sources over time. Therefore, it is essential to establish further knowledge on how sediment sources vary in different catchments and over multiple spatial and temporal scales, so that process-based models to estimate soil erosion and sediment transfer at the catchment scale can be better calibrated for these source-specific processes (Section 6.2.2).

In conclusion, through new empirical evidence and novel methodological approaches, this research underscores that understanding and conceptualising the linkages between the processes and process interactions underlying SS sources and transport across temporal scales, is key to improved quantification and prediction of SS transport in rivers, both in terms of improving predictive models, and identifying sediment management needs. Further development of this avenue of research will aid sustainable sediment management and safeguarding rivers and their geomorphological and ecological functioning.

APPENDICES

Appendix A The River Aire catchment

Total catchment area	879 km^2 (upstream on Leeds: 690km^2)
Altitude	15 – 200 m a.s.l.
Land use	Grassland (59%) Urban (25%) Heath and peat bogs (12%) Arable land (4%)
Geology	Carboniferous: Limestone and Shale (23%) Millstone Grit (46%) Coal measures (31%)
Soil	poorly draining loamy and clayey soils, with raw oligo-fibrous peats, and stagnohumic and stagnogley soils in the upper part, and brown earths and pelo-stagnogley soils in the middle and lower parts
Climate	Temperate
Precipitation (1961 and 2017)	1018 mm $year^{-1}$
River discharge (1961 and 2017)	Q_{50}: 10.05 m^3/s Q_{10}: 36.67 m^3/s Q_{95}: 3.67 m^3/s
Base Flow Index (BFI) (1961 and 2017)	0.49 (Armley)

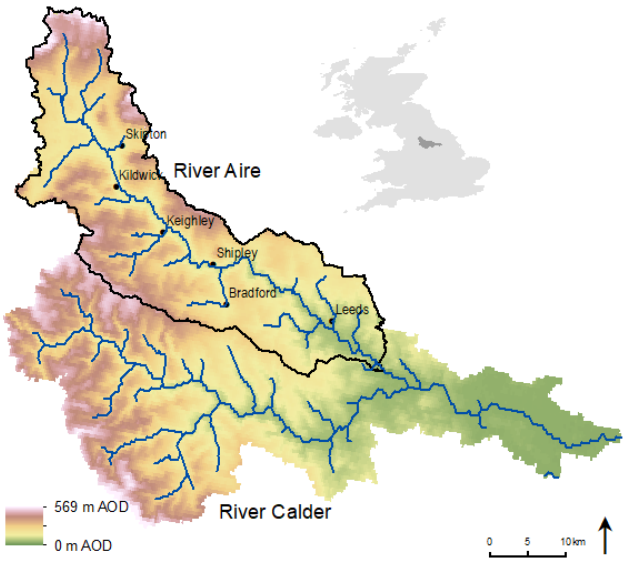

Figure: Topography of the Aire-Calder Catchment (Source: HydroShed)

Appendix B Suspended sediment concentration data: Environment Agency

	Upstream*	Middle*	Downstream*
Average	17.24	15.59	16.56
Min	1.00	1.00	1.00
Max	210.00	124.00	148.00
Standard deviation	25.29	20.40	20.40
Number of samples	209.00	213.00	213.00
Comments	No samples from 2010	No samples from 2010	Irregular samples No samples between 2007-2010
	The average standard deviation between same-day observations in different stations is 3 mg L^{-1}		

* corresponding to EA SS monitoring locations indicated in Figure 3-1

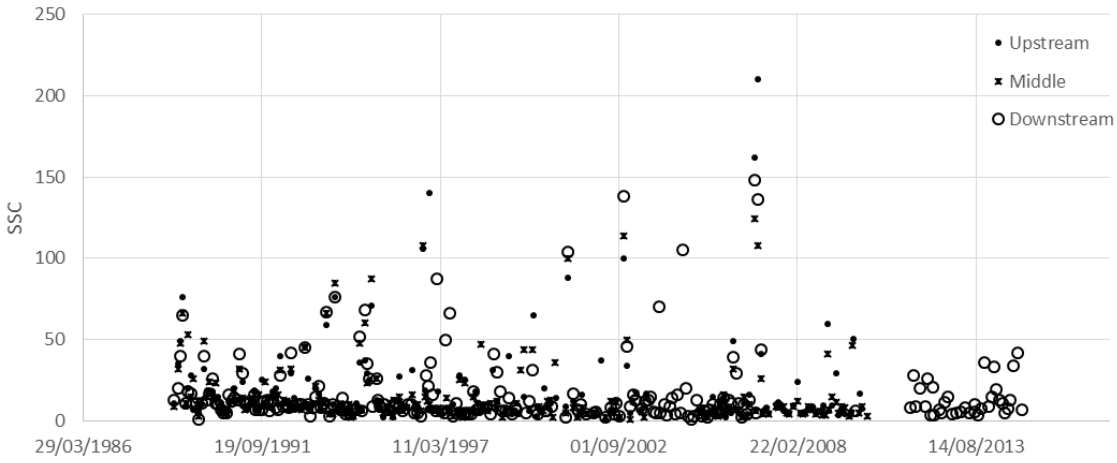

Figure: Suspended sediment concentrations measured by Environment Agency at three locations within the city of Leeds (Figure 3-1)

Appendix C Suspended sediment sampling

All suspended sediment samples used in this study were taken with a hand-held sampler from the side of the River Aire near Brewery Wharf in Leeds (A1). To test the distribution of the suspended sediment concentration along the width of the river a heavy sampler (model US DH-59) with winch was used from the footbridge (Centenary Bridge, CB) at Brewery Wharf (A2). The tests confirmed that the suspended sediment concentration did not vary significantly along the width of the river (Figure).

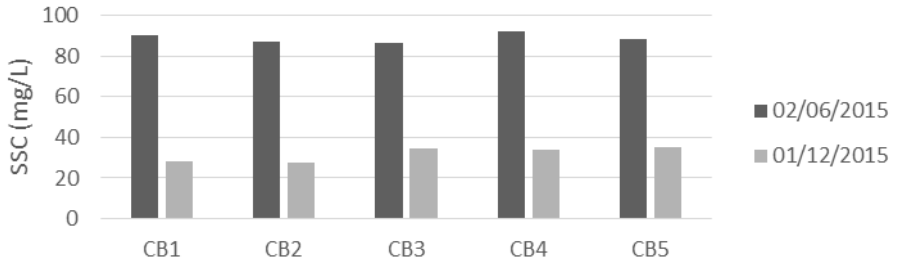

Figure: Suspended sediment concentrations measured along the width of the River Aire during two separate days based on samples taken with the US DH-59 sampler (CB5 is the side of the river where handheld samples were taken)

C.1 Hand-held sampler

- Note down location, date and time of sampling
- Use appropriate gloves and shoes with high grip, wear a life jacket
- Hold on to the railing with one hand
- Lower the sampler slowly into the river and bring back up
- Close the sampling bottle and store it
- Repeat if more volume is necessary (depending on the turbidity of the water)

C.2 Heavy sampler with winch

- Note down location, date and time of sampling
- Use appropriate gloves and shoes with high grip and a life jacket
- Set up the bridge board and secure it to the railing of the bridge.
- On person lifts the sampler over the railing and attach it to the wire while the other person is holding the handle of the winch and is standing on the footstep of the bridge board.
- Move the bridge board forward until the sampler cannot touch the bridge.
- Carefully lower the sampler down to the water surface by turning the handle of the winch

- Lower the sampler from the water surface to the bottom and back at a uniform rate
- Move the bridge board backwards and lift the sampler back over the railing.
- Take out the bottle vertically and close it.
- Repeat if more volume is necessary (depending on the turbidity of the water)

Figure: Hand-held depth integrating hand-held suspended sediment sampler

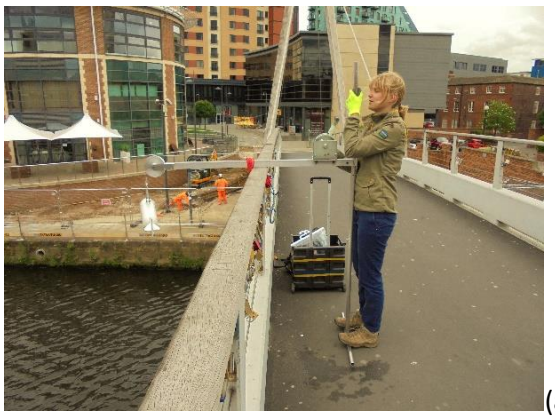
(a)

(b)

Figure: Heavy depth integrating suspended sediment sampler (US DH-59): (a) lowering the sampler down from a bridge using a winch; (b) taking a full water bottle out of the sampler

Appendix D Sediment filtering

Suspended sediment from water samples is retained by filtration with a portable filtration set, including a manual and electrical vacuum pump and quartz fibre filters to retain the suspended sediment.

- Prepare the filtration set, make sure the filtration set is clean and place a pre-weighted 47mm glass fibre filter in position, use tweezers to handle the filter.
- Homogenize the water in the bottle first, so that none of the suspended matter load is settled at the bottom. Then poor the water onto the filter.
- Use a vacuum pump to create a partial vacuum to suck the water through the filter. Once all the water is passed, take the filter out and place it in a plastic disk to dry.
- All filters are oven dried at 105˚C for two hours before weighed again to determine the suspended sediment concentration.
- Samples may be air-dried by exposure to ambient air until transferred to the lab.

Cooper et al. (2014b) tested the temporal stability of sediment samples for DRIFTS and they concluded that once oven dried at 105 °C for 2 h, sediment retained on filters can be stored at room temperature in an air-tight environment for several months without risk of degradation.


(a)

(b)

Figure: Sediment filter setup: (a) portable filter set with manual vaccum pump; (b) electrical vacuum pump

Appendix E Sediment source sample preparation

E.1 Storage

All samples are stored in labelled polythene bags and air-dried (Figure a). Once completely dry, all samples are sieved to < 2mm to remove stones and large pieces of organic material (e.g. grass).

E.2 Disaggregate clasts

Particles larger than 50 µm increase scattering significantly resulting in noisy spectra and low absorption intensities in the infrared region (Cooper et al., 2014a). To reduce this noise and minimise the impact of size selective transport due to different grain size distributions between the source samples and the suspended sediment, the source samples DRIFTS measurements will only be conducted on the <63 µm fraction of the source samples (Brosinsky et al., 2014b; Cooper et al., 2014a; Poulenard et al., 2012; Smith and Blake, 2014). Organic material was not removed since studies have demonstrated that organic carbon is strongly related to the origin of the sediment, so that the use of correction factors can lead to important changes in source apportionment (Smith and Blake, 2014). The samples are firstly mixed with demineralised water. To disaggregate clasts, the samples are then placed in a sonic bath for seven minutes and sieved to <63 µm (Figure b, c).

E.3 Filter samples

The samples are filtered on quartz fibre filters (between 50 and 100mg) and oven-dried for two hours at 105˚C (Cooper et al., 2014a; Pulley et al., 2015) (Figure d,e).

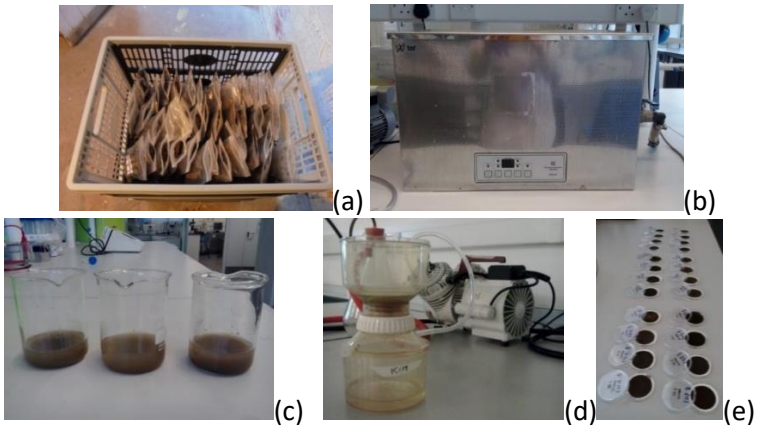

Figure: Sediment source samples are: (a) stored in polyethylene bags; (b) mixed with demineralised water and placed in a sonic bath for 7 minutes; (c) wet sieved to <63µm; (d) filtered on quartz fibre filters; and (e) oven-dried for two hours at 105˚C.

Appendix F DRIFTS analysis of sediment samples

F.1 Spectroscopy

F.1.1 Principle

Spectroscopy is based on the interaction of electromagnetic radiation with matter. Molecular spectroscopy includes absorption, emission, fluorescence and scattering processes at the molecular level, while atomic spectroscopy encompasses the analysis of wavelength dependence of absorption and emission of electromagnetic radiation by atoms and ions of an element (Ahmad et al., 2001). Molecular spectroscopy is characterized by low-energy radiation (Infrared, visible, UV), which causes vibration of the molecule or the transit of outer electrons from low- to high-energy state. Covalently bonded molecules have a characteristic rotational– vibrational structure unique to the mass of the atoms and strength of the bonding between them (Cooper et al., 2014b). When an IR beam passes through a sample, a fraction of the incident light is absorbed depending on the vibrations of the bonds within the molecules. This results in a spectrum characterized by absorption bands specific for particular compounds, which can serve as a chemical fingerprint for the analysed sample (Beasley et al., 2014; Raphael, 2011). Molecular spectroscopy can therefore be used to identify compounds within a sample such as organic carbon, carbonates, phosphates, iron content and clay (Brosinsky et al., 2014a; Viscarra Rossel et al., 2006). Contrarily, atomic spectroscopy is based on high-energy electromagnetic radiation which causes the inner electrons to transit within the atom (Zhang, 2007). Atomic spectroscopy has the capacity to identify individual elements. Methods based on atomic spectroscopy include X-ray fluorescence (XRF), inductively coupled plasma-optical emission spectrometry (ICP-OAS) and Atomic absorption spectrometry (AAS).

F.1.2 Infrared spectrometry

In this study, IR spectroscopy (MIR: 4000-400cm^{-1}) was used. Two main types of infrared spectrometers exist: dispersive and Fourier transform (FT) spectrometers (Zhang, 2007). The major difference is that the FT spectrometers produce the infrared spectrum more rapidly compared to dispersive instruments and it has a greater sensitivity (Pavia et al., 2001). A mathematical algorithm, FT, is used to convert the raw wavelength data into the actual spectra of the samples (Beasley et al., 2014). In Diffuse Reflectance Infrared Fourier Transform spectrometry (DRIFTS) a beam of multi-frequency MIR light is targeted onto the sample. This will cause molecular vibration unique to the bonds making up the molecule, resulting in an infrared absorption pattern unique to the molecule. The

light that is not absorbed is either reflected or refracted, whereby only the diffusely reflected fraction is used in the DRIFTS procedure (Cooper et al., 2014a).

F.2 Measuring

F.2.1 Preparation

Two main preparation methods are proposed in literature. The first one is semi-destructive and involves the grounding of the sediment-covered filters and the subsequent analysis of the entire sample (Cooper et al., 2014b). The second approach is performing the measurements directly on the filters (or by scraping of the dry sediment collected on the filters) (Poulenard et al., 2012). In this study, all samples were measured directly on the filters. All filters where carefully cut into small rounds to fit into the spectrometer (figure 1).

Empty filters were measured with DRIFTS to retain background signals. Also filters with varying amounts of material where tested to determine the minimum amount of sediment that should be retained in order to get a representative spectrum of the material. For a selected set of samples, raw material was also analysed for comparison.

F.2.2 Scanning

Samples were scanned at a 4cm-1 resolution across the 4000-400cm^{-1} spectrum with 32 co-added scans per spectrum. Less scans resulted in more noise on the resulting spectrum, while more scans did not improve the result significantly. The samples retained on the filters was carefully placed on a sample cup and introduced in the device. Background samples with a dedicated pellet and plain filter samples were regularly collected throughout the measurements to make sure the device did not pose any errors. Data was processed using the software provided by the manufacturer of the spectrometer


(a)

(b)

(c)

Figure: (a) all source samples retained on quartz fibre filters and (b) filters cut in small rounds to fit into the spectrometer; (b) sampling cup size

Appendix G Sediment fingerprinting

This document describes the steps in developing a PLSR model to estimate sediment source contributions to the suspended sediment. It includes four main steps: (i) data pre-processing; (ii) sediment source discrimination; (iii) analysis of experimental mixtures; (iv) construction of PLS models for each sediment source.

All computations were performed in the **software programme R**. The associated codes and spectral data are attached to this thesis in a **CD** in a folder named "Fingerprinting". To run the files in R, it is recommended to install the following packages:
install.packages("prospectr")
install.packages("reshape2")
install.packages('pls')
install.packages('sampling')

G.1 Data

In the folder, three datasets in .csv format are included:

- **SourceSamples**: DRIFTS spectra of the original source samples
- **MixturesSediment_CO2**: DRIFTS spectra of the experimental mixtures
- **SuspendedSediment_CO2**: DRIFTS spectra of the SS samples
- **BedSediment_CO2**: DRIFTS spectra of the BS samples

To avoid CO_2(gas) interference, discriminant analyses were performed for wavenumbers in the ranges 3800–2400 cm^{-1} and 2300–650 cm^{-1} (Poulenard et al., 2012, 2009).

G.2 R-files

There are 10 files containing R code in the Fingerprinting folder:

- **Preporcessing_sources**: applies mean centering and smoothing to the spectra of the source samples
- **Preprocessing**: applies mean centering and smoothing to the spectra of the SS, BS and experimental mixtures
- **Misc**: file to process and visualise spectral data, © 2006,2007 BjÃ¸rn-Helge Mevik (more information in the file)
- **DiscriminantAnalysis**: first runs the preprocessing_sources.R file and then applies a PCA and discriminant analysis based on Mahalanobis distances on the source sample spectra

- **Unmixing_model**: first runs the preprocessing.R file and then runs five separate PLSR models (one for each source), which are stored in five files:
  - **PLS_model_Limestone**
  - **PLS_model_Millstone**
  - **PLS_model_Coals**
  - **PLS_model_Riverbank**
  - **PLS_model_Urban**

In what follows, the methodologies are further explained in detail.

G.3 Data pre-processing

The resulting spectra from the DRIFTS analysis may contain variations (noise) due to a number of reasons: spectrometer drift, particle size variation, illumination stability, interference with the quartz fibre filters, etc. (Cooper et al., 2014b; Evrard et al., 2013; Martínez-Carreras et al., 2010a). To reduce the noise and to test the effect of it, signal processing was applied on the dataset. Cooper et al. (2014b) tested three common methods for spectral pre-treatment including (i) mean centering and 15-point first-order Savitzky–Golay filtering; (ii) Multiplicative Scatter Correction (MSC); and (iii) a combination of mean centering, filtering, and MSC. They concluded that mean centring and 15-point first-order Savitzky–Golay filtering produced the best results for sediment fingerprinting. They attributed these results to the fact that the MSC technique can remove spectral signals associated with the sediment chemical bounds so that important aspects of the sediment fingerprint are removed. This makes it more difficult to calibrate multivariate models for sediment fingerprinting (Cooper et al., 2014b). Also Martínez-Carreras et al. (2010a) concluded that mean-centering and filtering using a Savitzky-Golay algorithm produced good results in the context of sediment fingerprinting.

After testing the PLS models with and without pre-processing, it became clear that the pre-processing did not improve the results substantially as also found by Ge et al. (2014). However, Wold et al. (2001) recommends to centre the variables for better interpretation and numerical stability of the PLS models.

G.3.1 Mean centering

Mean centering transforms the matrix with the raw spectral data to a new matrix with columns that have a mean of zero, so that all spectra have a common baseline (Cooper et al., 2014b; Stevens and Lopez, 2015): $X_{c_{s\lambda}} = X_{s\lambda} - \bar{X}_{\lambda}$, whereby $X_{c_{s\lambda}}$ is the mean centered matrix with s samples and λ wavelengths, $X_{s\lambda}$

is the matrix with raw spectral values and $\bar{X}_\lambda$ represent the means of all spectral values at each wavelength.

G.3.2 Savitzky–Golay filtering

Savitzky–Golay filtering is a common pre-processing approach used in spectroscopic studies because it reduces noise, while preserving the shape of the spectrum and lower frequency trends which are important for the sediment fingerprint (Cooper et al., 2014b; Stevens and Lopez, 2015). The Savitzky–Golay algorithm is based on the weighted sum of neighbouring values: $x_j^* = \frac{1}{N}\sum_{h=-m}^{m} c_h x_{j+h}$, whereby x_j^* is the smoothed value, *N* is a normalizing coefficient, *m* is the number of neighbouring values at both sides of value *j* and c_h includes coefficients related to the chosen polynomial order and degree (Stevens and Lopez, 2015).

G.4 Sediment source discrimination

Statistical techniques are used to identify the source materials that are most different from each other. A principal component analysis (PCA) is performed on the DRIFTS signatures to determine the natural clustering of the samples. This first step will also reduce the dimensions of the dataset (source (sub)samples and DRIFTS-spectra) so that it can be used for discriminant analysis (DA).

G.4.1 Principal component analysis

PCA is performed on the spectral dataset of the sediment sources to check whether there are natural clusters present related to the sediment sources and to assess the variability and overlap between sediment source classes (Poulenard et al., 2009). Essentially, a PCA reduces a dataset with lots of variables (columns) and numerous measurements (rows) into a few principal components. These principal components are retrieved by transforming the variables into a set of linear, orthogonal combinations of these variables by rotating the axes of the original dataset in such a way that maximises the variance of the uncorrelated variables (Figure); the first principal component lies along the line with the greatest variation, and the second lies perpendicular to it.

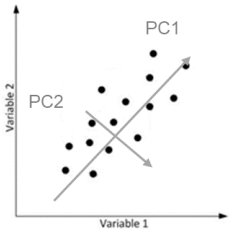

Figure: Visualisation of a two-dimensional PCA: rotating the axes of the original dataset in such a way that maximises the variance of the uncorrelated variables.

PCA reduces the dimensions of a dataset by factorizing a given spectral matrix $\boldsymbol{X}$, comprised of a set of samples and variables, into two matrices (figure): one matrix of scores ($\boldsymbol{U}$) and one matrix of loadings ($\boldsymbol{P}$), so that the residuals are minimized ($\boldsymbol{E}$) (Eq.1). The scores represent the samples in the new feature space (so the transformed variable values) based on the new set of variables (principal components) (Stevens and Lopez, 2015). Scores are calculated as linear combinations of the original data whereby weights $\boldsymbol{W}$ act as coefficients; or in other words, the weights provide represent how the original variables combine to form the new variables (Eq.2). The loadings represents the weights of the principal components on the original variables (wavelengths):

$$X = UP + E \quad (1)$$

$$U = XW \quad (2)$$

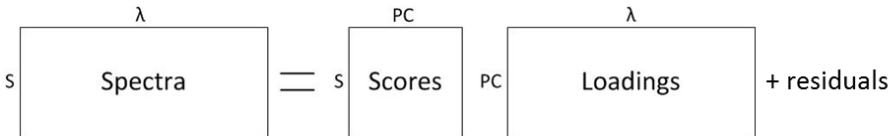

Figure: Principal component analysis on spectral dataset: the original matrix with S samples and λ wavelenghts is decomposed in a matrix with scores representing the new variables (PC's) for each sample, a matrix with scores representing the weights of all wavelengths on the PC's, and a matrix of residuals that are minimized.

G.4.2 Discriminant analysis

After performing a PCA, discriminant analysis (DA) is carried out to test whether the potential sediment sources can be discriminated based on their respective spectrum. The DA compares the distances between sample values to the centre of the class (i.e. sediment source) (Brosinsky et al., 2014a; Cooper et al., 2014a; Poulenard et al., 2012). Mahalanobis distances are preferred over Euclidian distances because it takes the variability of the DRIFTS spectrum into account. This means that Mahalanobis distances avoid misattribution issues caused by

the global spectra intensity (which increases the mean) (Poulenard et al., 2009; Stevens and Lopez, 2015). Mahalanobis distances can also be used to account for the correlation between variables (figure 2). The DA is performed on the scores of the PCA because this type of analysis requires fewer columns (variables) than rows (samples) to avoid a singular covariance matrix (Poulenard et al., 2009). PCA scores are by definition uncorrelated, so that correction for covariance is not required in this case (De Maesschalck et al., 2000). Mahalanobis distance (MD) between a set of observations and the mean of a particular class is calculated as: $MD = \sqrt{(x_i - \mu)C_x^{-1}(x_i - \mu)^T}$, with x_i a set observations of class *i*, μ the mean from a set of observations and C_x^{-1} the covariance matrix of the observations. MD's are calculated between the scores of the sources and the respective means of the sources. Pairwise comparisons are then performed of the MD's of the classes (sources). When the MD's of one class to the actual class centre is consistently smaller compared to the MD's of another class, it can be concluded that DRIFTS spectra can be used to discriminate between those two classes. Based on this analysis, a particular number of sources in retained for further analysis.

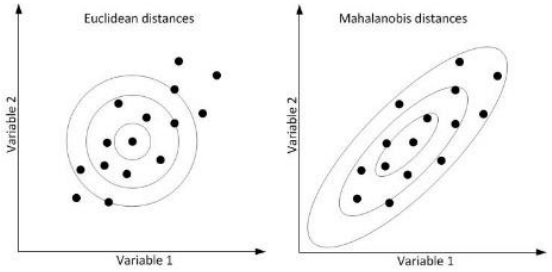

Figure: Illustration of the difference between Euclidean and Mahalanobis distances: when two variables are strongly correlated, Mahalanobis distances better represent the distances of the variables to the centre of the class

G.5 Construction of PLSR models

G.5.1 Construction of the PLS model

PLS regression (PLSR) is only recently developed as a means for modelling complicated data sets. Compared to multiple linear regression, PLSR is better able to handle data with strongly collinear, noisy and numerous X variables (such as spectra) (Karaman et al., 2013; Martens and Martens, 2000; Wold et al., 2001). In this study, PLSR is used to assess the relationship between DIRFTS spectra (X) and the weight contributions of the sediment sources (Y) in experimental mixtures. Separate PLS models are constructed for every sediment source. Similarly to PCA, the data are projected onto a new set of variables (PLS components).

In multiple linear regression, the relation between the response variables Y and the predictor variables X in its most simple form is described as:

$$Y = b_0 + b_1X_1 + b_2X_2 + \cdots + b_iX_i \quad (3)$$

However, in large highly collinear datasets containing more variables than samples, this approach is not suitable. Instead, PLSR decomposes the dataset into a set of new and orthogonal variables to work with. The difference with PCA is that instead of maximizing the variance within one dataset, PLS works by maximizing the covariance between two datasets based on the respective scores (or latent variables) (Stevens and Lopez, 2015) (figure).

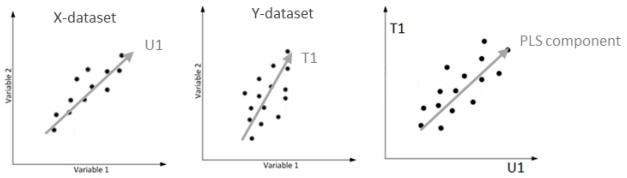

Figure: Visualisation of PLS: maximizing the covariance of the scores (U1 and T1) between two datasets X and Y

Similar to PCA, X-scores ($\boldsymbol{U}$) are computed as linear combinations of the original X variables with a set of weights $\boldsymbol{W}$ so that $\boldsymbol{X}$ can be expressed in terms of scores, loadings and residuals (Eq. 4 and 5). In addition to that, the Y dataset (here known source contributions) is also decomposed in scores ($\boldsymbol{T}$) and loadings ($\boldsymbol{F}$), but in such a way that the covariance between the X-scores $\boldsymbol{U}$ and the Y-scores $\boldsymbol{T}$ is maximized (Eq.6). As a result, X-scores can serve as good predictors of Y (Eq. 7). Equation 4 and 7 can be combined. So that the PLSS regression coefficients $\mathbf{B}$ can be described as $\mathbf{W} * \mathbf{F}$. The deviations between the observed and modelled responses is represented by the Y-residuals $\boldsymbol{Q}$ (Wold et al., 2001).

$$U = XW \quad (4)$$
$$X = UP + E \quad (5)$$
$$Y = TF + E' \quad (6)$$
$$Y = UF + Q \quad (7)$$
$$\mathrm{Y} = \mathrm{XW} * \mathrm{F} + \mathrm{Q} = \mathrm{BX} + \mathrm{Q} \quad (8)$$

In other words, if we can predict scores from Y based on scores from X by maximising the covariance between both, we can also predict Y. In addition, PLSR also models the “structure” of X and of Y, which provides additional information to understand the relationship between both datasets (Wold et al.,

2001). The scores $\boldsymbol{U}$ and $\boldsymbol{T}$ contain information about the different samples and their (dis)similarities regarding the model, while the regression coefficients and loadings $\boldsymbol{P}$ and $\boldsymbol{F}$ are important to understand which X-variables are the most important (large values) (Wold et al., 2001).

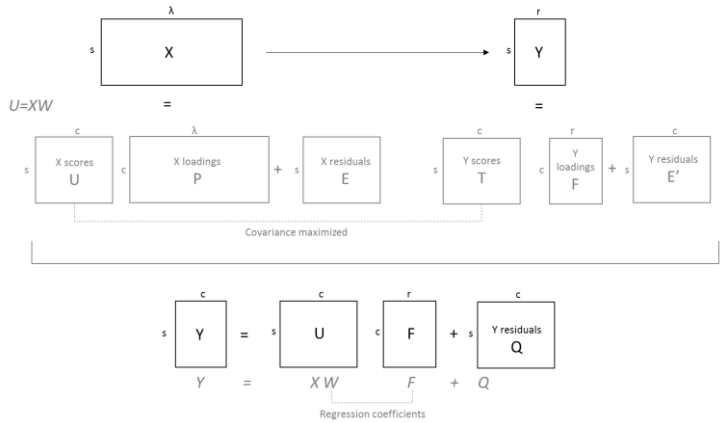

Figure: Conceptual representation of partial least squares regression

G.5.2 Model calibration

The dataset (X) is divided into two parts: 75% for calibration and 25% for validation. To randomly select the calibration set (X_c), the Kennard-Stone sampling algorithm was used. In a first step, the algorithm selects the sample (X_{c1}) in X which is closest to the mean of the entire dataset (determined by Mahalanobis distances), allocates it to X_c and removes it from X. In a second step, the sample (X_{c2}) in X which is most dissimilar to X_{c1} is selected, allocated to X_c and removed from X. In a third step, the sample (X_{c3}) is selected which is most dissimilar to the samples already in X_c, allocated to X_c and removed from X. This last step is repeated to select the remaining samples (2/3 of X).

To avoid under- or overfitting of the model, the best compromise between the description of the calibration set and the model predictive power (lowest predictive standard error) needs to be determined. In practice, this means that the appropriate number of components (i.e. the correct level of model complexity) needs to be determined (Evrard et al., 2013; Poulenard et al., 2012, 2009; Wold et al., 2001). A model underfits the data when too few components are included in the model which implies that an important structure of the data is left un-modelled. Overfitting on the other hand, occurs when too many components are taken into account, including too much noise and random variations from the data into the model (Martens and Martens, 2000).

The most used technique to assess the predictive uncertainty of the model with regards to the amount of components is re-sampling during calibration. In re-sampling techniques, different algorithms are used to generate new (hypothetical) sample sets from the observed data. These new sample sets are produced in an iterative process where the model is run each loop, which allows to calculate uncertainties (Martens and Martens, 2000; Poulenard et al., 2009; Wold et al., 2001).

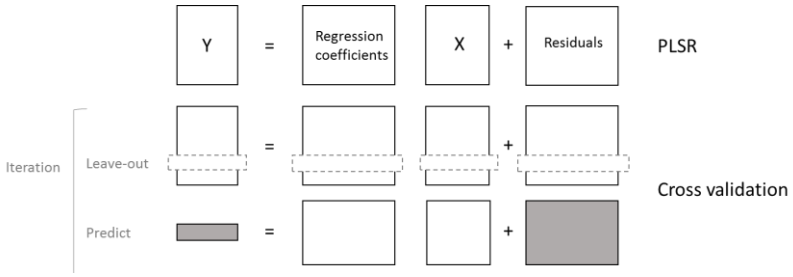

Figure: Re-sampling techniques for PLSR model and parameter uncertainty assessment.

Cross-validation is a way to calculate prediction diagnostics without the need for a separate prediction set, i.e. only with the calibration set. The PLS-models are in other words cross-validated using the data in the calibration set to tune the parameters of the models (Stevens and Lopez, 2015). Cross validation basically is the “re-estimation of all the parameters of the model n times, each time keeping one or more of the available objects (a “cross-validation segment”) as “secret” during the estimation and instead using this segment as a small “unknown” test set to check to obtained model’s predictive performance. When each of the available objects has been treated as secret and unknown, the squared lack of fit between the input data Y and the corresponding predictions of Y from the secret and unknown segments are used to calculate the mean squared error of prediction in Y” (Martens and Martens, 2000, p. 8).

Specifically, leave-one-out cross validation consists of holding-out one (randomly selected based on Kennard-Stone sampling) sample of the calibration set and fit the model with the remaining data. The model is then used to predict the value of the hold-out sample. These steps are repeated up to n times (where n is lower than the amount of samples in the calibration set). A sample that has been selected in one iteration, is returned to the calibration set and not selected anymore (Stevens and Lopez, 2015). The root mean squared error (RMSE) of cross validation can then be calculated and plotted against the number of components. The optimum number of components is the number with the lowest RMSE value (Poulenard et al., 2012, 2009).

Appendix H References

Ahmad, R., Artwright, M., Taylor, F., 2001. Analytical Methods for Environmental Monitoring. Pearson Education Limited, Essex.

Beasley, M.M., Bartelink, E.J., Taylor, L., Miller, R.M., 2014. Comparison of transmission FTIR, ATR, and DRIFT spectra: Implications for assessment of bone bioapatite diagenesis. J. Archaeol. Sci. 46, 16–22. doi:10.1016/j.jas.2014.03.008

Brosinsky, A., Foerster, S., Segl, K., Kaufmann, H., 2014a. Spectral fingerprinting: sediment source discrimination and contribution modelling of artificial mixtures based on VNIR-SWIR spectral properties. J. Soils Sediments 14, 1949–1964. doi:10.1007/s11368-014-0925-1

Brosinsky, A., Foerster, S., Segl, K., López-Tarazón, J.A., Piqué, G., Bronstert, A., 2014b. Spectral fingerprinting: characterizing suspended sediment sources by the use of VNIR-SWIR spectral information. J. Soils Sediments. doi:10.1007/s11368-014-0927-z

Cooper, R.J., Krueger, T., Hiscock, K.M., Rawlins, B.G., 2014a. High-temporal resolution fluvial sediment source fingerprinting with uncertainty: A Bayesian approach. Earth Surf. Process. Landforms. doi:10.1002/esp.3621

Cooper, R.J., Rawlins, B.G., Lézé, B., Krueger, T., Hiscock, K.M., 2014b. Combining two filter paper-based analytical methods to monitor temporal variations in the geochemical properties of fluvial suspended particulate matter. Hydrol. Process. 28, 4042–4056. doi:10.1002/hyp.9945

De Maesschalck, R., Jouan-Rimbaud, D., Massart, D.L.L., 2000. The Mahalanobis distance. Chemom. Intell. Lab. Syst. 50, 1–18. doi:10.1016/S0169-7439(99)00047-7

Evrard, O., Poulenard, J., Némery, J., Ayrault, S., Gratiot, N., Duvert, C., Prat, C., Lefèvre, I., Bonté, P., Esteves, M., 2013. Tracing sediment sources in a tropical highland catchment of central Mexico by using conventional and alternative fingerprinting methods. Hydrol. Process. 27, 911–922. doi:10.1002/hyp.9421

Ge, Y., Thomasson, J.A., Morgan, C.L.S., 2014. Mid-infrared attenuated total reflectance spectroscopy for soil carbon and particle size determination. Geoderma 213, 57–63. doi:10.1016/j.geoderma.2013.07.017

Karaman, I., Qannari, E.M., Martens, H., Hedemann, M.S., Knudsen, K.E.B., Kohler, A., 2013. Comparison of Sparse and Jack-knife partial least squares regression methods for variable selection. Chemom. Intell. Lab. Syst. 122, 65–77. doi:10.1016/j.chemolab.2012.12.005

Legout, C., Poulenard, J., Nemery, J., Navratil, O., Grangeon, T., Evrard, O., Esteves, M., 2013. Quantifying suspended sediment sources during runoff events in headwater catchments using spectrocolorimetry. J. Soils Sediments 13, 1478–1492. doi:10.1007/s11368-013-0728-9

Martens, H., Martens, M., 2000. Modified Jack-knife estimation of parameter uncertainty in bilinear modelling by partial least squares regression (PLSR). Food Qual. Prefer. 11, 5–16. doi:10.1016/S0950-3293(99)00039-7

Martínez-Carreras, N., Krein, A., Udelhoven, T., Gallart, F., Iffly, J.F., Hoffmann, L., Pfister, L., Walling, D.E., 2010a. A rapid spectral-reflectance-based fingerprinting approach for documenting suspended sediment sources during storm runoff events. J. Soils Sediments 10, 400–413. doi:10.1007/s11368-009-0162-1

Martínez-Carreras, N., Udelhoven, T., Krein, A., Gallart, F., Iffly, J.F., Ziebel, J., Hoffmann, L., Pfister, L., Walling, D.E., 2010b. The use of sediment colour measured by diffuse reflectance spectrometry to determine sediment sources: Application to the Attert River catchment (Luxembourg). J. Hydrol. 382, 49–63. doi:10.1016/j.jhydrol.2009.12.017

Pavia, D., Lampman, G., Kriz, G., 2001. Introduction to Spectroscopy. Thomson Learning, Inc, Madrid.

Poulenard, J., Legout, C., Némery, J., Bramorski, J., Navratil, O., Douchin, A., Fanget, B., Perrette, Y., Evrard, O.,

Esteves, M., 2012. Tracing sediment sources during floods using Diffuse Reflectance Infrared Fourier Transform Spectrometry (DRIFTS): A case study in a highly erosive mountainous catchment (Southern French Alps). J. Hydrol. 414–415, 452–462. doi:10.1016/j.jhydrol.2011.11.022

Poulenard, J., Perrette, Y., Fanget, B., Quetin, P., Trevisan, D., Dorioz, J.M., 2009. Infrared spectroscopy tracing of sediment sources in a small rural watershed (French Alps). Sci. Total Environ. 407, 2808–19. doi:10.1016/j.scitotenv.2008.12.049

Pulley, S., Foster, I., Antunes, P., 2015. The uncertainties associated with sediment fingerprinting suspended and recently deposited fluvial sediment in the Nene river basin. Geomorphology 228, 303–319. doi:10.1016/j.geomorph.2014.09.016

Raphael, L., 2011. Application of FTIR Spectroscopy to Agricultural Soils Analysis, in: (Ed.), P.G.N. (Ed.), Fourier Transforms - New Analytical Approaches and FTIR Strategies. InTech, pp. 385–404. doi:10.5772/15732

Savitzky, A., Golay, M.J.E., 1964. Smoothing and Differentiation of Data by Simplified Least Squares Procedures. Anal. Chem. 36, 1627–1639. doi:10.1021/ac60214a047

Smith, H.G., Blake, W.H., 2014. Sediment fingerprinting in agricultural catchments: A critical re-examination of source discrimination and data corrections. Geomorphology 204, 177–191. doi:10.1016/j.geomorph.2013.08.003

Stevens, A., Lopez, L.R., 2015. A Guide to Diffuse Reflectance Spectroscopy & Multivariate Calibration with the R Statistical Software.

Verheyen, D., Diels, J., Kissi, E., Poesen, J., 2014. The use of visible and near-infrared reflectance measurements for identifying the source of suspended sediment in rivers and comparison with geochemical fingerprinting. J. Soils Sediments 14, 1869–1885. doi:10.1007/s11368-014-0938-9

Viscarra Rossel, R. a., Walvoort, D.J.J., McBratney, A.B., Janik, L.J., Skjemstad, J.O., 2006. Visible, near infrared, mid infrared or combined diffuse reflectance spectroscopy for simultaneous assessment of various soil properties. Geoderma 131, 59–75. doi:10.1016/j.geoderma.2005.03.007

Wold, S., Sjostrom, M., Eriksson, L., 2001. PLS-regression : a basic tool of chemometrics. Chemom. Intell. Lab. Syst. 58, 109–130.

Zhang, C., 2007. Chapter 9: Atomic Spectroscopy for Metal Analysis, in: Fundamentals of Environmental Sampling and Analysis. John Wiley & Sons, Inc, Hoboken.